CASE STUDIES ON APPLICATION OF DATA INTEGRATION TECHNIQUES TO NONDESTRUCTIVE TESTING OF PAVEMENTS

Research Report 0-4393-3

Project Number 0-4393

Conducted for:
Texas Department of Transportation &
Federal Highway Administration

November 2005

Center for Transportation Infrastructure Systems
The University of Texas at El Paso
El Paso, TX 79968
(915) 747-6925

TECHNICAL REPORT STANDARD TITLE PAGE

1. Report No. FHWA/TX-05/0-4393-3	2. Government Accession No.	3. Recipient's Catalog No.
4. Title and Subtitle Case Studies on Application of Data Integration Techniques to Nondestructive Testing of Pavements		**5. Report Date** November 2005
		6. Performing Organization Code
7. Authors I. Abdallah, D. Yuan and S. Nazarian		**8. Performing Organization Report No.** Research Report 0-4393-3
9. Performing Organization Name and Address Center for Transportation Infrastructure Systems The University of Texas at El Paso El Paso, Texas 79968-0516		**10. Work Unit No.**
		11. Contract or Grant No. Project No. 0-4393
12. Sponsoring Agency Name and Address Texas Department of Transportation and the Federal Highway Administration. Research and Technology Implementation Office P.O. Box 5080 Austin, Texas 78763-5080		**13. Type of Report and Period Covered** Technical Report 9/03– 8/04
		14. Sponsoring Agency Code

15. Supplementary Notes
Project performed in Cooperation with the Texas Department of Transportation and the Federal Highway Administration.
Research Study Title: Integration of Non-Destructive Testing Data Analysis Techniques

16. Abstract
The nondestructive testing devices currently in use by TxDOT are the falling weight deflectometer, the seismic pavement analyzer, the portable seismic pavement analyzer, and ground penetrating radar, which provide thickness or modulus information. In many projects a number of these devices are used. Results do not always coincide and thus decisions on either to combine values or decide on one value need to be made. Data integration methods can be used to integrate the results from different devices in a synergistic way by utilizing the strengths of each method while minimizing the weaknesses. Two approaches were recommended: Joint Inversion Method and Data Fusion Method. These methods are implemented into two software packages called JIM and DFINE, respectively. This report contains the results from the implementation of the methods at several sites throughout Texas. The data integration methods provide more robust and realistic results than any traditional methods used individually.

17. Key Words Data fusion, Fuzzy logic, Seismic Nondestructive Testing, Deflection Nondestructive Testing	18. Distribution Statement No restrictions. This document is available to the public through the National Technical Information Service, 5285 Port Royal Road, Springfield, Virginia 22161, www.ntis.gov		
19. Security Classified (of this report) Unclassified	**20. Security Classified (of this page)** Unclassified	**21. No. of Pages** 226	**22. Price**

Form DOT F 1700.7 (8-69)

CASE STUDIES ON APPLICATION OF DATA INTEGRATION TECHNIQUES TO NONDESTRUCTIVE TESTING OF PAVEMENTS

by

Imad Abdallah, MSCE
Deren Yuan, Ph.D.
and
Soheil Nazarian, Ph.D., P.E.

Research Report 0-4393-3

The Center for Transportation Infrastructure Systems
The University of Texas at El Paso
El Paso, TX 79968-0516
(915) 747-6925

DISCLAIMERS

The contents of this report reflect the view of the authors who are responsible for the facts and the accuracy of the data presented herein. The contents do not necessarily reflect the official views or policies of the Texas Department of Transportation or the Federal Highway Administration. This report does not constitute a standard, a specification or a regulation.

The material contained in this report is experimental in nature and is published for informational purposes only. Any discrepancies with official views or policies of the Texas Department of Transportation or the Federal Highway Administration should be discussed with the appropriate Austin Division prior to implementation of the procedures or results.

NOT INTENDED FOR CONSTRUCTION, BIDDING, OR PERMIT PURPOSES

Imad Abdallah, MSCE
Deren Yuan, Ph.D.
Soheil Nazarian, Ph.D., P.E. (69263)

ACKNOWLEDGMENTS

EXECUTIVE SUMMARY

Nondestructive testing (NDT) technology has made substantial progress in the last two decades. Currently, four NDT devices, the Falling Weight Deflectometer (FWD), the Ground Penetrating Radar (GPR), the Seismic Pavement Analyzer (SPA), and the Portable Seismic Pavement Analyzer (PSPA), are available to TxDOT for collecting field data. Each of these technologies has strengths and weaknesses. However, when combined, they can provide a wealth of information not available when one method is used alone.

The ultimate NDT tool for the evaluation of all pavement systems in Texas would be a device that integrates these NDT tools. The first step toward a fully integrated hardware is a robust integration software. The objective of this project is to harvest the strength of different NDT methods and combine them in a way as to improve the parameters used in pavement design and evaluation. This project will examine the strengths and weaknesses of each device to develop a work plan for integrating information collected from each device in a practical manner.

Developing an algorithm for combining data from different NDT methods with the objective to assess the state of a pavement requires specialized technical capabilities beyond the requirements of conventional data analysis. It requires: (a) a good understanding of each of the NDT techniques being considered, (b) in-depth knowledge of probability and statistical techniques, cross-correlation techniques and techniques for normalizing and re-sampling; and (c) a good understanding of advanced analysis techniques such as artificial neural networks and expert systems. In that context, combining the data from different methods falls under the following two broad categories a) joint inversion, and b) data fusion.

The joint inversion method (JIM) was described in Research Report 0-4393-1. In JIM, the raw or processed data from two or more NDT devices are input to an advanced backcalculation program. A user-friendly software package has been developed for use by TxDOT personnel.

The concept of data fusion and the implementation of that concept were described in Research Report 0-4393-2. Data fusion can be used to integrate the results from different devices in a synergistic way by utilizing the strengths of each method while minimizing the weaknesses. Data fusion allows for logical combining and filtering of information to obtain a composite value or a basis for decision. A user-friendly software package called DFINE has also been developed to conveniently conduct data fusion.

In this report, the two methods have been applied to several sites to demonstrate the practical use of the procedures. Based on extensive field studies, the data integration methods provide more robust and realistic results than any traditional methods used individually.

IMPLEMENTATION STATEMENT

The nondestructive testing devices currently in use by TxDOT are the falling weight deflectometer, the seismic pavement analyzer, the portable seismic pavement analyzer, and ground penetrating radar, which provide thickness or modulus information. In many projects a number of these devices are used. Results do not always coincide and thus decisions on either to combine values or decide on one value need to be made. A user-friendly software package has been developed to implement the data fusion techniques for the devices named above. The software is ready for use on trial basis.

TABLE OF CONTENTS

LIST OF FIGURES

LIST OF TABLES

CHAPTER ONE

INTRODUCTION

PROBLEM STATEMENT

The most crucial information for assessing the road quality is the moduli and thickness of the pavement layers. With several different testing devices available today, there is no shortage of information that can be gathered. However, each method has its own strengths and weaknesses. When the results from multiple testing devices are conflicting, the dilemma arises over which one to accept. Such decisions should be made rationally. The following two approaches can be followed to achieve this goal:

(1) Integrating the input data from different devices into one reduction program. This process is called the Joint Inversion Method (JIM).
(2) Rationally reconciling the results from different methods to derive consistent results. This process is called data fusion.

The joint inversion method (JIM) is a backcalculation method that relies on the joint analysis of the raw data from the seismic-based and deflection-based methods. In this type of backcalculation, the inherent strength of each method dominates the analysis, resulting in a more robust and stable algorithm. JIM is thoroughly described in Abdallah et al. (2003) under Research Report 0-4393-1.

Data fusion is a process by which one source of data can be logically selected over another, or by which data from several available sources can be combined or "fused." As each method for analyzing pavements has its own strengths and weaknesses, it is only reasonable to attempt to utilize all methods to develop a better overall characterization of a pavement. As the parameters being measured are not "exact" and are subject to inherent errors, all information that has merit should be considered to some extent. The process involved in data fusion is elaborated in Williams et al. (2004) under Research Report 0-4393-2.

OBJECTIVE AND APPROACHES

The major objective of this study is to investigate the possibility and feasibility of developing joint inversion method and data fusion methods to combine test results from several different nondestructive (NDT) devices. Two software packages have been developed for this purpose.

In this report, the utility and usefulness of these two software packages are evaluated by applying them to the data collected at several locations in Texas using several NDT devices.

ORGANIZATION

Chapter 2 gives a brief overview of the joint inversion method and the data fusion method. A discussion on the strengths and weaknesses of those methods is also included.

Chapter 3 depicts the features and overall flaws of the two software packages developed under this project, namely JIM and DFINE. Snapshots taken from different windows of each software package are used to describe the execution and operation of the program. That chapter can be used as a quick guide to start utilizing either JIM or DFINE.

Several sites were visited and numerous data collected to demonstrate the feasibility of NDT data integration. A description of the sites is documented in Chapter 4.

Chapter 5 contains the overall analysis processes used in the data collection and reduction. One of the test sites is used as an example to illustrate the results of the entire process.

Chapter 6 contains the results of the analysis from data collected at all the sites. The results from JIM are compared to results from FWD backcalculation using MODULUS and from seismic data using SMART. Core data and GPR data collected at few sites are also included in the results. The strengths and limitations of the algorithm based on the results are also provided in this chapter.

Chapter 7 presents the summary and conclusions for this project.

CHAPTER TWO

BACKGROUND

INTRODUCTION

Perhaps the greatest concern in testing pavements is to determine the modulus of each pavement layer. Another concern is to accurately measure the thickness of as many layers as possible without having to core the road. Several devices and methods exist for estimating both modulus and thickness. Table 2.1 shows some of the devices currently in use and whether they can be used to determine modulus, thickness, or both. The two devices for collecting and analyzing data are the Falling Weight Deflectometer (FWD) and the Seismic Pavement Analyzer (SPA). The other two devices, the Portable Seismic Pavement Analyzer (PSPA) and the Ground Penetrating Radar (GPR), are supplementary.

Table 2.1 - Commonly Used NDT Devices

Device	Modulus	Thickness
Seismic Pavement Analyzer	Yes	Yes
Portable Seismic Pavement Analyzer	Top Layer	—
Falling Weight Deflectometer	Yes	—
Ground Penetrating Radar	—	Yes

The strength and weaknesses for each technology are different. For the FWD, further developments in the analysis procedures are needed to improve the stability and capabilities of current programs. Nonetheless, the greatest obstacle to a reliable implementation of the FWD is accurate determination of layer thickness and depth to shallow bedrock. The GPR measures the electric properties of the layers that can be translated to layer thickness and the uniformity of the pavement in terms of moisture and density. However, electric properties are not directly related to the mechanical properties used in structural evaluation. Seismic methods provide the thickness and moduli of different layers. However, the GPR is more convenient for thickness determination. In addition, the seismic moduli are small-strain moduli. These moduli should be converted to design moduli using nonlinear algorithms such as SMART.

Two main integration techniques were proposed under this project: a) Joint Inversion and b) Data Fusion. Figure 2.1 illustrates the overall integration scheme and the flow of information. The current analysis methods are illustrated to the left of the figure and the proposed analysis methods to the right. In current state, the analysis from each NDT device is performed separately usually by different persons. The engineer in charge then compares and analyzes the results from each method manually and subjectively. The flow of information for the current process is indicated by dotted lines. In the proposed data integration method, the data from each device are passed into an integration center where all the reduction, analysis and harmonization of the data are performed.
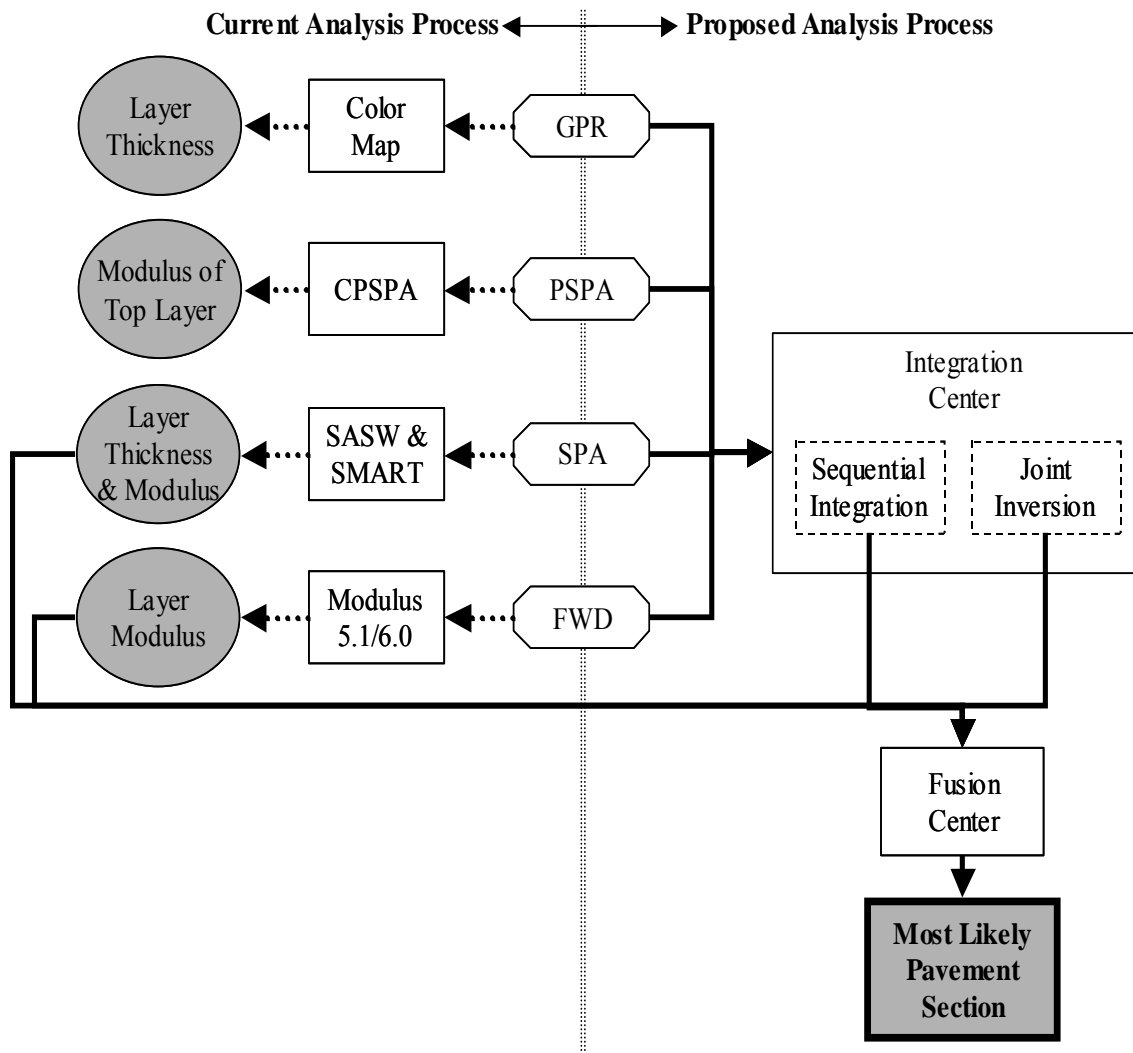
Figure 2.1 - Overall Schematic of Proposed Integration Tools

The joint inversion technique is based on the idea that information from different sources measuring the same phenomenon could be used jointly to support each other in describing that phenomenon. The first portion in the proposed analysis process in the figure depicts the joint integration technique. On the other hand, the data fusion technique is useful when more than one

set of results are obtained. The lower portion of Figure 2.1 depicts the flow and function of data fusion. If the user, for example, performs four different analyses (i.e. conventional analyses and integrated analyses), the outcome is four sets of results. The benefit of using data fusion is to rationally extract and estimate more-reliable results that can be used for evaluation.   In this chapter, the background information behind the joint inversion method and data fusion method, as applied to these devices, is briefly described.

JOINT INVERSION ALGORITHMS

In joint inversion, the data from different methods are interpreted simultaneously.   In that manner, the results are harmonized and are made consistent using objective criteria. Consider a pavement section at which FWD, SPA and GPR data are available. The engineer would like to determine the modulus and thickness of each layer. As indicated before, when the FWD is interpreted alone, the thickness has to be estimated.   Any uncertainty in thickness may significantly impact the backcalculated moduli.   Today, one can use the GPR to obtain the thickness of the layers and input them to the backcalculation program.   This will reduce the uncertainty in the input thickness; however, due to the non-uniqueness of the backcalculation algorithms, one is not ensured that the estimated moduli are accurate.

If the SPA data are available, one can harmonize the results even further since the SPA provides the moduli and thickness of each layer also. When the results of the FWD, GPR and SPA are combined, the moduli from the SPA and FWD have to corroborate with one another and the thickness from the GPR and SPA should agree. In that manner, at least in theory, the results should be more accurate and representative.

The approach taken for joint inversion technique under this project, as shown in Figure 2.2, is different. Both the seismic dispersion curve and the FWD deflections are used as input. The output is moduli of pavement layers. The algorithm is an iterative process that uses a single value decomposition routine (SVDC) to minimize the errors.

Figure 2.2 illustrates the flow of information and the process used to determine pavement layer moduli. Initially inputs from the FWD measurements are fed into the FWD forward model subroutine (BISAR) and inputs from the SPA measurements are fed into the seismic forward model subroutine with the initial pavement properties such as seed modulus, thickness, Poisson's ratio, and density of each layer. The function of each forward model is to calculate a theoretical response (i.e., deflection bowl for the FWD and dispersion curve for the seismic). The results of the two forward models are compared to the measured values. The error between the theoretical and measured results is calculated. If the error is less than a specified tolerance, the design moduli are reported. However, if the error is greater than the tolerance, the pavement parameters are adjusted and the process is repeated until the error is minimal.

DATA FUSION METHODS

In any application, accuracy and precision are important. When a phenomenon is measured, the resulting measurement contains error. The ideal situation would be the elimination or reduction of errors. However, that may prove impossible without extraordinary effort. Where multiple

```
┌─────────────────┐  ┌─────────────────┐  ┌─────────────────┐
│  Falling Weight │  │ Initial Pavement│  │   Dispersion    │
│  Deflection Data│  │   Properties    │  │   Curve Data    │
└─────────────────┘  └─────────────────┘  └─────────────────┘
         │                    │                    │
         ▼                    ▼                    ▼
  ┌─────────────┐      ┌──────────────┐     ┌──────────────────┐
  │ FWD Forward │─────▶│Error Function│◀────│ Seismic Forward  │
  └─────────────┘      └──────────────┘     └──────────────────┘
                              │
                              ▼
                        ◇───────────◇   Satisfied
                       ╱   Check     ╲ ──────────────┐
                       ╲  Tolerance? ╱               │
                        ◇───────────◇                │
                              │                      │
                       Not Satisfied                 │
                              ▼                       │
                       ┌──────────────┐               │
              ┌───────▶│    SSVDC     │               │
              │        └──────────────┘               │
              │         │          │                  │
              │         ▼          ▼                  │
       ┌─────────────┐ ┌──────────────┐ ┌─────────────────┐
       │ FWD Forward │▶│Error Function│◀│ Seismic Forward │
       └─────────────┘ └──────────────┘ └─────────────────┘
              │               │                         
              │               ▼                         
        Not Satisfied   ◇───────────◇                   
              └─────────╱   Check     ╲                 
                        ╲  Tolerance? ╱                 
                         ◇───────────◇                  
                              │   Satisfied             │
                              ▼                          
                       ┌──────────────┐                 │
                       │    Output     │◀───────────────┘
                       │ (Layer Moduli)│
                       └──────────────┘
```
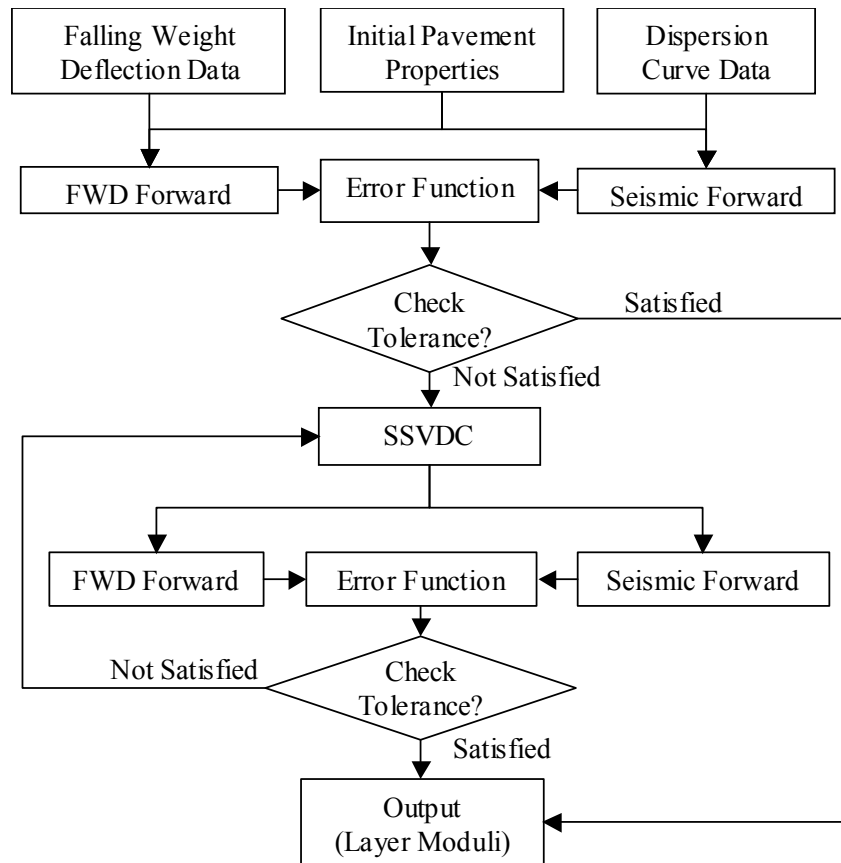
Figure 2.2 - Joint Inversion Algorithm Flowchart

devices are used to measure the same phenomenon, the resulting measurements can either support or contradict each other. Data fusion is a general term used to describe the processes by which results from different devices are combined with the purpose of arriving at more reliable or accurate results than the individual devices would arrive at on their own. The complexity of data fusion can range from a simple average to an artificial neural network.

One of the main basis for data fusion is that any event has some degree of "truth" associated with it. This truth can be represented by a probability, a weight, a distribution, or a plausibility interval. It is usually possible to obtain a weight from any of the methods just listed. Weights, in turn, can be used to combine readings from multiple devices. Once a systematic method for data manipulation and data filtering is defined, algorithms can then be developed to remove the burden of guess work for a person trying to make a decision.

Data fusion methods can be broken up into several categories. The two categories used to develop the data fusion program for this study are a) statistical method, b) fuzzy logic. The first category is statistical or "probabilistic" approaches to data fusion. The methods contained within are a weighted average that relies on statistical information such as mean and standard deviation. The other method is the fuzzy logic fusion method. The fuzzy logic method allows for the creation of rules that attempt to function in a manner that changes a subjective decision into a

mathematical rule. These decisions, in turn, can be used to combine or filter data. Several of these methods have been implemented in this study as reported in Research Report 0-4393-2 (Williams et al., 2004). The methods used are summarized below.

Statistical Weighted Average: The statistical weighted average method uses simple statistical values to combine data. From most sets of numbers, a mean and standard deviation can be obtained. Additionally, a standard deviation can be assumed in cases where one cannot be calculated. This usually happens when the size of the sample is small.

Fuzzy Logic: Fuzzy logic tries to handle vagueness or ambiguity that is the result of human thinking. The idea behind fuzzy logic is a way to imitate the decision process that relies on making a subjective decision with a decision algorithm formed by defining rules that will interpret the inputs and make a decision based on those rules. Fuzzy logic depends on the development of fuzzy sets. These fuzzy sets have no definite boundary, and thus events that occur within these sets often partially belong to two members of the set.

Once again, we highly recommend that the reader reviews Research Reports 0-4393-1 and 0-4393-2 for an in depth description of the methods summarized above.

NDT ANALYSES PROGRAMS

Several NDT analyses programs are used in this project to analyze data collected in the Field. The following section provides a brief description of each program.

Seismic Modulus Analysis and Reduction Tool (SMART)

SMART was designed for a flexible pavement system based on the classical layered elastic theory with a modification on the analysis of the structural response of the pavement system. The algorithm integrated in this program is a compromise between the simple linear model and comprehensive nonlinear model. This algorithm takes advantage of the speed of the linear analysis while incorporating the nonlinear behavior of the pavement layers. Although the algorithm is not strictly a nonlinear algorithm, it accounts for the nonlinear behavior of the pavement materials under actual truck traffic. The algorithm is referred to as an equivalent-linear analysis method.

Equivalent Linear Model: An equivalent-linear model is a model that in an approximate fashion can consider the load-induced nonlinear behavior based on the static linear elastic layered theory. An iterative process is employed to consider the nonlinearity of the pavement materials. The constitutive model adopted in the equivalent linear model is:

$$E = k_1 \sigma_c{}^{k_2} \sigma_d{}^{k_3} \tag{2.1}$$

In this equation, k_1, k_2 and k_3 are statistically determined coefficients. In Equation 2.1, the modulus at a given point within the pavement structure is related to the state of stress. Since the state of stress can be known only if the material properties, including modulus, are known, an iterative process has to be used to implement this stress-modulus relationship. The advantage of

the model presented in Equation 2.1 is that it is universally applicable to fine-grained and coarse-grained base and subgrade materials.

Equation 2.2 was slightly modified to incorporate the seismic modulus with the load-induced nonlinear modulus. Parameter k_1 in Equation 2.1 is replaced by a term that is a function of the seismic modulus and the stresses under seismic testing. Therefore, after arithmetic manipulation and substitution, the nonlinear modulus can be related to the seismic modulus through (Ke et al., 2002)

$$E = E_{seis} (\frac{\sigma_{c\_ult}}{\sigma_{c\_init}})^{k2} (\frac{\sigma_{d\_ult}}{\sigma_{d\_init}})^{k3} \qquad (2.2)$$

Compared to Equation 2.1, parameter k_1 is eliminated when the seismic modulus is considered as an input. Equation 2.2 can be used in an equivalent-linear model to obtain the modulus of a nonlinear material in SMART. This model is more elaborate and is detailed in Abdallah et al. (2003). The remaining nonlinear parameters k_2 and k_3 can be obtained from laboratory tests such as the resilient modulus tests. In the absence of laboratory testing, the k_2 and k_3 values can be approximated based on the material quality.

Figure 2.3 presents an overall depiction of the process used for performing the analysis using SMART. Step 1, in the figure, represents the field testing process. The SPA, a trailer-mounted device is used to collect seismic data. The data collection process is rapid with a complete testing cycle at one point taking less than one minute (lowering sources and receivers, making measurements, and withdrawing the equipment). Nazarian et al. (1993) contains the details of the SPA operations. Once the data is collected, the Spectral-Analysis-of-Surface-Waves (SASW) process is used to determine the small-strain modulus or "seismic modulus" of different layers. This is Step 2 in the process. Nazarian et al. (1993) provides detail explanation of the SASW process. Step 3, in the figure, illustrates where SMART fits into the overall procedure. SMART uses the seismic modulus from the SASW process as input to determine the design moduli of different layers.

Spectral Analysis of Surface Waves Method (SASW)

As discussed above, the SASW analysis works in conjunction with the SMART analysis, since the output of the SASW process is used as input to the SMART program. The SASW method is an in situ seismic evaluation technique for determining elastic moduli and thickness of a layered system, such as pavements. The method is based on the dispersion phenomenon of surface (Rayleigh) waves propagating in a layered system; that is, the waves of different frequencies or wavelengths travel with different velocities. The test process of this method, which has been automated, involves generation and detection of surface waves by impacting the surface of the pavement and monitoring and capturing the motion of the pavement surface at various points. A detailed discussion about the SASW method can be found in Nazarian (1984), Stokoe et al. (1994), and Hiltunen & Gucunski (1994).
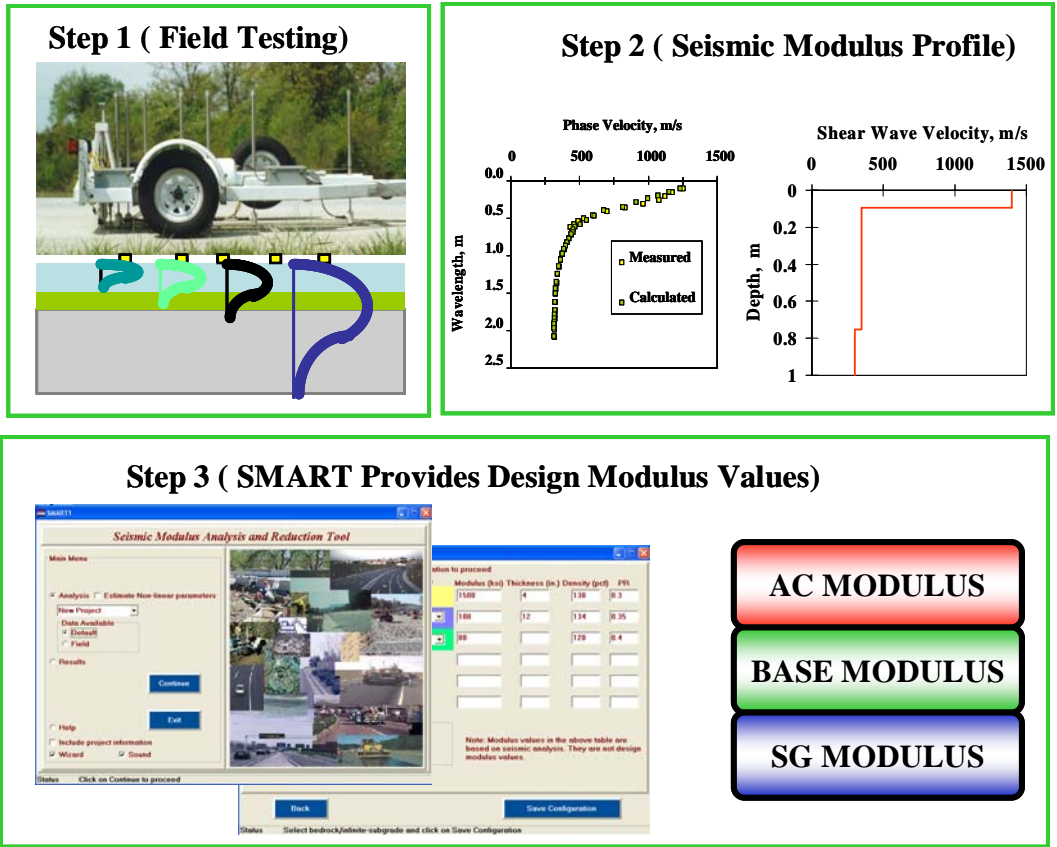
Figure 2.3 - Snapshots of the SMART Algorithm

Figure 2.4 illustrates a typical SASW testing procedure. The test is carried out using the SPA. A picture of the SPA is depicted in Step 1 of the figure. To conduct the testing with the SPA, elastic waves are generated by an impact source, detected by at least a pair of receivers (accelerometers and geophones), and recorded. The plot labeled waveform in Step 1 of the figure illustrates an example of the raw data from two receivers. This first step captures the information needed, using the NDT device. The next step is to convert the recorded signals (from the waveforms) to the frequency domain by means of a Fast Fourier Transform (FFT) algorithm to obtain the dispersion curve (phase velocity vs. frequency or wavelength). The phase lag between two receiver locations, at a given frequency, is used to calculate the phase velocity. This step is performed instantaneously and is typically conducted for a number of receiver spacings to cover a broad range of frequencies or wavelengths. At the same time, the phase velocities are being calculated and thus the dispersion curve is being developed. As the phase for each receiver spacing is determined, the software automatically displays the corresponding part of the dispersion curve. This is represented by the Dispersion Curve plot in Step 2. Once the raw dispersion data are obtained from several receiver spacings, averaging of these dispersion data will form a dispersion curve as indicated in the figure. Once the average dispersion curve is generated, the last step in the SASW process is the inversion. Step 3 in Figure 2.4 illustrates the use of the average dispersion curve as input in the inversion of the pavement profile. This process mainly involves a trial and error fitting routine in order to select the most appropriate set of moduli to represent the information measured for the pavement.
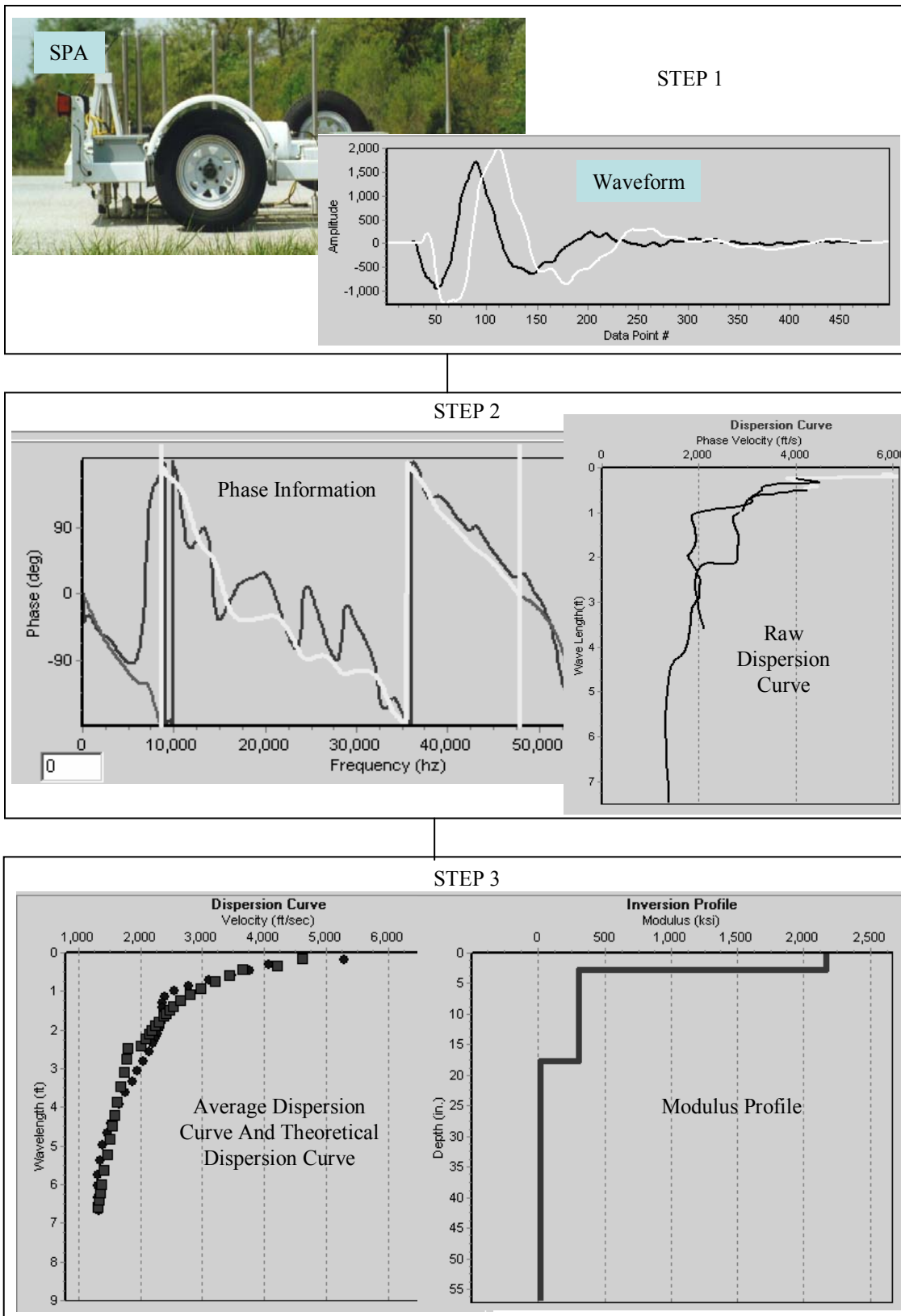
Figure 2.4 - Flow of SASW Analysis

Again this process has been automated in the software. As illustrated in Step 3 (Dispersion Curve plot) both the theoretical and measured "average" dispersion curves are shown. The plot labeled inversion profile shows a graphical representation of the layer moduli.

MODULUS

MODULUS is a linear elastic program that backcalculates layer moduli from FWD data. The backcalculation algorithm used in MODULUS is based on matching of a measured deflection bowl with a predicted deflection bowl to obtain material properties. The determination of pavement moduli using the static layer elastic backcalculation method is, by far, the most widely used procedure (Bush, 1980; Lytton, et al., 1985; Uzan, et al., 1990). The application of layered theory for in-situ material characterization requires the estimation of only one unknown parameter, the Young's modulus, of each layer. MODULUS is currently the analysis program used by TxDOT. Figure 2.5 shows snapshots of the program. The latest version of the program is windows based. MODULUS uses the deflection bowl measured using the FWD along with the thickness values of each layer and the range of the layer modulus for each layer. The range of the layer moduli are used as bounds for the algorithm used in the selection of the deflection bowl.
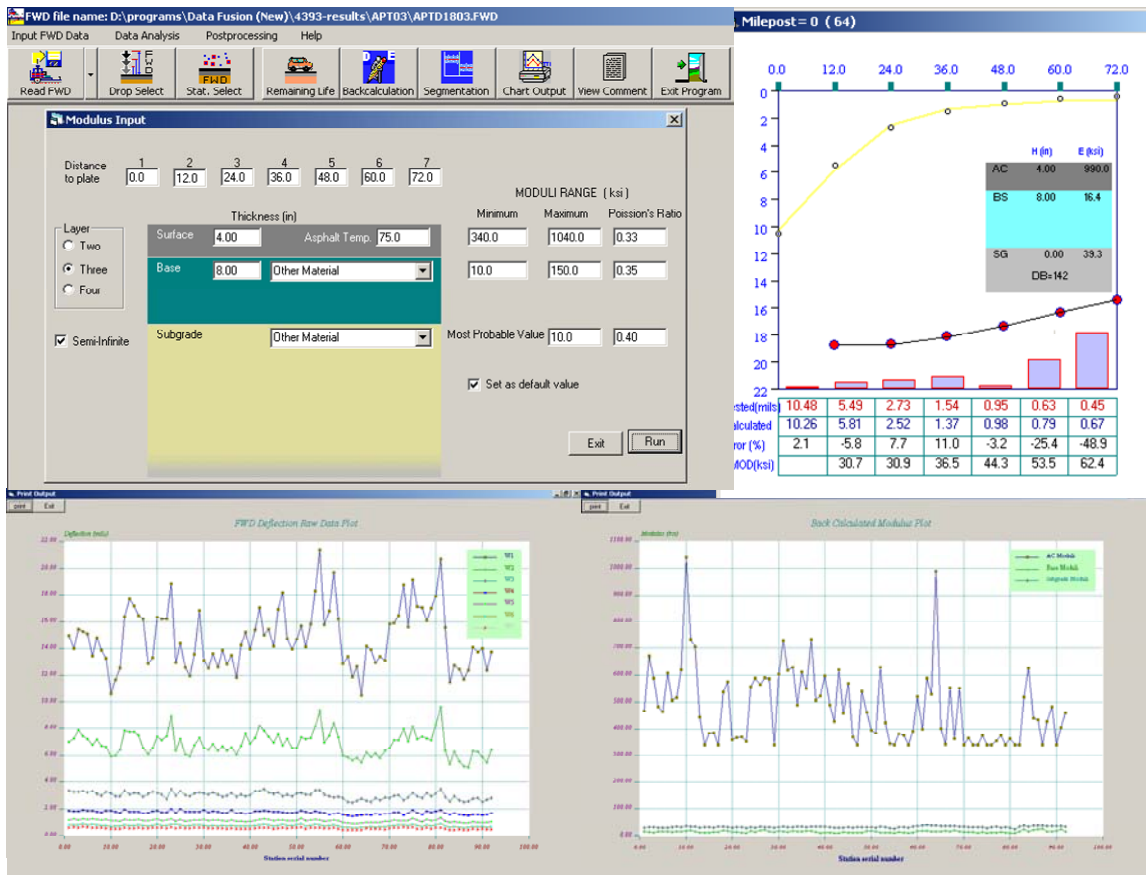
Figure 2.5 - Snapshots of MODULUS Program

CHAPTER THREE

DESCRIPTIONS OF JIM AND DFINE

INTRODUCTION

Two software packages were developed for the implementation of the data integration algorithm and data fusion algorithms. JIM (**J**oint **I**nversion **M**ethod) uses data from several NDT devices to estimate the layer moduli and layer thickness. The data fusion software that is used to harvest the wealth of information from combining the information from the various NDT analyses to provide a more informed decision on the state of the pavement system is DFINE (**D**ata **F**usion for **I**ntelligent **N**ondestructive **E**valuation).

A brief description of the two programs is presented in this chapter. A user's guide for JIM and DFINE is included in the installation files. Also, a training web site located at http://ctis.utep.edu makes available training modules for both programs. Both JIM and DFINE are windows-based programs. Snapshots taken from each of the software are included to present the features and overall flow of JIM and DFINE. This chapter can be used as a quick reference to start utilizing either JIM or DFINE.

JOINT INVERSION METHOD (JIM)

Main Menu

Figure 3.1 shows the start-up window of JIM. Four devices of interest (FWD, SPA, PSPA and GPR) are shown in the top portion of the window. Data from these four NDT devices can be used in the joint inversion analysis. Among the four devices, FWD and SPA are selected by default and data from both are required to perform the inversion to estimate layer moduli and layer thickness. The other two devices, PSPA and GPR, are used as complementary inputs to strengthen the joint inversion process. PSPA data are very stable for the top layer of a pavement system. In a three layer flexible pavement system PSPA provides a good indication of the ACP modulus. Likewise, the GPR provides a good indication of the thickness of the ACP layer and in certain cases the base layer. The information, if available, can be used to reduce the number of backcalculated parameters. The preliminary information necessary for the execution of the program is provided in this window as well. After the necessary information is provided, the "Next" or "Continue" button needs to be selected to proceed to the next window.

To start using JIM, a user is first required to enter information regarding the project test-site. This is accomplished by selecting the project options menu. On the left side, the user first specifies the project directory. The project directory is used to store the inputs and outputs of JIM. An option is provided for a user to create a new directory or open an existing directory. Once the project folder is selected, the right side of the window requires project information regarding a test site. An option is used to allow a user to load default project information. Upon completion, the "Update" button is selected to proceed to the next window.
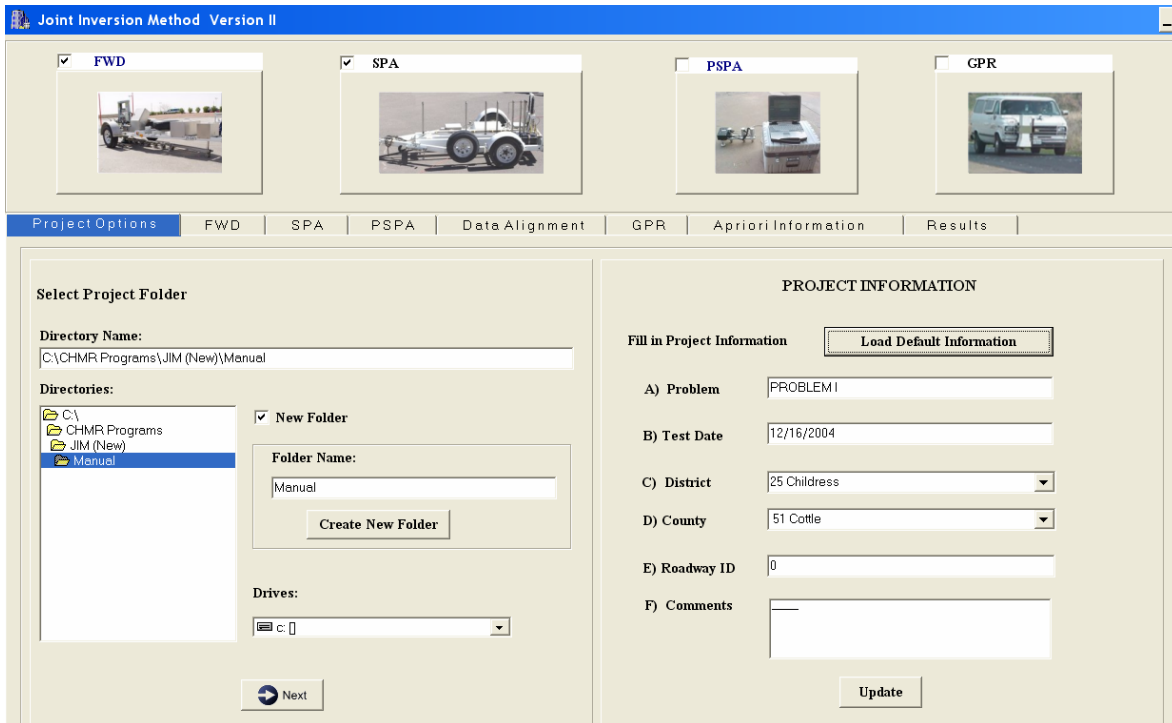
Figure 3.1 - Main Menu Window of JIM

FWD, SPA and PSPA Menus

The FWD Menu is used to load the necessary FWD files. The first option in this window is to select the FWD file (see Figure 3.2). When the option is selected, a pop-up window, as shown in Figure 3.2, appears that allows a user to browse for the appropriate FWD files. The file extension for the FWD data is ".fwd". After choosing an FWD file, a drop-down box appears that enables the user to select the appropriate drop height for the analysis. Then the "Continue" button is selected prompting the program to display the information from the FWD file on the FWD tab. Figure 3.3 displays the FWD data in both tabular and graphical form. The tabular format lists station number, comments, and load for the selected file. The graph on the right side displays seven FWD deflections versus the station identification. The two displays allow a user to view the graph of the FWD data and use the tabular form to prescreen the FWD deflection data. The user can decide on the stations to be included or excluded from the analysis by selecting/ deselecting each station. By default all stations in the FWD file are selected. Again, a user has to click the "Update" button to proceed further.

14
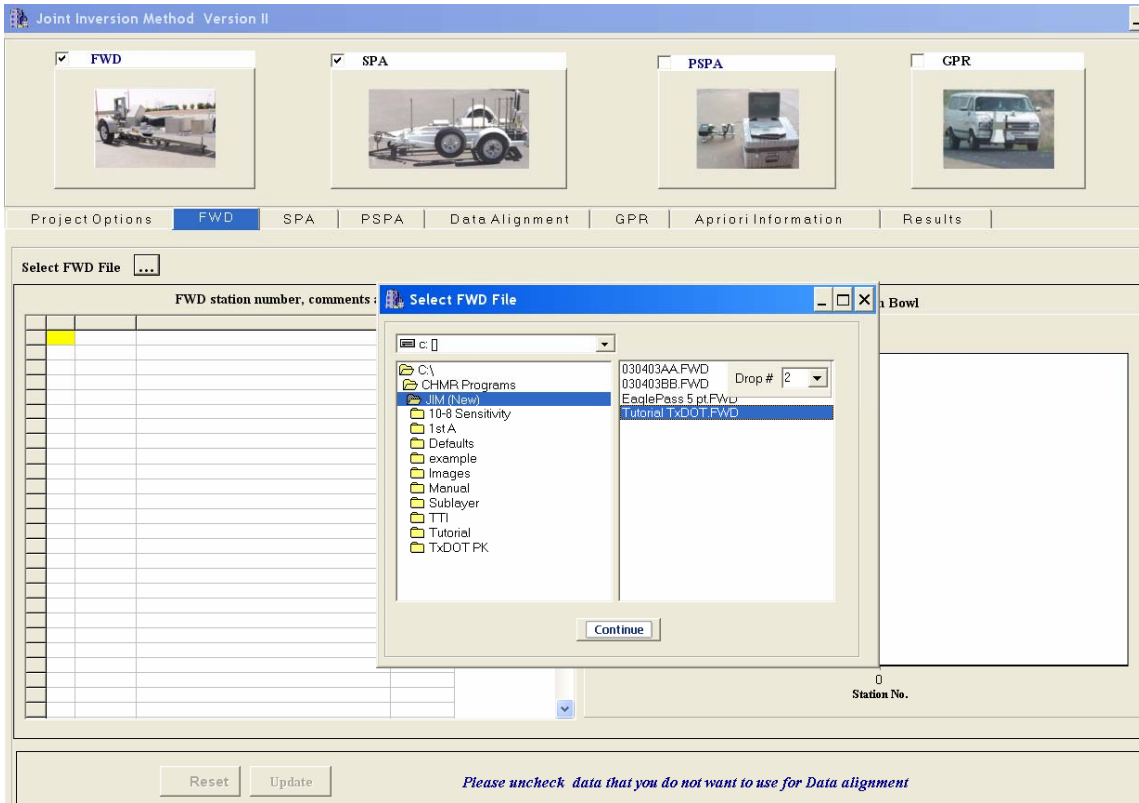
Figure 3.2 - Menu of Selecting FWD File in JIM
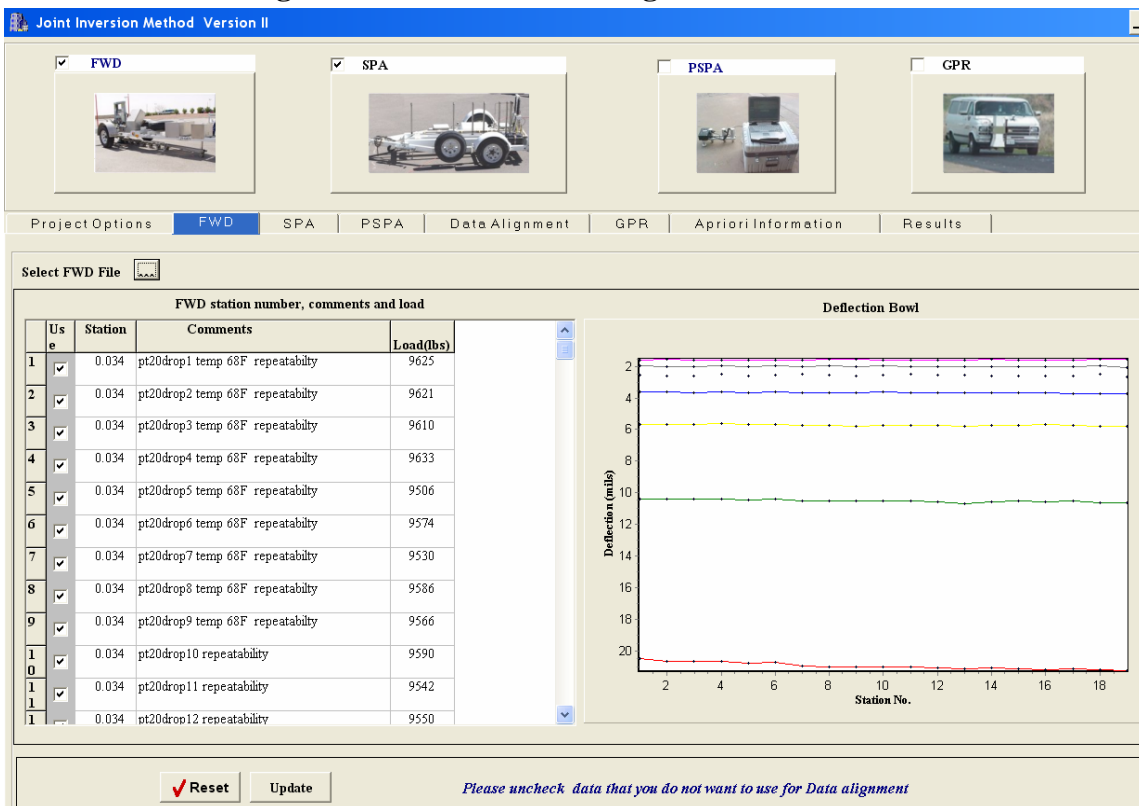
Figure 3.3 - Menu of Loaded FWD File in JIM

The next window to load is a menu similar to the FWD tab, the SPA menu. The SPA Menu is used to load the necessary SPA files. The process of selecting the SPA files is similar to the FWD. The file extension for the SPA data is ".stj". Figure 3.4 and 3.5 are snapshots of the SPA information windows. Figure 3.4 provides a view of the file selection menu, and Figure 3.5 displays the dispersion curve information from the file. The table lists station counter and the comments for the selected files. The graph on the right side displays the dispersion curves. As with the FWD, the two displays in Figure 3.5 allow the user to view the dispersion curves and use the tabular form to prescreen the data. Also, the user can decide on the stations to be included in or excluded from the analysis by selecting/deselecting each station. By default all stations in the SPA file are selected. Again, a user has to click the "Update" button to proceed further.
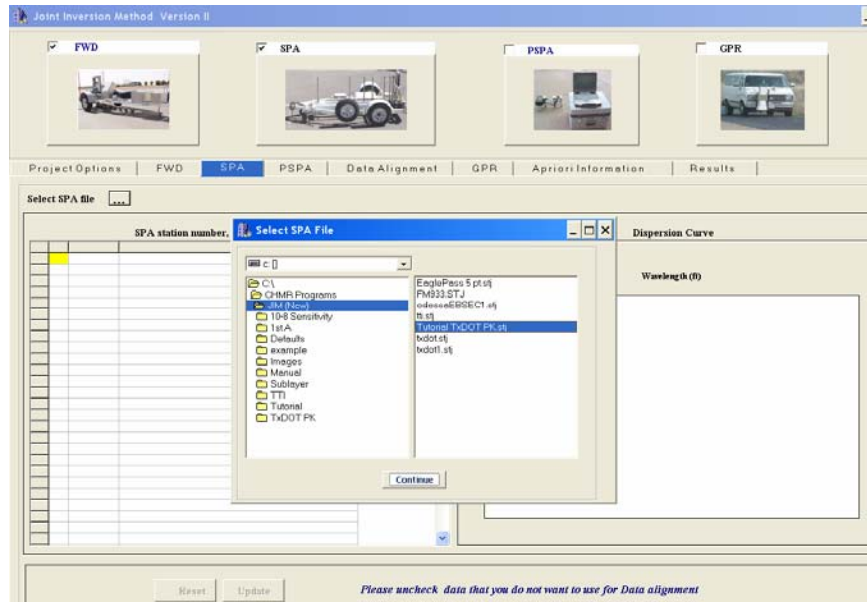
Figure 3.4 - Menu of Selecting SPA File in JIM
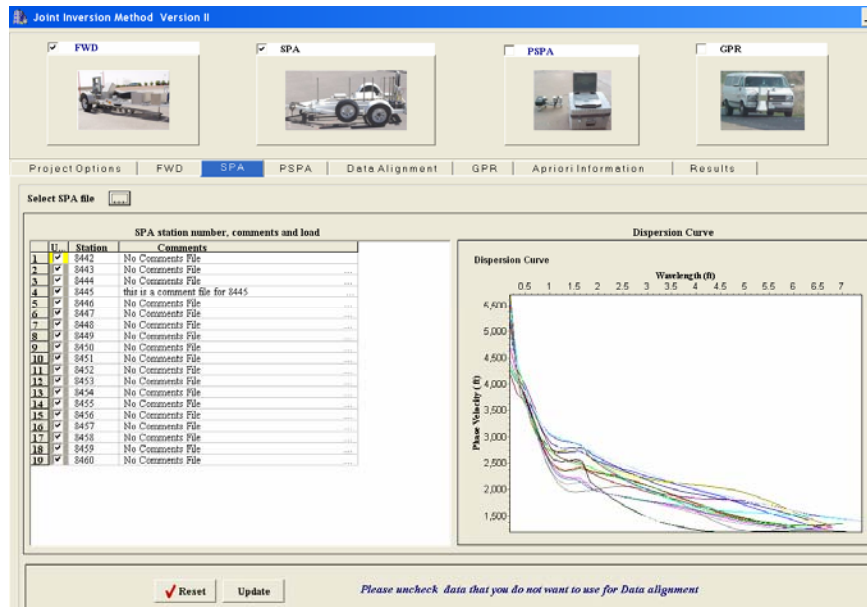
Figure 3.5 - Menu of Loaded SPA File in JIM

16

The use of the PSPA menus is optional. If PSPA data is available, a user will be prompted to proceed to the PSPA menu. The steps for selecting and loading PSPA data follow the same procedure as that of the FWD and SPA. The PSPA file has an extension ".pspa". Figure 3.6 shows a PSPA menu with a sample loaded PSPA file.
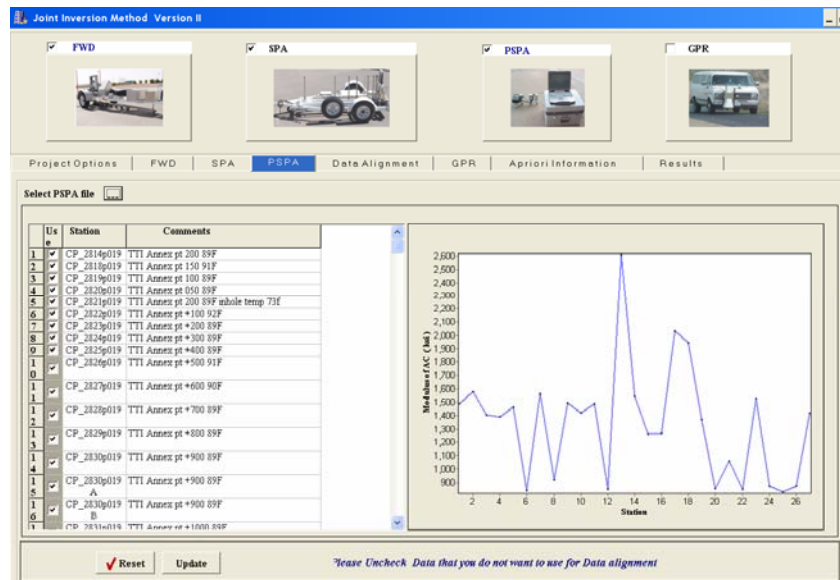
Figure 3.6 - Menu of Loaded PSPA File in JIM

Data Alignment

The next step of the process is to align the FWD, SPA and the PSPA data before proceeding to the next step. The NDT data may have been collected with various devices using different referencing systems. Therefore, aligning the data before analysis is crucial. JIM allows the user to align the data by using the comments provided during data collection. The data alignment tab, as presented in Figure 3.7, contains information (station number and comments) for the FWD, SPA, and PSPA. Several options are available for aligning the data in the case where: a) not all devices collected data in the same order, b) some devices repeated data collection, or c) missing data that was either not collected or removed due to irregularities in the data. For each method, the station number and comment can be: a) shifted up or down to match the comments from the other devices or b) deleted from the table. Also, a row from the entire table listed in Figure 3.7 can be removed. The data shown in this menu needs to be completely aligned with no missing data before proceeding to the next step. Providing detail comments in the data collection phase of each NDT device is very crucial to make data alignment easy. Once alignment is completed, the user can select the "Done Alignment" button to proceed.

GPR Menu

If GPR data is available, the user may select the GPR file with a file extension ".gpr". The file extension from COLORMAP, which is used to interpret GPR data, needs to change from "*.txt" to "*.gpr" in order to be used in JIM. This was done to distinguish the various types of input to JIM. The GPR data is presented in the top portion of the GPR tab as shown in Figure 3.8. The thickness of the ACP layer and base layer at regular increments are extracted from the GPR file and plotted.
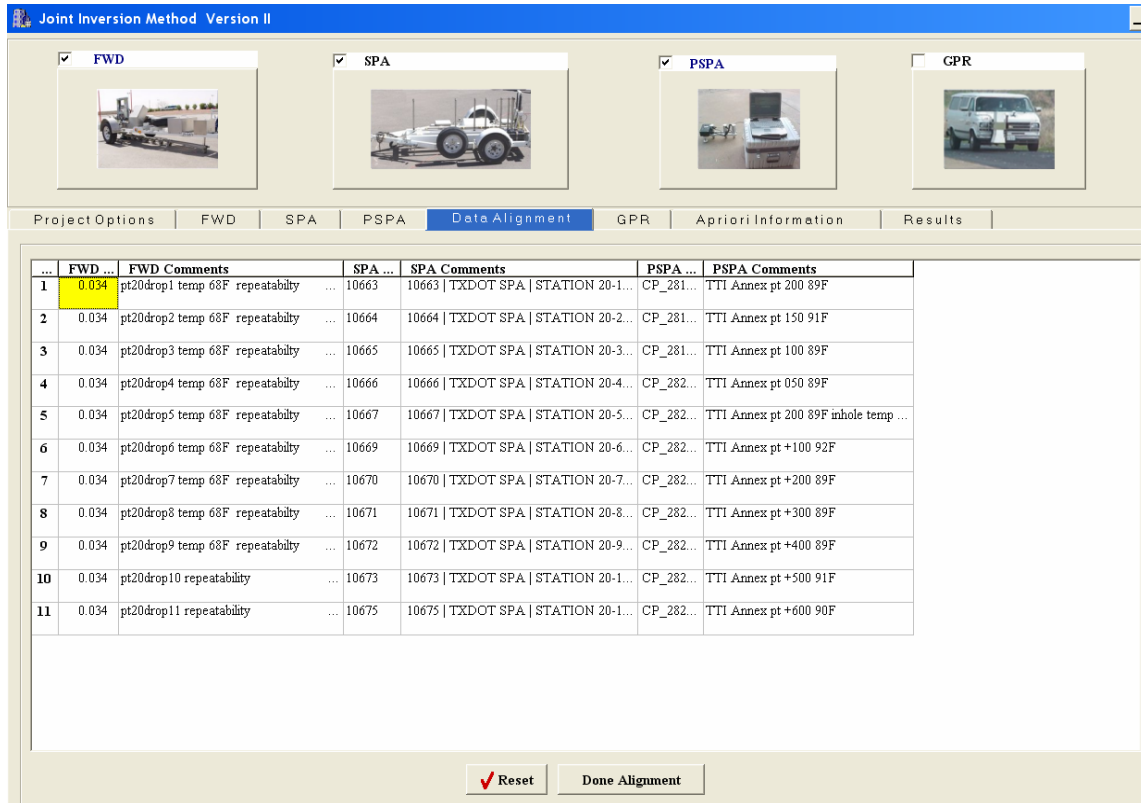
Figure 3.7 - Menu of Aligning Data Sets in JIM
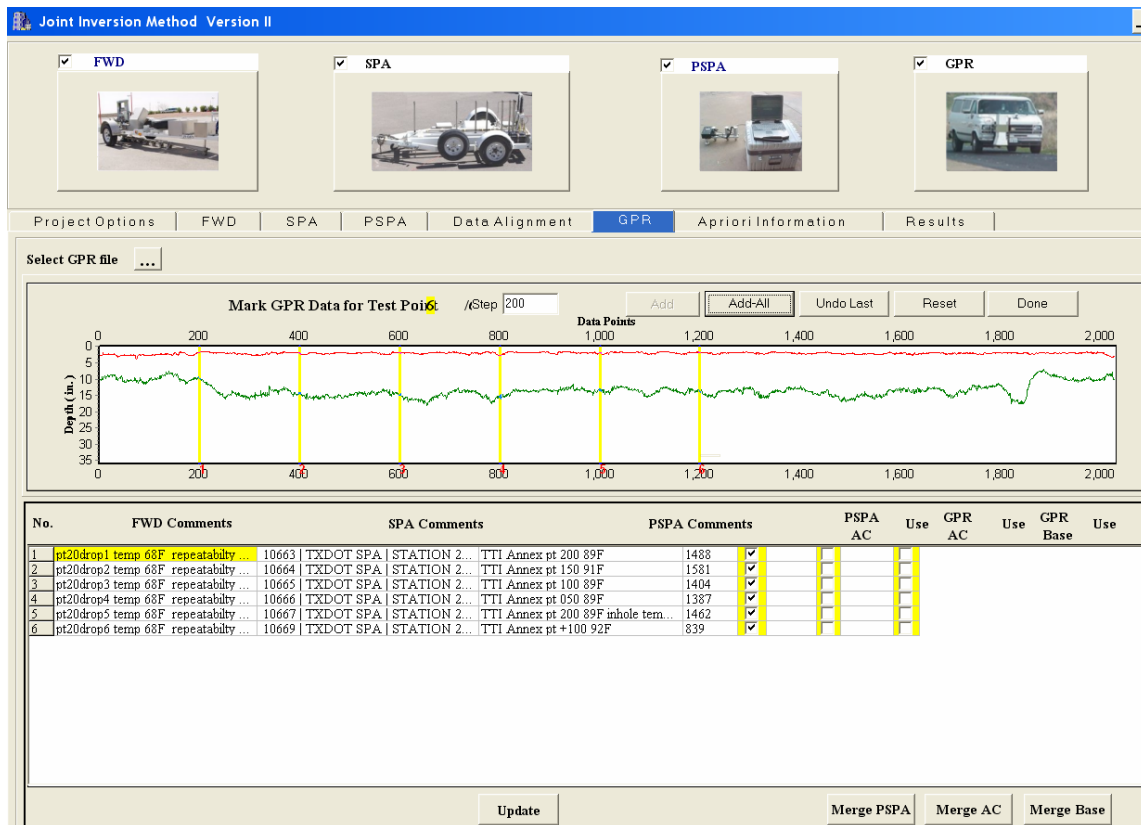
Figure 3.8 - Menu of Loaded GPR File in JIM

18

Since the GPR data is in a continuous form, but the FWD, SPA, and PSPA data are more in a discrete form, the GPR data needs to be tied to other devices. The user can mark the station location either by specifying the step for each station and selecting the adjacent "Select" button, or if the tests were conducted at equal spacings, an "Add All" button can be selected to mark all stations at the specified location. At each marked location a "yellow" bar shows the identification mark of each station. A user can either select "reset" button to repeat the GPR markings, or the "Done" button to complete aligning the GPR data. The bottom part of the GPR menu shows the final data alignment process. The GPR and PSPA data can be further processed. A user can average GPR data across the section being analyzed or across several subsections. The same can be performed on the PSPA data. Once the appropriate selections are made, the "Update" button is selected to proceed to the next step.

A Priori Information Menu

The last input tab is the "A Priori Information" tab (see Figure 3.9). The first option in this menu is the selection of the analysis option. Three analysis types are available: a) JIM, b) FWD, and c) SPA. The JIM analysis is by default the option selected since this is the analysis type the program is designed to perform. However, the program is capable of running the FWD analysis (excluding the SPA data) and likewise the SPA analysis (excluding the FWD data). The program performs analysis for JIM first, followed by the other two options, if selected. The lower portion of this menu shows a table for providing the a priori information of the pavement system such as layer thickness, layer moduli, nonlinear k_2 and k_3 parameters, Poisson's ratio, and layer density. This information is used as seed values in the inversion analysis. Also provided in this table is the option to select the parameters that need to be "backcalculated". A user can proceed to the analysis by selecting the "Continue" button. An animation window, depicting computer processing, signifies that the analysis is in progress. Based on data used and analysis method chosen, the analysis time could vary from 1 to 20 minutes.
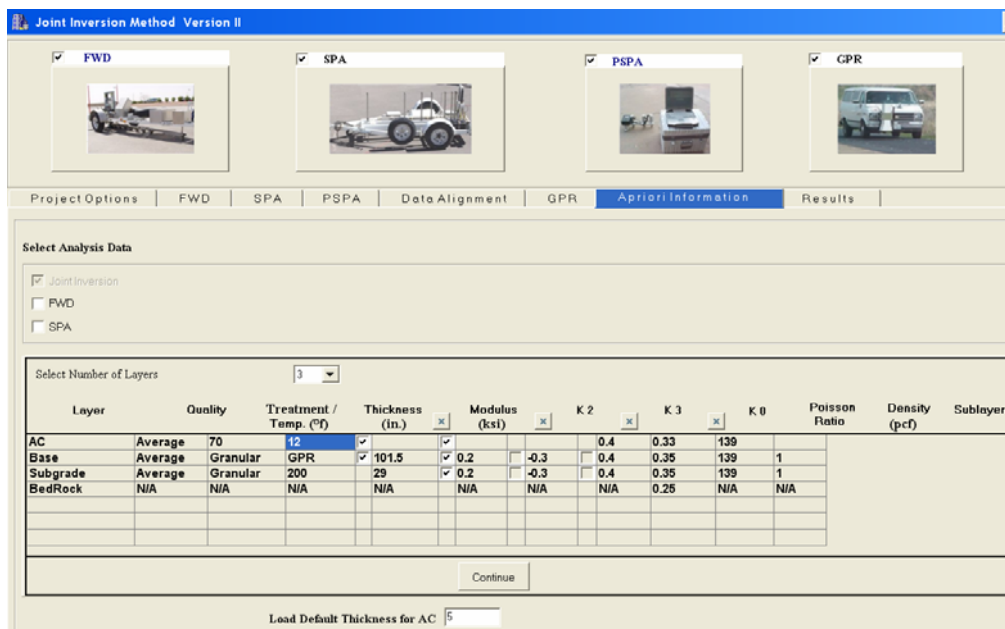
Figure 3.9 - Menu to Select Analysis Information in JIM

Results Menu

The default results window appears after the analysis is completed. The results menu provides two options to view the results: a) a profile view of the entire section analyzed and b) a station by station view. The profile section is presented first with two figures as shown in Figure 3.10. The top graph provides the results of the layer thickness in terms of depth versus station number. The "backcalculated" thickness is compared to the nominal or a priori thickness. The bottom graph shows the modulus for each station. Another option is to select the two types of layer moduli estimated based on the nonlinear analysis, namely: a) the conservative moduli and b) the average moduli. For a more detail scrutiny of the results of each station, the user can enter the station number in the edit box provided in the top of the menu, and select the adjacent button. This will switch the results menu to a station by station view. Figure 3.11 shows a snapshot of the detail results menu. The measured and backcalculated deflection bowls and/or dispersion curves are depicted in the left side of the menu. The right side of the menu contains the estimated profile and a summary table presenting the layer thickness and layer moduli. The user can easily access different stations by using the "→" and "←" button located on the top of the menu. Similar options are provided for the different moduli (conservative, average). All output files are saved under the same folder that the user creates at the beginning. The "Report.jim" file contains a summary report of the results.
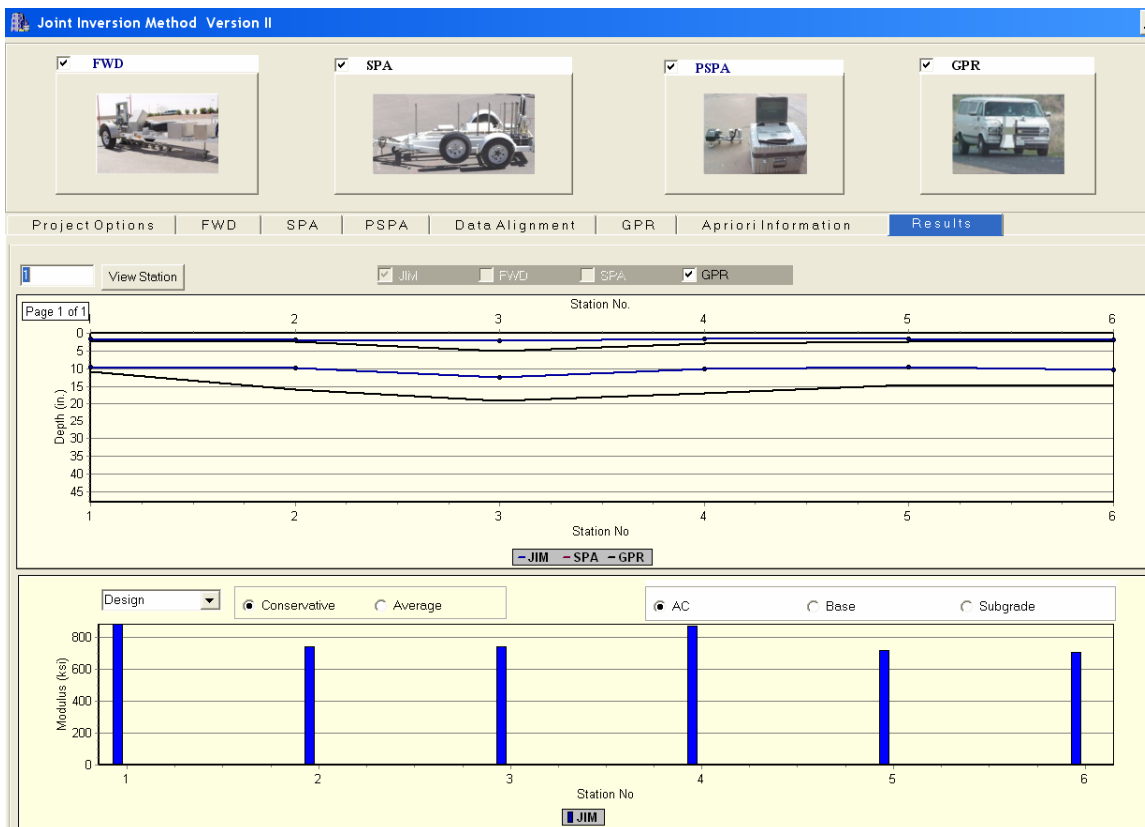
Figure 3.10 - Menu of Section Results in JIM
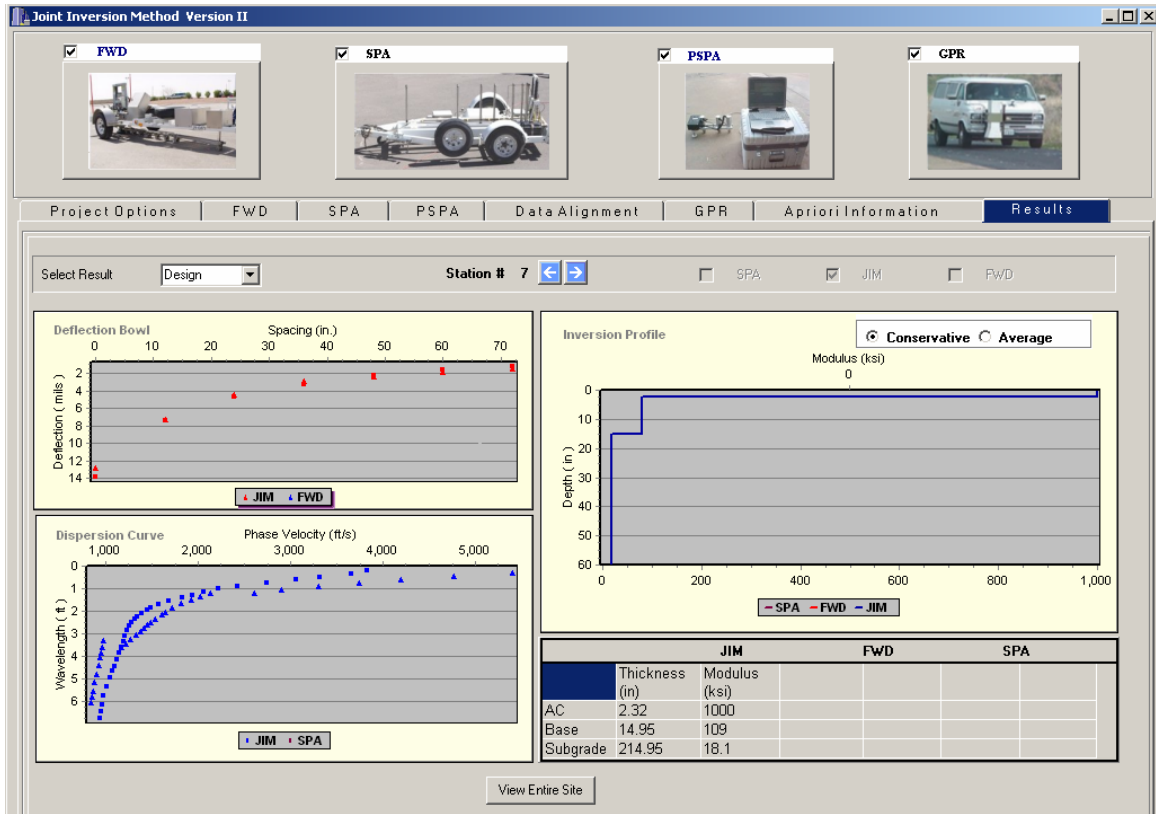
Figure 3.11 - Menu of Results of Each Station in JIM

DATA FUSION FOR INTELLIGENT NONDESTRUCTIVE EVALUATION OF FLEXIBLE PAVEMETNS (DFINE)

Main Menu

Figure 3.12 shows the start-up window or the main menu of DFINE. The main menu is divided into two main sections: a) Project Information and b) Data Preprocessing. The section on the left side provides a user with the capability to enter project information. The user is first required to select and/or create a project folder where all data is stored. Once the project information is created, the next step is to load in the project description. This type of information is either entered by the user, or if a default file was previously created, the default values are loaded. When finished, the "Next" button flashes prompting the user to proceed to the data preprocessing.

There are three stages for data preprocessing. Stage 1 allows the user to select the results files from the analysis methods that will be used in the fusion analysis. The program has been preset to load the following five types of data:

a) JIM results with file extension "*.jim",
b) SMART results with file extension "*.smart",
c) FWD results that require three file with the following extensions: "*.fwd", "*.asc", and "*.da1". The first file is the MODULUS input file and the latter two are produced by

21

MODULUS. The three files are necessary so that this program can be fully-compatible with MODULUS program.
d) GPR results with file extension "*.GPR",
e) Core results that can be input directly.
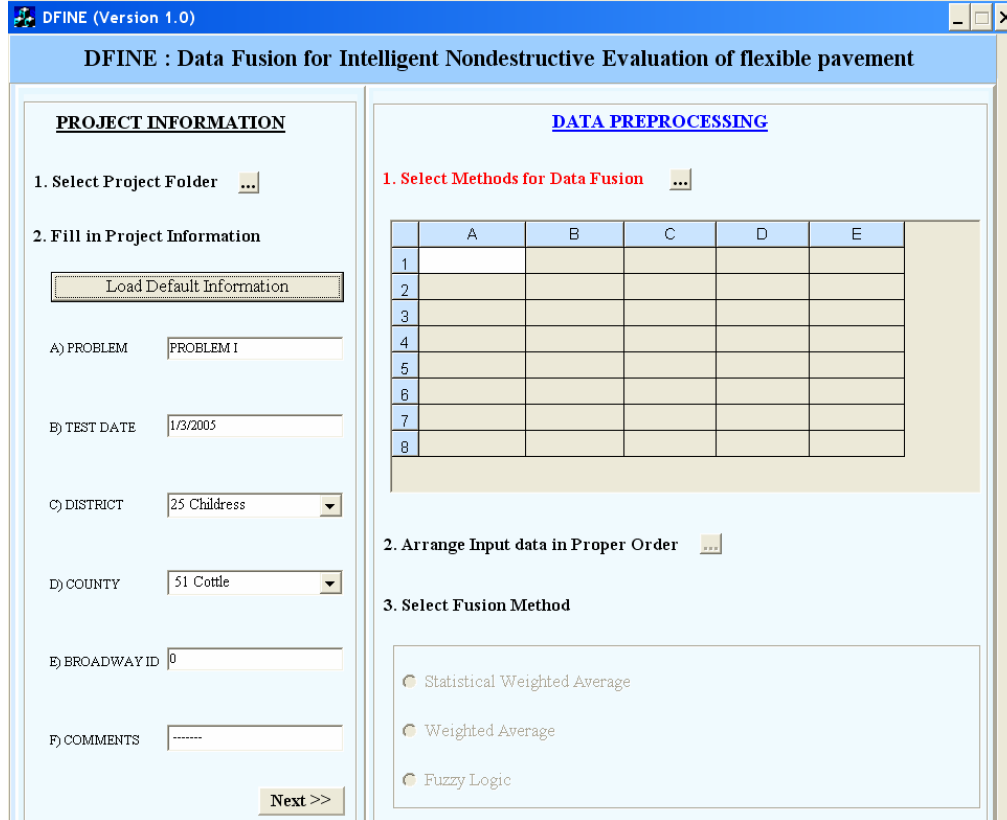
Figure 3.12 - Main Window of DFINE

Once a user selects "methods for data fusion" icon, a window prompts a user to select from eight options of data to be fused (see Figure 3.13). The methods available are:
- SMART (Conservative),
- SMART (Average),
- JIM (Conservative),
- JIM (Average),
- FWD,
- GPR and
- CORE.

SMART and JIM methods are repeated twice to provide a user the capability to select either the conservative or "minimum" moduli, or average moduli. After selecting a method, a user is prompted to enter the appropriate files. Once all the methods are chosen and the files selected, the user selects the "OK" button to continue. The files are processed and the thickness and moduli from each file are extracted. A summary of the parameters to be fused are then listed in the table of the main menu. The user can select or deselect any parameter for fusion analysis. Figure 3.14 highlights an example of the fusion parameter summary section.

22
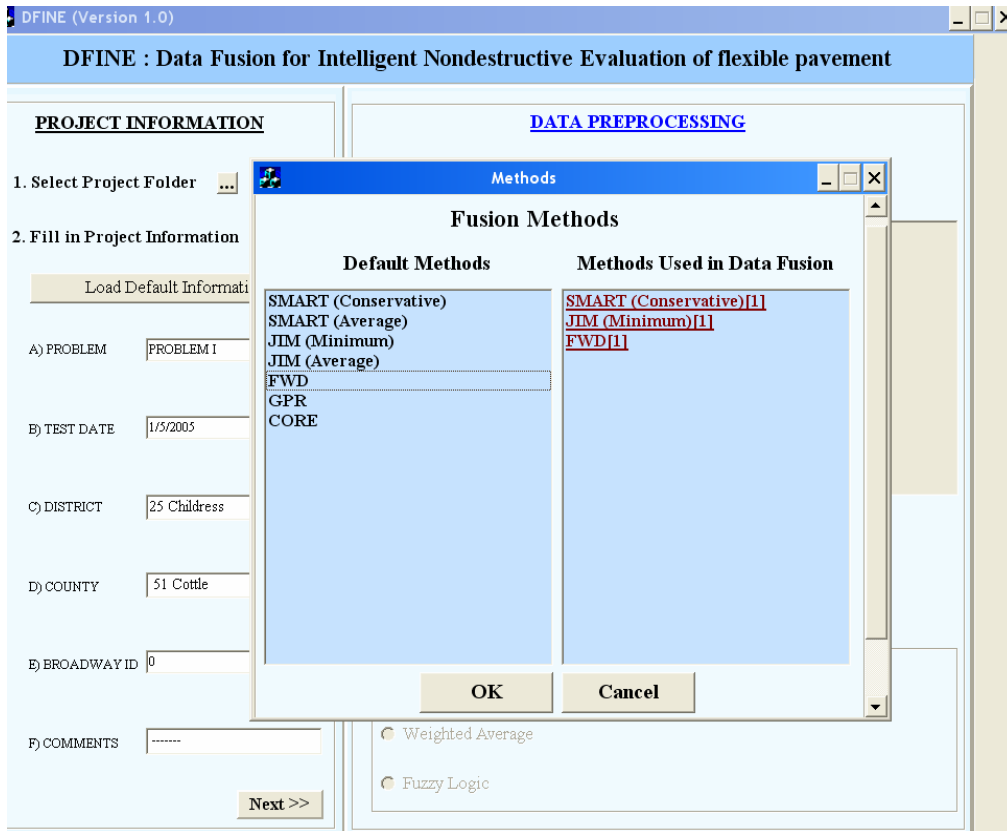
Figure 3.13 - Menu of File Selection of Fusion Methods in DFINE

Figure 3.14 - Options for Selecting Data Fusion Parameters in DFINE

Data Alignment

The second stage of data preprocessing is to align the data. After selecting the data alignment button, a tabulated data alignment window pops up as shown in Figure 3.15. The user needs to align the data using the comments to ensure that the data to be fused from different analyses are from the same stations. Data from JIM, SMART, and MODULUS are matched first. Once the data is matched, the user can enter core data where applicable. Core data can be in the form of thickness and/or the resilient or dynamic moduli from lab testing. Once this information is entered, the window can be closed.

Figure 3.15 - Menu of NDT Data Alignment in DFINE

GPR Menu

The next step is to align the GPR data. If the GPR data are available, a window appears allowing a user to harmonize the GPR data with data from other NDT analyses based on the station location. As presented in Figure 3.16, the GPR profile from the selected file is plotted. The plot shows the thickness of the ACP and base layers. The user can mark the stations either by specifying the step for each station and selecting the adjacent "Select" button, or if the tests were conducted at equal spacings, an "Add All" button can be selected to mark all stations at the specified location. At each marked location, a vertical line signifies the identification of the station. The user can select "reset" button to modify the GPR markings. The core information is identified on the graph at each location data was provided. Once the process is complete, the user proceeds to the next step by closing the GPR window. A summary of the data that is to be fused is presented next. A radio button menu on top of the summary table can be used to switch between each variable.

Results Menus

Stage 3 of the data preprocessing is to fuse the data. Three fusion options are available as shown in the bottom section of the main menu presented in Figure 3.12. The first two options are based on weighted averaging. TxDOT Report 0-4393-2 (Williams et al., 2004) presents the theory behind data fusion based on the weighted average. Figure 3.17 shows the results of the fusion based on the statistical weighted average and weighted average, respectively. The results are presented in a similar manner for both fusion methods since the only difference is the mathematics involved in fusing the data. A radio button menu on the top of the results window can be used to switch between viewing the fused results of different parameters. The results are presented with first showing a table with its respective statistics such as mean (average), standard deviation, and coefficient of variation. The table also includes additional parameters that can be modified to impact the fused data for the weighted average method (see Figure 3.17b). The bottom half of the menu contains the results in both tabular and graphical manners. The graphical representation contains a comparison of the fused results with the typical averages for each method.

24
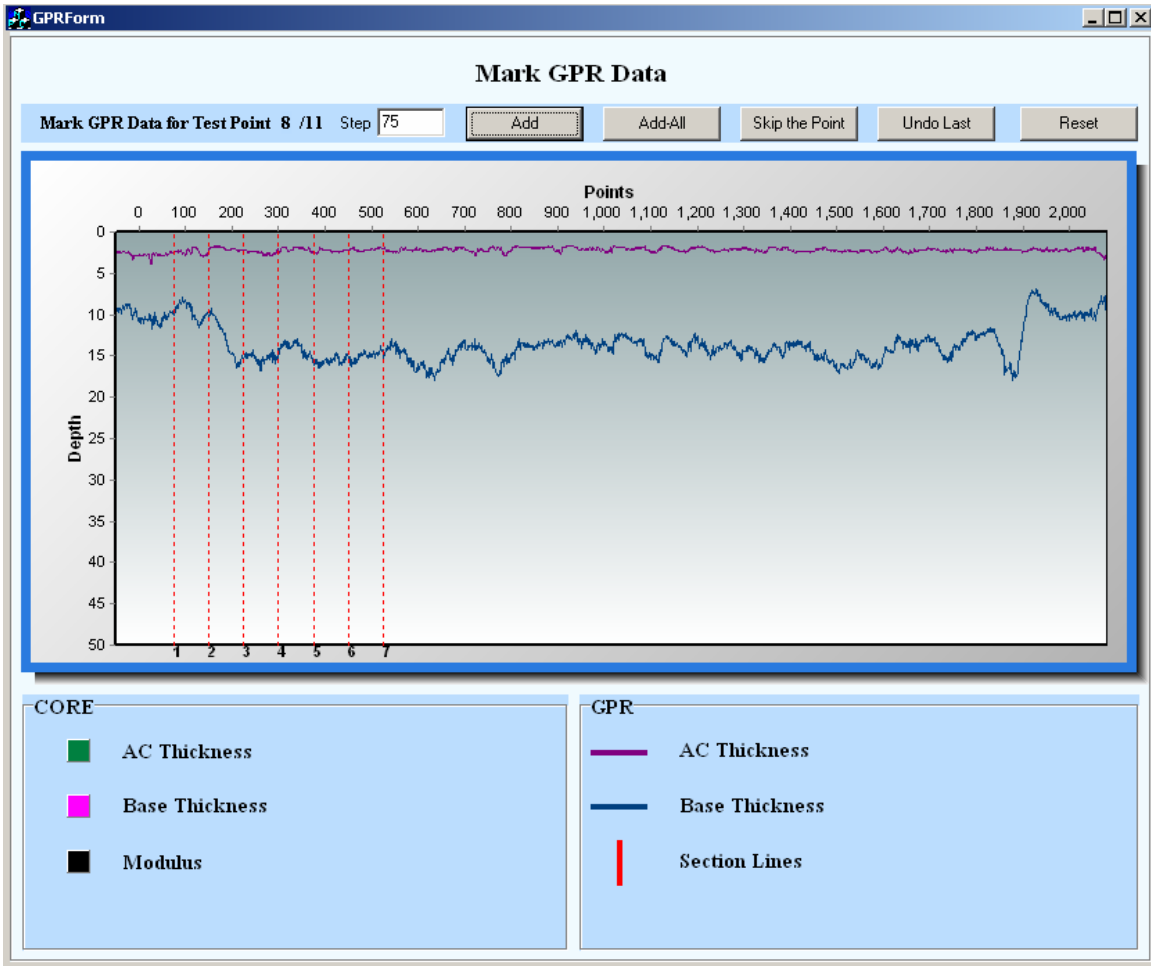
Figure 3.16 - Menu of Alignment of GPR Data in DFINE
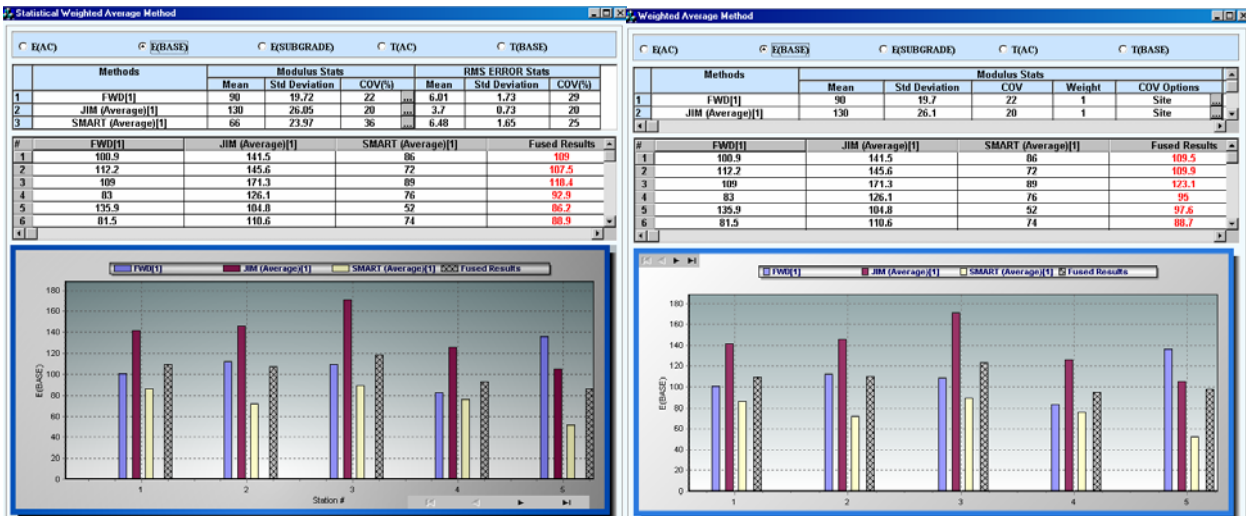
a) Statistical Weighted Average   b) Weighted Average

Figure 3.17 - Menu of Statistical Weighted Average and Weighted Average in DFINE

The third fusion method is based on the fuzzy logic method. The fuzzy logic method, which is a tool that captures human ambiguity, is based on fuzzy sets formed by defining rules and decisions based on those rules. Figure 3.18 shows the results of DFINE using fuzzy logic. The top part contains the fuzzy logic membership functions and the fuzzy rules used. The two fuzzy logic membership functions in DFINE are based on the standard deviation of the data and the Backcalculation RMS error based on the results of the NDT analysis tools. Each membership function is predefined with default values. To modify the membership function, the user can double-click on the graph. Figure 3.19 shows and example of that. The fuzzy sets have several shapes as detailed in Report 0-4393-2 (Williams et al., 2004). Membership function in DFINE varies from three to seven fuzzy sets. A default of five fuzzy sets ranging from very low, to low, to average, to high, to very high, is included in the software. The shape of each set is based on four values or limits which are defined depending on the type of membership function. Fuzzy rules are used to connect the fuzzy sets or membership functions.
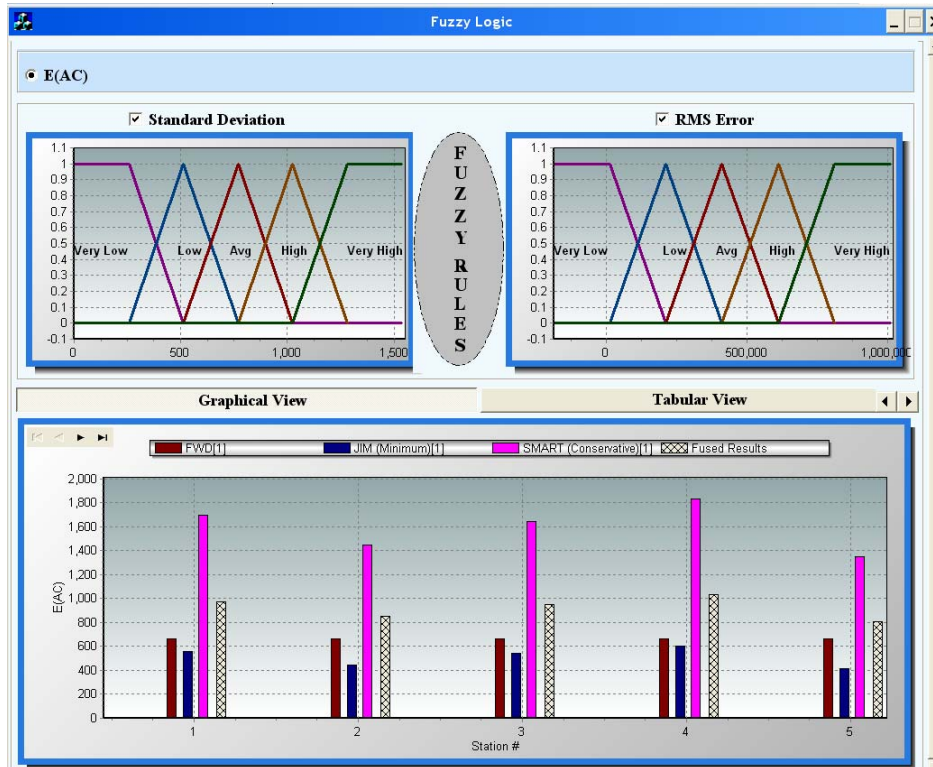
Figure 3.18 - Menu of Data Fusion Based on Fuzzy Logic in DFINE

Fuzzy rules are basic mathematical functions that determine the weights for fusing the data. To access the fuzzy rules, a single-click on the oval between the membership functions labeled fuzzy rules is necessary. The fuzzy rules menu or "rules editor" is shown in Figure 3.20. The rules editor provides the user a means to adjust the set of default rules. The rules are specified on the top of the window and the functions to add, change, and delete a rule is located at the bottom of the window. Once the rule changes are finalized, the user can save the changes and close the window. This updates the results in the fuzzy logic results menu. Referring back to Figure 3.19, the bottom section of the fuzzy logic results menu contains the fused results as well as the results from each analysis method both in graphical and tabular formats.
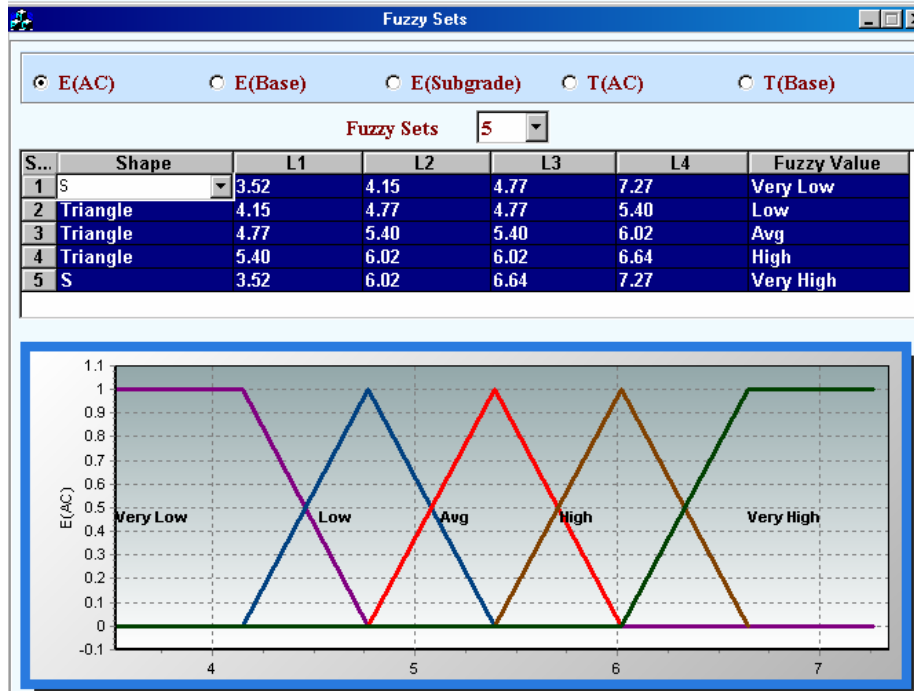
Figure 3.19 - Menu of Defining Fuzzy Sets for Membership Functions in DFINE
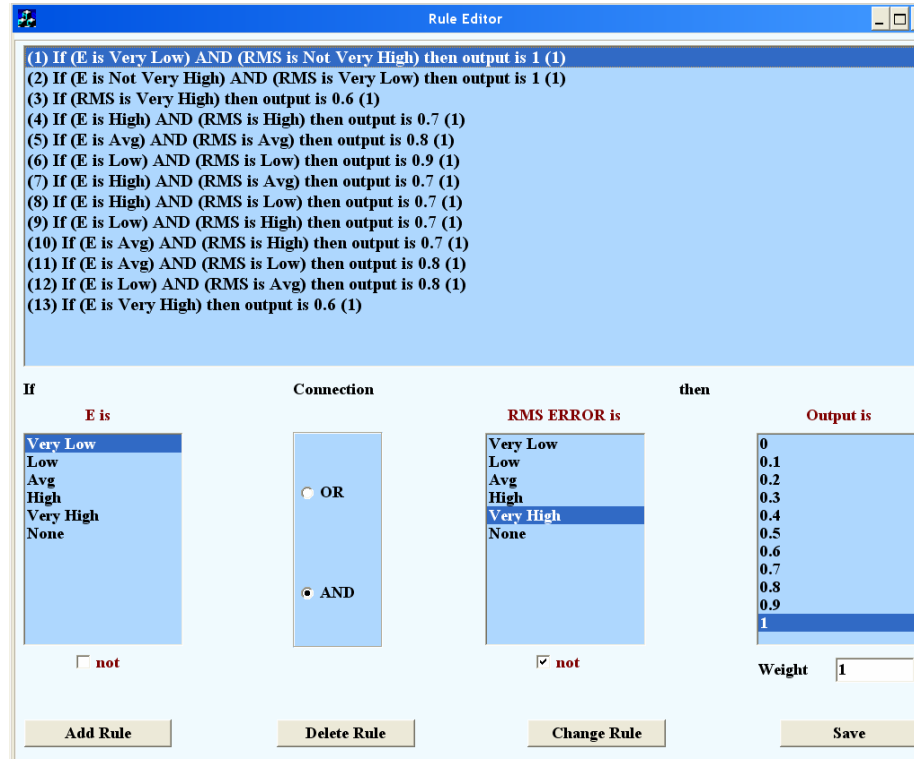
Figure 3.20 - Menu of Fuzzy Logic Rule Editor in DFINE

Further details on using JIM and DFINE is provided in the Help Guide provided with each program.

CHAPTER FOUR

SITE DESCRIPTION

INTRODUCTION

Once the algorithms and programs were developed, the next step was to visit several site across Texas to demonstrate the feasibility of JIM and DFINE. A description of each site followed by the types of data collected is presented in this chapter.

LOCATION OF SITES

Figure 4.1 shows the site locations and Table 4.1 provides the detail information about the pavement structure at each section tested. The selected sites were located in the different districts across Texas.

Figure 4.1 - Location of Sites for Data Collection

Table 4.1- Pavement Structure Sites and NDT Devices Used.

District	Site Location	Layer Thickness (in.)		Section Tested	NDT Devices
		ACP	Base		
Amarillo	FM 1062	4	10	Five Sections	FWD, SPA, PSPA, and GPR
El Paso	TxDOT Parking Lot	2.0	6.0	One Section (repeated 6-times)	FWD & SPA
Bryan	Rut Ride section (TTI Annex)	2	8.0/14.0	Three Sections	FWD, SPA, PSPA, and GPR
Laredo	Eagle Pass	2.0	12.0	Two Sections	FWD & SPA
Odessa	IH I-20 (Ward)	5.0	18.0	Four Sections	FWD & SPA
	IH I-20 (Ector)	3.5	22.0	Four Sections	FWD & SPA
Lubbock	US380	2.0	10.0	Four Sections	FWD & SPA
Austin	APT Site*	2	8	Four Sections	FWD, SPA & PSPA

* - The APT Site in Austin was visited twice (December 2003, September 2004)

FM-1062 (Amarillo): The Amarillo site, which was located on FM 1062, consisted of nominally, 4 in. of ACP placed in two layers, over 10 in. of base, over subgrade. Five different base types were used at this site. The basic constituent of all base types was a local flexible base material normally used by Amarillo District. However, most sections were stabilized by different stabilizers. These materials and corresponding station numbers are included in Table 4.2.

Table 4.2 - Section Information for the FM1062 Site

Section	Stabilizing Agent	Station No.
1	3% Roadbond	215 to 230
2	2% Cement Kiln Dust (CKD)	230 to 245
3	8% Fly Ash (Type C)	245 to 260
4	3% Lime	260 to 275
5	Control (None)*	275 to 289+50

* A layer of Geogrid was used

TxDOT Parking Lot (El Paso): The first site tested was a parking lot located in El Paso District. At this site, extensive data was collected to assess the repeatability of the devices and algorithms. Examples of field testing efforts at the site are shown in Figure 4.2. The pavement was a thin three layer system consisting of 2 in. of asphalt-concrete pavement (ACP) layer over 6 in. of a granular base layer. The section was 300 ft in length divided up into twenty test points at 15 ft intervals. This site was tested using the FWD and SPA, since the PSPA and GPR were not available at the time. As presented in Table 4.1, this pavement section was tested six times to assess the repeatability of the devices and algorithms. The results from the repeatability of the devices were reported in Research Report 0-4393-1, Abdallah et al. (2003). Also included in the first report were the results from JIM for the first set of data collected. The results of all six repeats for this section are included in this report.

Figure 4.2 - FWD and SPA Devices in Operation at TxDOT Parking Lot (El Paso)

TTI Annex Rut Ride section - (Bryan): The TTI Rut-Ride section located at the TTI Riverside Annex was another ideal site. Since there was no need for traffic control, multiple data sets using the various NDT devices were gathered. Figure 4.3 provides an illustration of the pavement cross-section. The site was made up of three pavement sections. The first and last sections were constructed with a 6 in. flexible base over 8 in. of lime-treated subgrade (subbase) and the middle section contained a 14 in. thick flexible base. The ACP layer throughout the site had a thickness of 2 in. The first and last sections were analyzed as a four-layer pavement system and the middle section as a three-layer system. The site was 2,000 ft long, pre-marked at 50-ft intervals. The site was divided into twenty-five testing points as indicated in Figure 4.3. The first five points were tested at 50 ft increments to cover the first section. The next sixteen points were tested at 100 ft increments to cover the second pavement section (section with 14 in. flexible base). The last section was tested with four points collected at 50 ft spacing. Figure 4.4 shows the FWD, SPA, and GPR operating at the test site. This site was also tested with the PSPA. The repeatability of the GPR and PSPA was assessed at this test section and reported in Report 0-4393-1 (Abdallah et al., 2003). The results of the analysis are presented in this report.
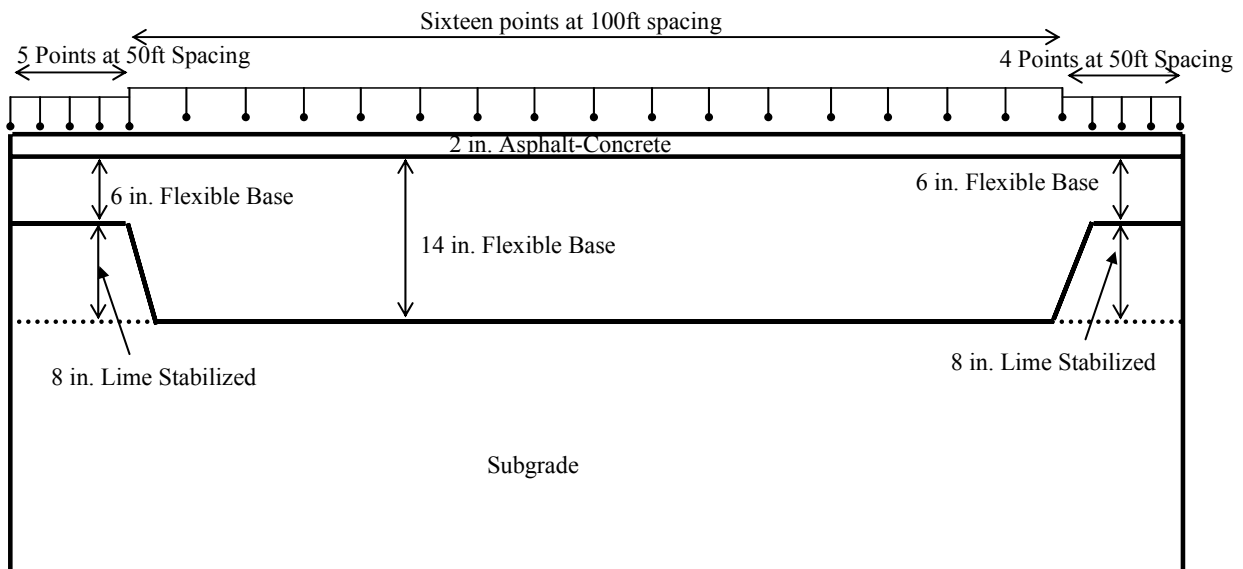
Figure 4.3 - Schematic of the Test Setup and Test Section at the TTI Test Site

Figure 4.4 - FWD, SPA, and GPR Data at the TTI Test Site

Eagle Pass Inspection Facility (Laredo): At this site, the FWD and SPA data were collected and provided by TxDOT. The pavement section at this site composed of three layers with a 2 in. poor quality ACP layer over a 12 in. thick lime-treated base over subgrade.

IH - I20 (Odessa, Ward): The FWD and SPA data were collected at 0.1 mile intervals over five pavement sections located between Mile Posts 48 to 65 on westbound right lane. Table 4.3 contains the section information. The pavement sections composed of three layers with a 5 in. thick ACP, over 18 in. of base, over subgrade.

Table 4.3 - Section Information for IH-I20 Westbound Right Lane of Ward County

Section	Nominal Thickness, in.		Section Extent, miles	
	ACP	**Base**	**Beginning**	**Ending**
1			0.5	1.5
2			1.8	2.8
3	5.0	18.0	4.7	5.7
4			11.3	12.3
5			15.3	16.3

IH - I20 (Odessa, Ector): Similar to the other Odessa site, the FWD and SPA data were collected at 0.1-mile intervals over four sections near Pecos, TX, three sections in the eastbound lane and one in the westbound lane. The pavement sections consisted of 3.5 in. of ACP layer, over 22 in. of granular base, over subgrade. This site was tested as part of a forensic study to determine the causes of early pavement failure at this site. Figure 4.5 shows a series of photos taken during the data collection process.

a) Distress of AC Layer   b) Coring Activity

c) Asphalt Core Sample   d) Asphalt Debonding
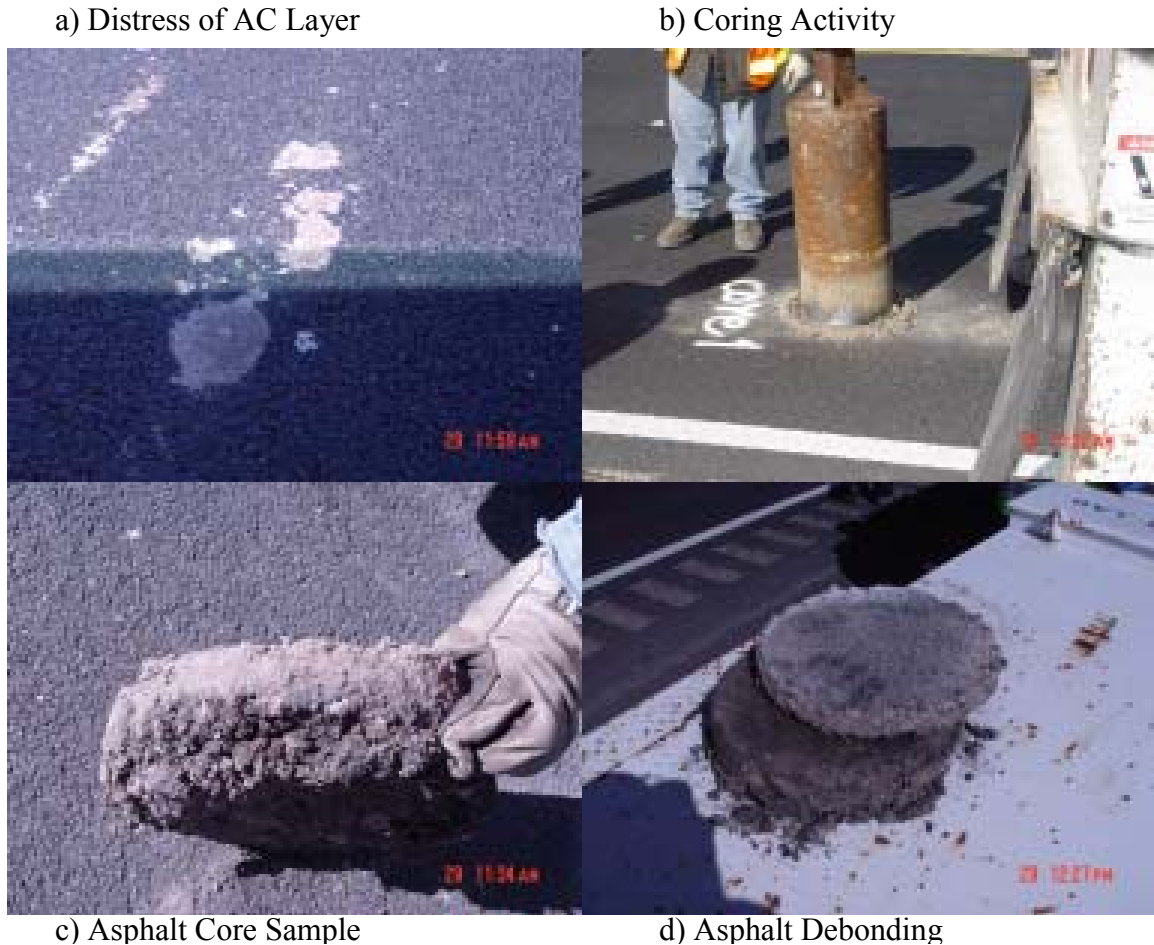
Figure 4.5 - Photos of the Odessa Section Indicating Structural Distress

US380 (Lubbock): Four sections of the US 380, located in Lubbock were tested with the FWD and SPA. The pavement sections consisted of 2 in. of ACP, over 10 in. of cemented-treated base over subgrade.

APT Site (Austin): The accelerated pavement test (APT) site provided an ideal site to collect data for illustrating the applicability of JIM and DFINE. This was a well-controlled pavement section located at the J.J. Pickle Research Campus of the University of Texas and required no traffic control. Data were collected with the FWD, SPA and PSPA. The pavement section was composed of 2 in. of ACP over 8 in. of base over a clayey subgrade. Three different base materials were used at this site. Figure 4.6 shows a view of the APT pavement section. The site is divided into 4 main lanes and two shoulders each close to 330 ft in length. This site was visited twice, once in December of 2003 and once in September of 2004. The labeling scheme used in both visits is indicated in Figure 4.6. Figure 4.7a and 4.7b show the NDT devices during data collection. Figure 4.7c shows the Texas Mobile Load Simulator (MLS) device that is used for the accelerated pavement testing at this site. Figure 4.7d is the location of the grid or pad for the MLS testing section. The grid was tested in December of 2003 (MLS was not on the test pad at that time). However, on the second visit, the MLS was mobilized at the test pad, and therefore, no data was collected at that location.
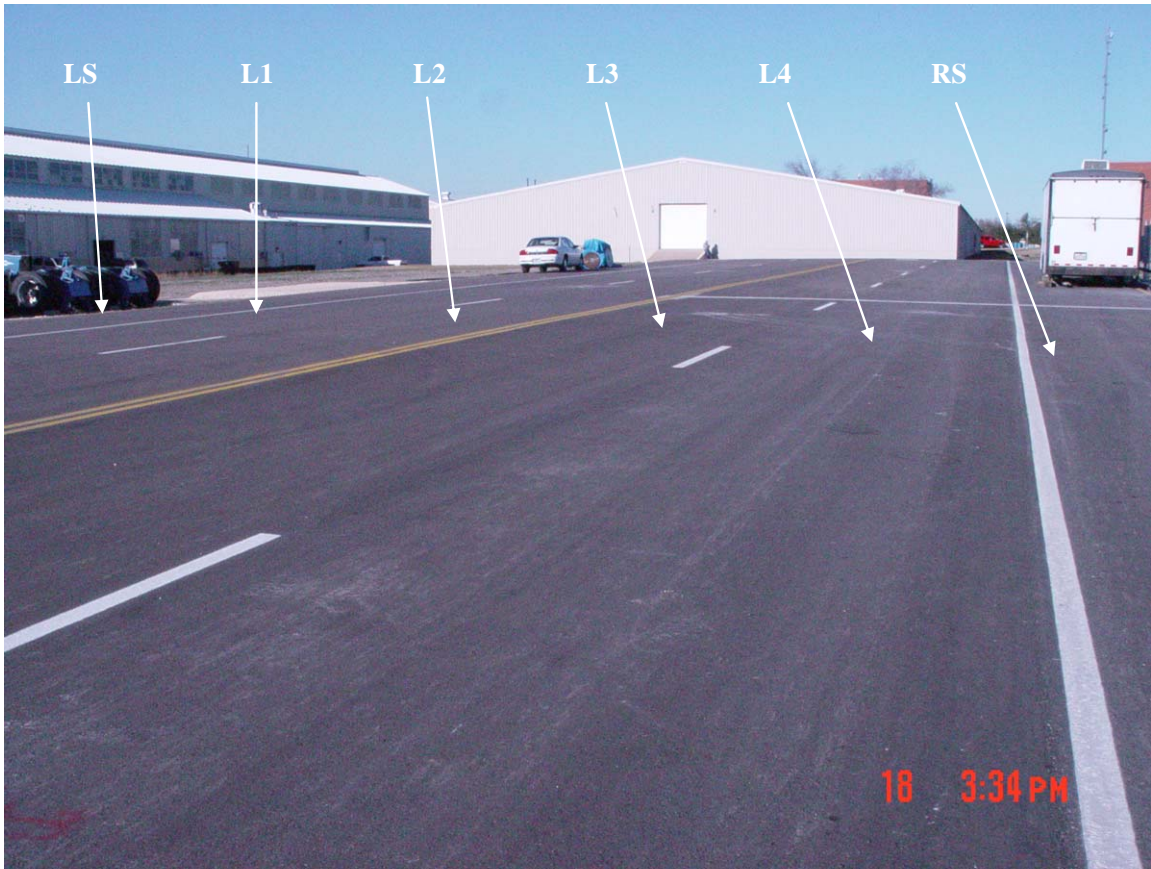
Figure 4.6 - Picture of the APT Test Section

a) SPA at APT site

b) PSPA at APT Site

c) MLS Device

d) MLS Test Pad

Figure 4.7 - Pictures of the NDT Devices and MLS Pad at APT Site

CHAPTER FIVE

TESTING PROCEDURES AND DATA REDUCTION

INTRODUCTION

A detailed description of the analysis and testing procedures used to process and reduce the data is presented next. One of the test sites is used as an example to illustrate the process.

DATA ANALYSIS DATA REDUCTION

In any algorithm development process, the ultimate goal is to test the results from the proposed methodology and determine its feasibility and accuracy. In this project, both JIM and DFINE needed to be tested by applying them to field data from several sites. In addition to comparing the results from these algorithms with existing analysis techniques, one of the original goals of this project was to validate the results with a well calibrated test site.

Figure 5.1 illustrates the process followed to perform the analyses. To obtain all the necessary information, the following main tasks had to be carried out:

1. Field Testing
2. Lab Testing
3. Data Analysis
4. Interpretation of Results

The first task was field testing, which consisted of collecting at a minimum: a) seismic data with the SPA and b) deflection data with the FWD. Optional NDT methods that could be used to collect data were PSPA and GPR. The second task was to perform laboratory tests, ranging from measurements on cores (modulus and thickness), to dynamic modulus tests to obtain the ACP modulus, to resilient modulus tests on base and subgrade to obtain modulus and nonlinear parameters. Under normal circumstances for Task 3, the analysis performed would be based on JIM. However, since the intent was to compare the results of JIM with other NDT analysis tools, SMART and MODULUS software packages were also used to analyze the data.

```
    ┌─────────────────┐         ┌─────────────────┐
    │          (1)    │────────▶│          (2)    │
    │  Field Testing  │         │   Lab Testing   │
    └─────────────────┘         └─────────────────┘
             │                           │
             │        ┌─────────────────┐│
             │        │          (3)    │◀┘
             │        │  Data Analysis  │
             │        └─────────────────┘
             │                 │
    ┌─────────────────┐        │
    │          (4)    │◀───────┘
    │  Interpretation │
    │    of Results   │
    └─────────────────┘
```
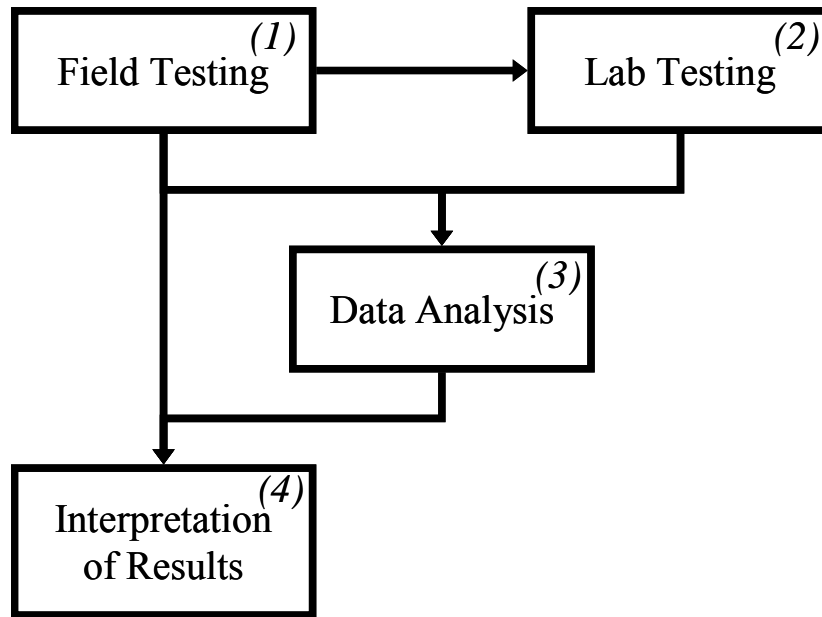
Figure 5.1 - Flowchart of Validation Process

SMART (Abdallah et al., 2002) uses seismic data along with nonlinear parameters of base and subgrade as inputs to determine layer moduli. MODULUS (Uzan et al., 1988) in turn uses FWD deflection as input to estimate layer moduli. PSPA and GPR analyses were performed if those devices were used in data collection process. As part of Task 3, the results from all the analyses were fused using DFINE. The final step in the process (Task 4) consisted of comparing the analyses results and identifying the limitations and advantages of JIM and DFINE. To illustrate the entire process, the procedure and results will be presented and discussed in detail for the rut-ride site at the TTI Annex.

The importance of following a data collection protocol to enable data synchronization during data integration was emphasized in Research Report 0-4393-1. Both the FWD and SPA data collection programs allowed for operators to input comments for each station. The synchronization was carried out by matching the comments input during data collection. To facilitate the synchronization, the following steps were followed when possible.

Pre-test: The NDT integration tools require at least two testing devices, namely FWD and SPA. Coordination on the following issues needed to be carried out:

a) Station referencing - The referencing system for every project was different. With the FWD, the operator used a distance measuring instrument (DMI) to mark the test locations. Once the FWD test was complete, the operator marked the location and labeled each test point. The station label was provided in the comments. The remaining NDT devices followed the FWD.

   A better practice would be to mark and label each station, before the tests begin. Marking and labeling each test point first, ensures the test operation is systematic and allows for the

devices to be independent of one another. This procedure seems to be the most effective in the field.

b) Order of devices - Several equipment-arrangements were tried. However, there was not one arrangement that seemed the most favorable. The coordination was more important than the order of devices. All devices require similar test time of approximately less than one minute. The only suggestion regarding the testing order of the devices is to have the PSPA accompany either the SPA or FWD. The portability of the PSPA allows the FWD or SPA operator to perform the PSPA test simultaneously.

Two items that are crucial during the testing process are proper commenting and temperature measurement.

a) Comments - The comments are the key factor for synchronizing the data during data analyses. The testing team needs to agree on a labeling system to be included in the comments field of each device. This makes it easier to utilize the module in JIM and or DFINE. For example, one of the devices broke down at one site and the tests were performed out of order. But since the comments were thorough, it was easy to align data from this device with the other devices. In another case, the equipment operated effectively, but on several occasions one of the NDT operators repeated the test at one or more points. At this site the operators did not provide complete comments. The data alignment process was very tedious.

b) Temperature measurements - The temperature measurements protocols seem to vary at each site. For instance, temperature measurements were sometimes performed at the beginning and end of the project. In another case, temperature measurements were performed sporadically. And yet, in another instance, temperature measurement was carried out for every point. The operator's experience and weather conditions dictate the frequency of temperature measurements. Temperature correction is very important for the ACP layer, and frequently ignored during data reduction or not included if it is not easily accessed.

Post-test: The main function after the testing is complete is to have the data from all tests in one folder. The operators need to coordinate the data transfer and provide the data to the person whose task is to perform the data reduction in a timely manner.

The steps above proved very useful for the data collection team for the later test sections. This information should be provided to the operators before visiting the test site if multiple NDT devices are to be used.

Field Testing

As described in Chapter 4, the rut-ride section located at the TTI annex was one of the first sites tested under this project. The data collection process consisted of conducting nondestructive tests with the GPR, FWD, SPA and PSPA. This site was pre-marked at 50 ft increments starting at station number -200 to 1800 (see Figure 5.2). As discussed previously, the pavement contained three sections. Five points were tested from Section 1, 16 points from Section 2, and 4 points from Section 3, for a total of twenty five stations. The pre-marking of the site, allowed for
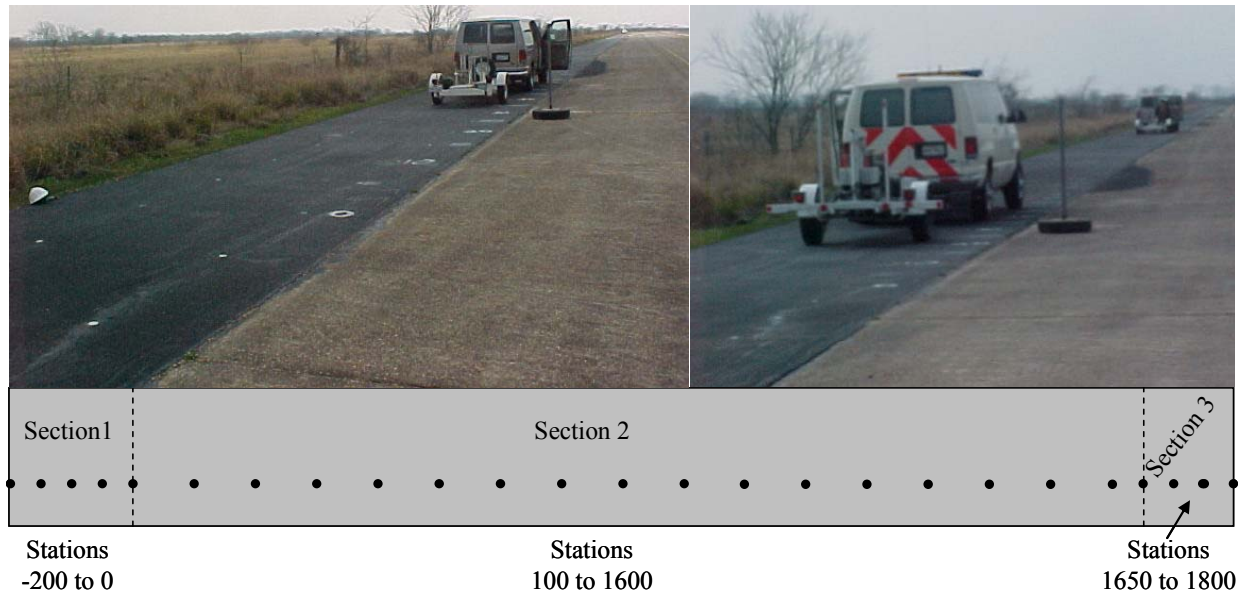
Figure 5.2 - Rut Ride Section at TTI Annex

the operators to be consistent in the station labeling. Temperature measurements were also the operators to be consistent in the station labeling. Temperature measurements were also included in the comments. No trenching or coring was performed at this site; therefore, laboratory testing was not performed.

Data Analysis

The procedure used to analyze the data can be summarized in the following steps:

> Step 1: Use the SASW software to determine the ideal dispersion curve from the SPA test data.
> Step 2: Use the SASW software to determine the seismic modulus profile using the ideal dispersion curve from Step 1.
> Step 3: Use SMART with the results of Step 2 to determine design modulus profile.
> Step 4: Use MODULUS with the FWD deflections to determine modulus profile.
> Step 5: Use JIM with the ideal dispersion curve and the measured deflections to determine the pavement modulus and thickness profile.
> Step 6: Retrieve GPR data from COLORMAP and extract discrete thickness for each test location.
> Step 7: Reduce PSPA data to determine the modulus of ACP.
> Step 8: Use results from MODULUS, SMART, and JIM in DFINE.

The results of the data analysis processes are discussed next.

SPA-SASW Analysis: The reduction of the SASW data is a two-step process (Nazarian et al., 1995). The first step consists of constructing an idealized dispersion curve, variation in phase velocity with wavelength. Once a dispersion curve is determined, an inversion (backcalculation)

38

algorithm is used to estimate the shear wave velocity profile of the pavement section (Step 2 of the data analysis process). The shear wave velocity can be readily converted to seismic modulus. This reduction scheme is performed for each test point.

The results from Step 1 of the data analysis process for this test site are presented in Figure 5.3. The figure shows the idealized dispersion curves for the three sections outlined in Figure 5.2. Also plotted is the average dispersion curve of each section. As the results in the figure indicate the variability is reasonable. The results of all 25 points tested show that the curves are reasonably similar at short wavelengths. For few stations in Figures 5.3a and 5.3b, the dispersion curves did not follow the trend especially at the long and intermediate wavelengths. This provides a preliminary indication that the ACP layer is more uniform across the section as compared to the base layer and subgrade layers.
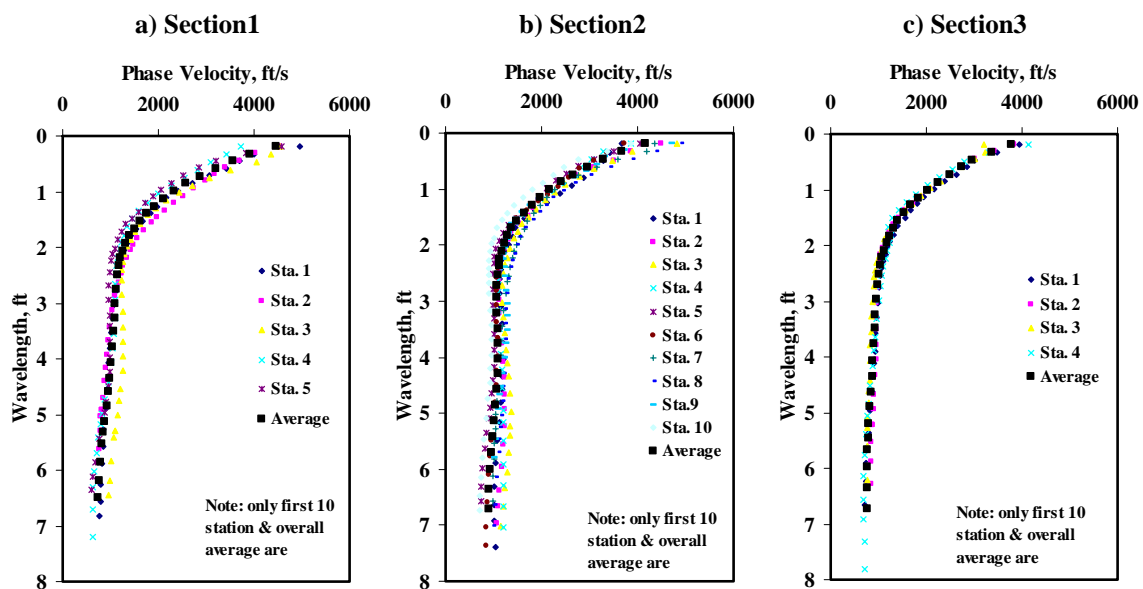
Figure 5.3 - Idealized Dispersion Curve for the Rut Ride Section at TTI Annex

Once the dispersion curve is constructed, several inversion scenarios can be used. Typically, the inversion process is performed to estimate the modulus of each layer only. However, if the thickness is not well known, both the thickness and modulus can be estimated. For this case study, the inversion process was performed two times. The first was based on the assumption that the layer thicknesses were known and only the seismic layer moduli were estimated. The second case was to estimate both the thickness and the seismic modulus of each layer. To compare the two cases, the dispersion curve and seismic modulus profile for the three sections are presented in Figure 5.4. Figures 5.4a, 5.4c, and 5.4e depict the measured dispersion curves plotted against the two calculated dispersion curves when only layer moduli were calculated and when both layer thickness and layer moduli were calculated. The calculated dispersion curves were generated using the seismic modulus profile depicted in Figures 5.4b, 5.4d and 5.4f. The experimental and calculated dispersion curves compare favorably in both cases for all three sections. The RMS errors provided in the pavement profiles show the closeness of the fit between the measured and calculated dispersion curves. The RMS error ranges from 6% to 8% for this site.
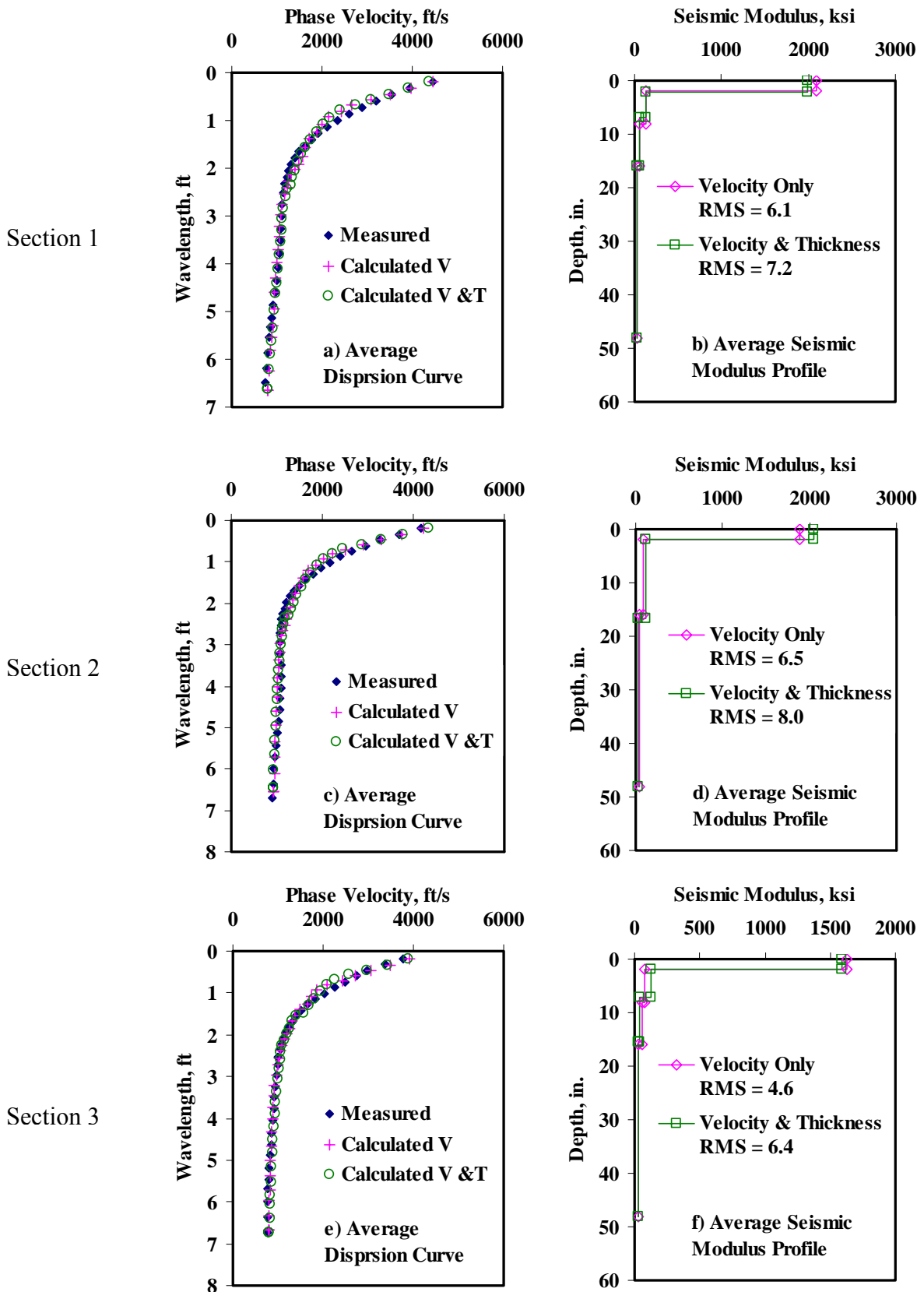
Figure 5.4 - Typical Results of SASW Data Reduction Processes

Table 5.1 and 5.2 summarize the results for all test points at this site for the two inversion processes. The average, standard deviation and coefficient of variation (COV) are included in each table. The COVs are similar for both cases. In general the ACP and subgrade layers demonstrate less variability than the base layer for both cases. The seismic moduli were then used in SMART to estimate the design moduli of each layer.

Table 5.1 - Results of SASW Analysis for Estimating Seismic Moduli at Rut Ride Section
a) Section 1

Station No.	Modulus, ksi				RMS Error, %
	ACP	Base	Subbase	SG	
1	2121	101	61	28	4.5
2	2424	206	38	27	5.5
3	2429	159	80	33	5.9
4	1641	128	50	27	7.8
5	1823	87	50	27	6.8
Average	2088	136	56	29	6.1
Std Dev	354	48	16	2.6	-
COV	17%	35%	28%	9%	-

b) Section 2

Station No.	Modulus, ksi			RMS Error, %
	ACP	Base	Subgrade	
6	1854	117	44	6.9
7	2127	101	44	7.4
8	2271	122	44	8.3
9	1678	105	44	8.0
10	1679	76	36	7.1
11	1677	105	36	5.9
12	2103	133	30	3.2
13	2425	144	34	4.2
14	2039	101	44	6.4
15	1496	53	42	6.3
16	1611	44	36	6.0
17	1884	126	36	10.3
18	1946	53	44	6.7
19	1683	51	41	4.9
20	1918	87	44	5.9
21	1826	92	36	6.3
Average	1889	94	40	6.5
Std Dev	255	31	4.7	-
COV	14%	33%	12%	-

c) Section 3

Station No.	Modulus, ksi				RMS Error, %
	ACP	Base	Subbase	SG	
22	1796	72	36	30	7.1
23	1707	107	44	41	3.1
24	1435	61	79	27	4.0
25	1586	78	57	27	4.0
Average	1631	80	54	31	4.6
Std Dev	156	20	19	6.7	-
COV	10%	25%	35%	21%	-

Table 5.2 - Results of SASW Analysis for Estimating Seismic Moduli and Thicknesses at Rut Ride Section

a) Section 1

Station No.	Thickness, in.			Modulus, ksi				RMS Error,%
	ACP	Base	Subbase	ACP	Base	Subbase	SG	
1	2.2	5.5	8.6	2040	112	57	29	4.3
2	2.2	4.8	7.4	1946	144	71	34	9.7
3	2.2	4.8	9.6	2171	135	72	24	7.7
4	2.0	4.8	9.6	1677	144	69	24	8.2
5	1.8	4.8	9.6	2093	138	55	24	6.3
Average	2.1	4.9	9.0	1985	135	65	27	7.2
Std Dev	0.2	0.3	1.0	191	13	8	4.3	-
COV	9%	6%	11%	10%	10%	13%	16%	-

b) Section 2

Station No.	Thickness, in.		Modulus, ksi			RMS Error, %
	ACP	Base	ACP	Base	Subgrade	
6	2.1	15.4	1651	116	27	8.0
7	1.9	15.4	2396	109	27	9.6
8	1.8	15.4	2587	130	27	10.5
9	2.2	15.4	1568	72	33	12.7
10	1.8	15.4	1952	101	27	8.0
11	2.1	15.4	1660	109	27	5.9
12	2.2	12.9	2052	134	30	2.9
13	2.0	16.7	2477	150	24	4.1
14	1.8	15.4	2604	154	27	6.2
15	1.8	13.7	1833	73	27	6.8
16	1.8	12.6	1824	74	27	7.9
17	1.8	12.6	1933	245	27	16.1
18	2.2	15.4	1669	49	33	8.0
19	1.8	15.4	2052	62	27	5.1
20	1.8	15.4	2169	105	27	6.4
21	1.8	12.6	2341	163	27	10.3
Average	1.9	14.7	2048	115	30	8.0
Std Dev	0.2	1.3	347	49	2.4	-
COV	9%	9%	17%	42%	8%	-

c) Section 3

Station No.	Thickness, in.			Modulus, ksi				RMS Error, %
	ACP	Base	Subbase	ACP	Base	Subbase	SG	
22	1.9	5.4	7.2	1575	120	33	28	9.4
23	2.1	5.6	10.4	1600	123	45	38	3.3
24	2.2	4.8	9.4	1157	131	43	30	7.2
25	1.8	4.8	6.4	2044	144	35	24	5.5
Average	2.0	5.2	8.4	1594	130	39	29	6.4
Std Dev	0.2	0.4	1.9	362	11	6	6.3	-
COV	9%	8%	22%	23%	8%	15%	22%	-

As for the case where the layer thicknesses were estimated, the thickness of the ACP layer was close to the nominal thickness of 2 in. For Section 1 and Section 3, with a four-layer system pavement, a base thickness of approximately 5 in. was estimated (as compared to the nominal thickness of 6 in.) and a subbase thickness of 8 in. to 9 in. (as compared to the nominal thickness of 8 in.). The base thickness of Section 2 was also close to the nominal thickness of 14 in. The thickness from the SASW program will later be compared to those of JIM and GPR.

SMART Analysis: SMART was used to estimate the design moduli using seismic moduli. Seismic moduli from the SASW analysis and the nonlinear parameters for the base and subgrade layer were used as input to calculate the variation in design modulus within each pavement layer. Ideally, the nonlinear parameters for the base and subgrade should be determined from lab testing. In the absence of that, the default values for k_2 and k_3 obtained from similar materials in the area were used. Since SMART (Ke el al., 2002) is based on a nonlinear algorithm, two sets of design moduli (i.e., conservative and average) were reported for the base and subgrade. The conservative values correspond to the minimum modulus determined for each layer whereas the average values correspond to the weighted average of the moduli within the layer. SMART also provides the surface deflections at the FWD sensor locations based on the design moduli as described in Ke et al. (2002). These deflections can be compared with the FWD deflections measured at the same points as an independent check of the validity of the results from SMART.

The conservative and average moduli for the entire site are presented in Table 5.3. Also included in the table are the RMS errors calculated between the deflections measured with the FWD and those estimated by SMART. The deflections calculated using the moduli from SMART exhibit an average RMS error close to 6% across the site. The COVs of the layer moduli were less than 20% for the ACP and subgrade indicating a reasonable consistency across the site. The base exhibited a COV close to 30% to 35%. A point by point comparison with other methods will be presented later in the chapter.

FWD Analysis: The backcalculation program MODULUS was used to estimate the moduli of the layers using the deflections measured with the FWD. The FWD deflections measured at this site are presented in Table 5.4. The COVs for the deflections are less than 15% for Sections 1 and 2, and less than 33% for Section 3. The deflections from the second drop height (load close to 9000 lbs) were used in the analysis. The reported FWD deflections were normalized to 9000 lbs using the following equation:

$$d_i^{Normalized} = d_i\left(\frac{9000}{Load_{Actual}}\right) \quad i = 0 \, to \, 6 \tag{5.2}$$

where d_i is the measured deflection at sensor i and $Load_{Actual}$ is the measured load.

The backcalculated moduli are presented in Table 5.5 along with the associated RMS errors after the completion of backcalculation. MODULUS uses the error per sensor as a convergence method as compared to SMART and SASW software packages that use RMS errors. To uniformly compare the results, the RMS error was determined for each station.

Table 5.3 - Results of SMART Analysis for Estimating Design Moduli at Rut Ride Section
a) Section 1

| Station No. | Modulus, ksi | | | | | | | RMS Error, % |
| | ACP | Base | | Subbase | | Subgrade | | |
		Cons.	Avg.	Cons.	Avg.	Cons.	Avg.	
1	619	55	76	29	33	18.0	24.0	4.5
2	707	90	128	21	22	17.0	23.0	5.5
3	709	77	123	39	45	21.0	28.0	5.9
4	479	53	88	25	27	17.0	23.0	7.8
5	532	45	63	25	27	17.0	23.0	6.8
Average	**609**	**64**	**96**	**28**	**31**	**18**	**24**	**6.1**
Std Dev	**103.1**	**18.8**	**28.7**	**6.9**	**8.8**	**1.7**	**2.2**	**-**
COV	**17%**	**29%**	**30%**	**25%**	**29%**	**10%**	**9%**	**-**

b) Section 2

| Station No. | Modulus, ksi | | | | | RMS Error, % |
| | ACP | Base | | Subgrade | | |
		Cons.	Avg.	Cons.	Avg.	
6	557	60	86	27.0	38.0	6.9
7	639	50	72	27.0	37.0	7.4
8	683	64	89	27.0	38.0	8.3
9	504	53	76	27.0	37.0	8.0
10	505	38	52	22.0	30.0	7.1
11	504	52	74	22.0	31.0	5.9
12	632	69	95	19.0	26.0	3.2
13	729	76	104	22.0	29.0	4.2
14	613	51	73	27.0	37.0	6.4
15	450	30	35	25.0	35.0	6.3
16	484	25	28	22.0	30.0	6.0
17	566	65	91	23.0	31.0	10.3
18	585	31	36	27.0	37.0	6.7
19	506	30	34	25.0	35.0	4.9
20	576	46	62	27.0	37.0	5.9
21	549	45	64	22.0	31.0	6.3
Average	**568**	**49**	**67**	**24**	**34**	**6.5**
Std Dev	**76.7**	**15.3**	**24.0**	**2.7**	**3.9**	**-**
COV	**14%**	**31%**	**36%**	**11%**	**12%**	**-**

c) Section 3

| Station No. | Modulus, ksi | | | | | | | RMS Error, % |
| | ACP | Base | | Subbase | | Subgrade | | |
		Cons.	Avg.	Cons.	Avg.	Cons.	Avg.	
22	548	41	52	25	26	22.0	31.0	7.1
23	521	46	75	25	26	25.0	35.0	3.1
24	438	42	46	36	43	17.0	23.0	4.0
25	484	46	58	27	31	17.0	23.0	4.0
Average	**498**	**44**	**58**	**28**	**32**	**20**	**28**	**4.5**
Std Dev	**47.7**	**2.6**	**12.5**	**5.3**	**8.0**	**3.9**	**6.0**	**-**
COV	**10%**	**6%**	**22%**	**19%**	**25%**	**19%**	**21%**	**-**

Table 5.4 - Measured FWD Deflections for Rut Ride Section
a) Section 1

Station No.	Normalized Deflection, mils (12 in. Spacing)						
	d0	d1	d2	d3	d4	d5	d6
1	16.9	10.8	6.7	4.3	3.5	2.6	2.1
2	16.0	10.9	6.7	4.2	3.4	2.5	2.1
3	11.7	8.1	5.4	3.7	3.1	2.3	1.9
4	13.9	8.6	5.6	3.7	3.1	2.3	1.9
5	14.2	8.4	5.5	3.7	3.1	2.4	2.0
Average	**14.5**	**9.4**	**6.0**	**3.9**	**3.2**	**2.4**	**2.0**
Std Dev	**2.0**	**1.4**	**0.6**	**0.3**	**0.2**	**0.1**	**0.1**
COV	**14%**	**15%**	**11%**	**8%**	**6%**	**6%**	**5%**

b) Section 2

Station No.	Normalized Deflection, mils (12 in. Spacing)						
	d0	d1	d2	d3	d4	d5	d6
6	12.7	7.6	4.7	3.3	2.8	2.2	1.8
7	11.6	6.9	4.2	3.0	2.6	2.1	1.7
8	11.8	6.7	4.2	3.0	2.6	2.0	1.6
9	12.3	7.1	3.4	2.4	2.2	1.8	1.5
10	10.3	5.6	3.7	2.7	2.5	1.9	1.6
11	12.7	6.7	3.8	2.5	2.2	1.7	1.4
12	12.2	7.1	4.2	2.8	2.3	1.8	1.4
13	11.2	6.4	3.7	2.4	2.1	1.6	1.2
14	12.3	6.8	3.9	2.6	2.0	1.5	1.2
15	13.4	7.1	4.4	2.8	2.3	1.7	1.4
16	15.4	8.5	5.1	3.4	2.8	2.1	1.6
17	11.7	6.5	4.3	3.0	2.5	1.8	1.4
18	11.4	5.8	3.7	2.7	2.4	1.9	1.5
19	13.3	6.6	4.1	2.9	2.6	2.0	1.5
20	15.8	8.1	4.6	3.0	2.6	1.9	1.5
21	13.5	7.0	3.8	2.5	2.0	1.5	1.2
Average	**12.6**	**6.9**	**4.1**	**2.8**	**2.4**	**1.8**	**1.5**
Std Dev	**1.4**	**0.7**	**0.4**	**0.3**	**0.3**	**0.2**	**0.2**
COV	**11%**	**11%**	**11%**	**11%**	**11%**	**11%**	**11%**

c) Section 3

Station No.	Normalized Deflection, mils (12 in. Spacing)						
	d0	d1	d2	d3	d4	d5	d6
22	11.7	6.0	3.6	2.5	2.0	1.5	1.2
23	18.8	10.3	4.7	2.8	2.0	1.5	1.2
24	20.1	11.2	5.4	3.0	2.2	1.6	1.3
25	27.4	12.5	6.0	3.7	2.8	2.0	1.5
Average	**19.5**	**10.0**	**4.9**	**3.0**	**2.3**	**1.7**	**1.3**
Std Dev	**6.4**	**2.8**	**1.0**	**0.5**	**0.4**	**0.2**	**0.1**
COV	**33%**	**28%**	**21%**	**18%**	**16%**	**13%**	**11%**

Table 5.5 - Results of MODULUS Analysis for Estimating Design Moduli at Rut Ride Section

a) Section 1

Station No.	Modulus, ksi				Error/ Sensor %	Depth to Bedrock, in.	RMS Error, %
	ACP	Base	Subbase	Subgrade			
1		150	19	16.4	2.8		3.3
2		150	25	16.1	3.2		3.5
3	500	150	85	18.6	3.8	300	3.9
4		150	46	18.3	2.1		2.5
5		120	57	18.2	2.6		3.6
Average	**500**	**144**	**47**	**18**	**3**	**300**	**3.4**
Std Dev	**-**	**13.6**	**26.5**	**1.2**	**0.6**	**-**	**-**
COV	**-**	**9%**	**57%**	**7%**	**22%**	**-**	**-**

b) Section 2

Station No.	Modulus, ksi			Error/ Sensor %	Depth to Bedrock, in.	RMS Error, %
	ACP	Base	Subgrade			
6		101	20.7	4.4		4.7
7		112	22.7	5.6		5.9
8		109	22.9	5.1		5.8
9		83	26.2	9.5		10.7
10		136	25.5	6.3		8.8
11		82	25.6	4.7		5.4
12		95	23.8	4.0		3.4
13		99	27.1	4.8		2.3
14	500	84	26.1	4.9	300	1.1
15		79	23.7	3.9		6.8
16		69	19.7	3.4		2.5
17		107	23.6	2.4		11.4
18		108	25.7	5.9		2.4
19		84	23.6	5.6		2.1
20		61	21.6	3.9		3.1
21		70	26.6	4.8		7.0
Average	**500**	**92**	**24**	**5**	**300**	**5.2**
Std Dev	**-**	**19.5**	**2.2**	**1.6**	**-**	**-**
COV	**-**	**21%**	**9%**	**32%**	**-**	**-**

c) Section 3

Station No	Modulus, ksi				Error/ Sensor %	Depth to Bedrock, in.	RMS Error, %
	ACP	Base	Subbase	Subgrade			
22		107	68	27.6	2.3	300	3.3
23	500	98	10	25.6	2.1	174	2.3
24		90	10	22.9	2.5	131	3.5
25		38	13	18.8	2.4	300	6.3
Average	**500**	**83**	**25**	**24**	**2**	**226**	**3.8**
Std Dev	**-**	**30.6**	**28.5**	**3.8**	**0.1**	**-**	**-**
COV	**-**	**37%**	**114%**	**16%**	**6%**	**-**	**-**

The RMS errors are reasonably small for all test points with an average of about 5%. The modulus of the ACP layer was fixed to 500 ksi, since the thickness of the ACP layer was less than 3 in. The average base moduli vary from 83 ksi to 144 ksi with a COV of 37% for Section 3, 21% for Section 2 and 9% for Section 1. The average subbase moduli range from 47 ksi to 25 ksi. The COV of the subbase layer is rather large at 57% and 114% for Sections 1 and 3, respectively. The average subgrade modulus is close to 20 ksi with a COV of less than 16%. These results will be further compared with results of the average layer moduli reported from SMART and JIM.

JIM Analysis: As with the SASW analysis, the joint inversion analysis, which incorporates data from SPA and FWD, was carried out twice. First, only layer moduli were estimated. In this case, the results from the GPR were used to fix the thickness of the ACP and base layers and the PSPA moduli were assigned to the ACP layer. The average GPR thicknesses of the ACP and base layers for Sections 1, 2, and 3 were determined and assigned to the corresponding sections. Likewise, the moduli of the ACP layer were the averages of PSPA moduli from points in Sections 1, 2, and 3, respectively. In the second case, the analysis was performed so that the layer thicknesses and moduli could be estimated. As such, the nominal thicknesses were introduced in the analysis as seed values.

The thicknesses estimated by the GPR are compared to the nominal values in Figure 5.5. The thickness of the ACP layer compares well with the nominal value. The base thickness agrees well with the nominal values for Section 2. The base thicknesses for Sections 1 and 3 are a few inches different from the suggested nominal thickness values.

The variation in the ACP modulus from PSPA along the site is shown in Figure 5.6. The values are fairly consistent. Based on the repeatability and documented history of the accuracy of GPR and PSPA, the thickness of the ACP and base layers and the modulus of the ACP layer were not backcalculated.

The results from the two backcalculation schemes (with and without thickness backcalculation) are summarized in Tables 5.6 and 5.7. Without backcalculating the thicknesses, the minimum and average moduli estimated by JIM for the base and subbase layers are similar to SMART (see Table 5.6). Overall, the layer moduli vary by less than 15%.

From Table 5.7, the layer thicknesses estimated by JIM for the ACP layer are approximately 2 in., which correspond to the GPR and nominal thicknesses. The base layer thickness is close to the 6 in. nominal thickness, but less than the GPR thickness for Section 1. For Section 2, the thickness based on JIM was greater than both the GPR and nominal thicknesses of 14 in. For Section 3, the base thickness from JIM is less than the nominal thickness of 8 in. The COV of the ACP thickness is less than 20%, for the base layer less than 30%, and for the subbase as high as 50%. As stated above, the ACP layer moduli were not backcalculated. For the lower layers (base, subbase, and subgrade), the variability of the layer moduli are less for the average values compared to the minimum values. Overall, the variability of the moduli reported from both runs in JIM is less than 20%. For the base results (conservative and average) for Section 2 and conservative subbase moduli of Section 3 exhibited a slight increase in variability of 31%, 27% and 24% respectively (see Table 5.6). The other exception is for the conservative subbase
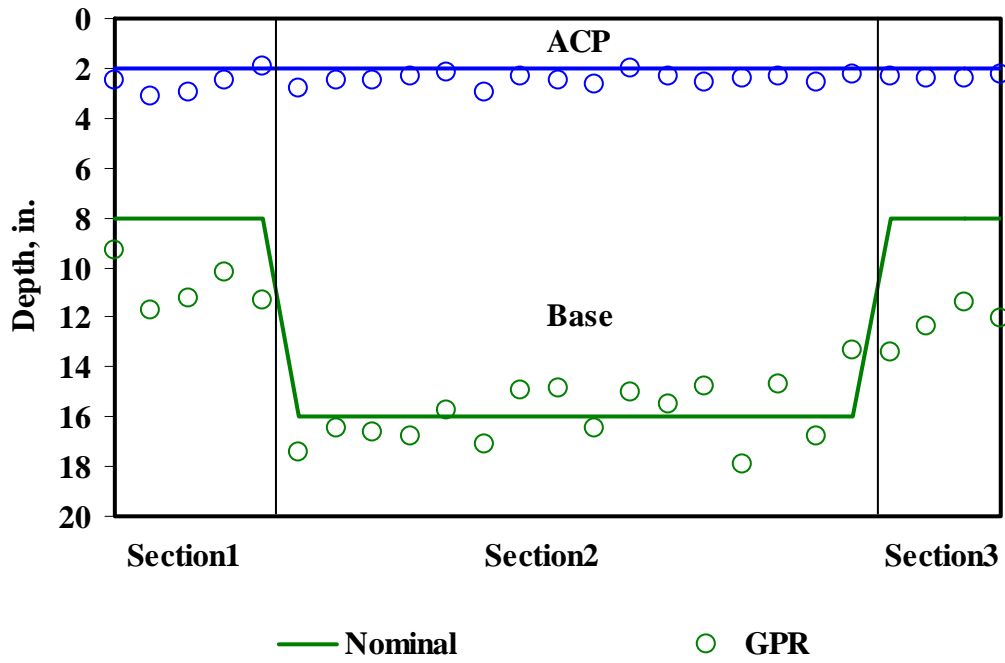
Figure 5.5 - Results of GPR Thicknesses for the Rut Ride Section
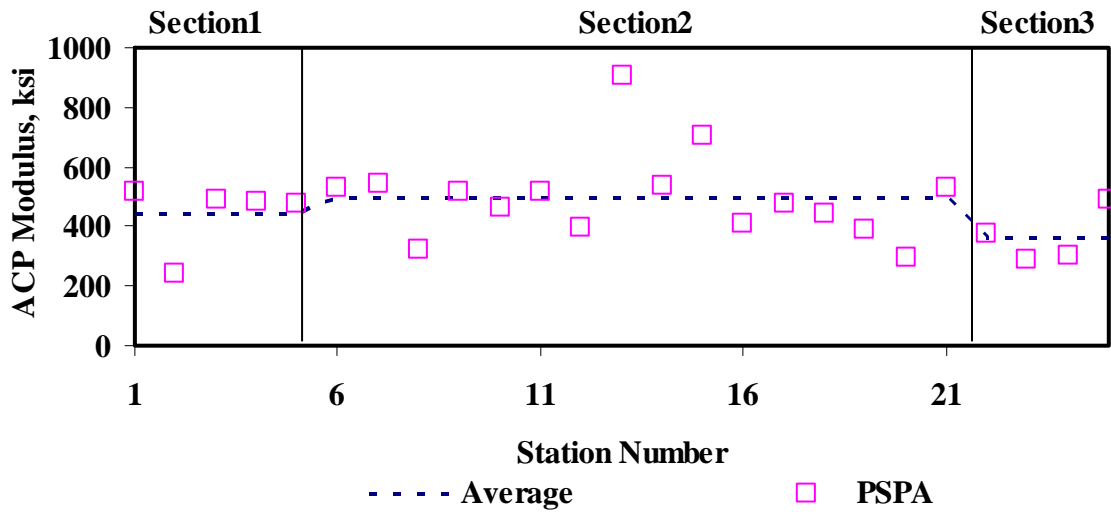
Figure 5.6 - Moduli of Asphalt Concrete Pavement Layer from PSPA Analysis for Rut Ride Section

Table 5.6 - Results of JIM Analysis for Estimating Design Moduli at Rut Ride Section
a) Section 1

| Station No. | Modulus, ksi | | | | | | | RMS Error, % |
| | ACP | Base | | Subbase | | Subgrade | | |
		Cons.	Avg.	Cons.	Avg.	Cons.	Avg.	
1		55	94	32	55	11.2	12.1	2.6
2		55	99	32	55	12.8	13.9	3.4
3	441	72	107	39	60	12.9	13.8	3.5
4		50	90	27	50	13.3	14.5	3.0
5		54	86	32	50	12.3	13.3	3.1
Average	**441**	**57**	**95**	**32**	**54**	**12**	**13**	**3.1**
Std Dev	**-**	**8.3**	**8.2**	**4.2**	**4.3**	**0.8**	**0.9**	**-**
COV	**-**	**15%**	**9%**	**13%**	**8%**	**7%**	**7%**	**-**

b) Section 2

| Station No. | Modulus, ksi | | | | | RMS Error, % |
| | ACP | Base | | Subgrade | | |
		Cons.	Avg.	Cons.	Avg.	
6		80	141	13.8	14.9	3.3
7		83	146	15.2	16.5	3.9
8		100	171	15.3	16.6	3.8
9		70	126	18.4	20.1	4.5
10		56	105	17.8	19.5	4.5
11		60	111	17.7	19.3	3.0
12		79	139	16.4	17.9	2.1
13	499	87	152	18.7	20.3	2.9
14		65	119	18.6	20.4	3.5
15		39	73	17.3	19.1	4.7
16		32	62	14.2	15.6	4.3
17		64	118	16.2	17.6	2.4
18		48	93	18.6	20.5	4.6
19		38	76	16.7	18.4	4.2
20		60	111	15.1	16.5	3.5
21		46	89	18.8	20.7	2.3
Average	**499**	**63**	**114**	**17**	**18**	**3.6**
Std Dev	**-**	**19.4**	**30.9**	**1.7**	**1.9**	**-**
COV	**-**	**31%**	**27%**	**10%**	**10%**	**-**

c) Section 3

| Station No. | Modulus, ksi | | | | | | | RMS Error, % |
| | ACP | Base | | Subbase | | Subgrade | | |
		Cons.	Avg.	Cons.	Avg.	Cons.	Avg.	
22		64	96	39	59	19.0	20.5	3.0
23	363	56	93	23	50	17.2	18.6	2.8
24		59	96	27	55	17.6	19.0	3.8
25		54	91	27	56	13.6	14.6	3.0
Average	**363**	**58**	**94**	**29**	**55**	**17**	**18**	**3.2**
Std Dev	**-**	**4.5**	**2.6**	**7.0**	**3.4**	**2.3**	**2.5**	**-**
COV	**-**	**8%**	**3%**	**24%**	**6%**	**14%**	**14%**	**-**

Table 5.7 - Results of JIM Analysis for Estimating Design Moduli and Thicknesses at Rut Ride Section

a) Section 1

Station No.	Thickness, in.			Modulus, ksi								RMS Error, %
	ACP	Base	Subbase	ACP	Base		Subbase		Subgrade		
					Cons.	Avg.	Cons.	Avg.	Cons.	Avg.	
1	2.5	6.2	6.6		80	105	27	51	11.6	12.5	2.2
2	2.9	3.6	4.6		68	97	34	58	11.7	12.6	2.2
3	2.8	8.7	13.6	441	87	103	44	62	12.0	12.8	2.5
4	2.0	7.4	7.1		79	100	27	55	12.8	13.8	2.5
5	1.9	6.6	10.2		56	102	26	47	12.6	13.7	3.1
Average	**2.4**	**6.5**	**8.4**	**441**	**74**	**101**	**32**	**55**	**12**	**13**	**2.5**
Std Dev	**0.4**	**1.9**	**3.5**	**-**	**12.2**	**3.0**	**7.5**	**5.6**	**0.5**	**0.6**	**-**
COV	**18%**	**29%**	**42%**	**-**	**16%**	**3%**	**24%**	**10%**	**4%**	**5%**	**-**

b) Section 2

Station No.	Thickness, in.		Modulus, ksi					RMS Error, %
	ACP	Base	ACP	Base		Subgrade		
				Cons.	Avg.	Cons.	Avg.	
6	2.3	20.0		82	106	13.0	13.8	3.5
7	2.1	20.0		84	110	13.9	14.8	3.8
8	2.4	20.0		93	118	13.4	14.2	4.3
9	2.0	20.0		83	108	16.5	17.6	4.5
10	1.8	20.0		75	100	16.8	18.0	3.1
11	2.0	19.7		78	104	16.9	18.1	2.8
12	2.7	18.1		84	109	16.0	17.1	2.3
13	2.8	19.1	499	84	109	17.9	19.2	2.9
14	2.3	17.3		81	107	18.3	19.7	3.3
15	1.5	17.4		65	93	16.4	17.7	2.2
16	1.7	14.3		44	86	14.0	15.2	2.9
17	2.4	16.7		75	101	15.8	17.0	2.0
18	1.9	20.0		65	90	15.7	16.9	3.2
19	1.7	18.8		68	93	15.4	16.6	2.4
20	2.0	18.2		83	108	14.9	16.0	3.3
21	2.1	15.5		50	94	18.8	20.4	2.2
Average	**2.1**	**18.4**	**499**	**75**	**102**	**16**	**17**	**3.0**
Std Dev	**0.4**	**1.8**	**-**	**13.2**	**8.8**	**1.7**	**1.9**	**-**
COV	**17%**	**10%**	**-**	**18%**	**9%**	**11%**	**11%**	**-**

c) Section 3

Station No.	Thickness, in.			Modulus, ksi								RMS Error, %
	ACP	Base	Subbase	ACP	Base		Subbase		Subgrade		
					Cons.	Avg.	Cons.	Avg.	Cons.	Avg.	
22	2.1	4.4	17.3		80	98	38	58	18.7	20.4	2.1
23	1.9	3.6	10.0	363	88	104	29	56	17.1	18.8	2.6
24	1.8	5.1	4.1		85	104	35	58	16.0	17.4	2.7
25	1.9	3.2	10.7		102	107	29	58	13.3	14.5	2.4
Average	**1.9**	**4.1**	**10.5**	**363**	**89**	**103**	**33**	**58**	**16**	**18**	**2.5**
Std Dev	**0.1**	**0.8**	**5.4**	**-**	**9.3**	**3.5**	**4.5**	**0.9**	**2.3**	**2.5**	**-**
COV	**6%**	**21%**	**51%**	**-**	**10%**	**3%**	**14%**	**2%**	**14%**	**14%**	**-**

50

moduli for the cases when both thickness and moduli were backcalculated, which was 24% (see Table 5.7). For this section the JIM results show consistency with low variability across each section for both runs.

The average moduli from the two backcalculation schemes using JIM are compared graphically in Figures 5.7. The moduli for the ACP layer for the two cases were the same since the PSPA moduli was fixed in the analysis. However, for the base, subbase and subgrade layers, the moduli from the two cases compare favorably. The base layer moduli of Section 2 for the case where only layer moduli were backcalculated exhibit higher moduli and a larger variability than when both thickness and moduli were backcalculated, as reported in Tables 5.6 and 5.7. This could be attributed to the GPR thickness values for base layer of 13.5 in., used in the case where only layer moduli was backcalculated, compared to the backcalculated thickness values which are higher with an average thickness of 18 in. For the remaining layers (bottom layers), the results are very close, almost overlapping for most of the stations. The next step was to compare the results from JIM with the results of the other analyses.

Comparison of Results from Different Analyses

The thicknesses estimated from JIM are compared with those from the GPR and SASW analyses in Figure 5.8. From Figure 5.8a, the ACP thicknesses from all three approaches are similar, with JIM values being amid the other two. Overall, thicknesses from JIM compare very reasonably to the as-built thickness. As shown in Figure 5.8b, the thickness of the base estimated by JIM is comparable to those obtained from the GPR and SASW analyses for Sections 1 and 3. In Section 2, however, the thickness from JIM is greater than those reported by the GPR and SASW analyses.

The ACP moduli estimated from JIM, SMART and MODULUS are compared in Figure 5.9a. In the JIM analysis, the average moduli from PSPA were used in the backcalculation process. Also, in MODULUS, the ACP modulus was fixed at 500 ksi since the layer thickness was less than 3 in. At some points, the modulus estimated by SMART are greater than those from JIM, and exhibit more variability.

The base moduli are compared in Figure 5.9b. Sections 1 and 3 were analyzed as four-layer pavement systems. The average moduli estimated from JIM seem closer to the SMART results for Section 1. However, for Section 3, the results are closer to those for MODULUS. For Section 2, moduli from JIM are greater than those from MODULUS and SMART.

Figure 5.9c contains the comparison of subbase moduli for Sections 1 and 3 (four-layer pavement systems). The results from JIM seem more consistent than the results from SMART or MODULUS. From Figure 5.9d, the subgrade moduli from JIM for all three sections seem consistent. The moduli from SMART are more variable and higher since the seismic tests only sample the top 2 ft of the subgrade as opposed to the FWD which estimates the moduli at greater depth.

The backcalculation RMS errors from the three analyses are compared in Figure 5.10. The RMS errors are reasonably low for all three methods with the averages of less than 10%. JIM analyses demonstrated the lowest RMS error across the three sections.
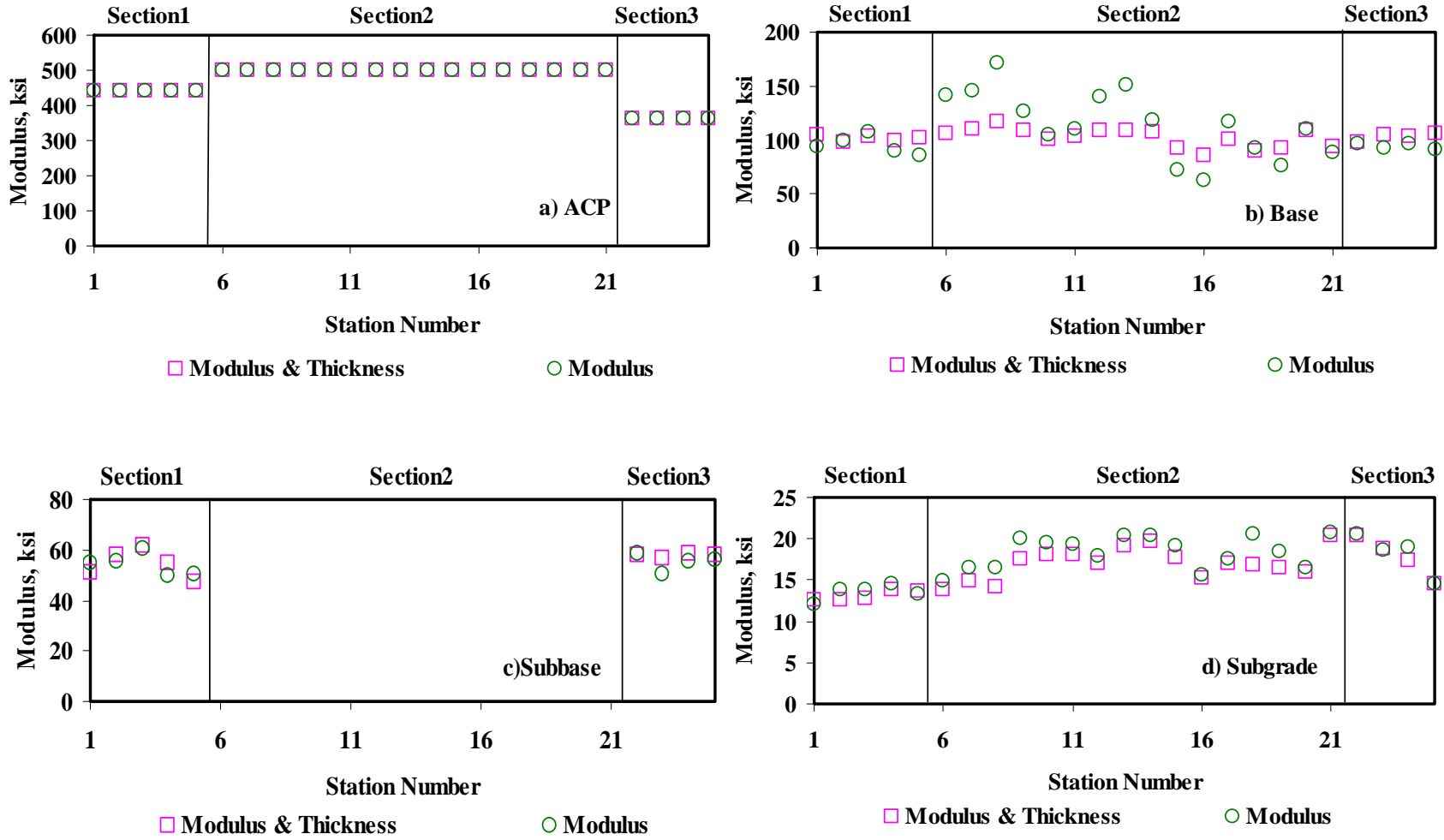
Figure 5.7 - Comparison of Moduli from JIM for Rut Ride Section with Constant and Backcalculated Thicknesses
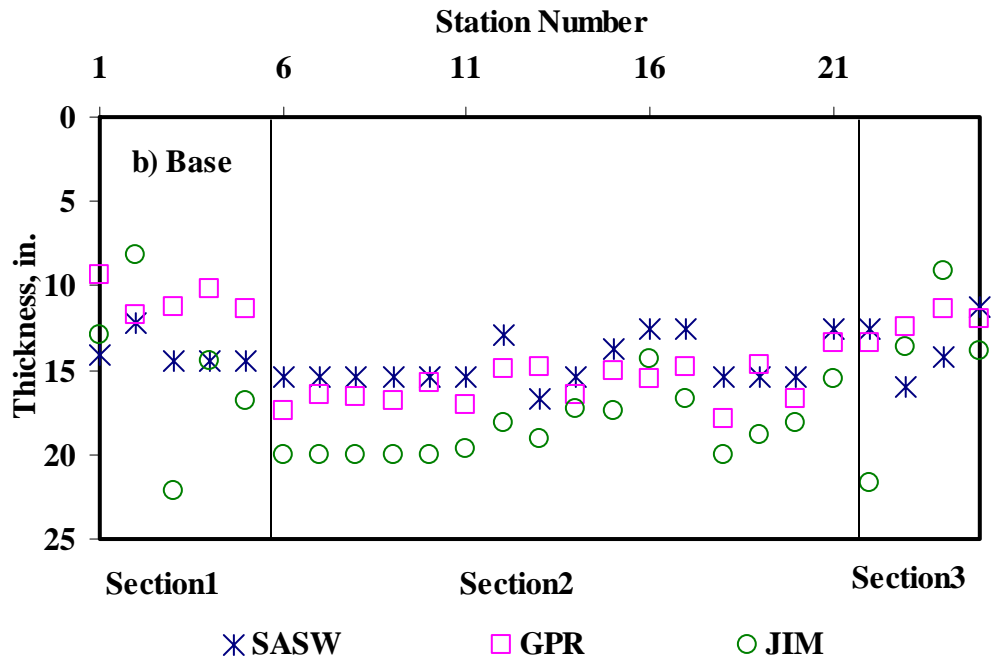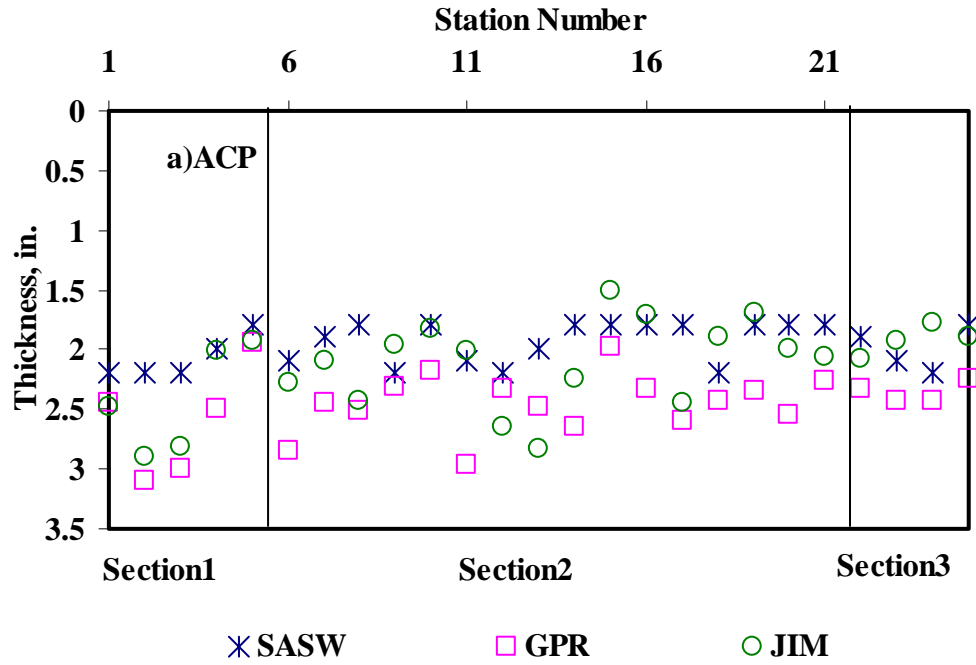
Figure 5.8 - Comparison of Thicknesses from Different Analyses for Rut Ride Section
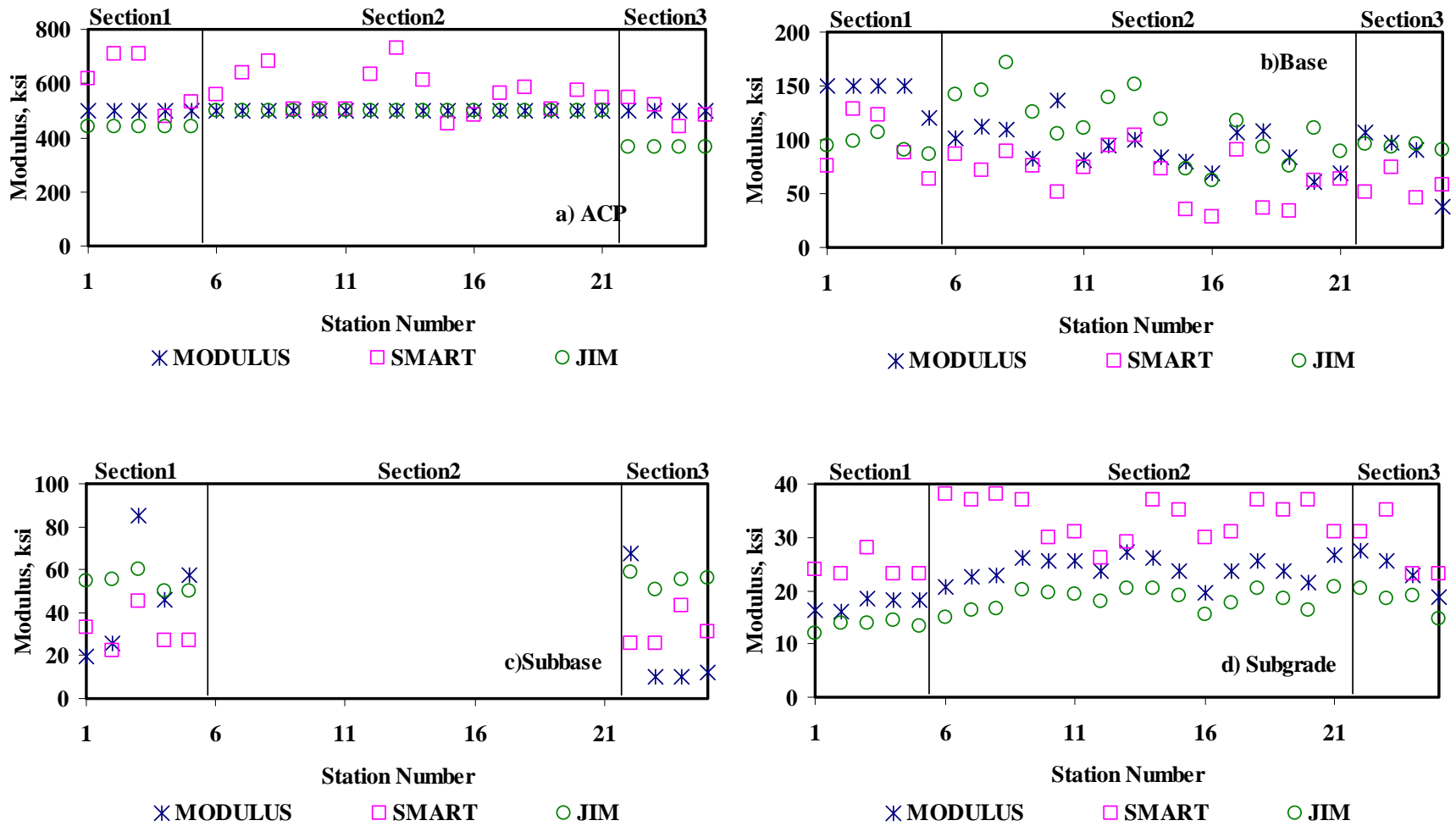
Figure 5.9 - Comparison of Design Moduli from Different Analyses for Rut Ride Section
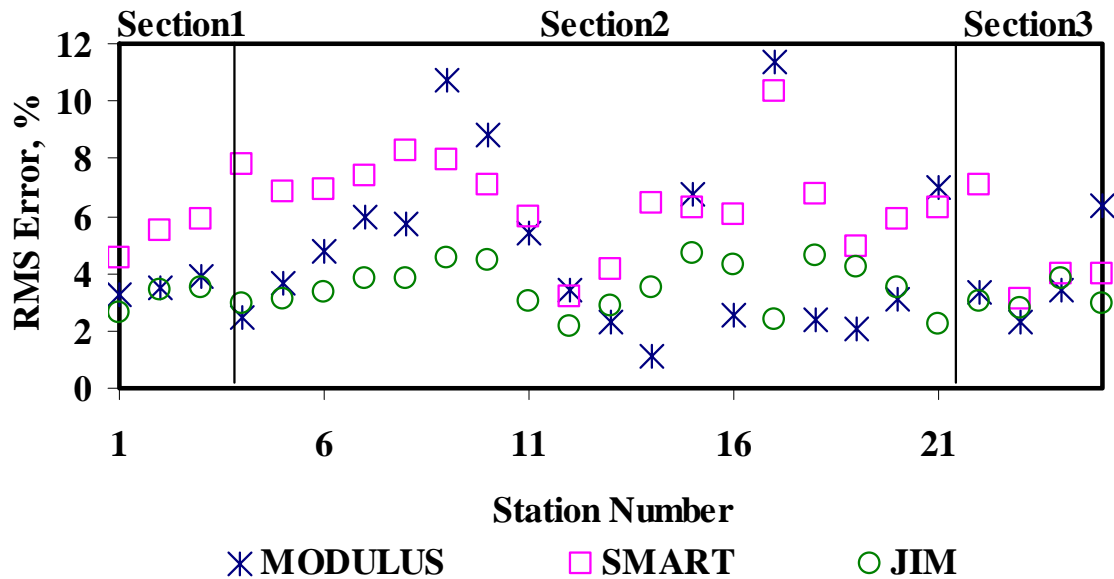
Figure 5.10 - Comparison of Backcalculation RMS Errors for Rut Ride Section

DATA FUSION OF RESULTS FROM TTI RIDE RUT SITE

The next step in the process is fusing the results from different analyses using DFINE. The data that were fused are presented in Table 5.8. The average layer moduli for the base, subbase, and subgrade for JIM, SMART and MODULUS were used in the data fusion. As discussed in Chapter 3, DFINE uses three fusion techniques: a) statistical weighted average (SWA), b) weighted average (WA), and c) fuzzy logic (FL).

The statistical weighted average and weighted average methods are fairly similar in the way that their data is fused since they are both a variation of the traditional average method. In the statistical weighted average method, the uncertainty based on the statistical information of the data being fused is used as weighting factor to bias the results. The lower the variability of one set of results (indicating more consistency in the results) is, the larger the weighting factor for that set will be. The assumption is that the results with lower variability are more reliable, and therefore, more weight can be assigned to those results. The COV of each data set is used in determining the corresponding weighting factor.

The weighted average method is basically a modification on the traditional average method where each data point from the NDT analysis is assumed to be perfect (no variability). This method does not use any of the inherent statistics from the NDT analysis results when averaging. The results from the NDT analyses are averaged station by station (no variability is computed). Once the results of each station are computed, then the site statistics are obtained (average, stddev, and COV). This method produces the lowest site variability of the three fusion methods since no error from the analysis is considered. The weighted average method used in DFINE works as the traditional weighted average by default, but with the possibility to assign a

55

Table 5.8 - Summary of Moduli Used in Data Fusion

a) Section 1

Station No.	Modulus, ksi														RMS Error, %
	JIM				RMS Error, %	SMART				RMS Error, %	MODULUS				
	ACP	Base	SB	SG		ACP	Base	SB	SG		ACP	Base	SB	SG	
1		94	55	12	2.6	619	76	33	24	4.5		150	19	16	3
2		99	55	14	3.4	707	128	22	23	5.5		150	25	16	3
3	441	107	60	14	3.5	709	123	45	28	5.9	500	150	85	19	4
4		90	50	14	3.0	479	88	27	23	7.8		150	46	18	3
5		86	50	13	3.1	532	63	27	23	6.8		120	57	18	4
Avg.	441	95	54	13	3.1	609	96	31	24	6.1	500	144	47	18	3.4
Std Dev	-	8.2	4.3	0.9	-	103	28.7	8.8	2.2	-	-	13.6	26.5	1.2	-
COV	-	9%	8%	7%	-	17%	30%	29%	9%	-	-	9%	57%	7%	-

b) Section 2

Station No.	Modulus, ksi											RMS Error, %
	JIM			RMS Error, %	SMART			RMS Error, %	MODULUS			
	ACP	Base	SG		ACP	Base	SG		ACP	Base	SG	
6		141	15	3.3	557	86	38	6.9		101	21	5
7		146	16	3.9	639	72	37	7.4		112	23	6
8		171	17	3.8	683	89	38	8.3		109	23	6
9		126	20	4.5	504	76	37	8.0		83	26	11
10		105	20	4.5	505	52	30	7.1		136	26	9
11		111	19	3.0	504	74	31	5.9		82	26	5
12		139	18	2.1	632	95	26	3.2		95	24	3
13	499	152	20	2.9	729	104	29	4.2	500	99	27	2
14		119	20	3.5	613	73	37	6.4		84	26	1
15		73	19	4.7	450	35	35	6.3		79	24	7
16		62	16	4.3	484	28	30	6.0		69	20	3
17		118	18	2.4	566	91	31	10.3		107	24	11
18		93	21	4.6	585	36	37	6.7		108	26	2
19		76	18	4.2	506	34	35	4.9		84	24	2
20		111	16	3.5	576	62	37	5.9		61	22	3
21		89	21	2.3	549	64	31	6.3		70	27	7
Avg.	499	114	18	3.6	568	67	34	6.5	500	92	24	5.2
Std Dev	-	30.9	1.9	-	76.7	24.0	3.9	-	-	19.5	2.2	-
COV	-	27%	10%	-	14%	36%	12%	-	-	21%	9%	-

c) Section 3

Station No.	Modulus, ksi														RMS Error, %
	JIM				RMS Error, %	SMART				RMS Error, %	MODULUS				
	ACP	Base	SB	SG		ACP	Base	SB	SG		ACP	Base	SB	SG	
22		96	59	20	3.0	548	52	26	31	7.1		107	68	28	3
23	363	93	50	19	2.8	521	75	26	35	3.1	500	98	10	26	2
24		96	55	19	3.8	438	46	43	23	4.0		90	10	23	3
25		91	56	15	3.0	484	58	31	23	4.0		38	13	19	6
Avg.	363	94	55	18	3.2	498	58	32	28	4.5	500	83	25	24	3.8
Std Dev	-	2.6	3.4	2.5	-	47.7	12.5	8.0	6.0	-	-	30.6	28.5	3.8	-
COV	-	3%	6%	14%	-	10%	22%	25%	21%	-	-	37%	114%	16%	-

56

modification factor or a weight to each data set (analysis method) based on the user's perceptions for established accuracy of the analysis method for certain conditions. For this case study, no weighting factor was assigned. Therefore, the results from the weighted average method in this report are similar to those of the traditional weighted average method.

Fuzzy Logic is the third fusion technique used in DFINE. One of the main steps in this method is the development of the fuzzy sets. These fuzzy sets have no definite boundary. Events that occur within these sets often partially belong to two members of the set.

Fuzzy logic provides membership functions made of fuzzy sets that are used to classify results. DFINE uses two functions to fuse the data: a) the standard deviation and b) the backcalculation RMS error. The standard deviation is calculated based on the results of each method for the section. The RMS error is based on the error of the backcalculation process of each analysis. Therefore, the RMS error method can only be used to fuse results of methods that use backcalculation (i.e., JIM, SMART, and MODULUS). This method cannot be used with the PSPA or GPR.

For this case study, both membership functions (i.e., standard deviation and RMS error) were used. Each membership function was made of five fuzzy sets ranging from very low, low, average, high, and very high. The fuzzy sets are defined by "fuzzy" shapes that are constrained by limits. Table 5.9 lists the boundary limits for the fuzzy sets for each membership function based on the standard deviation criteria for the ACP layer (Table 5.9a), base (Table 5.9b), subbase (Table 5.9c) and subgrade (Table 5.9d). Finally, Table 5.9e lists the limits of the fuzzy sets based on the RMS error criteria.

Report 0-4393-2 (Williams et al., 2004) provides more detailed information about the shapes of the membership functions. The "fuzzy" shape and limits of each fuzzy set is defined in Table 5.9 as well. The shapes used for the five fuzzy sets are Z, Λ, Λ, Λ, and S. Each fuzzy shape is defined by four limits. These limits designated *L1* through *L4* to specify the boundary of each class or fuzzy set. In general for each fuzzy set, the lower limit is defined by *L1* and the upper limit is defined by *L4*. The limits, *L2* and *L3,* are used to define the inner constraints of the fuzzy sets. For a triangular shape, the inner limits *L2* and *L3* are equal, indicating the peak of the triangle. On the other hand, the Z and S shapes have distinct L2 and L3 limits to define the slanted parts of the shapes.

To briefly expand on the setup of a membership function, an example from DFINE using the standard deviation of the ACP modulus with five fuzzy sets is presented in Figure 5.11 starting with very low standard deviation (Fussy Set 1) to very high standard deviation (Fuzzy Set 5). The shapes of the five fuzzy sets are shown in Figure 5.11. The limits of each set are calculated from the standard deviation of the results of the methods being fused. The value of the limits depends on the shape of the class being used. The first set is Z-shaped by default, and is set for the very low standard deviations. The limits of the Z-shape (first fuzzy set) are: L1 equal to 0 ksi, L2 equal to 26 ksi, L3 equal to 52 ksi, and L4 equal to 155 ksi. The remaining fuzzy sets for this function are defined similarly as indicated in Figure 5.11. As indicated in Figure 5.11, membership functions can have overlapping fuzzy sets. In such cases, a value belongs to both sets, and would trigger twice depending on the fuzzy rules used. The sets and limits for each

Table 5.9 - Boundaries for Membership Functions for Rut Ride Section
a) Standard Deviation of ACP Modulus

| Fuzzy Sets | | Membership Boundary (Limits) | | | |
| | | Standard Deviation | | | |
Type	Shape	L1	L2	L3	L4
Very Low	Z	0.0	25.9	51.8	155.4
Low	Triangle, Λ	25.9	51.8	51.8	77.7
Average	Triangle, Λ	51.8	77.7	77.7	103.6
High	Triangle, Λ	77.7	103.6	103.6	129.5
Very High	S	0.0	103.6	129.5	155.4

b) Standard Deviation of Base Modulus

| Fuzzy Sets | | Membership Boundary (Limits) | | | |
| | | Standard Deviation | | | |
Type	Shape	L1	L2	L3	L4
Very Low	Z	0.0	20.1	40.2	120.5
Low	Triangle, Λ	20.1	40.2	40.2	60.2
Average	Triangle, Λ	40.2	60.2	60.2	80.3
High	Triangle, Λ	60.2	80.3	80.3	100.4
Very High	S	0.0	80.3	100.4	120.5

c) Standard Deviation of Subbase Modulus

| Fuzzy Sets | | Membership Boundary (Limits) | | | |
| | | Standard Deviation | | | |
Type	Shape	L1	L2	L3	L4
Very Low	Z	0.0	9.1	18.1	54.4
Low	Triangle, Λ	9.1	18.1	18.1	27.2
Average	Triangle, Λ	18.1	27.2	27.2	36.3
High	Triangle, Λ	27.2	36.3	36.3	45.3
Very High	S	0.0	36.3	45.3	54.4

d) Standard Deviation of Subgrade Modulus

| Fuzzy Sets | | Membership Boundary (Limits) | | | |
| | | Standard Deviation | | | |
Type	Shape	L1	L2	L3	L4
Very Low	Z	0.0	3.4	6.8	20.3
Low	Triangle, Λ	3.4	6.8	6.8	10.2
Average	Triangle, Λ	6.8	10.2	10.2	13.5
High	Triangle, Λ	10.2	13.5	13.5	16.9
Very High	S	0.0	13.5	16.9	20.3

e) Standard Deviation of RMS Error

| Fuzzy Sets | | Membership Boundary (Limits) | | | |
| | | Standard Deviation | | | |
Type	Shape	L1	L2	L3	L4
Very Low	Z	3.6	4.2	4.8	7.3
Low	Triangle, Λ	4.2	4.8	4.8	5.4
Average	Triangle, Λ	4.8	5.4	5.4	6.1
High	Triangle, Λ	5.4	6.1	6.1	6.7
Very High	S	3.6	6.1	6.7	7.3
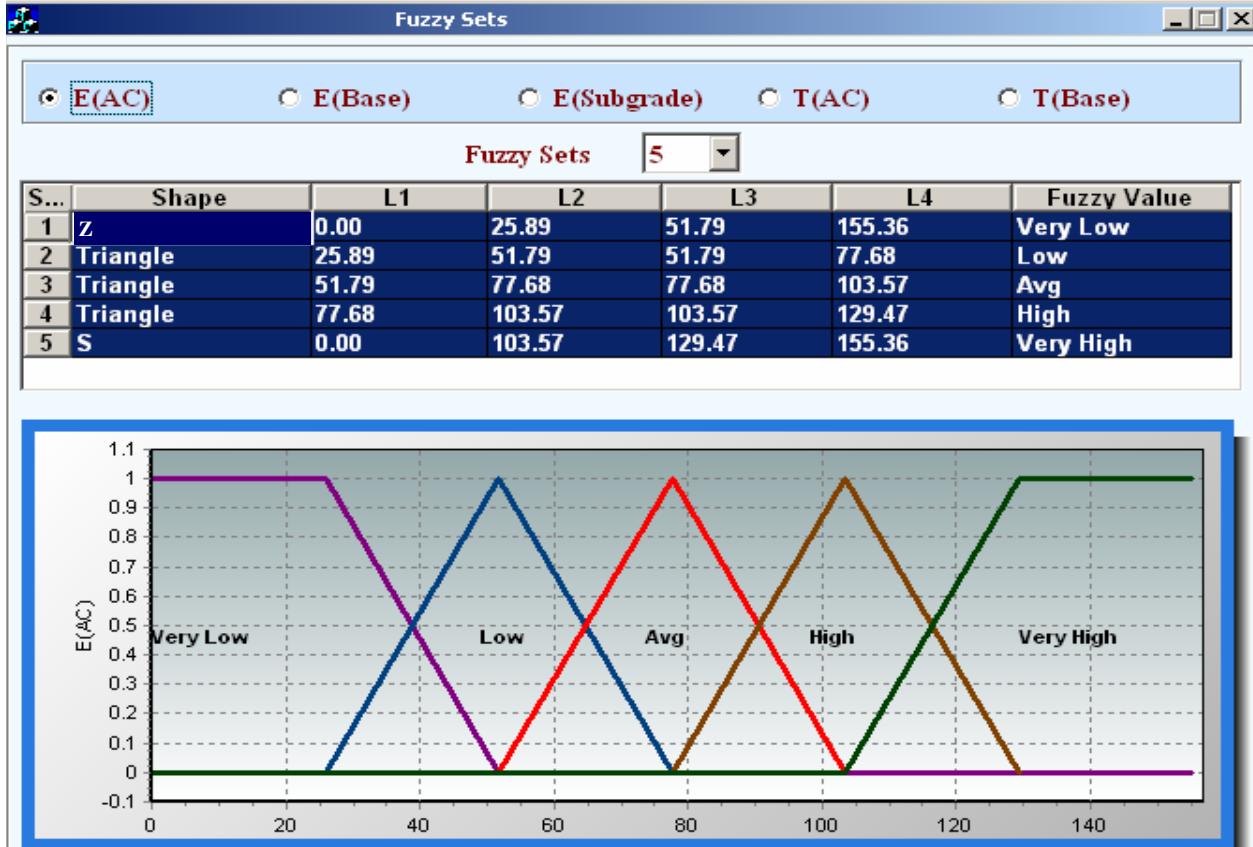
Figure 5.11 - Standard Deviation Fuzzy Set of ACP Modulus for Rut Ride Section

function shown in Figure 5.11 are obtained automatically based on preset conditions in the program. However, a user can vary the number of fuzzy sets from one to seven, or can change the limits manually using the grid or table shown in the top part of Figure 5.11. Once the membership functions are setup, the next step is to develop the fuzzy rules.

Chapter 3 explains the use membership functions with fuzzy rules. Briefly, the rules are a set of logical statements that assign weights based on the triggering of different membership functions. The rules are developed using the fuzzy operator. When a decision must be made between two degrees of membership, the operators used are primarily *AND* and *OR*, or, as would be thought of in probability, intersection and union. Another basic operator used is the *NOT* (complement) operator. A set number of default rules are provided for triggering the standard deviation function and the RMS error function. Figure 5.12a shows the default fuzzy rules in DFINE. As indicated in the figure, the rules combine both the standard deviation and the RMS error in the fusion based on fuzzy logic. The first rule that is highlighted in Figure 5.12a is:

$$IF\ (E\ is\ Very\ Low)\ AND\ (RMS\ is\ NOT\ Very\ High)\ Then\ OUTPUT\ is\ 1(1) \qquad (5.3)$$

where E is defined in this case as the standard deviation of modulus, and RMS is the RMS Error. Therefore, the rule states that if the standard deviation triggers the very high fuzzy set and the RMS error does not trigger the Very High fuzzy set, then the weight assigned to that fused parameter is 1. The value of one is multiplied by the results of the membership function(s). The

a) Fuzzy Rules   **b) Membership Value**

(1) If (E is Very Low) AND (RMS is Not Very High) then output is 1 (1)
(2) If (E is Not Very High) AND (RMS is Very Low) then output is 1 (1)
(3) If (RMS is Very High) then output is 0.6 (1)
(4) If (E is High) AND (RMS is High) then output is 0.7 (1)
(5) If (E is Avg) AND (RMS is Avg) then output is 0.8 (1)
(6) If (E is Low) AND (RMS is Low) then output is 0.9 (1)
(7) If (E is High) AND (RMS is Avg) then output is 0.7 (1)
(8) If (E is High) AND (RMS is Low) then output is 0.7 (1)
(9) If (E is Low) AND (RMS is High) then output is 0.7 (1)
(10) If (E is Avg) AND (RMS is High) then output is 0.7 (1)
(11) If (E is Avg) AND (RMS is Low) then output is 0.8 (1)
(12) If (E is Low) AND (RMS is Avg) then output is 0.8 (1)
(13) If (E is Very High) then output is 0.6 (1)
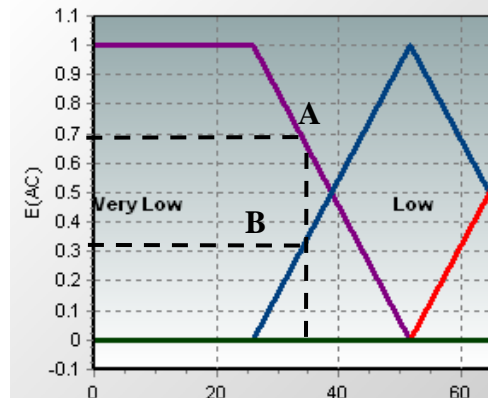
Figure 5.12 - Default Fuzzy Rules used in DFINE

value on the membership function is y-axis value of the fuzzy set. Figure 5.12b shows an example of determining the membership value if that rule is triggered. If the standard deviation of an input is 35 ksi, as indicated in the figure by the dash-line, two fuzzy sets will be triggered. The first fuzzy set (very low) will have a membership value close to 0.7 (point A). The second fuzzy set (Low) triggered will have a membership value of 0.3 (point B). Therefore, for this input value any rule that has the fuzzy set of "Very Low" or "Low" will use a membership value of 0.7 or 0.3, respectively. The designation of "*(1)*" at the end of Equation 5.3 provides additional flexibility to adjust the weight by that value. The process illustrated in this example is carried out for each modulus from each of the analysis methods for assigning weights. Further description and illustrations of the use of the rules is provided in Williams et al. (2004).

In most cases, a user does not need to modify the default values for the three fusing techniques. Once the data from the NDT methods are selected, the values can be automatically fused using any of the three fusing techniques. The results for the Rut Ride site for Section 1 are presented in Figure 5.13 for each pavement layer. The average and one standard deviation bounds are shown. The first three results in each graph are from the standard averaging of the results from each of the analysis methods. The last three results indicate the fused values of the three methods. In the SWA and FL methods, by default, very little weights are assigned to moduli that are not backcalculated (e.g. the ACP modulus from MODULUS). A user however, can modify the default weights. The results of the fused value are therefore not appreciably impacted by a parameter that is not backcalculated.

In each of the graphs in Figure 5.13, the mean modulus is the most likely value for that layer. A summary of the results from all three sections for this site are presented in Table 5.10. The variability of the fused value is typically less than each individual method. As shown in Table 5.10, most of the fused results show low COVs which indicate more certainty on the result of the fused values. The improvement in the moduli of the base and subbase after data fusion as compared to the FWD backcalculation (MODULUS) is of significance.

60
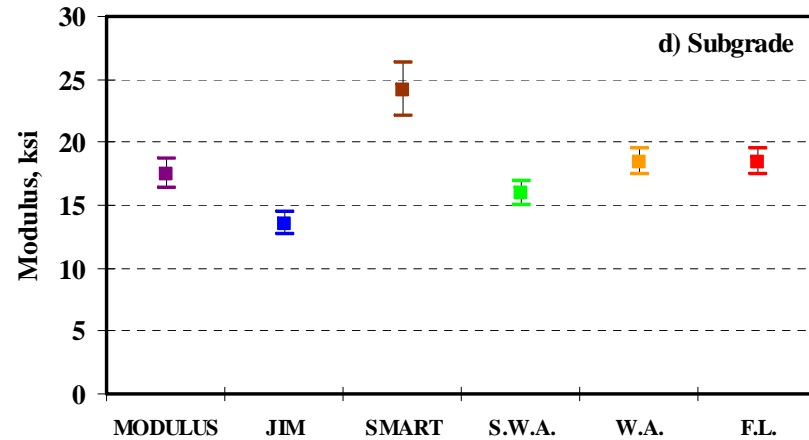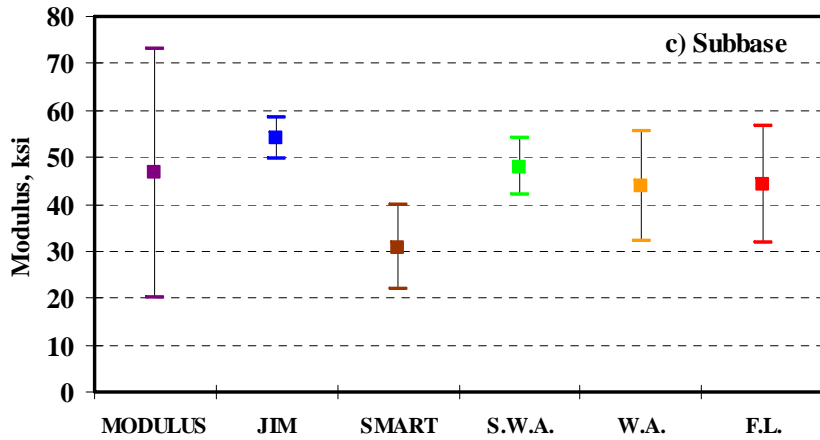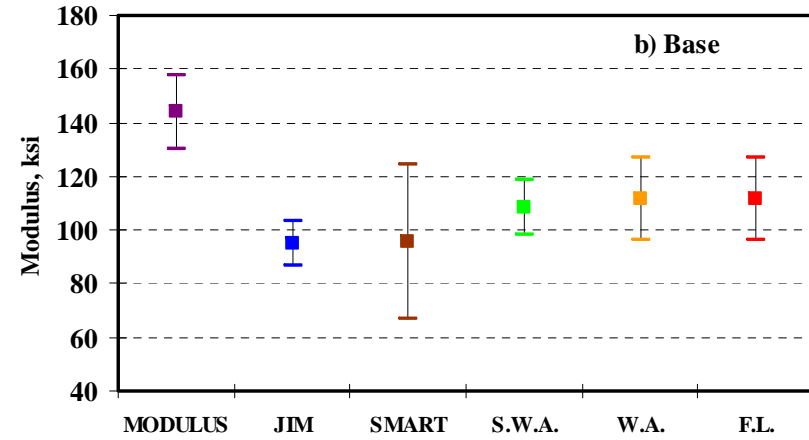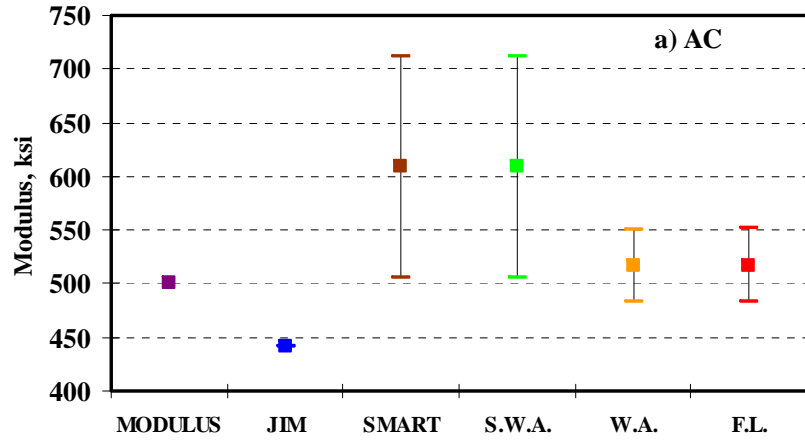
Figure 5.13 - Comparison of Design Moduli before and after Data Fusion for Section 1 of Rut Ride Site

Table 5.10 - Design Moduli with Corresponding Variability before and after Data Fusion for Rut Ride Site

Section No.	Method	Modulus, ksi							
		ACP		Base		Subbase		Subgrade	
		Avg.	*COV*	Avg.	*COV*	Avg.	*COV*	Avg.	*COV*
1	**MODULUS**	500	-	144	*9%*	47	*57%*	18	*7%*
	JIM	441	-	95	*9%*	54	*8%*	14	*7%*
	SMART	609	*17%*	96	*30%*	31	*29%*	24	*9%*
	SWA	*609*	*17%*	*108*	*10%*	*48*	*13%*	*16*	*6%*
	WA	*517*	*7%*	*112*	*14%*	*44*	*27%*	*18*	*6%*
	FL	*517*	*7%*	*112*	*14%*	*44*	*28%*	*18*	*6%*
2	**MODULUS**	500	-	90	*22%*	-	-	24	*9%*
	JIM	499	-	114	*27%*	-	-	18	*11%*
	SMART	568	*14%*	67	*36%*	-	-	34	*12%*
	SWA	*568*	*14%*	*87*	*25%*	*-*	*-*	*22*	*9%*
	WA	*522*	*5%*	*96*	*17%*	*-*	*-*	*25*	*6%*
	FL	*524*	*5%*	*95*	*17%*	*-*	*-*	*25*	*6%*
3	**MODULUS**	500	-	83	*37%*	25	*114%*	24	*16%*
	JIM	363	-	94	*3%*	55	*6%*	18	*14%*
	SMART	498	*10%*	58	*22%*	32	*25%*	28	*21%*
	SWA	*498*	*10%*	*86*	*5%*	*53*	*8%*	*21*	*14%*
	WA	*454*	*4%*	*70*	*16%*	*46*	*21%*	*23*	*16%*
	FL	*460*	*5%*	*67*	*17%*	*44*	*23%*	*24*	*17%*

62

CHAPTER SIX

CASE STUDIES

INTRODUCTION

The data analysis process described in Chapter 5 was carried out for a number of sites to determine the reasonableness of the programs JIM and DFINE. The detailed results from each step of the analysis are included in Appendices A through I.   The results from all sites are summarized and analyzed in this chapter. Some of the sites were visited either by UTEP or TxDOT personnel as part of forensic studies. In those cases, supporting information was not available.

RESULTS FROM BACKCALCULATION AND DATA FUSION ANALYSES

For each site, the summary of the layer moduli using JIM, SMART and MODULUS is presented first. As indicated before, JIM and SMART report estimated conservative and average moduli for the base and subgrade. The average moduli are used here for comparison purposes. For sections with the nominal ACP thickness less than 3 in., the modulus for backcalculation with MODULUS was fixed to 500 ksi. The backcalculated thickness using JIM is provided in the appendices. Even though the backcalculation of thickness was performed using JIM, the results are not summarized in this chapter except for the sites where the GPR data were also available. The main focus of this chapter is in the comparison of the backcalculated moduli.

The second part of the results is the outcome of the data fusion using DFINE. The assumption made for all case studies presented in this chapter is that the results from all the NDT analyses are valid and therefore included in the data fusion. The default settings in DFINE were used for fusion in all case studies. For the statistical weighted average (SWA) method, no adjustments were made to the weighting factors. The weighted average (WA) method was used assuming each method to be equally as important (as mentioned in Chapter 4). This is basically a simple station-by-station averaging where the results of each analysis are averaged for each station and then the site statistics are obtained. The Fuzzy Logic (FL) analyses were carried out with two membership functions (standard deviation, and RMS error) each with five fuzzy sets. Basically the same configuration used in Chapter 5 for the Rut Ride section at TTI annex was used throughout. Also as mentioned earlier, if a layer had a fixed modulus for all stations (i.e. in the

case of thin pavement sections using MODULUS), no weight was assigned to eliminate them from the SWA analysis. As for the FL method, a default weight of 0.5 was assigned so that those values would minimally impact the FL analysis.

FM1062 (Amarillo)
This site was one of the more controlled sites as far as data collection and support information. Data were collected with the FWD, SPA, PSPA, and GPR. The DCP was also used at this site. The site consisted of five experimental sections constructed with a base material stabilized in five different fashions. The pavement sections consisted of a three-layer system with a nominally 3-in.-thick ACP over 10 in. of base over subgrade.

The results of the analyses of this site are summarized in Tables 6.1 through 6.6. The site was analyzed as a four layer system since the DCP results indicated that the top half of the base layers at almost all sites were significantly different than the bottom half (see Table 6.1).

Table 6.1 - Variations of Moduli and Thickness of Base layer from DCP

Section		1 (Roadbond)		2 (CKD)		3 (Fly Ash)		4 (Lime)		5 (Control)	
Core		1	2	1	2	1	2	1	2	1	2
Upper Layer	**Modulus, ksi**	49	41	47	52	26	30	72	69	37	52
	Thickness, in.	Refusal at 5 in.		4.8	4.4	3.7	3.6	4.1	3.5	3.6	3.3
Lower Layer	**Modulus, ksi**	No data		159	229	90	69	229	229	80	96
	Thickness, in.			5.0	5.4	4.0	4.7	5.7	6.3	5.4	6.3
Section Modulus, ksi		45		126		56		167		72	
Section Thickness, in.		10 (assumed)		9.8		8.0		9.8		9.4	

Since the PSPA and core results were available, they were incorporated in the analysis with JIM. The ACP moduli were fixed to the values determined by the PSPA, and the layer thicknesses were based on the GPR results.

The ACP moduli from the PSPA (reported under JIM in Table 6.3) vary from 300 ksi to 400 ksi which is slightly greater than results from SMART. The COVs of moduli from the five sections are less than 8% from the PSPA and less than 14% for SMART. The seismic moduli measured on the cores retrieved from the sites are compared with the field moduli in Table 6.2. The average lab moduli from cores compare reasonably well with the field moduli.

Table 6.2 - Variations of Seismic Moduli and Thickness of ACP Layer from Cores

Section	1 (Roadbond)		2 (CKD)		3 (Fly Ash)		4 (Lime)		5 (Control)	
Core	1	2	1	2	1	2	1	2	1	2
Modulus, ksi	360	421	386	400	369	354	359	336	308	348
Thickness, in.	4.0	3.8	4.0	4.0	4.0	4.5	4.0	4.0	4.0	3.8
Section Modulus, ksi	391		393		361		348		328	
PSPA Modulus, ksi	419		366		402		376		333	
SMART Modulus, ksi	287		299		301		321		253	
Section Thickness, in.	3.9		4.0		4.3		4.0		3.9	

Table 6.3 - Comparison of Backcalculated Results for FM 1062

Section No.		JIM				RMS Error, %	SMART				RMS Error, %	MODULUS				RMS Error, %
		Modulus, ksi					Modulus, ksi					Modulus, ksi				
		ACP	UB	LB	SG		ACP	UB	LB	SG		ACP	UB	LB	SG	
RB	Avg.	419	40	55	16	8.0	287	26	26	21	9.0	500	18	14	22	3.4
	Std Dev	-	6.5	7.6	1.6	-	29.1	6.2	4.2	1.5	-	-	4.8	5.4	2.4	-
	COV	-	16%	14%	10%	-	10%	24%	16%	7%	-	-	27%	38%	11%	-
CKD	Avg.	366	39	62	17	5.1	299	24	29	22	7.5	500	44	30	22	4.4
	Std Dev	-	7.1	9.2	1.5	-	21.2	5.7	4.6	0.0	-	-	21.9	34.3	1.9	-
	COV	-	18%	15%	9%	-	7%	24%	16%	0%	-	-	50%	115%	8%	-
Flyash	Avg.	402	43	65	14	4.2	301	30	33	22	7.5	500	15	16	20	4.8
	Std Dev	-	7.2	10.1	1.9	-	27.9	5.3	4.2	0.0	-	-	7.1	8.1	2.7	-
	COV	-	16%	15%	14%	-	9%	18%	13%	0%	-	-	47%	51%	14%	-
Lime	Avg.	376	60	82	19	4.8	321	68	57	22	7.2	500	52	76	26	4.5
	Std Dev	-	15.0	21.4	3.4	-	33.8	14.7	18.7	1.0	-	-	15.8	54.8	4.0	-
	COV	-	25%	26%	18%	-	11%	22%	33%	5%	-	-	31%	72%	16%	-
Control	Avg.	333	33	54	18	7.1	253	37	48	22	7.5	500	13	85	24	3.8
	Std Dev	-	5.4	6.2	3.3	-	35.1	8.2	9.7	1.5	-	-	9.1	53.8	4.4	-
	COV	-	16%	12%	19%	-	14%	23%	20%	7%	-	-	72%	63%	18%	-

The moduli of the upper base from the three methods are presented in Table 6.3. The moduli from JIM and SMART are generally greater than the backcalculated moduli from MODULUS

The COVs of the upper base moduli are the smallest for the results from JIM and the greatest for MODULUS. In some cases, the COVs of the upper base moduli from JIM are much smaller than SMART. From all three analyses, the base treated with CKD is the stiffest. From MODULUS and JIM, the lime-treated base is the second stiffest, while from SMART the base treated with fly ash is the second stiffest. The trends exhibited by MODULUS and JIM are in agreement with those reported for the DCP.

From JIM, the modulus of the lower base for each section is always greater than the upper base, as anticipated. SMART and MODULUS do not exhibit the same trend. For SMART, the moduli of the upper and lower bases are generally similar; whereas for the MODULUS a general trend between the upper and lower cannot be found. The least variability in the lower base modulus is observed with SMART, followed by JIM. The COVs of the moduli from MODULUS are typically greater than 40%.

Resilient modulus tests were also carried out on the five base blends. Tests were carried out at 15 different deviatoric stresses and confining pressures to characterize the nonlinear behavior of the materials. The nonlinear relationship considered is:

$$M_R = K_1 \, \sigma_c^{K2} \, \sigma_d^{K3} \tag{6.1}$$

were M_R = resilient modulus, σ_c = confining pressure and σ_d = deviatoric stress. Parameters K_1 through K_3 are determined through curve fit to the data collected.

The results from the resilient modulus tests are summarized in Table 6.4. The specimens, which were nominally 6 in. in diameter and 12 in. in height, were prepared, compacted and cured as per TxDOT specifications. Since TxDOT does not have any provisions for the mixing and preparing specimens with Roadbond, the specification provided by the supplier was followed.

Parameter K_1 is an indication of the modulus at small stresses. For that term, the CKD provided the stiffest material followed by the Roadbond and fly ash. The raw material provided the least stiff material. Parameter K_2 provides information with regards to strength hardening of the materials. In that sense, the CKD is the least stress sensitive material and the raw base the most. Parameter K_3, which can be used to interpret the strain-softening of the materials, is similar for all five materials.

Table 6.4 - Resilient Modulus Test Results

Stabilizing Agent	Nonlinear Parameters*				Representative Modulus, ksi			
	K_1, ksi	K_2	K_3	R^2	Lab	JIM	SMART	MODULUS
3% Roadbond	72	0.21	-0.14	0.93	69	48	26	16
2% CKD	422	0.00	-0.14	0.90	289	51	27	35
8% Fly Ash	49	0.27	-0.12	0.93	55	54	32	15
3% Lime	25	0.44	-0.12	0.92	37	72	63	64
Control (None)	10	0.61	-0.11	0.96	20	44	43	48

To compare the lab moduli under comparable conditions under wheel loads, the resilient modulus at a confining pressure of 5 psi and deviatoric stress of 15 psi was calculated and reported in Table 6.4. In this case, the CKD is the stiffest material followed by Roadbond and Fly ash.

Seismic modulus tests were also carried out on the materials. Since seismic tests are nondestructive, the same specimen can be tested repeatedly with time. The moisture susceptibility test as described in Tex-149 was carried out on each specimen. The specimen preparation for these tests is different to be more representative of the behavior of the material in the field. For all materials, the base, additives and necessary amount of water to achieve optimum moisture content was thoroughly mixed and compacted in a concrete mold equipped with small holes at the bottom. The specimen was then air-dried for twenty four hours and tested to obtain the initial seismic modulus. The specimen was then placed in a 40°C oven for four days, after which transferred into a shallow water container and allowed to soak water for 6 days. Each day, the specimen was tested to obtain the seismic modulus. The modulus immediately after removing the specimen from the oven is termed the maximum seismic modulus. The residual seismic modulus is the average moduli of the last three days of soaking.

The seismic moduli described above are reported for the five materials in Table 6.5. The initial moduli correspond to moduli shortly after the placement and compaction of the materials in the field. In this case, the CKD provide the highest modulus followed by fly ash and lime. The Roadbond and the raw materials exhibited similar but lower initial moduli as compared to the other materials. As indicated in Nazarian et al. (2003), an initial modulus of about 100 ksi is considered reasonable for a durable and well-constructed base.

Table 6.5 - Seismic Modulus Test Results on Base Materials

Stabilizing Agent	Field Modulus, ksi			Seismic Lab Modulus			
	JIM	SMART	MODULUS	Initial, ksi	Maximum, ksi	Residual, ksi	Residual-to-Peak Ratio
3% Roadbond	48	26	16	68	214	21	0.10
2% CKD	51	27	35	575	668	653	0.98
8% Fly Ash	54	32	15	162	345	141	0.41
3% Lime	72	63	64	165	433	136	0.31
Control (None)	44	43	48	62	186	17	0.09

The maximum modulus, relate to the undesirable condition when the base layer is allowed to excessively dry before it is covered. The best materials are those that would not exhibit large differences between the initial and maximum moduli. In this term, the CKD is performing better than the other materials.

The residual modulus exhibit the softening of a well-constructed base when exposed to moisture. An ideal base would provide residual modulus that is close to the initial modulus. Nazarian et al. (2003) suggest that for un-stabilized flexible bases, the ratio of the residual to peak modulus may

be a good indicator of the long term performance of the material. The value of 0.09 for the control material indicates that the raw material may exhibit excessive softening due to exposure to moisture. The Roadbond material exhibits a similar pattern. The other three materials demonstrate less softening tendency when exposed to moisture.

It should be emphasized that the laboratory test results provide information about the suitability of the material assuming good construction practice. Field tests can be used to obtain information about the quality of construction and the material.

The subgrade layer moduli from the three analyses are fairly similar. MODULUS yields slightly higher subgrade moduli as compared to JIM and SMART. The backcalculation RMS errors for the three methods are reasonably low for this site, with SMART providing the highest mismatch.

The thicknesses of the ACP and base layers from JIM, GPR and SASW are compared with the representative thicknesses measured in the field in Figure 6.1. As a reminder, the SASW analysis is part of the analysis performed for SMART (see Chapter 5). As shown in Figure 6.1a, all three analyses methods exhibit similar trends, with the Roadbond and control sections having a thinner ACP layer and the section with lime-treated base being the thickest. The thicknesses from JIM vary between 2 in. to 2.5 in., the SASW method between 2.5 in. to 3 in., and the GPR between 3 in. to 3.5 in. However, the thicknesses from the cores vary between 4 in. and 4.5 in. All three methods under estimated the thickness. JIM seems to be reporting the thickness of the upper ACP since the ACP was placed in two lifts approximately a year apart. The SASW under-predicts the thickness of the ACP perhaps because the lower layer was less stiff as the top ACP layer.

The thicknesses of the base layer are presented in Figure 6.1b. The SASW thicknesses vary between 9 in. and 10 in. JIM thicknesses are similar to those from the SASW for three of the five sections. The JIM thickness for the CKD section is smaller than the SASW thickness, and for the lime treated section greater. The thicknesses from the GPR vary between 10 in. and 14 in. The actual base thickness from the DCP is between 8 in. and 10 in.

The results from the data fusion activities are summarized in Table 6.6. Overall, the fused ACP moduli are fairly consistent across the sections. This statement also applies to the subgrade fused moduli.

The fused values for the base layer show that the upper base values for Roadbond are as low as the control section. The trend is worse for the lower base where Roadbond is lower in some cases than the control section. This is a case where combining the results from all three methods is not the best solution since there is a large difference in the results of the NDT analyses. MODULUS results in Table 6.3 reports layer moduli to be very low, at 14 ksi in some cases. This indicates that a very bad base layer exists. Additional information about the site as the result of DCP analysis suggests that the base is much stronger. JIM and SMART are more representative of the results. In this case, the choice for fusing the data would improve if MODULUS is excluded from the analysis. As for the subgrade, the results seem representative of all the three fusion methods.

Station Number

| | Rb | CKD | Flyash | Lime | Control |

a) ACP

✳—— SASW   ☐—— GPR   ◯—— JIM   + Core

Station Number

| | Rb | CKD | Flyash | Lime | Control |

b) Base

✳—— SASW   ☐—— GPR   ◯—— JIM
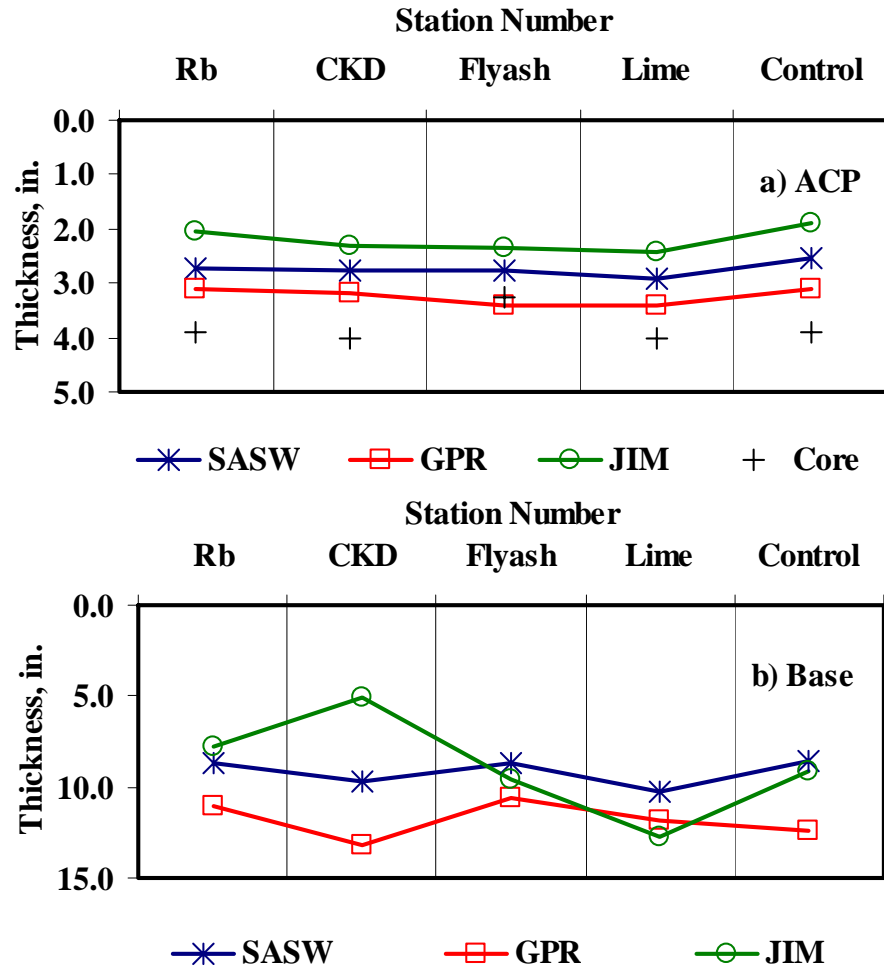
Figure 6.1 - Comparison of Thickness Values for FM 1062

Table 6.6 - Data Fusion Results for FM 1062

Method	Section No.	Modulus, ksi							
		ACP		Upper Base		Lower Base		Subgrade	
		Avg.	COV	Avg.	COV	Avg.	COV	Avg.	COV
SWA	RB	287	10%	26	18%	33	13%	18	6%
	CKD	299	7%	39	25%	49	29%	19	8%
	Flyash	301	9%	28	39%	31	33%	18	4%
	Lime	321	11%	76	16%	81	27%	19	7%
	Control	253	14%	22	47%	33	22%	19	9%
WA	RB	402	3%	28	11%	32	8%	20	7%
	CKD	388	2%	36	26%	39	26%	21	8%
	Flyash	401	3%	29	18%	38	14%	19	8%
	Lime	399	3%	61	15%	72	23%	22	11%
	Control	362	4%	28	36%	62	35%	21	14%
FL	RB	342	6%	32	17%	32	19%	20	6%
	CKD	338	5%	35	19%	51	22%	20	4%
	Flyash	352	5%	30	24%	35	14%	18	7%
	Lime	388	6%	65	13%	73	14%	22	11%
	Control	344	10%	25	42%	41	25%	21	15%

TxDOT Parking Lot (El Paso)

The TxDOT parking lot site was analyzed as a three layer system with 2-in.-thick ACP over 6 in. of granular base over subgrade. This site had one section that was tested six times for repeatability purposes. Data was collected with the SPA and FWD. The summary of the six tests are presented in Table 6.7. The first observation made is that the results from each test seem repeatable for all the three analyses. The average moduli are fairly close for each repeated tests. As far as the comparison across the three sets of results (JIM, SMART, and MODULUS), the layer moduli reported by JIM for the ACP and base layers are higher than those from both SMART and MODULUS. The results of the subgrade layer are similar for all three methods with JIM being slightly lower. On the other hand, the variability of JIM results is much smaller than the results of the other two methods, especially for the base layer. The COV values for the ACP layer are similar for JIM and SMART (less than 20%). The base layer moduli using JIM show consistency with COVs of around 20%. However, for the SMART and MODULUS the variability is twice as high reaching 50% in some cases. For the subgrade layer, the three methods yield similar results with similar COVs, with the results from SMART being more variable. The RMS errors for all three methods were reasonably low with JIM having the least error. This site demonstrates JIM results to be the most consistent of the three.

The results from the data fusion process using DFINE are summarized in Table 6.8 along with the simple averages of the results from JIM, SMART and MODULUS results. For this particular case, where the section was tested six times, the results from all repeat tests are combined.

In general, each method provides a different set of moduli. Without a means of fusing the data, a person interpreting the results can only use subjective means to select the set of layer moduli to use. One solution could be selecting the set of results with the lowest overall variability, which in this case is JIM. However, by using DFINE and fusing the three methods, a more rational estimation of the layer moduli is carried out. For this site, the ACP and subgrade average moduli from the three fusion methods are comparable. The average moduli of the base from the three fusion methods vary from a minimum of 118 ksi to a maximum of 151 ksi. For this layer, the modulus of the base is more influenced by the nonlinear modulus obtained from the seismic methods as opposed to the deflection-based methods. This occurs because the base layer is too thin to substantially impact the deflection basin.

Another aspect of the data fusion results is the variability associated with it. For the base layer, the COVs are much smaller for the WA and FL methods with values of 27% and 29% as compared to the SWA with a COV of 42%. The same pattern is also reflected in the results of the ACP layer. This pattern can be interpreted as the WA and FL techniques providing results with higher level of certainty as compared to the values reported from the SWA method. The variability in the reported subgrade moduli is similar for all the three fusion techniques.

Eagle Pass Inspection Facility (Laredo)

Two sections of this site were tested by TxDOT personnel as a part of a forensic study. This section was analyzed as a 2-in.-thick ACP over 12 in. of base over subgrade. The base was slightly stabilized with cement. The two sections analyzed were Strip 2 and Strip 4 as listed in Table 6.9. The moduli from JIM, SMART and MODULUS are consistently greater for Strip 2 as compared to Strip 4. The average ACP modulus for JIM is comparable to SMART (ACP

70

Table 6.7 - Comparison of Backcalculated Results for TxDOT Parking Lot

Section No.		JIM				SMART				MODULUS			
		Modulus, ksi			RMS Error, %	Modulus, ksi			RMS Error, %	Modulus, ksi			RMS Error. %
		ACP	Base	SG		ACP	Base	SG		ACP	Base	SG	
Test 1	Average	570	214	17	2.8	471	176	21	5.7	500	73	21	7.0
	Std Dev	92.0	38.3	1.6	-	69.6	76.2	6.0	-	-	36.3	2.1	-
	COV	16%	18%	10%	-	15%	43%	28%	-	-	49%	10%	-
Test 2	Average	563	212	17	2.8	456	179	20	5.6	500	69	21	7.1
	Std Dev	79.1	37.6	1.8	-	74.6	78.9	3.2	-	-	35.0	2.2	-
	COV	14%	18%	10%	-	16%	44%	16%	-	-	51%	10%	-
Test3	Average	564	209	17	2.7	473	173	21	5.5	500	67	21	6.6
	Std Dev	79.6	48.1	1.8	-	79.3	74.1	3.9	-	-	34.1	2.2	-
	COV	14%	23%	11%	-	17%	43%	19%	-	-	51%	10%	-
Test 4	Average	586	211	17	2.6	518	165	17	5.1	500	70	21	7.0
	Std Dev	78.8	40.2	1.7	-	48.8	69.7	3.8	-	-	30.7	2.2	-
	COV	13%	19%	10%	-	9%	42%	22%	-	-	44%	10%	-
Test5	Average	584	196	17	2.8	509	166	17	4.8	500	66	21	6.9
	Std Dev	108.3	47.2	1.8	-	68.8	72.8	2.9	-	-	28.6	2.2	-
	COV	19%	24%	11%	-	14%	44%	18%	-	-	44%	10%	-
Test 6	Average	573	203	17	2.8	503	169	17	5.5	500	62	21	6.3
	Std Dev	84.7	45.0	1.8	-	70.0	77.3	2.7	-	-	28.3	2.5	-
	COV	15%	22%	11%	-	14%	46%	16%	-	-	45%	12%	-

Table 6.8 - Data Fusion Results of the Average of All Six Tests for TxDOT Parking Lot

Method	Modulus, ksi					
	ACP		Base		Subgrade	
	Average	*COV*	Average	*COV*	Average	*COV*
JIM	**573**	*15%*	**208**	*21%*	**17**	*10%*
SMART	**489**	*14%*	**171**	*44%*	**19**	*20%*
MODULUS	**500**	-	**68**	*47%*	**21**	*10%*
SWA	**538**	*12%*	**118**	*42%*	**19**	*7%*
WA	**536**	*8%*	**151**	*27%*	**19**	*8%*
FL	**533**	*7%*	**140**	*29%*	**19**	*7%*

Table 6.9 - Comparison of Backcalculated Results for Eagle Pass Inspection Facility (Laredo)

Section No		JIM			RMS Error, %	SMART			RMS Error, %	MODULUS			RMS Error, %
		Modulus, ksi				Modulus, ksi				Modulus, ksi			
		ACP	Base	SG		ACP	Base	SG		ACP	Base	SG	
Strip2	**Average**	**490**	**240**	**28**	**3.7**	**420**	**223**	**39**	**6.0**	**500**	**105**	**41**	**12.0**
	Std Dev	*86.5*	*37*	*8*	*-*	*64.6*	*63.5*	*9.6*	*-*	*-*	*40.3*	*13.2*	*-*
	COV	*18%*	*15%*	*28%*	*-*	*15%*	*28%*	*25%*	*-*	*-*	*38%*	*32%*	*-*
Strip4	**Average**	**440**	**203**	**26**	**3.8**	**389**	**167**	**38**	**6.4**	**500**	**93**	**36**	**11.1**
	Std Dev	*175.7*	*54.2*	*6.1*	*-*	*119.7*	*91.2*	*7.4*	*-*	*-*	*57.4*	*9.7*	*-*
	COV	*40%*	*27%*	*23%*	*-*	*31%*	*55%*	*20%*	*-*	*-*	*62%*	*27%*	*-*

modulus was fixed in MODULUS). The ACP layer modulus is less variable for Strip 2 (with a COV of up to 18%) than for Strip 4 (with a COV of up to 40%) from both JIM and SMART with the highest variability being 40% for Strip 4. This occurs because the ACP along Strip 4 contained more severe cracks than Strip 2. The average base moduli were the highest for JIM and the lowest for MODULUS. The base moduli from JIM were comparable to those from SMART. This indicates that the seismic results influence the modulus of the base more than the deflections. The COVs of base moduli from JIM are much smaller than those from the SMART and MODULUS for both Strip 2 and Strip 4, indicating that the seismic and deflection results are complementing one another. For the subgrade, JIM yields lower moduli than SMART and MODULUS. As such, the deflections from FWD are controlling the results from the subgrade layer. The subgrade modulus COVs from the three methods are fairly close, with the FWD providing the highest variability. The RMS errors from backcalculation are the highest from the FWD with about 12%, and the lowest from JIM with less than 4%. This is another indication that the seismic results and the deflections contain complementary information that can provide moduli with greater certainty.

The results of the data fusion process using DFINE for Strip 2 and 4 are summarized in Table 6.10. Since the average moduli from the ACP and subgrade from JIM, SMART, and MODULUS are reasonably similar, the fused values are also reasonably similar. The benefit of the fused values is the reduced uncertainty reflected in the COVs. For the base layer, the fused moduli are somewhere between those obtained from MODULUS and those from the JIM and SMART. Since the backcalculation errors are smaller for JIM and SMART and since the material was stabilized the higher moduli seem more plausible. Even though all three data fusion processes exhibit a reduced uncertainty for both sections, the COVs are lower for the WA and FL methods.

Table 6.10 - Data Fusion Results for Eagle Pass Inspection Facility (Laredo)

Method	Modulus, ksi					
	ACP		Base		Subgrade	
	Average	COV	Average	COV	Average	COV
JIM	465	29%	222	21%	27	26%
SMART	405	23%	195	42%	39	23%
MODULUS	500	-	99	50%	38	30%
SWA	424	24%	146	46%	30	20%
WA	459	16%	169	29%	34	19%
FL	451	12%	165	31%	33	20%

IH - I20 (Odessa – Ward County)
This site nominally consisted of 5 in. of ACP over 18 in. of granular base over subgrade. This site was tested before the site was rehabilitated. The main concern was with the quality of in-place base due to moisture migration in some areas. The site was divided into four sections. Sections 1, 2 and 4 were particularly of interest because of perceived moisture migration and surface cracks. As shown in Table 6.11, this site consisted of a fairly strong pavement. The DCP tested were attempted at a number of locations in all four sections by the District staff, but in all cases it could not be penetrated more than a couple of inches.

Table 6.11 - Comparison of Backcalculated Results for I20 Odessa (next to Ward)

Section No.		JIM				SMART				MODULUS			
		Modulus, ksi			RMS Error, %	Modulus, ksi			RMS Error, %	Modulus, ksi			RMS Error, %
		ACP	Base	SG		ACP	Base	SG		ACP	Base	SG	
1	Average	586	145	52	3.3	465	112	129	6.2	561	62	71	9.8
	Std Dev	85.6	47	15	-	53.9	34.4	12.0	-	163.4	15.4	19.8	-
	COV	15%	33%	28%	-	12%	31%	9%	-	29%	25%	28%	-
2	Average	682	137	55	2.9	516	122	137	5.3	803	49	76	6.0
	Std Dev	94.5	29.6	24.4	-	57.6	31.4	15.4	-	252.5	16.9	32.7	-
	COV	14%	22%	44%	-	11%	26%	11%	-	31%	34%	43%	-
3	Average	914	224	57	3.0	692	184	128	6.0	1682	96	80	5.4
	Std Dev	76.9	33.0	19.0	-	50.5	38.8	17.3	-	394.3	22.7	31.1	-
	COV	8%	15%	33%	-	7%	21%	14%	-	23%	24%	39%	-
4	Average	706	140	50	3.4	545	119	131	5.4	935	48	70	10.0
	Std Dev	62.8	31.6	8.6	-	37.2	16.8	17.7	-	318.6	12.1	11.4	-
	COV	9%	23%	17%	-	7%	14%	14%	-	34%	25%	16%	-

From JIM, SMART and MODULUS, Section 3 exhibited significantly higher ACP modulus. SMART provides reasonably similar ACP moduli for the other three sections, while MODULUS provides lower moduli for Section 1. The ACP moduli from SMART exhibit a much lower variability (with the highest COV being 12%), while the COV from MODULUS is the highest (with the lowest COV of 23%). Since the thickness of the ACP layer is about 5 in., the ACP moduli estimated by JIM are somewhat affected by the deflections from FWD. As such, JIM provides somewhat higher moduli than the SMART. The base moduli estimated by JIM are somewhat greater than those from SMART, with base modulus from MODULUS for all sections being significantly lower. For this site, the COVs of the base moduli from the three methods are close ranging from 15% to 34%. For the subgrade layer, moduli from JIM and MODULUS are reasonably close with JIM estimating slightly lower values in most cases. This can be translated to the fact that the moduli of the subgrade from JIM are for the most part controlled by the deflection data. The subgrade moduli from SMART are much greater than those from the other two methods. This occurs because the seismic data only samples the first couple of feet of the subgrade, whereas the FWD samples the subgrade much deeper. The COVs of subgrade moduli are rather small for the SMART and typically much greater for the MODULUS and JIM, probably because of the vicinity of a stiff subgrade layer near the surface. The RMS errors from backcalculation for all three methods are less than 10% with JIM exhibiting the lowest errors and the MODULUS the highest.

The averages of the three methods and the fused results for the four sections analyzed at this site are presented in Table 6.12. For this site, the ACP layer modulus was highest for MODULUS with a value of 995 ksi and a variability of 29% and lowest for SMART with a value of 555 ksi and a variability of 9%. The ACP modulus value for JIM is in between the other two methods reported. The moduli from MODULUS and SMART for the lower layers exhibit a different trend. SMART reports stiff base and very stiff subgrade with values of 134 ksi and 131 ksi respectively. On the other hand, MODULUS reports a weaker base and subgrade with values of 64 ksi and 74 ksi respectively. JIM provides a compromise of the two methods with a stiff base layer with a value of 162 ksi and a subgrade closer to what MODULUS reports with a value of 54 ksi. The variability of the fused results for the ACP layer is similar with COVs less than 16%. The fused moduli for the base layer vary from 94 ksi for SWA to 120 ksi for WA. The fused results of the subgrade are consistent at around 85 ksi for all fused methods. Overall, the results show a good quality ACP, base and subgrade layers for this site.

Table 6.12 - Data Fusion Results for I20 Odessa (next to Ward)

Method	Modulus, ksi					
	ACP		Base		Subgrade	
	Average	*COV*	Average	*COV*	Average	*COV*
JIM	722	*12%*	162	*22%*	54	*30%*
SMART	555	*9%*	134	*23%*	131	*12%*
MODULUS	995	*29%*	64	*27%*	74	*32%*
SWA	601	*10%*	94	*25%*	80	23%
WA	753	*16%*	120	*17%*	86	17%
FL	708	*13%*	114	*18%*	88	16%

IH - I20 (Odessa – Ector County)
The section nominally consisted of as a 3.5-in.-thick ACP over a 22-in.-thick base over subgrade. This site was visited as part of a forensic study to investigate and verify the strength of the base layer. Four sections of this road were tested. Section 1 exhibited evidence of rutting and in some area pumping. The other three sections contained the early indications of these types of distress.

The results from the JIM, SMART and MODULUS analyses are summarized in Table 6.13. The ACP moduli estimated from both JIM and SMART, ranging between 300 ksi and 375 ksi, indicate that the layer is below average. On the other hand the moduli estimated with MODULUS indicate that the ACP for Sections 1 and 4 being reasonable while Sections 2 and 3 were consistently weak. The lower than expected moduli from all sections were verified by performing laboratory seismic tests and by determining the air voids of cores extracted from the site (about 12%). While the COVs from JIM and SMART were typically less than 20%, the COVs from MODULUS were typically in excess of 30%.

The base moduli also varied between those estimated by JIM and SMART and those of MODULUS. Moduli from SMART indicate that the base is reasonably strong with values ranging from 70 ksi to 90 ksi, contradicting the results of MODULUS where the base moduli where about 35 ksi. From JIM, the base moduli are closer to SMART than MODULUS indicating that the seismic method is controlling the results of JIM analysis more than the FWD deflections. The DCP results, when it could penetrate through base, indicate an average modulus of about 55 ksi, with top 5 in. being less stiff and the bottom layer being stiffer than 80 ksi.
The COVs of the base moduli from JIM varied from 20% to 40%, from SMART from 20% to 30%, and from MODULUS from 20% to 60%.

The subgrade moduli from MODULUS and SMART were reasonably similar and in the range of about 80 ksi. But the moduli from JIM were consistently lower than those from SMART and MODULUS being in the range of 60 ksi. An explanation of this trend is warranted. Based on extensive past experience at this site location (Abdallah et al., 2002), the subgrade is reasonably thin and reasonably soft. A stiff layer is encountered at about a depth of 4 ft to 5ft from the pavement surface. As such the soft subgrade is about 15 in. to 20 in. thick. Under this condition, the FWD analysis typically over-estimates the modulus of the subgrade. To compensate for this over-estimation, the base modulus is under-estimated. The SMART analysis would typically miss this layer if the subgrade is modeled as a single layer. As such, the moduli obtained from the MODULUS and SMART are fortuitously close. At this site, when the deflection and seismic data are combined in JIM, the moduli of the base are controlled by the seismic data, as indicated before. This will allow for the deflection data to control the estimation of the moduli of the subgrade. As such, the subgrade moduli estimated by JIM are lower than the other two methods. However, based on our past experience, the reported subgrade moduli for JIM is higher than it should have been, and are composite values for the actual subgrade and the stiff underlying layer.

Finally, the RMS errors due to backcalculation are usually lower than 10% for the three methods, with JIM yielding the lowest values and MODULUS the highest.

76

Table 6.13 - Comparison of Backcalculated Results for I20 Odessa

Section No.		JIM				SMART				MODULUS			
		Modulus, ksi			RMS Error, %	Modulus, ksi			RMS Error, %	Modulus, ksi			RMS Error, %
		ACP	Base	SG		ACP	Base	SG		ACP	Base	SG	
1	Average	373	70	48	3.6	329	69	84	4.6	512	31	65	9.0
	Std Dev	64.8	15	17	-	51.6	16.4	13.3	-	248.2	18.0	22.7	-
	COV	17%	22%	36%	-	16%	24%	16%	-	48%	58%	35%	-
2	Average	334	76	59	3.9	313	72	87	5.6	394	34	85	8.8
	Std Dev	36.2	14.6	14.3	-	29.6	20.2	13.8	-	119.1	7.5	30.2	-
	COV	11%	19%	24%	-	9%	28%	16%	-	30%	22%	35%	-
3	Average	346	96	63	4.9	322	90	102	5.0	318	37	107	12.7
	Std Dev	62.5	36.1	21.6	-	42.6	24.1	12.0	-	115.6	21.8	92.2	-
	COV	18%	38%	35%	-	13%	27%	12%	-	36%	59%	86%	-
4	Average	362	84	58	4.7	316	91	101	4.9	529	31	86	10.5
	Std Dev	64.2	16.6	18.8	-	49.9	20.7	14.8	-	219.8	7.1	37.2	-
	COV	18%	20%	32%	-	16%	23%	15%	-	42%	23%	43%	-

The site average moduli for each method and fused values are summarized in Table 6.14. JIM and SMART results match more closely than the results of MODULUS. For this site, moduli from MODULUS exhibit the highest variability for all layers. The ACP moduli from the fused results vary between 330 ksi to 370 ksi. The SWA method reported the lowest values for all layers. WA and FL methods reported similar results. The COVs did not exceed 25% in all cases.

Table 6.14 - Data Fusion Results for I20 Odessa

Method	Modulus, ksi					
	ACP		Base		Subgrade	
	Average	COV	Average	COV	Average	COV
JIM	354	16%	82	25%	57	31%
SMART	320	14%	81	26%	94	15%
MODULUS	438	39%	33	41%	86	50%
SWA	332	12%	50	20%	76	16%
WA	371	17%	65	16%	79	23%
FL	360	16%	62	16%	79	15%

US380 (Lubbock)
Four sections were tested on US 380 near Lubbock. The pavement system consisted of a 2-in.-thick ACP (several layers of surface treatment) over a 10-in.-thick base over subgrade. The results from the analyses at this site are summarized in Table 6.15. The ACP moduli from JIM and SMART are similar with an average moduli close to 300 ksi. However, the COVs of the ACP moduli from for both JIM and SMART are quite high. Such a high variability is contributed to the nature of the mix used and the distresses observed at the site. The ACP modulus from MODULUS was fixed at 500 ksi, since the layer was only 2 in. thick.

The base moduli from JIM are greater than those from either SMART or MODULUS. The reason for this matter can be attributed to the contribution of the deflections to the determination of the base modulus. The base moduli estimated by MODULUS were around 20 ksi, which seems low based on the field observations. This could also be due to fixing the ACP modulus at 500 ksi. For SMART the base moduli are around 50 ksi to 60 ksi, while JIM yields base moduli in the range of 80 ksi to 110 ksi. The COVs for base moduli are the lowest for JIM, followed by SMART and MODULUS.

The subgrade moduli were fairly similar for JIM and MODULUS (in the range of 13 ksi to 19 ksi), indicating that the deflections are controlling the determination of the subgrade modulus more than seismic data. SMART on the other hand yields moduli that are in the range of 20 ksi to 26 ksi). In terms of backcalculation mismatch, the RMS errors are the lowest for JIM, reasonably low for SMART and reasonably high for MODULUS

The site averages and fused values are summarized in Table 6.16. The fused ACP moduli for the four sections are around 300 ksi to 350 ksi, mostly controlled by the seismic methods. The fused base moduli are lower for the SWA method because of the influence of the results from MODULUS. The fused base moduli are similar from the WA and FL methods, and more influenced by JIM and SMART. The fused subgrade moduli fall in a reasonably narrow band, and mostly influenced by the MODULUS and JIM results.

Table 6.15 - Comparison of Backcalculated Results for US380

Section No.		JIM Modulus, ksi			JIM RMS Error, %	SMART Modulus, ksi			SMART RMS Error, %	MODULUS Modulus, ksi			MODULUS RMS Error, %
		ACP	Base	SG		ACP	Base	SG		ACP	Base	SG	
EB1	Average	299	83	17	4.1	241	48	25	5.3	500	20	19	34.9
	Std Dev	94.7	39	8	-	91.4	28.8	3.6	-	-	24.7	8.5	-
	COV	32%	48%	45%	-	38%	60%	14%	-	-	126%	46%	-
EB2	Average	330	101	13	4.2	320	62	24	5.7	500	20	14	23.2
	Std Dev	117.5	31.1	4.4	-	86.4	25.4	3.3	-	-	21.7	5.6	-
	COV	36%	31%	34%	-	27%	41%	14%	-	-	107%	39%	-
WB1	Average	320	109	15	4.0	293	62	26	5.7	500	20	17	23.0
	Std Dev	144.1	36.1	5.1	-	124.1	30.2	5.8	-	-	16.1	6.7	-
	COV	45%	33%	34%	-	42%	49%	22%	-	-	80%	40%	-
WB2	Average	262	84	14	4.7	248	56	20	8.4	500	14	14	39.1
	Std Dev	55.9	32.5	3.4	-	54.1	29.7	1.9	-	-	7.5	3.9	-
	COV	21%	39%	25%	-	22%	53%	10%	-	-	53%	27%	-

Table 6.16 - Data Fusion Results for US380

Method	Modulus, ksi					
	ACP Average	COV	Base Average	COV	Subgrade Average	COV
JIM	303	34%	94	37%	15	34%
SMART	276	32%	57	51%	24	15%
MODULUS	500	-	19	92%	16	38%
SWA	292	28%	49	69%	18	19%
WA	359	15%	57	39%	18	19%
FL	337	18%	54	42%	18	17%

APT Section (Austin)

This section was constructed specifically to perform accelerated testing using the Texas Mobile Load Simulator (MLS). The section is divided into four lanes with two shoulders. In Lane 1 of the section, a grid was marked identifying the pad for the first MLS test. The pavement section at this site nominally consisted of 2 in. of ACP over 8 in. of granular base over several layers of clayey subgrade with a stiff layer at a depth of about 100 in. from the pavement surface.

This section was tested twice. In December 2003, the four lanes and the proposed test pad in Lane 1 were tested (see Figures 4.6 and 4.7). During the second visit to the APT section in September 2004, five lanes were tested including three of the lanes tested in 2003 plus the two shoulder lanes. Since the MLS was already was in place, the pad could not be tested. Also due to the malfunction of the FWD, the data from Lane 3 could not be analyzed with JIM. Data presented here is based on tests with the FWD, SPA and PSPA.

The results from the December 2003 tests are summarized in Table 6.17. In the JIM analysis, the ACP moduli from the PSPA were used as fixed values. On the average, the ACP moduli from the JIM and SMART vary between 430 ksi and 510 ksi. The COVs of the ACP moduli for all four sections are less than 12%. The moduli of the base layer from JIM and SMART are similar as well with a value of about 85 ksi to 110 ksi. The base moduli from MODULUS are smaller with a value of about 35 ksi to 50 ksi. The variability in the base moduli for the JIM and SMART is similar and generally less than 20%. For MODULUS, the COVs are typically greater than 20%. The subgrade moduli are the lowest for SMART (around 20 ksi), and the highest for MODULUS (about 30 ksi). Subgrade moduli from JIM are between these two extremes, indicating that the JIM moduli are reasonably equally influenced by the seismic and deflection data. The subgrade modulus COVs are reasonably small for all three methods with a value of less than 15%. The backcalculation RMS errors reported for JIM and SMART are less than 8%, indicating a reasonably good fit between the measured and calculated values. However, the backcalculation RMS errors for MODULUS are significantly greater since they are about 30%. Upon further investigation, this error is largely contributed from the difference between the measured and predicted values of the last two sensors.

The results of the data collected at this site show low variability and good consistency across the sections. As such, the fusion results are comparable to each other. Table 6.18 contains the fusion results. The fused ACP moduli for all sections are on the average around 480 ksi. For the base layer, the average fused modulus is 80 ksi. And for the subgrade, the fused moduli are about 25 ksi. The variability is very low ranging from 3% to 20%. Most of the COVs are close to 10%.

The results from the second visit are included in Table 6.19. The ACP moduli from PSPA for the five lanes are again reported under JIM. These moduli for the three lanes tested in December 2003 (Lane 1, Lan2 and Lane 4) are on the average close to 575 ksi with COVs ranging from 7% to 15%. The moduli from the September 2004 tests are about 100 ksi greater than those measured in December 2003, perhaps due to maturing of the ACP and the weaknesses with temperature adjustment algorithm. The ACP moduli from SMART are somewhat smaller than those from PSPA, but the variability is larger with COV values ranging from 12% to 25%. This occurs because the PSPA source generates wavelengths that are shorter than the SPA; therefore materials closer to the surface are better sampled with the PSPA.

80

Table 6.17 - Comparison of Backcalculated Results for APT (December 2003)

Section No.		JIM			JIM RMS Error, %	SMART			SMART RMS Error, %	MODULUS			MODULUS RMS Error, %
		Modulus, ksi				Modulus, ksi				Modulus, ksi			
		ACP*	Base	SG		ACP	Base	SG		ACP	Base	SG	
L1	Average	435	109	25	2.7	526	99	20	5.3	500	46	29	31.9
	Std Dev	40.0	16	1	-	42.3	13.2	2.1	-	-	9.9	1.7	-
	COV	9.2%	15%	5%	-	8%	13%	10%	-	-	21%	6%	-
L2	Average	509	86	25	3.0	471	96	21	8.0	500	49	29	31.0
	Std Dev	47.3	24.0	1.2	-	44.6	15.3	1.9	-	0.0	14.8	1.5	-
	COV	9.3%	28%	5%	-	9%	16%	9%	-	0%	30%	5%	-
L3	Average	445	102	27	2.7	432	101	21	5.6	500	39	31	31.1
	Std Dev	31.2	13.4	2.9	-	52.5	15.5	3.2	-	-	12.1	3.2	-
	COV	7.0%	13%	11%	-	12%	15%	16%	-	-	31%	10%	-
L4	Average	448	94	27	2.6	510	94	20	5.8	500	37	31	30.6
	Std Dev	26.4	14.1	3.0	-	49.5	6.3	2.6	-	-	11.9	3.7	-
	COV	5.9%	15%	11%	-	10%	7%	13%	-	-	32%	12%	-
PAD	Average	445	103	24	2.6	524	98	19	6.3	500	46	28	32.4
	Std Dev	35.2	17.3	1.2	-	57.7	17.3	2.5	-	-	11.7	2.0	-
	COV	7.9%	17%	5%	-	11%	18%	13%	-	-	26%	7%	-

* - Based on PSPA results

Table 6.18 - Data Fusion Results for APT (December 2003)

Method	Modulus, ksi					
	ACP		Base		Subgrade	
	Average	COV	Average	COV	Average	COV
JIM	456	-	99	17%	26	7%
SMART	493	10%	98	14%	20	12%
MODULUS	500	-	43	28%	30	8%
SWA	493	10%	75	16%	25	4%
WA	483	3%	79	10%	25	5%
FL	486	4%	78	11%	25	6%

Table 6.19 - Comparison of Backcalculated Results for APT (September 2004)

Section No.		JIM				SMART				MODULUS			
		Modulus, ksi			RMS Error, %	Modulus, ksi			RMS Error, %	Modulus, ksi			RMS Error, %
		ACP*	Base	SG		ACP	Base	SG		ACP	Base	SG	
L1	Average	640	84	25	4.6	579	109	21	7.2	500	43	28	40.9
	Std Dev	76.2	13	2	-	69.5	20.5	1.4	-	-	7.6	2.4	-
	COV	12%	16%	8%	-	12%	19%	6%	-	-	18%	8%	-
L2	Average	553	83	26	4.5	453	99	21	7.6	500	41	30	39.6
	Std Dev	68.0	22.7	1.5	-	77.4	30.7	2.1	-	-	10.1	1.7	-
	COV	12%	27%	6%	-	17%	31%	10%	-	-	25%	6%	-
L4	Average	545	95	27	3.5	458	110	23	6.2	500	49	31	36.8
	Std Dev	63.8	16.4	2.3	-	77.4	30.3	2.9	-	-	16.0	2.3	-
	COV	12%	0.2	0.1	-	17%	28%	13%	-	-	33%	7%	-
LL	Average	587	87	26	4.9	472	127	22	7.4	500	52	30	38.9
	Std Dev	42.1	18.4	1.6	-	116.6	28.6	2.1	-	-	12.1	2.1	-
	COV	8%	21%	6%	-	25%	23%	10%	-	-	23%	7%	-
RL	Average	665	66	22	7.2	402	91	23	6.5	500	25	25	31.1
	Std Dev	102.4	36.2	2.1	-	101.0	41.8	2.3	-	-	11.3	2.2	-
	COV	15%	55%	10%	-	25%	46%	10%	-	-	46%	9%	-

* - Based on PSPA results

The base moduli from JIM and SMART are consistent across the sections between the December 2003 and September 2004. The base moduli for the right shoulder are perhaps due to the infiltration of moisture associated with the grading of the site. The base moduli from MODULUS are also consistent between tests carried out in December and September, with an average modulus of around 45 ksi. Again, the right shoulder exhibits smaller moduli as compared to the other lanes

The subgrade moduli from the December 2003 and September 2004 tests are similar for all three methods. The same goes for the variability in subgrade moduli where the COVs are less than 10%. Similar to the December 2003 test results, the backcalculation RMS errors for MODULUS are high compared to the RMS errors of JIM and SMART.

The fused values for this experiement are presented in Table 6.20. Similar to the fused results from data collected in December 2003, the averages moduli are consistent with low COVs across the sections. In this case, the COVs of the WA and FL are much lower, around 6%, for the ACP layer than those of the SWA which range from 10% to 25%. The average fused moduli for the base layer are between 60 ksi and 80 ksi and for the subgrade layer the value is close to 25 ksi.

Table 6.20 - Data Fusion Results for APT (September 2004)

Method	Modulus, ksi					
	ACP		Base		Subgrade	
	Average	*COV*	Average	*COV*	Average	*COV*
JIM	598	-	77	*21%*	25	*7%*
SMART	473	*19%*	107	*29%*	22	*10%*
MODULUS	500	-	42	*29%*	29	*8%*
SWA	475	*19%*	56	*21%*	25	*4%*
WA	541	*3%*	76	*19%*	25	*4%*
FL	518	*6%*	73	*20%*	25	*5%*

CHAPTER SEVEN

SUMMARY AND CONCLUSION

Nondestructive testing technology has made substantial progress in the last two decades. Currently, four NDT devices, the Falling Weight Deflectometer, the Ground Penetrating Radar, the Seismic Pavement Analyzer, and the Portable Seismic Pavement Analyzer, are available to TxDOT for collecting field data. Each of these technologies has been proven instrumental in providing information regarding pavement properties. There are limitations to the capabilities of each of the NDT tools. For this reason, one method has not dominated and proven superior over the others.

As a step towards a fully integrated system, a pilot integration of the software using the current hardware was attempted in this research project. The objective was to harvest the strength of different NDT methods and combine them in a way as to improve the accuracy of the strength parameters used in pavement design and evaluation.

In this project, the strengths and weaknesses of each device were examined to develop a work plan for integrating information collected from each device in a practical manner. The following two approaches were developed: a) joint inversion, and b) data fusion.

The joint inversion method (JIM) was described in Research Report 0-4393-1. In JIM, the raw or processed data from two or more NDT devices are input to an advanced backcalculation program. A user-friendly software package has been developed for use by TxDOT personnel.

The concept of data fusion and the implementation of that concept as pertained to this study were described in Research Report 0-4393-2. Data fusion can be used to integrate the results from different devices in a synergistic way by utilizing the strengths of each method while minimizing the weaknesses. Data fusion allows for logical combining and filtering of information to obtain a composite value or a basis for decision. A user-friendly software package called DFINE has also been developed to conveniently conduct data fusion.

In this report, the two methods have been applied to several sites to demonstrate the practical use of the procedures.

The software package JIM provides the capability of incorporating NDT data from GPR and PSPA as fixed input into the joint analysis in addition to the seismic and FWD data. This provides engineers flexibility to reduce the non-uniqueness inherent in backcalculation while maintaining accuracy. Based on extensive field studies and results from several sites, the joint inversion method provided more robust and realistic results than any traditional methods used individually. The procedure is particularly attractive in the situations where MODULUS has shown weakness in resolving ACP and base moduli values.

Based on the sites analyzed, the moduli from the seismic analysis for the ACP were representative of the materials encountered in the field. Also, the base and subgrade moduli reported by JIM were more consistent with lower variability in comparison with traditional backcalculation methods.

The data fusion methods for the fusion of NDT pavement data was demonstrated using the case studies in this report. The premise of fusing data is to improve accuracy and precision when multiple devices are used to measure the same phenomenon. The fusion methods in DFINE show much promise and potential. This project demonstrated the feasibility and verification of using data fusion to aid pavement analyst in circumstances where multiple devices are used to either support or contradict each other. The fusion tools can be utilized with the purpose of arriving at a more reliable or accurate result than the individual devices would arrive on their own.

The overall results of DFINE showed the ability of the algorithm to rationally combine results from the various NDT analyses. Three methods were used to fuse the data. Considering fusing all three NDT analyses, the fuzzy logic method showed more reasonable outcome compared to the statistical weighted average and the weighted average methods.

REFERENCES

- Abdallah, I., Yuan, D., and Nazarian, S. (2002). "Validation of Software Developed for Determining Design Modulus from Seismic Testing." *Center for Highway Materials Research: Research Report No. 0-1780-5*, The University of Texas at El Paso, El Paso, Texas.

- Abdallah, I., Yuan, D., Nazarian, S., and Ferregut C. (2003). "Feasibility of Integration of Non-Destructive Testing Data Analysis Techniques" *Center for Transportation Infrastructure Systems: Research Report No. 0-4393-1*, The University of Texas at El Paso, El Paso, Texas.

- Bush A. J. (1980), "Development of the Nondestructive Testing for Light Aircraft Pavements," Phase I, Evaluation of NDT Device Report No. FAA-RD-80-9, Washington, D.C.

- Hiltunen, D. R. and Gucunski, N. 1994. Annotated Bibliography on SASW. Geophysical Characterization of Sites, R. D. Woods editor, Oxford and IBH Publishing Comp., New Delhi, 27-34.

- Ke, L., Nazarian, S., Abdallah, I., and Yuan, D., (2002), "A Sensitivity Study of Parameters Involved in Design with Seismic Moduli," Research Report 0-1780-2, Center for Highway Materials Research, the University of Texas at El Paso.

- Lytton R. L., Roberts, R. L., and Stoffels, S., (1985), "Determination of Asphaltic Concrete Pavement Structural Properties by Nondestructive Testing," NCHRP Report No. 10-27, Texas A & M University, College Station, Texas.

- Nazarian, S. 1984. In Situ Determination of Elastic Moduli of Soil Deposits and Pavement Systems by Spectral-Analysis-of-Surface-Waves Method, Ph.D. Dissertation, Department of Civil Engineering, The University of Texas at Austin.

- Nazarian, S. and Desai, M. R. (1993), "Automated Surface Wave Method: Field Testing," Journal of Geotechnical Engineering Division, ASCE, Vol. 119, No. GT7, New York, NY, pp. 1094-1111.

- Nazarian, S., Yuan D. and Baker M. R. (1995), "Rapid Determination of Pavement Moduli with Spectral-Analysis-of-Surface-Waves Method," Research Report 1243-1F, Center for Geotechnical and Highway Materials Research, The University of Texas at El Paso, El Paso, TX, 76 p.

- Nazarian, S., Yuan, D., Tandon, V., and Arellano, M. (2003). "Quality Management of Flexible Pavement Layers with Seismic Methods" *Center for Transportation Infrastructure Systems: Research Report No. 0-1735-3*, The University of Texas at El Paso, El Paso, Texas.

- Stokoe II, H.K., Wright, S.G., Bay, J.A. & J.M. Roesset 1994. Characterization of Geotechnical Sites by SASW Method. In R.D. Woods (ed) Geotechnical Characterization of Sites, Oxford and IBH Publ. Comp., New Delhi, India, 15-26, 1994.

- Uzan J., and Lytton, R. L., (1990), "Analysis of Pressure Distribution Under Falling Weight Deflectometer Loading," Journal of Transportation Engineering, ASCE, Vol. 116, No. 2, New York, NY, pp. 246-251.

- Uzan, J., Scullion, T., Michalek, C. H., and Parades, M., Lytton, R. L. (1988). "A Microcomputer Based Procedure for Backcalculating Layer Moduli from FWD Data." *Texas Transportation Institute: Research Report No. 1123-1*, Texas A&M University, College Station, Texas.

- Williams, R.R., Abdallah, I., and Nazarian, S. (2004). "Implementing Data Fusion Techniques in Non-Destructive Testing of Pavements" *Center for Transportation Infrastructure Systems: Research Report No. 4393-2*, The University of Texas at El Paso, El Paso, Texas.

88

APPENDIX A - Results of Analyses for FM 1062 (Amarillo)

Table A.1 - Results of SASW Analysis for Estimating Seismic Moduli

Section No.		Modulus, ksi				RMS Error, %
		ACP	U. Base	L. Base	Sg	
Rb	Average	824	26	30	24.9	9.2
	Std Dev	83	7	7	3.3	-
	COV	10%	26%	23%	13%	-
CKD	Average	833	40	46	26.5	7.5
	Std Dev	59	9	7	0.0	-
	COV	7%	22%	14%	0%	-
Fly ash	Average	792	30	37	26.5	7.5
	Std Dev	73	5	6	0.0	-
	COV	9%	17%	17%	0%	-
Lime	Average	836	68	72	26.8	7.2
	Std Dev	88	15	25	1.3	-
	COV	11%	22%	34%	5%	-
Control	Average	647	37	49	26.9	7.5
	Std Dev	89	8	10	1.7	-
	COV	14%	22%	20%	6%	-

Table A.2 - Results of SASW Analysis for Estimating Seismic Moduli and Thicknesses

Section No.		Thickness, in.			Modulus, ksi				RMS Error, %
		ACP	U. Base	L. Base	ACP	U. Base	L. Base	Sg	
Rb	Average	2.7	3.9	4.7	1214	44	74	23.1	8.6
	Std Dev	0.3	1.1	1.0	162	8	13	4.4	-
	COV	10%	28%	21%	13%	19%	17%	19%	-
CKD	Average	2.8	4.6	5.1	1106	62	89	23.9	6.9
	Std Dev	0.2	1.2	1.1	100	13	20	3.7	-
	COV	6%	25%	22%	9%	21%	23%	15%	-
Fly ash	Average	2.8	3.9	4.8	1113	54	92	25.8	7.3
	Std Dev	0.1	0.7	1.0	65	11	21	4.1	-
	COV	5%	18%	22%	6%	20%	23%	16%	-
Lime	Average	2.9	4.5	5.7	975	88	123	23.3	8.1
	Std Dev	0.3	0.8	0.4	52	16	27	3.6	-
	COV	9%	17%	7%	5%	18%	22%	16%	-
Control	Average	2.6	3.8	4.9	931	62	92	26.7	6.8
	Std Dev	0.4	0.5	1.2	101	12	24	4.2	-
	COV	15%	14%	24%	11%	20%	26%	16%	-
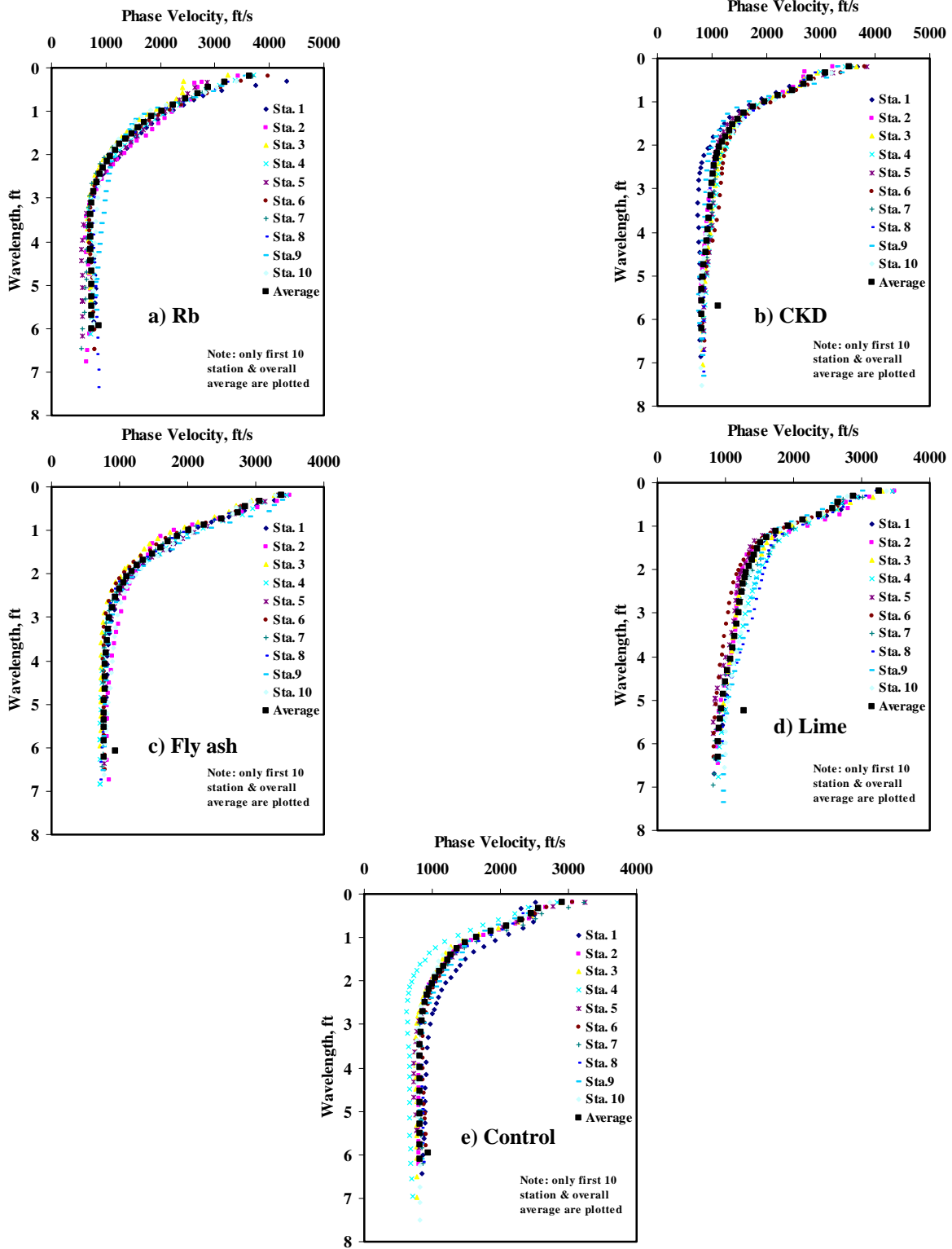
Figure A.1 - Results of Dispersion Curve from SASW Analysis

Figure A.2 - Results of SASW Data Reduction Process (Rb)

Figure A.3 - Results of SASW Data Reduction Process (CKD)

93

Figure A.4 - Results of SASW Data Reduction Process (Fly ash)

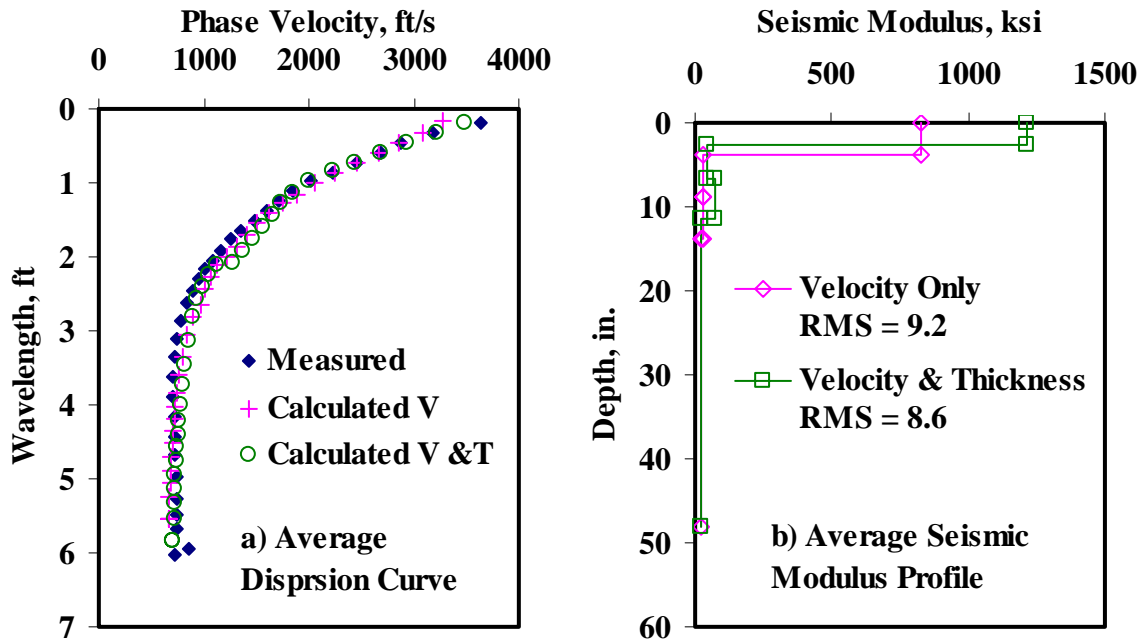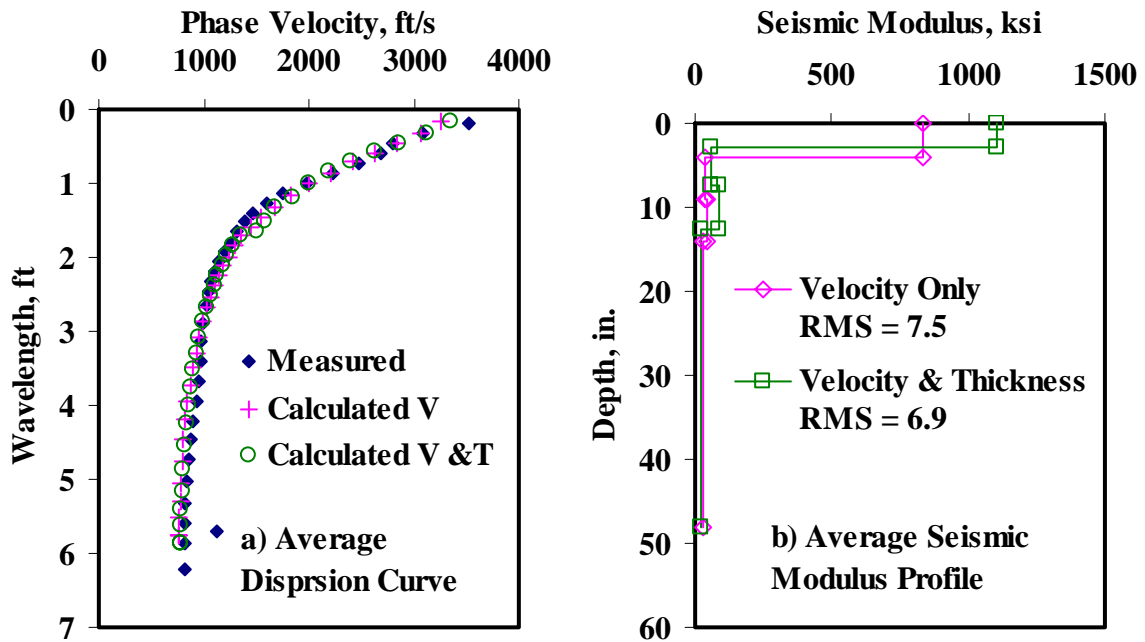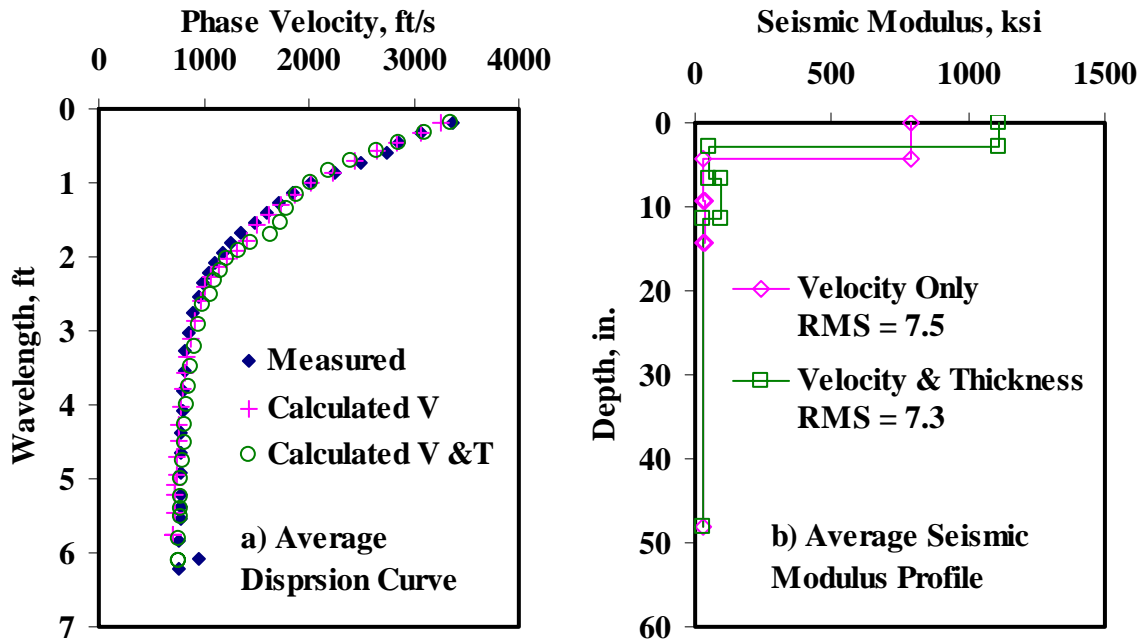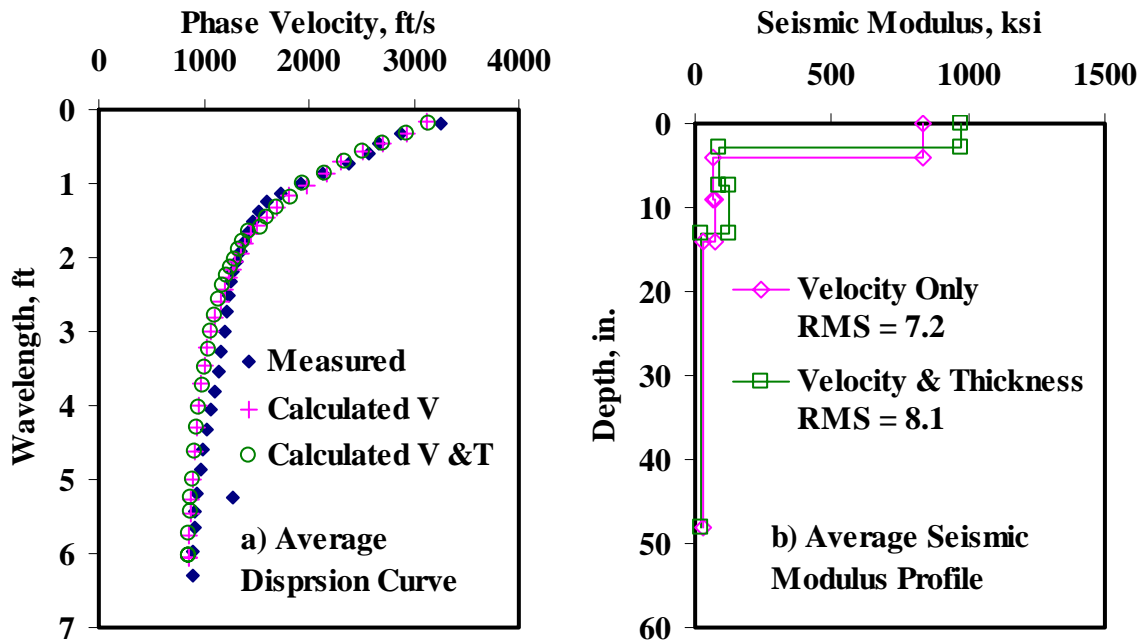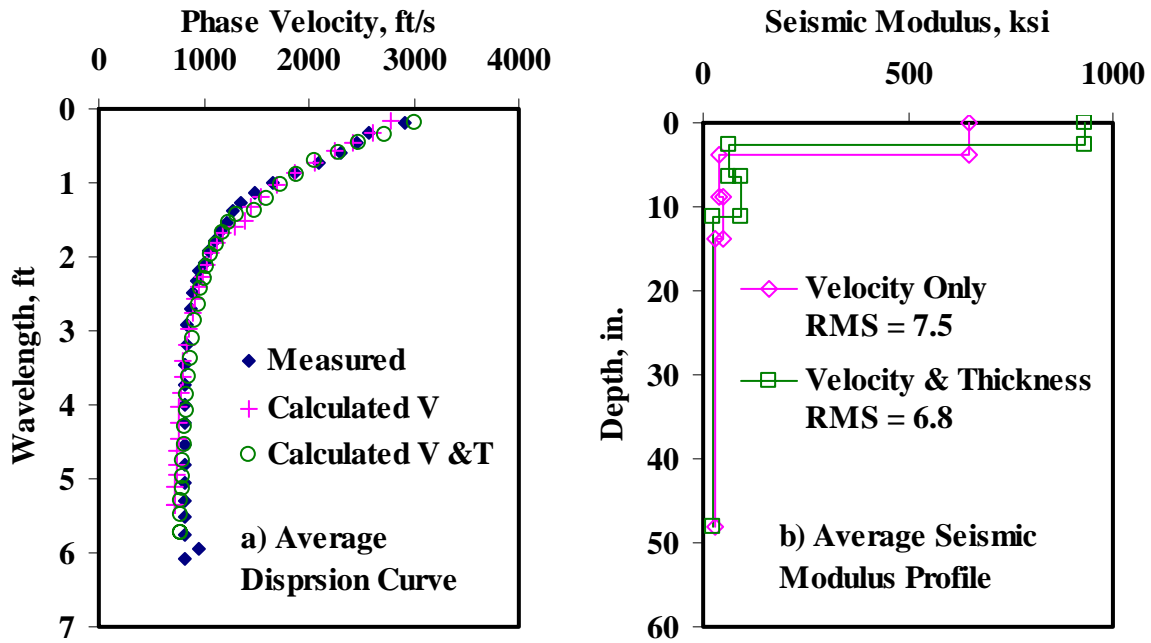**Figure A.5 - Results of SASW Data Reduction Process (Lime)**
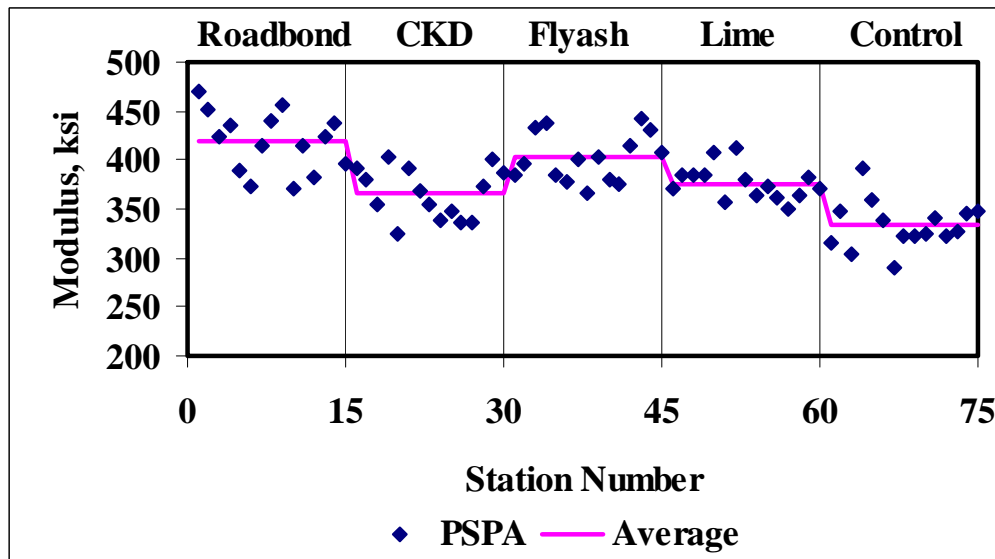
Figure A.6 - Results of SASW Data Reduction Process (Control)

Figure A.7 - Results of PSPA Data Reduction Process

Table A.3 - Results of PSPA Analysis for Estimating Moduli

Section No.	Modulus, ksi		
	Average	Stdev	*COV*
Rb	419	31	*7%*
CKD	366	26	*7%*
Fly ash	402	25	*6%*
Lime	376	17	*5%*
Control	333	24	*7%*

Table A.4 - Results of SMART Analysis for Estimating Design Moduli

Section No.		Modulus, ksi							RMS Error, %
		ACP	Upper Base		Lower Base		Subgrade		
			Cons.	Avg.	Cons.	Avg.	Cons.	Avg.	
Rb	Average	287	25	26	23	26	15	21	9.0
	Std Dev	29.1	5.9	6.2	3.0	4.2	0.9	1.5	-
	COV	10%	23%	24%	13%	16%	6%	7%	-
CKD	Average	299	23	24	28	29	16	22	7.5
	Std Dev	21.2	5.7	5.7	4.6	4.6	0.4	0.0	-
	COV	7%	25%	24%	16%	16%	2%	0%	-
Fly ash	Average	301	30	30	28	33	16	22	7.5
	Std Dev	27.9	5.3	5.3	2.3	4.2	0.5	0.0	-
	COV	9%	18%	18%	8%	13%	3%	0%	-
Lime	Average	321	67	68	52	57	16	22	7.2
	Std Dev	33.8	14.1	14.7	19.1	18.7	0.8	1.0	-
	COV	11%	21%	22%	37%	33%	5%	5%	-
Control	Average	253	37	37	48	48	16	22	7.5
	Std Dev	35.1	8.2	8.2	9.7	9.7	1.1	1.5	-
	COV	14%	23%	23%	20%	20%	7%	7%	-

Table A.5 - Summary Statistics of Measured FWD Deflections

Section No.		Normalized Deflection, mils (12 in. Spacing)						
		d0	d1	d2	d3	d4	d5	d6
Rb	Average	25.3	12.3	5.0	3.1	2.2	1.8	1.4
	Std Dev	3.9	1.5	0.6	0.3	0.2	0.2	0.1
	COV	16%	12%	12%	11%	10%	9%	8%
CKD	Average	19.1	9.9	5.0	3.2	2.2	1.7	1.4
	Std Dev	2.3	1.4	0.5	0.3	0.2	0.1	0.1
	COV	12%	14%	11%	8%	8%	9%	10%
Fly ash	Average	26.1	13.2	5.9	3.5	2.4	1.9	1.6
	Std Dev	3.5	1.8	0.9	0.5	0.3	0.2	0.2
	COV	14%	14%	15%	13%	12%	11%	10%
Lime	Average	14.7	7.6	4.4	2.9	2.0	1.5	1.3
	Std Dev	2.7	1.7	1.0	0.6	0.4	0.3	0.2
	COV	19%	23%	22%	20%	19%	18%	17%
Control	Average	23.9	10.0	4.4	2.9	2.2	1.7	1.4
	Std Dev	3.6	1.5	0.7	0.5	0.4	0.3	0.3
	COV	15%	15%	15%	17%	18%	16%	18%

Table A.6 - Results MODULUS Analysis for Estimating Design Moduli

Section No.		Modulus, ksi				RMS Error, %
		ACP	Upper Base	Lower Base	Subgrade	
Rb	**Average**	**500**	**18**	**14**	**22**	**3.4**
	Std Dev	*-*	*4.8*	*5.4*	*2.4*	*-*
	COV	*-*	*27%*	*38%*	*11%*	*-*
CKD	**Average**	**500**	**44**	**30**	**22**	**4.4**
	Std Dev	*-*	*21.9*	*34.3*	*1.9*	*-*
	COV	*-*	*50%*	*115%*	*8%*	*-*
Fly ash	**Average**	**500**	**15**	**16**	**20**	**4.8**
	Std Dev	*-*	*7.1*	*8.1*	*2.7*	*-*
	COV	*-*	*47%*	*51%*	*14%*	*-*
Lime	**Average**	**500**	**52**	**76**	**26**	**4.5**
	Std Dev	*-*	*15.8*	*54.8*	*4.0*	*-*
	COV	*-*	*31%*	*72%*	*16%*	*-*
Control	**Average**	**500**	**13**	**85**	**24**	**3.8**
	Std Dev	*-*	*9.1*	*53.8*	*4.4*	**-**
	COV	*-*	*72%*	*63%*	*18%*	**-**

Table A.7 - Results of JIM Analysis for Estimating Design Moduli

Section No.		Modulus, ksi							RMS Error, %
		ACP	Upper Base		Lower Base		Subgrade		
			Cons.	Avg.	Cons.	Avg.	Cons.	Avg.	
Rb	**Average**	**419**	**39**	**40**	**38**	**55**	**14**	**16**	**8.0**
	Std Dev	*-*	*6.4*	*6.5*	*5.9*	*7.6*	*1.4*	*1.6*	**-**
	COV	*-*	*16%*	*16%*	*15%*	*14%*	*10%*	*10%*	**-**
CKD	**Average**	**366**	**25**	**39**	**44**	**62**	**15**	**17**	**5.1**
	Std Dev	*-*	*4.7*	*7.1*	*7.0*	*9.2*	*1.3*	*1.5*	**-**
	COV	*-*	*19%*	*18%*	*16%*	*15%*	*9%*	*9%*	**-**
Fly ash	**Average**	**402**	**43**	**43**	**48**	**65**	**13**	**14**	**4.2**
	Std Dev	*-*	*7.2*	*7.2*	*8.1*	*10.1*	*1.7*	*1.9*	**-**
	COV	*-*	*16%*	*16%*	*17%*	*15%*	*13%*	*14%*	**-**
Lime	**Average**	**376**	**60**	**60**	**63**	**82**	**17**	**19**	**4.8**
	Std Dev	*-*	*14.9*	*15.0*	*17.7*	*21.4*	*2.9*	*3.4*	**-**
	COV	*-*	*25%*	*25%*	*28%*	*26%*	*17%*	*18%*	**-**
Control	**Average**	**333**	**33**	**33**	**40**	**54**	**16**	**18**	**7.1**
	Std Dev	*-*	*5.4*	*5.4*	*5.0*	*6.2*	*2.9*	*3.3*	**-**
	COV	*-*	*16%*	*16%*	*12%*	*12%*	*18%*	*19%*	**-**

Table A.8 - Results of JIM Analysis for Estimating Design Moduli and Thicknesses

| Section No.		Thickness, in.			Modulus, ksi							RMS Error ,%
					ACP	Upper Base		Lower Base		Subgrade		
		ACP	U. Base	L. Base		Cons.	Avg.	Cons.	Avg.	Cons.	Avg.	
Rb	Average	2.1	5	3	419	81	87	125	143	15	17	4.0
	Std Dev	0.2	2.0	0.8	-	5.5	3.0	21.2	4.8	1.3	1.5	-
	COV	12%	39%	30%	-	7%	3%	17%	3%	9%	9%	-
CKD	Average	2.3	2	3	366	56	87	100	142	16	18	2.4
	Std Dev	0.2	0.3	0.8	-	2.8	2.2	3.6	2.7	1.2	1.3	-
	COV	9%	14%	30%	-	5%	3%	4%	2%	8%	7%	-
Fly ash	Average	2.3	3	6	402	88	91	96	104	14	16	3.4
	Std Dev	0.3	1.0	2.5	-	4.5	2.5	10.9	1.9	1.6	1.8	-
	COV	11%	29%	40%	-	5%	3%	11%	2%	11%	12%	-
Lime	Average	2.4	2	10	376	93	94	118	146	18	20	2.8
	Std Dev	0.4	0.4	0.8	-	2.8	2.6	12.9	3.0	2.6	3.0	-
	COV	15%	15%	7%	-	3%	3%	11%	2%	15%	15%	-
Control	Average	1.9	6	3	333	86	89	121	142	17	19	3.5
	Std Dev	0.3	2.1	1.5	-	4.4	3.6	18.8	4.3	2.9	3.3	-
	COV	16%	35%	48%	-	5%	4%	16%	3%	17%	18%	-

98
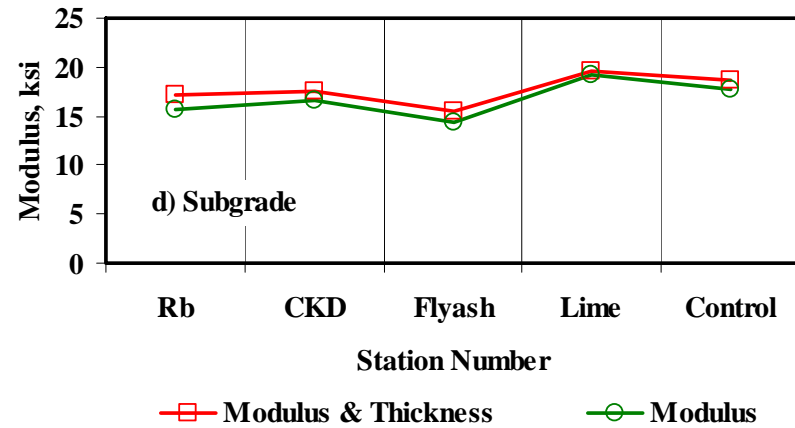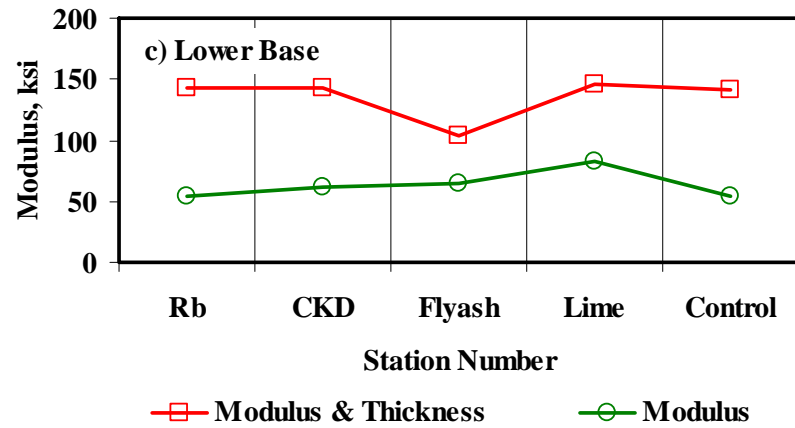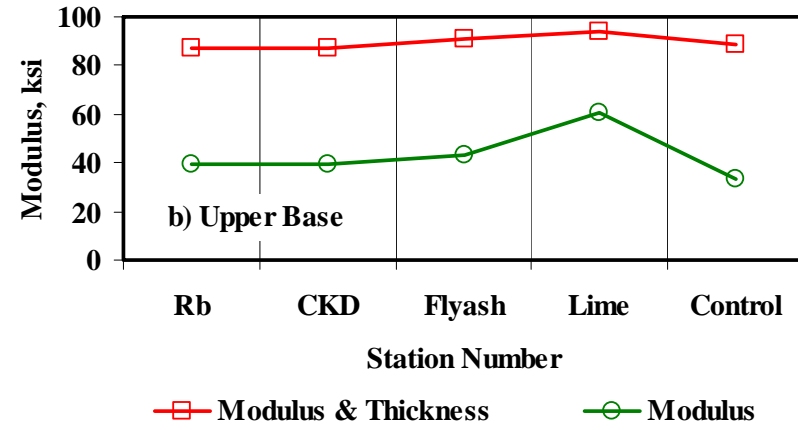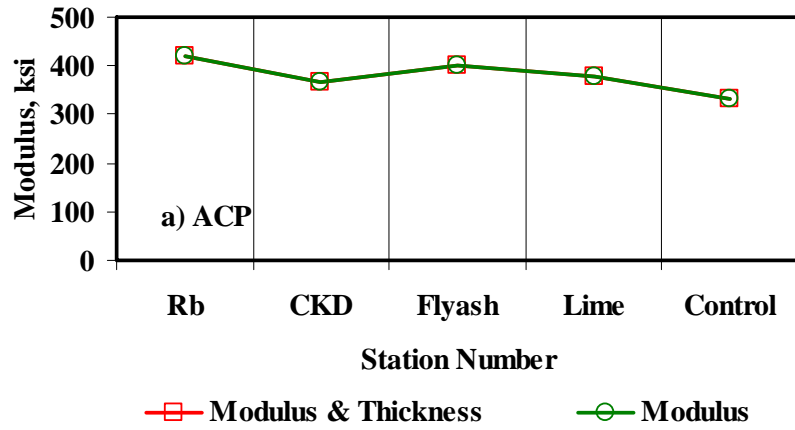
Figure A.8 - Comparison of Design Moduli from JIM Analysis with Constant and Backcalculated Thickness
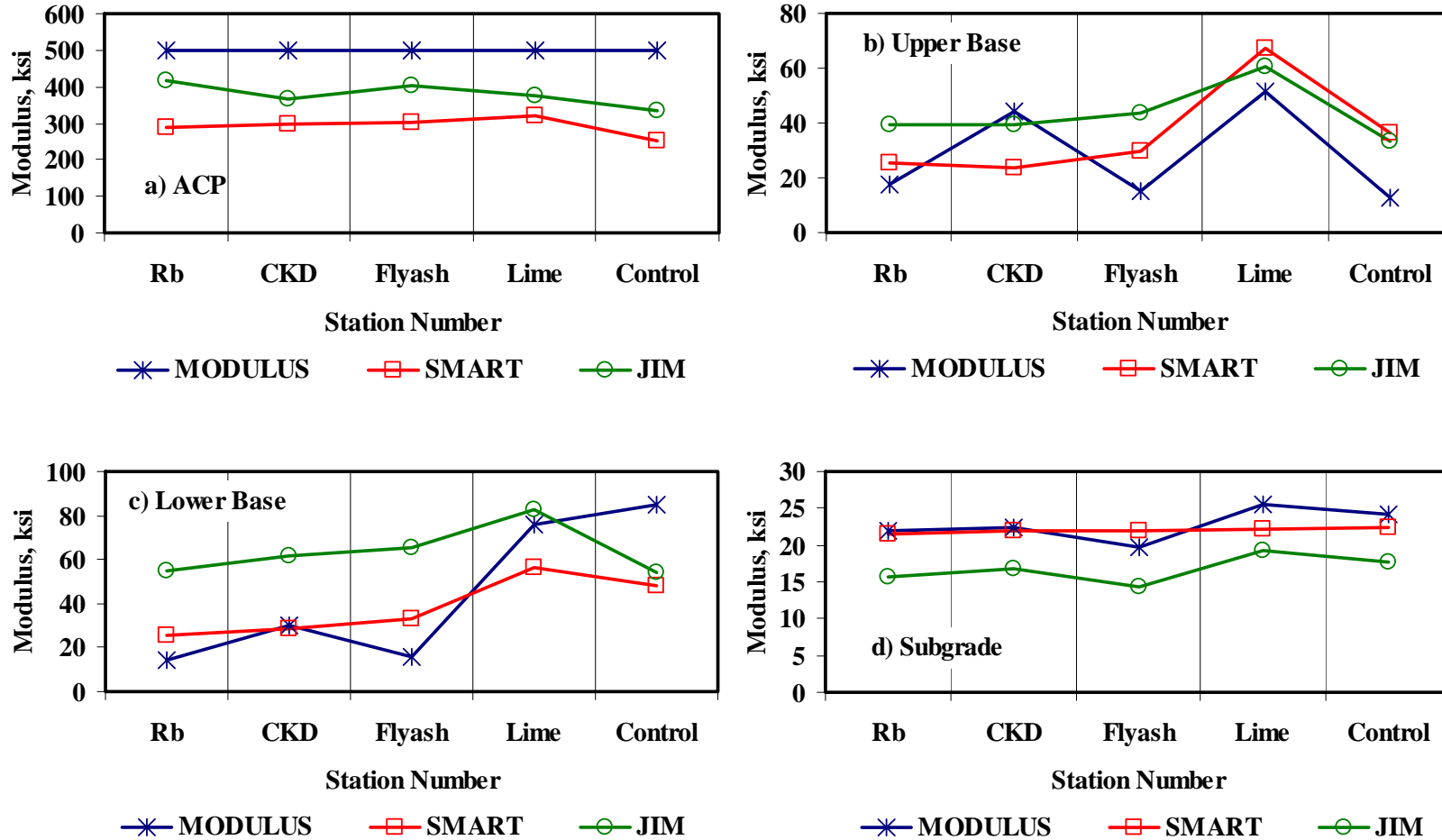
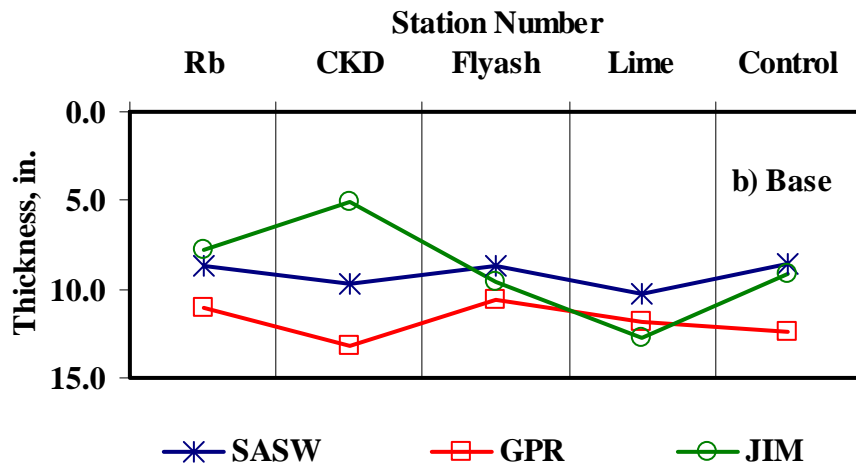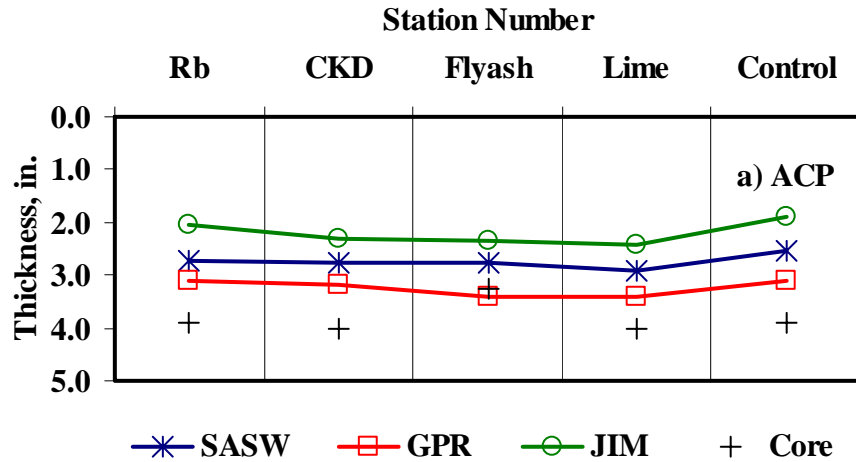**Figure A.9 - Comparison of Design Moduli from Different Analyses**

Figure A.10 - Comparison of Layer Thickness from Different Analyses
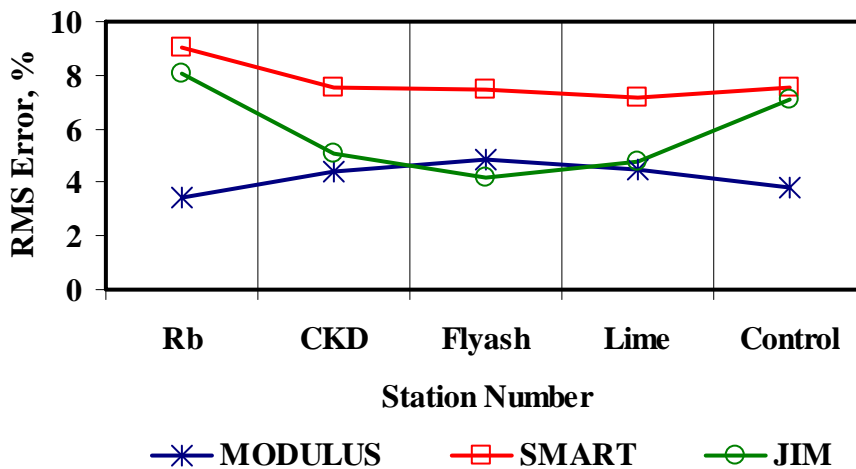

Figure A.11 - Comparison of RMS Error from Different Analyses

Table A.9 - Summary of Design Modulus Values with Data Fusion Results

| Section No.	Method	Modulus, ksi							
		ACP		Upper Base		Lower Base		Subgrade	
		Average	COV	Average	COV	Average	COV	Average	COV
Roadbond	MODULUS	500	-	18	24%	14	30%	22	11%
	JIM	419	-	40	16%	55	14%	16	10%
	SMART	287	10%	26	24%	26	16%	21	7%
	SWA	287	10%	26	18%	33	13%	18	6%
	WA	402	3%	28	11%	32	8%	20	7%
	FL	342	6%	32	17%	32	19%	20	6%
CKD	MODULUS	500	-	44	50%	26	121%	22	8%
	JIM	366	-	39	18%	62	15%	17	9%
	SMART	299	7%	24	24%	29	16%	22	0%
	SWA	299	7%	39	25%	49	29%	19	8%
	WA	388	2%	36	26%	39	26%	21	8%
	FL	338	5%	35	19%	51	22%	20	4%
Fly ash	MODULUS	500	-	15	47%	15	50%	20	14%
	JIM	402	-	43	16%	65	15%	14	14%
	SMART	301	9%	30	18%	33	13%	22	0%
	SWA	301	9%	28	39%	31	33%	18	4%
	WA	401	3%	29	18%	38	14%	19	8%
	FL	352	5%	30	24%	35	14%	18	7%
Lime	MODULUS	500	-	52	31%	76	72%	26	16%
	JIM	376	-	62	25%	82	26%	19	18%
	SMART	321	11%	68	22%	57	33%	22	5%
	SWA	321	11%	76	16%	81	27%	19	7%
	WA	399	3%	61	15%	72	23%	22	11%
	FL	388	6%	65	13%	73	14%	22	11%
Control	MODULUS	500	-	13	72%	85	63%	24	18%
	JIM	333	-	33	16%	54	12%	18	19%
	SMART	253	14%	37	23%	48	20%	22	7%
	SWA	253	14%	22	47%	33	22%	19	9%
	WA	362	4%	28	36%	62	35%	21	14%
	FL	344	10%	25	42%	41	25%	21	15%

102
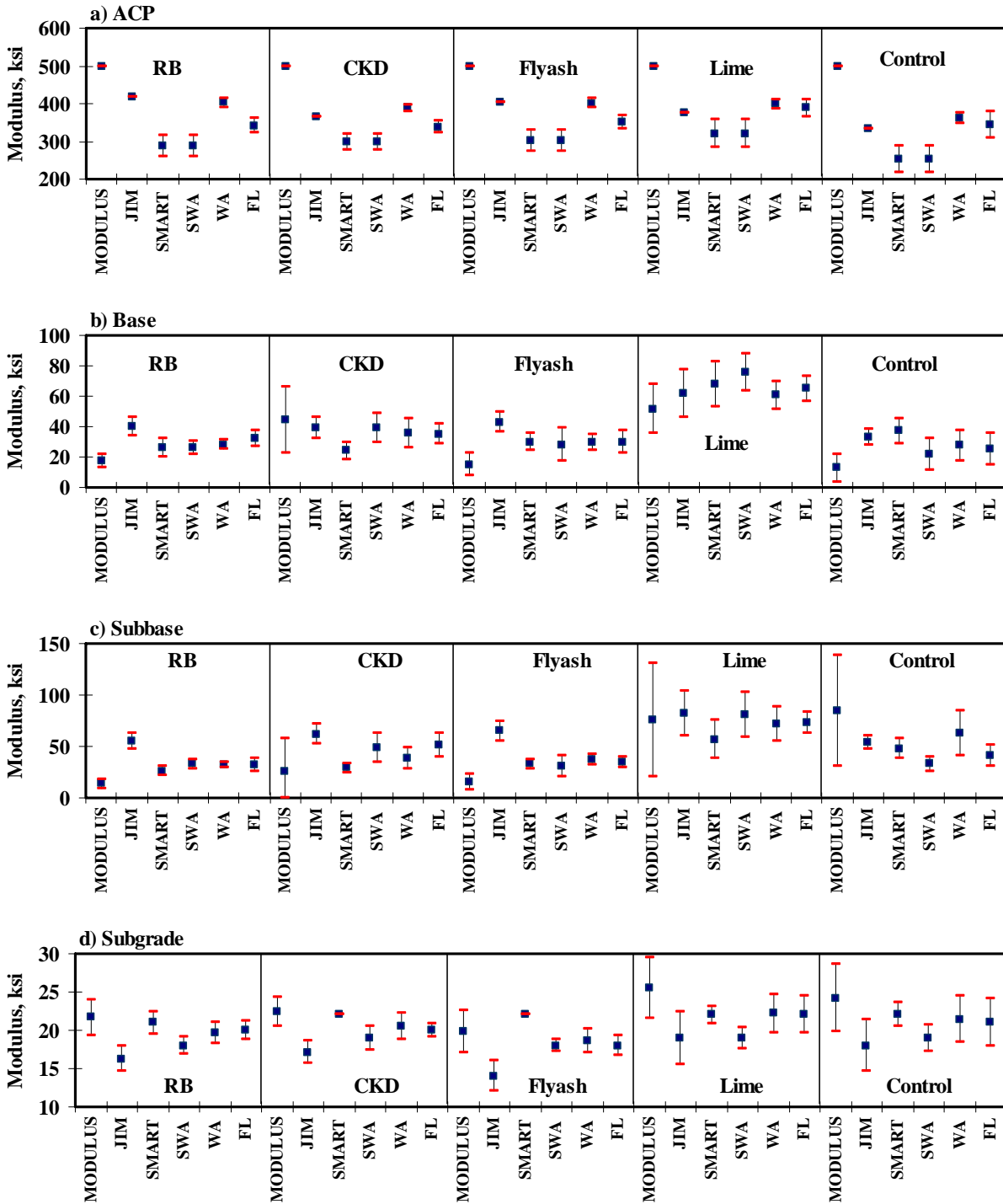
Figure A.12 - Statistical Comparison of Design Moduli of Different Analyses and Data Fusion Techniques

APPENDIX B - RESULTS OF ANALYSES FOR TXDOT PARKING LOT SITE (EL PASO)

Table B.1 - Results of SASW Analysis for Estimating Seismic Moduli

Section No.		Modulus, ksi			RMS Error, %
		ACP	Base	subgrade	
Test 1	Average	1615	279	26	5.7
	Std Dev	238	108	7	-
	COV	15%	39%	28%	-
Test 2	Average	1564	281	25	5.6
	Std Dev	255	110	4	-
	COV	16%	39%	16%	-
Test 3	Average	1621	275	25	5.5
	Std Dev	271	102	5	-
	COV	17%	37%	18%	-
Test 4	Average	1621	272	21	5.1
	Std Dev	153	97	5	-
	COV	9%	36%	22%	-
Test 5	Average	1594	273	20	4.9
	Std Dev	215	102	4	-
	COV	14%	37%	18%	-
Test 6	Average	1575	277	20	5.5
	Std Dev	218	106	3	-
	COV	14%	38%	17%	-

Table B.2 - Results of SASW Analysis for Estimating Seismic Moduli and Thicknesses

| Section No.		Thickness, in.		Modulus, ksi			RMS Error, %
		ACP	Base	ACP	Base	subgrade	
Test 1	Average	2.0	6.2	1824	200	26	6.9
	Std Dev	0.2	0.6	333	39	5	-
	COV	9%	9%	18%	19%	19%	-
Test 2	Average	2.0	6.0	1786	210	26	6.4
	Std Dev	0.2	0.7	325	28	5	-
	COV	9%	11%	18%	13%	18%	-
Test 3	Average	2.1	6.0	1729	177	27	7.2
	Std Dev	0.2	0.5	303	18	4.0	-
	COV	9%	9%	18%	10%	15%	-
Test 4	Average	2.1	6.1	1738	180	26	6.1
	Std Dev	0.2	0.7	201	17	5	-
	COV	8%	11%	12%	9%	18%	-
Test 5	Average	2.0	6.0	1667	187	25	7.0
	Std Dev	0.2	0.6	202	20	4	-
	COV	9%	11%	12%	11%	14%	-
Test 6	Average	2.0	6.1	1710	184	25	7.2
	Std Dev	0.2	0.7	231	22	6	-
	COV	9%	11%	14%	12%	18%	-
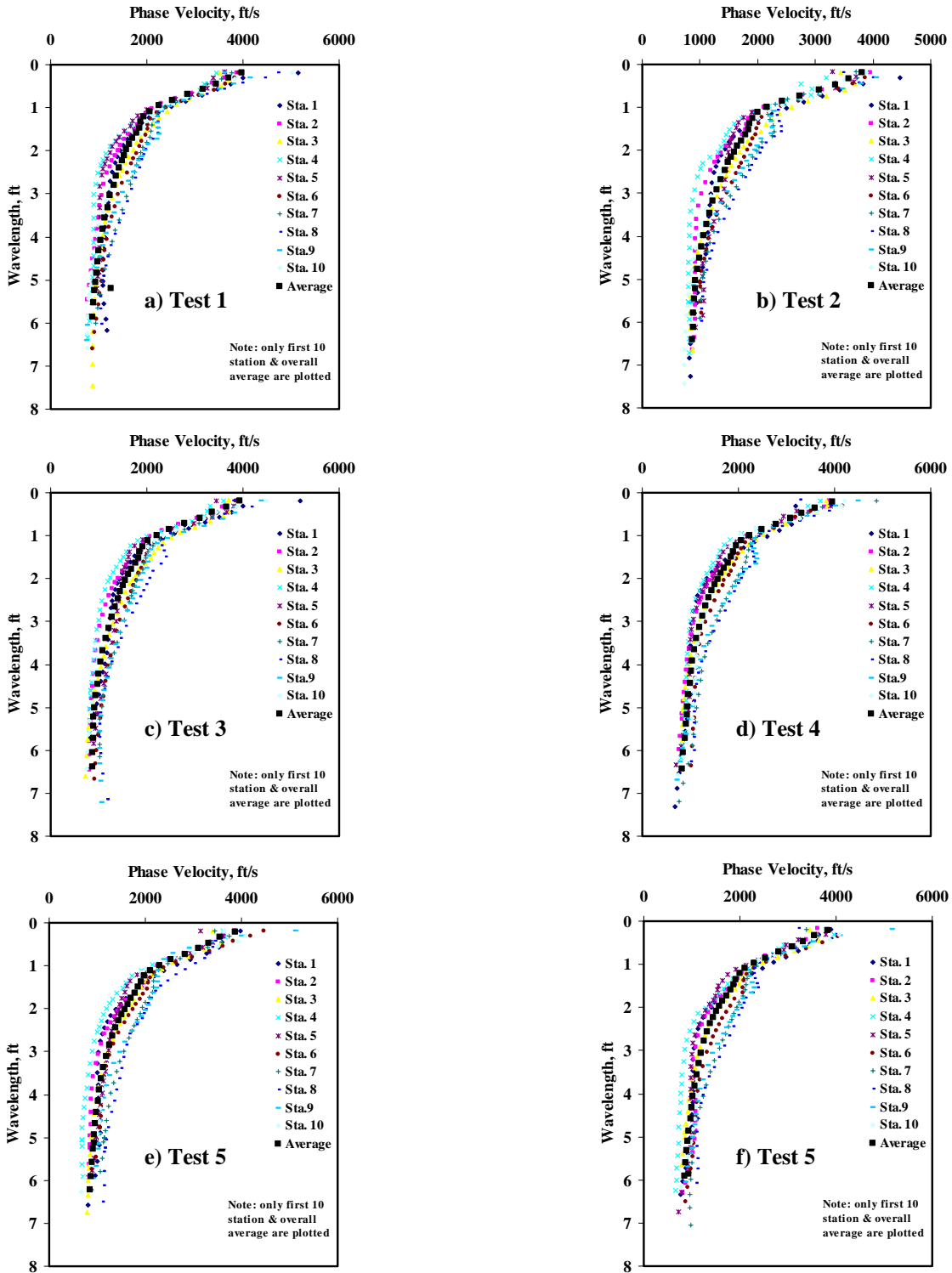
Figure B.1 - Results of Dispersion Curve from SASW Analysis

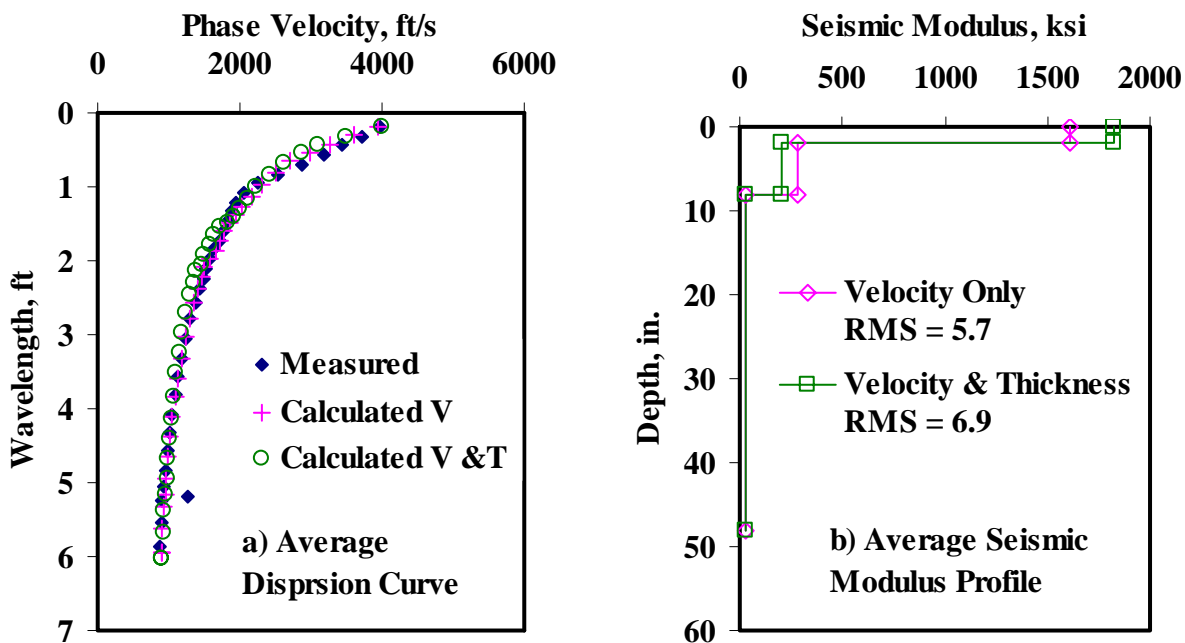**Figure B.2 - Results of SASW Data Reduction Process (Test1)**
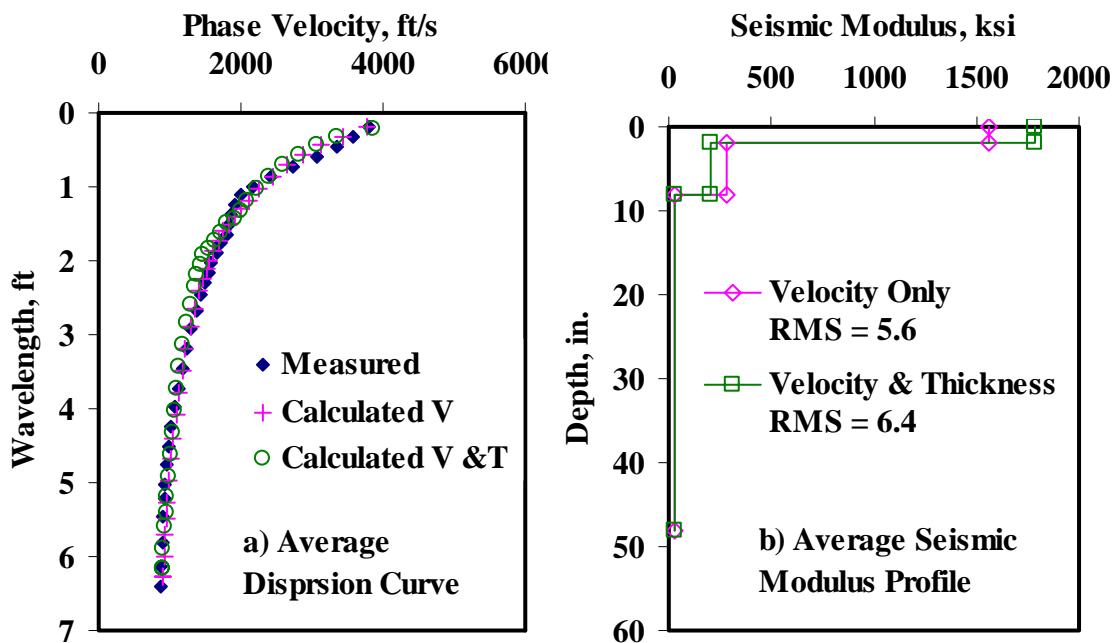

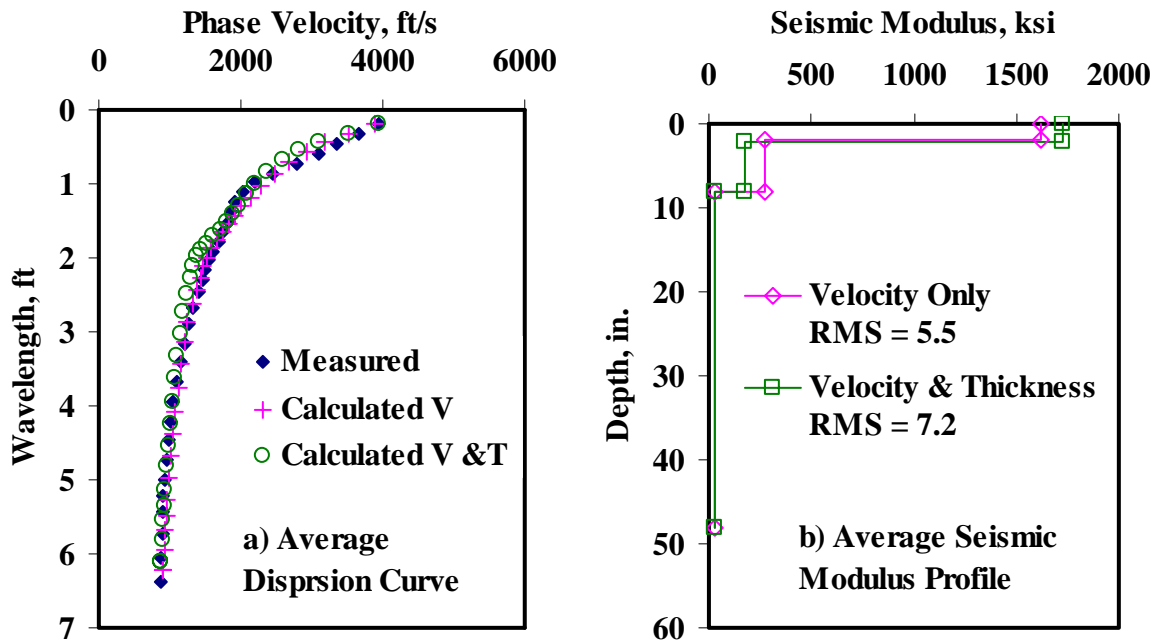**Figure B.3 - Results of SASW Data Reduction Process (Test2)**

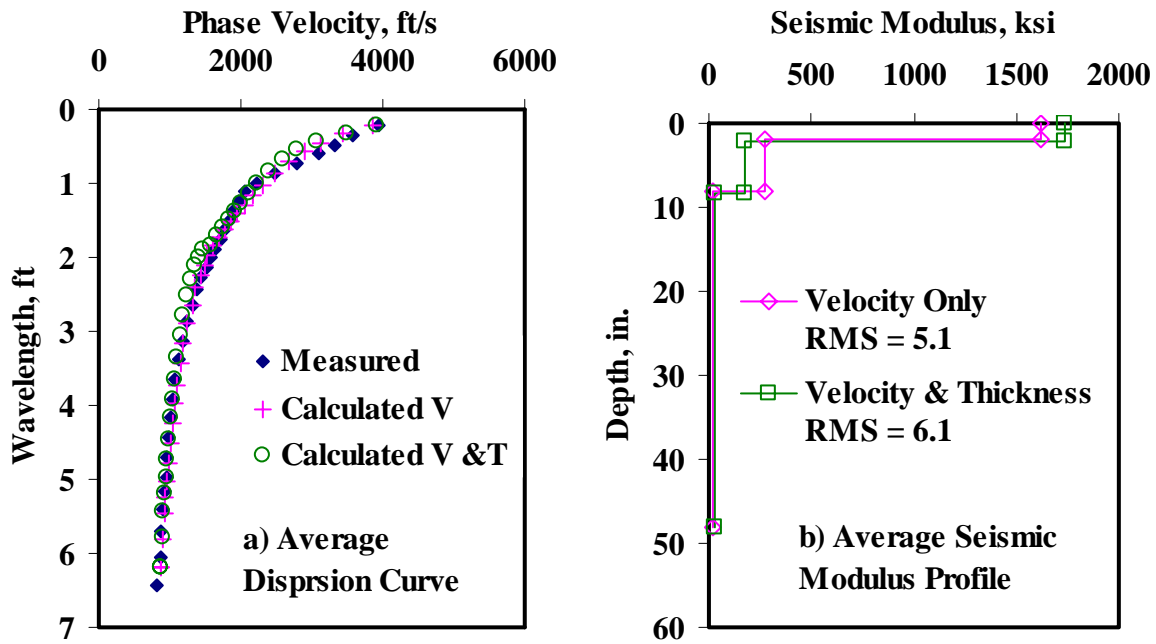**Figure B.4 - Results of SASW Data Reduction Process (Test3)**

Figure B.5 - Results of SASW Data Reduction Process (Test4)
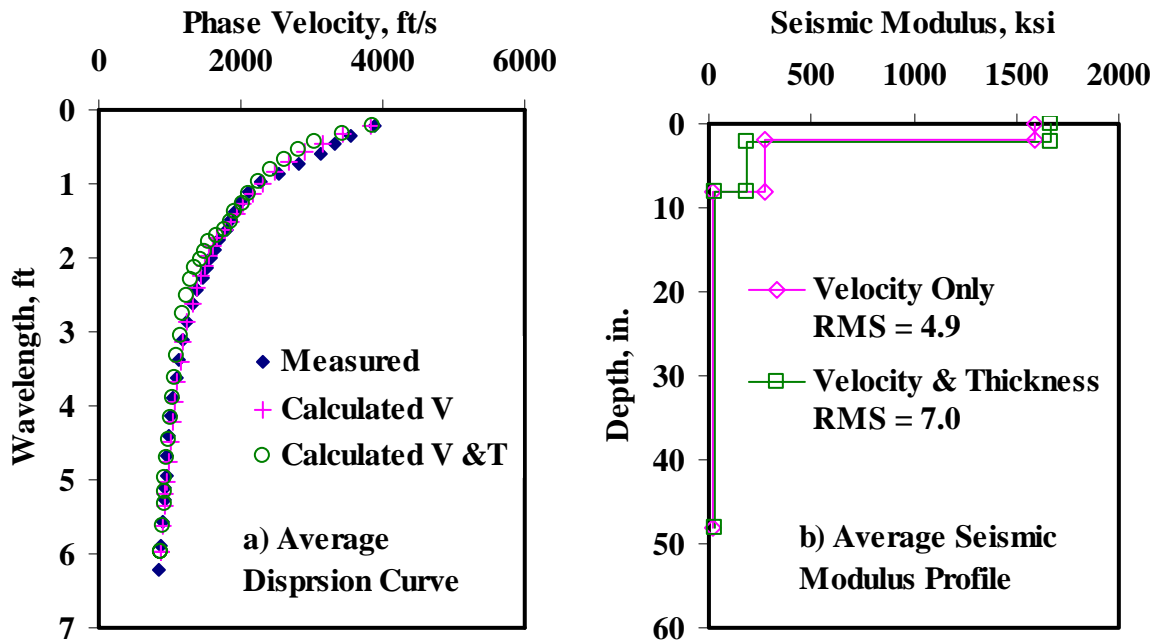
110

Figure B.6 - Results of SASW Data Reduction Process (Test5)
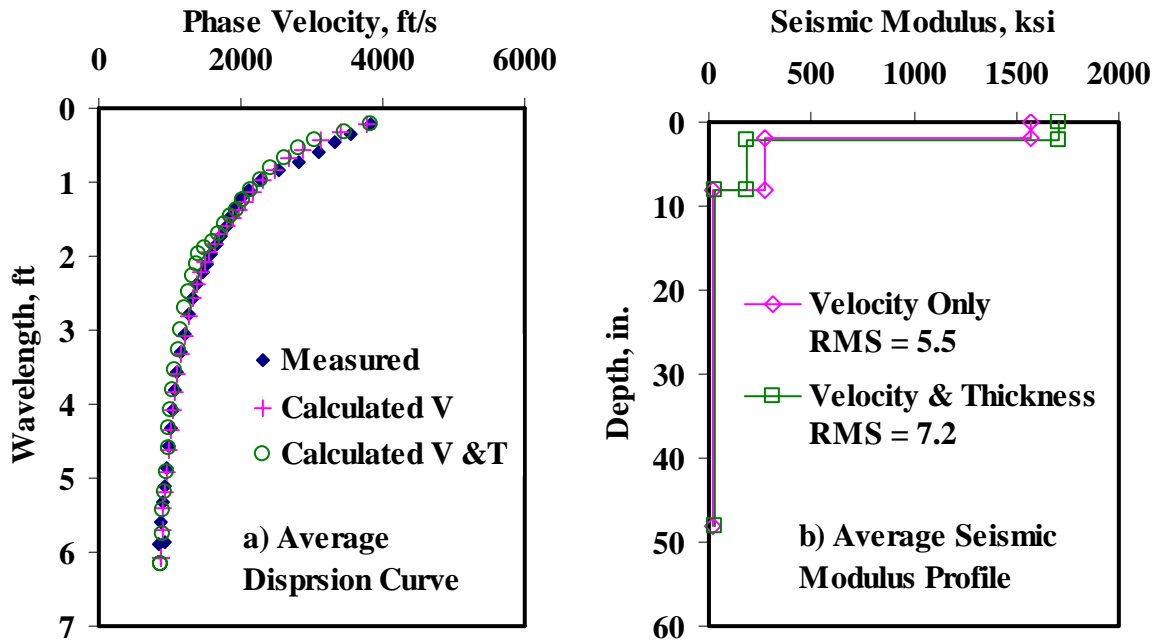

Figure B.7 - Results of SASW Data Reduction Process (Test6)

Table B.3 - Results of SMART Analysis for Estimating Design Moduli

Section No.		ACP	Base Cons.	Base Avg.	Subgrade Cons.	Subgrade Avg.	RMS Error, %
			Modulus, ksi				
Test 1	Average	471	124	176	14	21	5.7
	Std Dev	69.6	54.1	76.2	3.6	6.0	-
	COV	15%	44%	43%	26%	28%	-
Test 2	Average	456	125	179	13	20	5.6
	Std Dev	74.6	55.6	78.9	1.9	3.2	-
	COV	16%	45%	44%	14%	16%	-
Test3	Average	473	122	173	14	21	5.5
	Std Dev	79.3	52.6	74.1	2.5	3.9	-
	COV	17%	43%	43%	19%	19%	-
Test 4	Average	518	118	165	11	17	5.1
	Std Dev	48.8	49.7	69.7	2.5	3.8	-
	COV	9%	42%	42%	22%	22%	-
Test5	Average	509	118	166	11	17	4.8
	Std Dev	68.8	51.6	72.8	1.9	2.9	-
	COV	14%	44%	44%	18%	18%	-
Test 6	Average	503	121	169	11	17	5.5
	Std Dev	70.0	54.1	77.3	2.1	2.7	-
	COV	14%	45%	46%	20%	16%	-

Table B.4 - Summary Statistics of Measured FWD Deflections

Section No.		d0	d1	d2	d3	d4	d5	d6
		Normalized Deflection, mils (12 in. Spacing)						
Test 1	Average	19.6	9.8	5.1	3.2	2.3	1.8	1.4
	Std Dev	3.3	1.0	0.5	0.3	0.2	0.2	0.1
	COV	17%	11%	10%	10%	9%	9%	10%
Test 2	Average	20.2	9.9	5.2	3.3	2.3	1.8	1.4
	Std Dev	3.4	1.1	0.6	0.3	0.2	0.2	0.1
	COV	17%	11%	11%	11%	9%	10%	10%
Test3	Average	20.5	10.0	5.2	3.3	2.3	1.8	1.4
	Std Dev	3.5	1.1	0.6	0.3	0.2	0.2	0.1
	COV	17%	11%	11%	10%	10%	10%	11%
Test 4	Average	20.0	9.9	5.3	3.3	2.3	1.8	1.4
	Std Dev	3.1	1.1	0.5	0.3	0.2	0.2	0.1
	COV	16%	11%	10%	10%	10%	9%	10%
Test5	Average	20.5	9.9	5.3	3.3	2.3	1.8	1.4
	Std Dev	3.1	1.1	0.6	0.3	0.2	0.2	0.1
	COV	15%	11%	11%	10%	10%	9%	10%
Test 6	Average	20.8	9.9	5.2	3.3	2.3	1.8	1.4
	Std Dev	3.1	1.2	0.6	0.4	0.3	0.2	0.2
	COV	15%	12%	12%	12%	11%	9%	11%

Table B.5 - Results MODULUS Analysis for Estimating Design Moduli

Section No.		Modulus, ksi			RMS Error, %
		ACP	Base	Subgrade	
Test 1	Average	500	73	21	7.0
	Std Dev	-	36.3	2.1	-
	COV	-	49%	10%	-
Test 2	Average	500	69	21	7.1
	Std Dev	-	35.0	2.2	-
	COV	-	51%	10%	-
Test3	Average	500	67	21	6.6
	Std Dev	-	34.1	2.2	-
	COV	-	51%	10%	-
Test 4	Average	500	70	21	7.0
	Std Dev	-	30.7	2.2	-
	COV	-	44%	10%	-
Test5	Average	500	66	21	6.9
	Std Dev	-	28.6	2.2	-
	COV	-	44%	10%	-
Test 6	Average	500	62	21	6.3
	Std Dev	-	28.3	2.5	-
	COV	-	45%	12%	-

Table B.6 - Results of JIM Analysis for Estimating Design Moduli

Section No.		Modulus, ksi					RMS Error, %
		ACP	Base		Subgrade		
			Cons.	Avg.	Cons.	Avg.	
Test 1	Average	570	99	214	15	17	2.8
	Std Dev	92.0	20.1	38.3	1.4	1.6	-
	COV	16%	20%	18%	9%	10%	-
Test 2	Average	563	98	212	15	17	2.8
	Std Dev	79.1	19.8	37.6	1.5	1.8	-
	COV	14%	20%	18%	10%	10%	-
Test3	Average	564	97	209	15	17	2.7
	Std Dev	79.6	25.2	48.1	1.5	1.8	-
	COV	14%	26%	23%	10%	11%	-
Test 4	Average	586	98	211	15	17	2.6
	Std Dev	78.8	21.4	40.2	1.5	1.7	-
	COV	13%	22%	19%	10%	10%	-
Test5	Average	584	90	196	15	17	2.8
	Std Dev	108.3	24.5	47.2	1.6	1.8	-
	COV	19%	27%	24%	11%	11%	-
Test 6	Average	573	94	203	15	17	2.8
	Std Dev	84.7	23.4	45.0	1.5	1.8	-
	COV	15%	25%	22%	10%	11%	-

Table B.7 - Results of JIM Analysis for Estimating Design Moduli and Thicknesses

| Section No. | | Thickness, in. | | Modulus, ksi | | | | | RMS Error, % |
| | | | | ACP | Base | | Subgrade | | |
		ACP	Base		Cons.	Avg.	Cons.	Avg.	
Test 1	Average	2.6	8	503	141	167	15	17	2.6
	Std Dev	0.6	1.4	59.2	42.5	30.3	1.4	1.7	-
	COV	22%	17%	12%	30%	18%	9%	10%	-
Test 2	Average	2.6	8	486	139	164	15	16	2.6
	Std Dev	0.7	1.2	50.8	36.7	29.4	1.5	1.7	-
	COV	27%	16%	10%	26%	18%	10%	10%	-
Test3	Average	2.6	8	503	128	161	15	16	2.5
	Std Dev	0.5	1.6	51.8	58.0	34.6	1.5	1.8	-
	COV	20%	20%	10%	45%	22%	10%	11%	-
Test 4	Average	2.5	8	514	146	170	15	16	2.4
	Std Dev	0.5	1.2	36.6	50.0	33.3	1.5	1.8	-
	COV	21%	16%	7%	34%	20%	10%	11%	-
Test5	Average	2.6	8	491	138	165	14	16	2.5
	Std Dev	0.6	1.2	53.2	50.3	37.6	1.6	1.9	-
	COV	23%	16%	11%	36%	23%	11%	12%	-
Test 6	Average	2.5	8	500	143	170	14	16	2.6
	Std Dev	0.6	1.4	56.3	56.0	41.4	1.5	1.7	-
	COV	23%	19%	11%	39%	24%	10%	11%	-
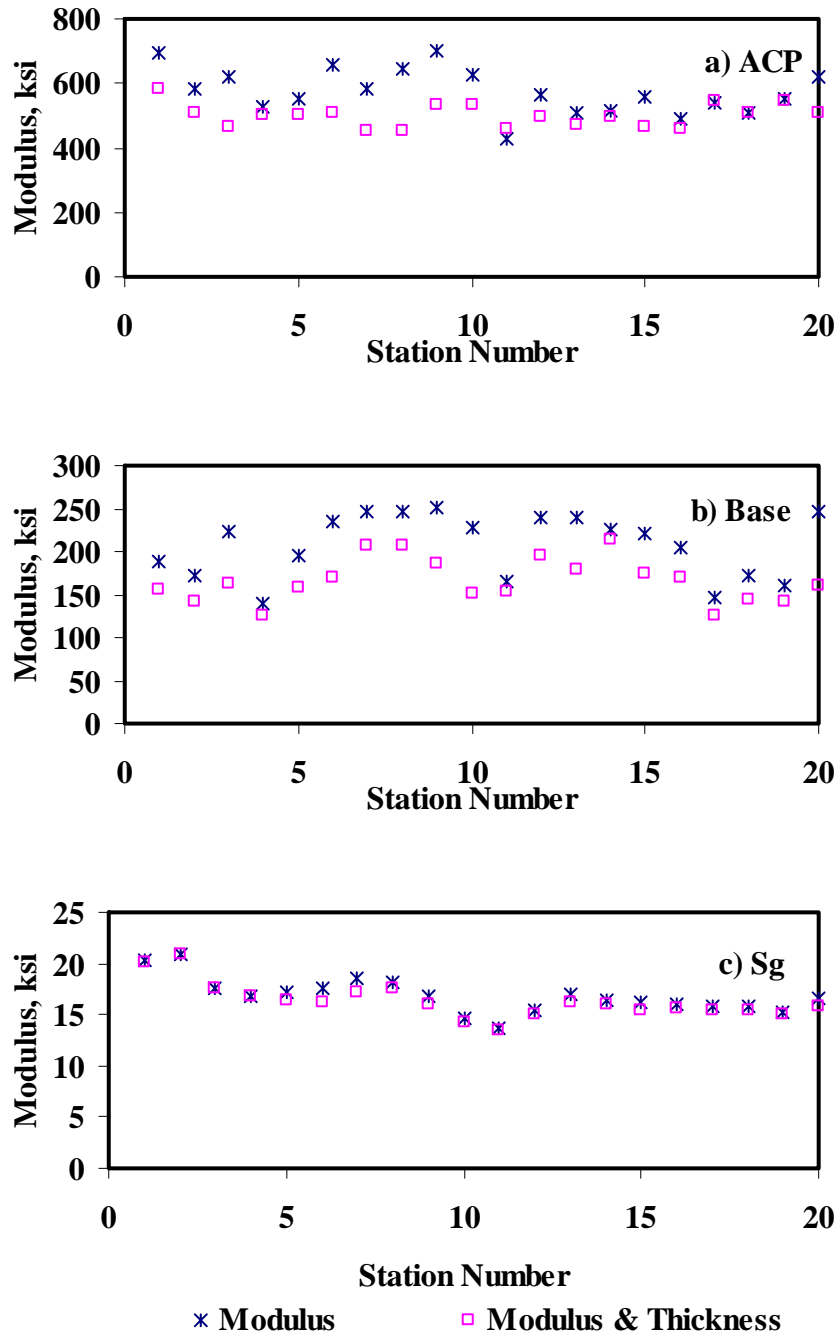
Figure B.8 - Comparison of Design Moduli from JIM Analysis with Constant and Backcalculated Thicknesses
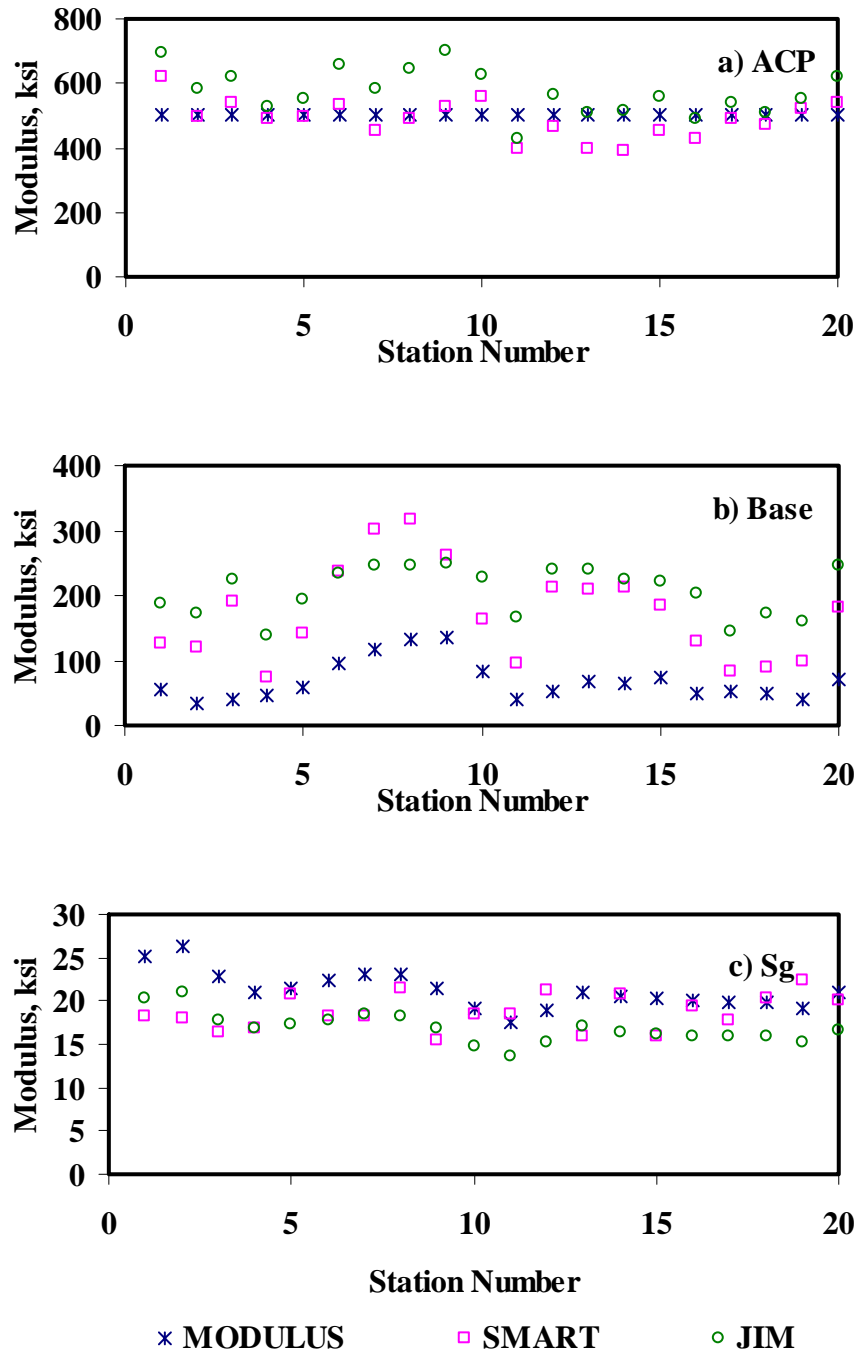
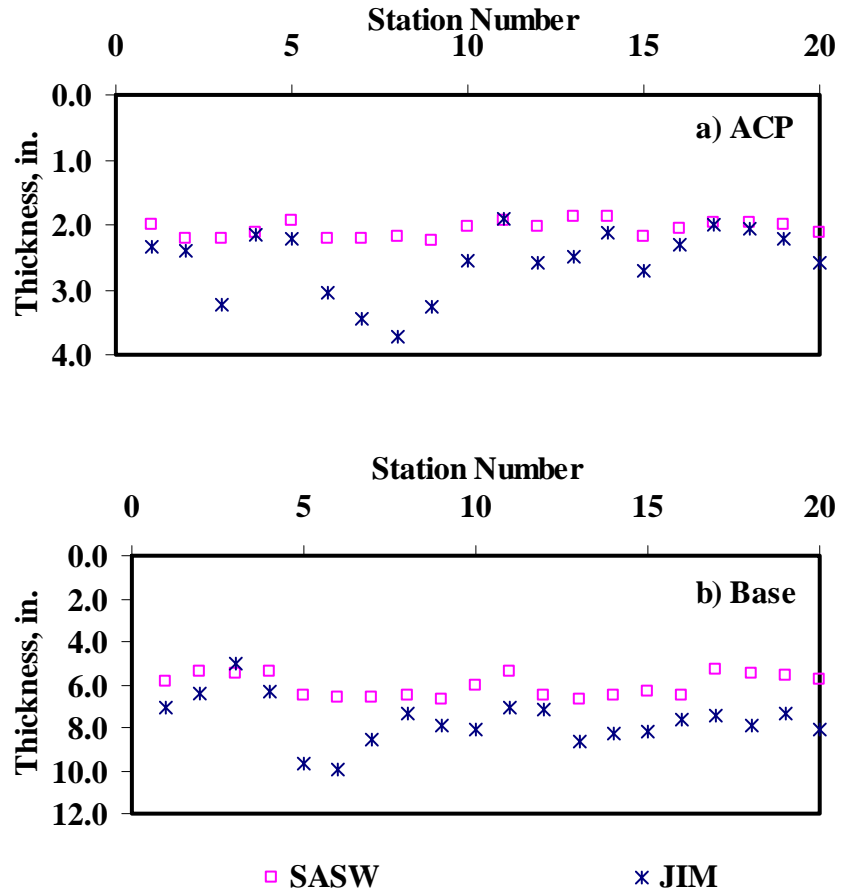**Figure B.9 - Comparison of Design Moduli from Different Analyses**

Figure B.10 - Comparison of Layer Thickness from Different Analyses
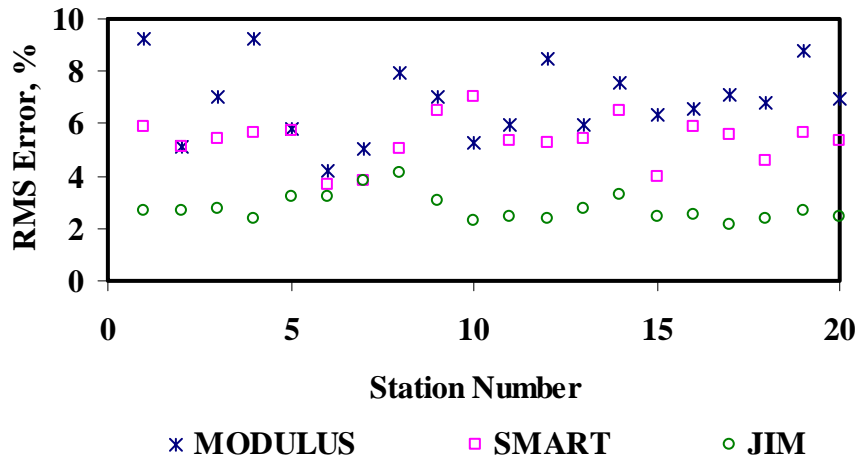

Figure B.11 - Comparison of RMS Error from Different Analyses

Table B.8 - Summary of Design Modulus Values with Data Fusion Results

| Section No.	Method	Modulus, ksi					
		ACP		Base		Subgrade	
		Average	*COV*	Average	*COV*	Average	*COV*
Test 1	MODULUS	500	-	73	49%	21	10%
	JIM	570	16%	214	18%	17	10%
	SMART	471	15%	176	43%	21	28%
	SWA	531	13%	126	44%	19	7%
	WA	531	8%	156	28%	20	10%
	FL	516	9%	147	30%	20	8%
Test 2	MODULUS	500	-	69	51%	21	10%
	JIM	563	14%	212	18%	17	10%
	SMART	456	16%	179	44%	20	16%
	SWA	524	13%	127	41%	19	7%
	WA	520	8%	155	28%	20	7%
	FL	516	7%	143	28%	20	6%
Test 3	MODULUS	500	-	67	51%	21	10%
	JIM	564	14%	209	23%	17	11%
	SMART	473	17%	173	43%	21	19%
	SWA	535	14%	124	43%	19	7%
	WA	527	8%	153	27%	20	8%
	FL	534	9%	146	31%	20	6%
Test 4	MODULUS	500	-	70	44%	21	10%
	JIM	586	13%	211	19%	17	10%
	SMART	518	9%	165	42%	17	22%
	SWA	554	8%	119	39%	19	8%
	WA	548	6%	149	25%	19	9%
	FL	550	6%	138	28%	19	7%
Test 5	MODULUS	500	-	66	44%	21	10%
	JIM	584	19%	196	24%	17	11%
	SMART	509	14%	166	44%	17	18%
	SWA	539	12%	103	41%	18	7%
	WA	550	9%	143	27%	18	7%
	FL	543	7%	126	31%	19	7%
Test 6	MODULUS	500	-	62	45%	21	12%
	JIM	573	15%	203	22%	17	11%
	SMART	503	14%	169	46%	17	16%
	SWA	545	11%	105	42%	18	9%
	WA	539	7%	147	28%	18	9%
	FL	539	6%	136	30%	19	10%
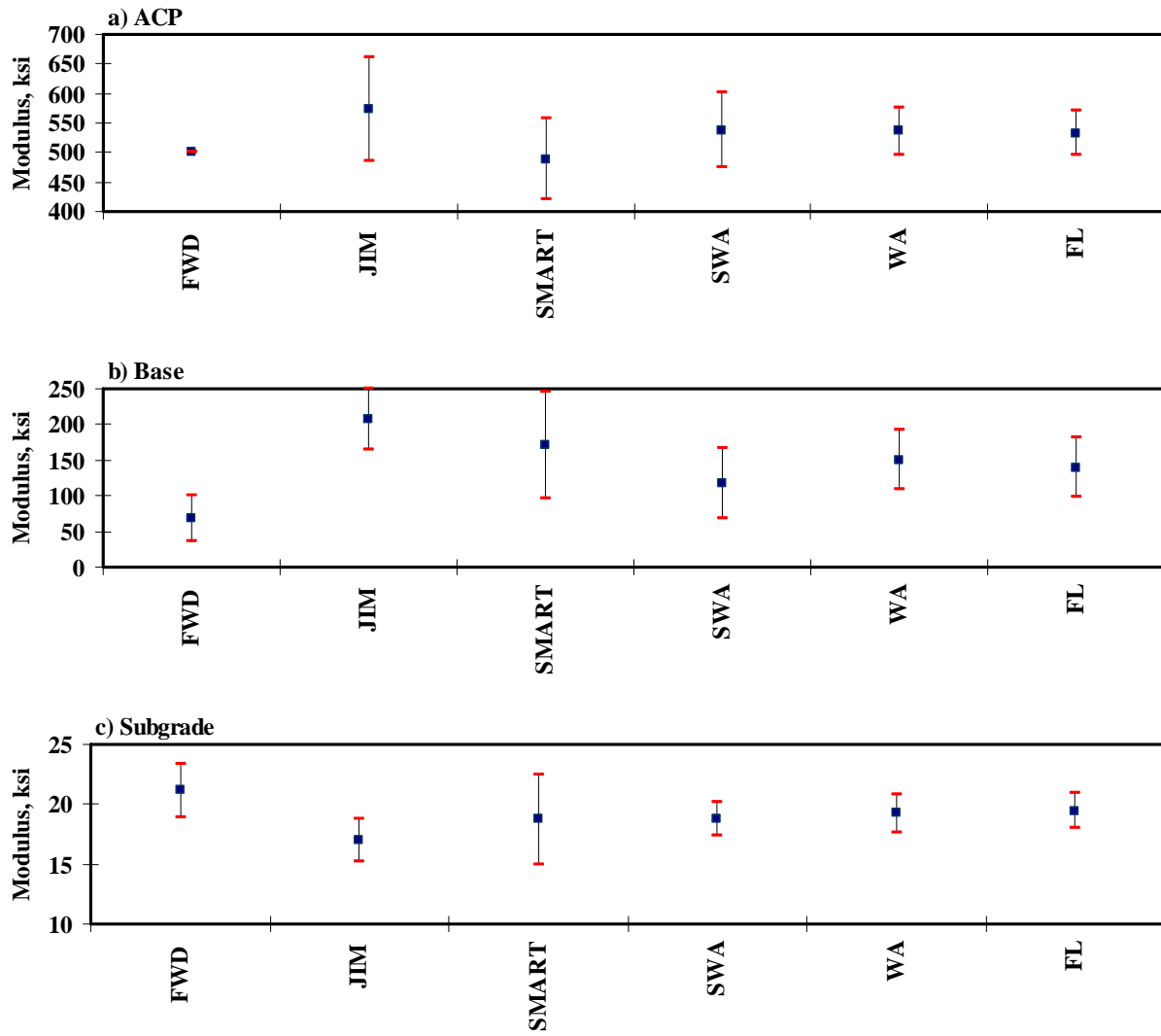
Figure B.12 - Statistical Comparison of Design Moduli of Different Analyses and Data Fusion Techniques

119

APPENDIX C - RESULTS OF ANALYSES FOR RUT RIDE SECTION AT TTI ANNEX (BRYAN)

Table C.1 - Results of SASW Analysis for Estimating Seismic Moduli

Section No.		Modulus, ksi				RMS Error, %
		ACP	Base	Subbase	Subgrade	
1	**Average**	**2088**	**136**	**56**	**28.5**	**6.1**
	Std Dev	*354*	*48*	*16*	*2.6*	*-*
	COV	*17%*	*35%*	*28%*	*9%*	*-*
2	**Average**	**1889**	**94**	**-**	**39.8**	**6.5**
	Std Dev	*255*	*31*	*-*	*4.7*	*-*
	COV	*14%*	*33%*	*-*	*12%*	*-*
3	**Average**	**1631**	**80**	**54**	**31.4**	**4.6**
	Std Dev	*156*	*20*	*19*	*6.7*	*-*
	COV	*10%*	*25%*	*35%*	*21%*	*-*

Table C.2 - Results of SASW Analysis for Estimating Seismic Moduli and Thicknesses

Section No.		Thickness, in.			Modulus, ksi				RMS Error, %
		ACP	Base	SB	ACP	Base	SB	SG	
1	**Average**	**2.1**	**4.9**	**9.0**	**1985**	**135**	**65**	**27.1**	**7.2**
	Std Dev	*0.2*	*0.3*	*1.0*	*191*	*13*	*8*	*4.3*	*-*
	COV	*9%*	*6%*	*11%*	*10%*	*10%*	*13%*	*16%*	*-*
2	**Average**	**1.9**	**14.7**	**-**	**2048**	**115**	**-**	**27.9**	**8.0**
	Std Dev	*0.2*	*1.3*	*-*	*347*	*49*	*-*	*2.4*	*-*
	COV	*9%*	*9%*	*-*	*17%*	*42%*	*-*	*8%*	*-*
3	**Average**	**2.0**	**5.2**	**8.4**	**1594**	**130**	**39**	**29.4**	**6.4**
	Std Dev	*0.2*	*0.4*	*1.9*	*362*	*11*	*6*	*6.3*	*-*
	COV	*9%*	*8%*	*22%*	*23%*	*8%*	*15%*	*22%*	*-*

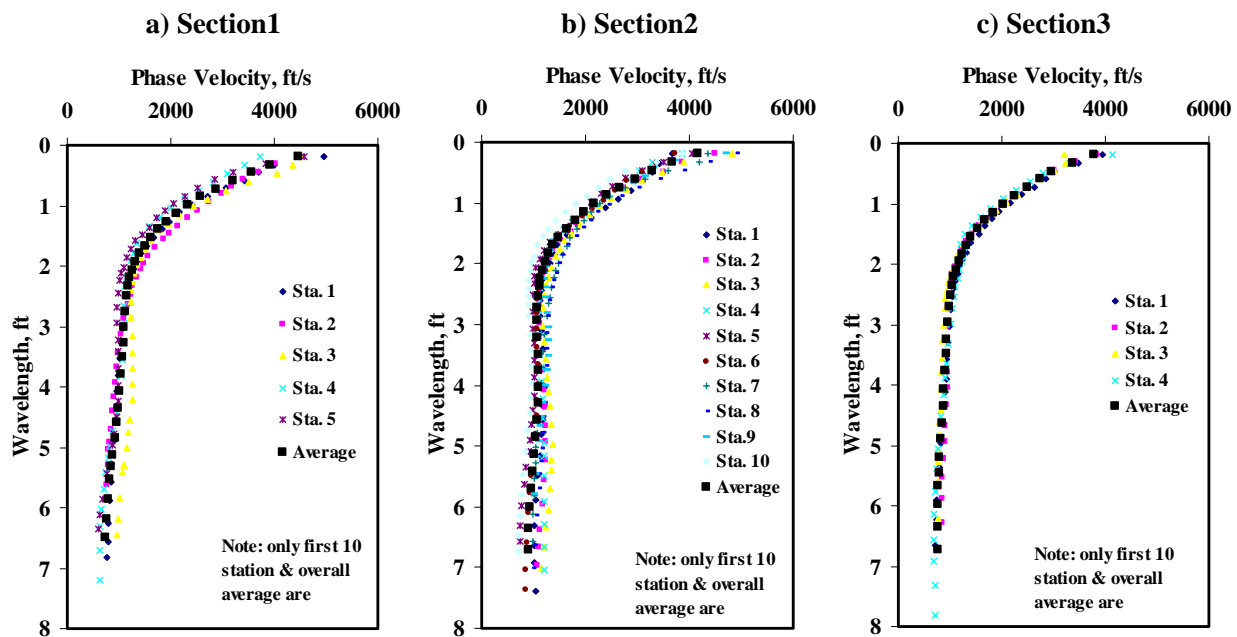a) Section1   b) Section2   c) Section3

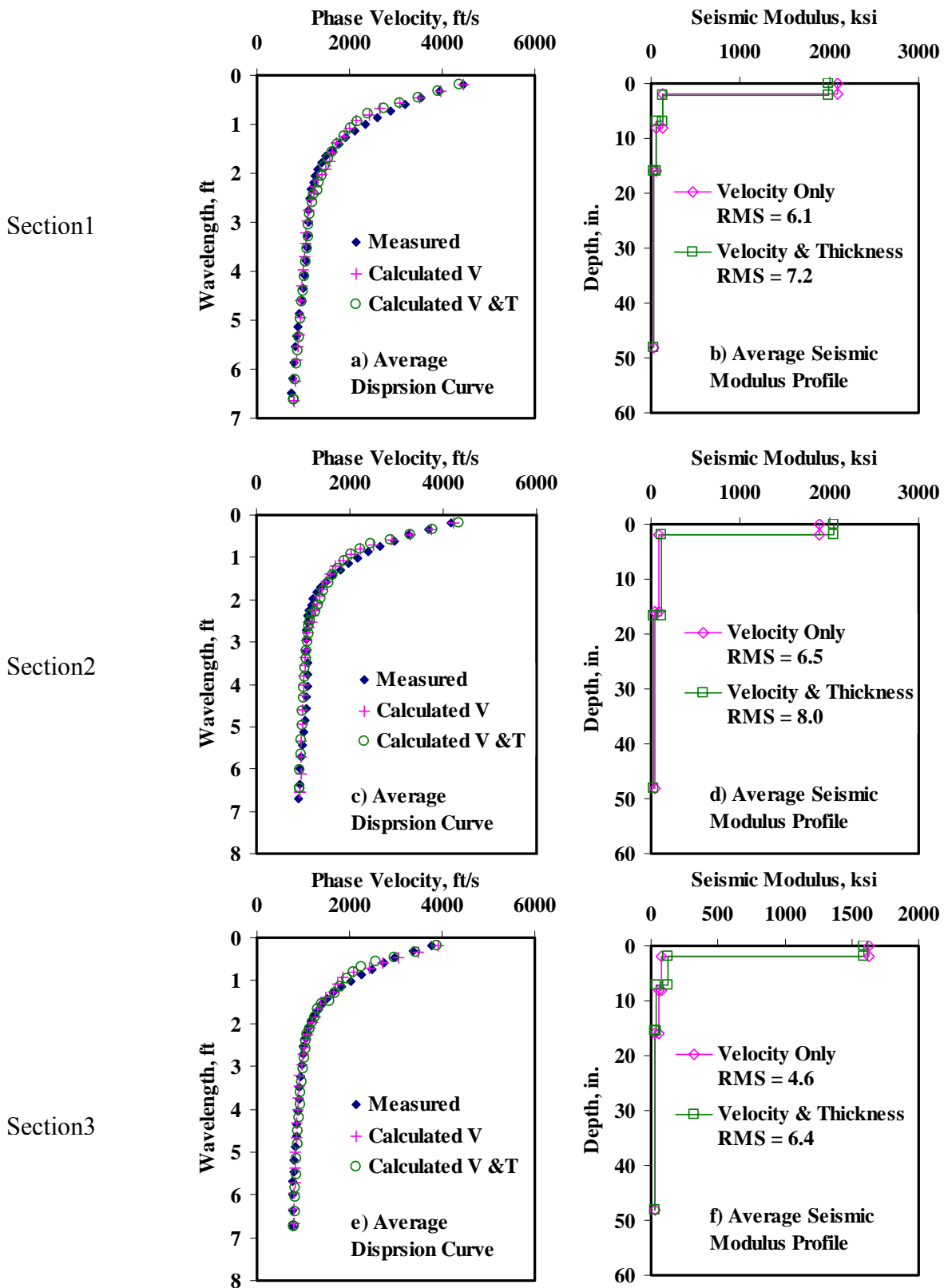**Figure C.1 - Results of Dispersion Curve from SASW Analysis**

Figure C.2 - Results of SASW Data Reduction Process

Table C.3 - Results of SMART Analysis for Estimating Design Moduli

Section No.		ACP	Base		Subbase		Subgrade		RMS Error, %
			Cons.	Avg.	Cons.	Avg.	Cons.	Avg.	
1	**Average**	**609**	**64**	**96**	**28**	**31**	**18**	**24**	**6.1**
	Std Dev	*103.1*	*18.8*	*28.7*	*6.9*	*8.8*	*1.7*	*2.2*	*-*
	COV	*17%*	*29%*	*30%*	*25%*	*29%*	*10%*	*9%*	*-*
2	**Average**	**568**	**49**	**67**	**-**	**-**	**24**	**34**	**6.5**
	Std Dev	*76.7*	*15.3*	*24.0*	*-*	*-*	*2.7*	*3.9*	*-*
	COV	*14%*	*31%*	*36%*	*-*	*-*	*11%*	*12%*	*-*
3	**Average**	**498**	**44**	**58**	**28**	**32**	**20**	**28**	**4.5**
	Std Dev	*47.7*	*2.6*	*12.5*	*5.3*	*8.0*	*3.9*	*6.0*	*-*
	COV	*10%*	*6%*	*22%*	*19%*	*25%*	*19%*	*21%*	*-*

(Modulus, ksi header spans ACP, Base, Subbase, Subgrade columns)

Table C.4 - Summary Statistics of Measured FWD Deflections

Section No.		d0	d1	d2	d3	d4	d5	d6
1	**Average**	**14.5**	**9.4**	**6.0**	**3.9**	**3.2**	**2.4**	**2.0**
	Std Dev	*2.0*	*1.4*	*0.6*	*0.3*	*0.2*	*0.1*	*0.1*
	COV	*14%*	*15%*	*11%*	*8%*	*6%*	*6%*	*5%*
2	**Average**	**12.6**	**6.9**	**4.1**	**2.8**	**2.4**	**1.8**	**1.5**
	Std Dev	*1.4*	*0.7*	*0.4*	*0.3*	*0.3*	*0.2*	*0.2*
	COV	*11%*	*11%*	*11%*	*11%*	*11%*	*11%*	*11%*
3	**Average**	**19.5**	**10.0**	**4.9**	**3.0**	**2.3**	**1.7**	**1.3**
	Std Dev	*6.4*	*2.8*	*1.0*	*0.5*	*0.4*	*0.2*	*0.1*
	COV	*33%*	*28%*	*21%*	*18%*	*16%*	*13%*	*11%*

(Normalized Deflection, mils (12 in. Spacing) header spans d0–d6)

Table C.5 - Results MODULUS Analysis for Estimating Design Moduli

Section No.		Modulus, ksi				RMS Error, %
		ACP	Base	Subbase	Subgrade	
1	Average	500	144	47	18	3.4
	Std Dev	-	13.6	26.5	1.2	-
	COV	-	9%	57%	7%	-
2	Average	500	92	-	24	5.2
	Std Dev	-	19.5	-	2.2	-
	COV	-	21%	-	9%	-
3	Average	500	83	25	24	3.8
	Std Dev	-	30.6	28.5	3.8	-
	COV	-	37%	114%	16%	-

Table C.6 - Results of JIM Analysis for Estimating Design Moduli

Section No.		Modulus, ksi							RMS Error, %
		ACP	Base		Subbase		Subgrade		
			Cons.	Avg.	Cons.	Avg.	Cons.	Avg.	
1	Average	441	57	95	32	54	12	13	3.1
	Std Dev	-	8.3	8.2	4.2	4.3	0.8	0.9	-
	COV	-	15%	9%	13%	8%	7%	7%	-
2	Average	499	63	114	-	-	17	18	3.6
	Std Dev	-	19.4	30.9	-	-	1.7	1.9	-
	COV	-	31%	27%	-	-	10%	10%	-
3	Average	363	58	94	29	55	17	18	3.2
	Std Dev	-	4.5	2.6	7.0	3.4	2.3	2.5	-
	COV	-	8%	3%	24%	6%	14%	14%	-

Table C.7 - Results of JIM Analysis for Estimating Design Moduli and Thicknesses

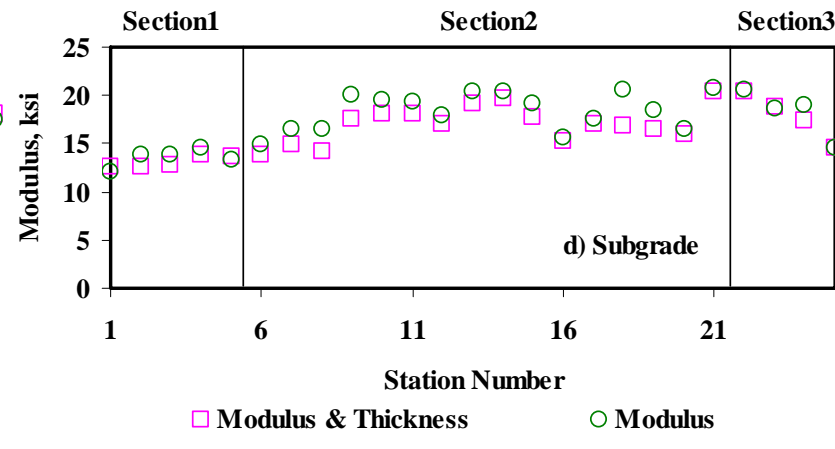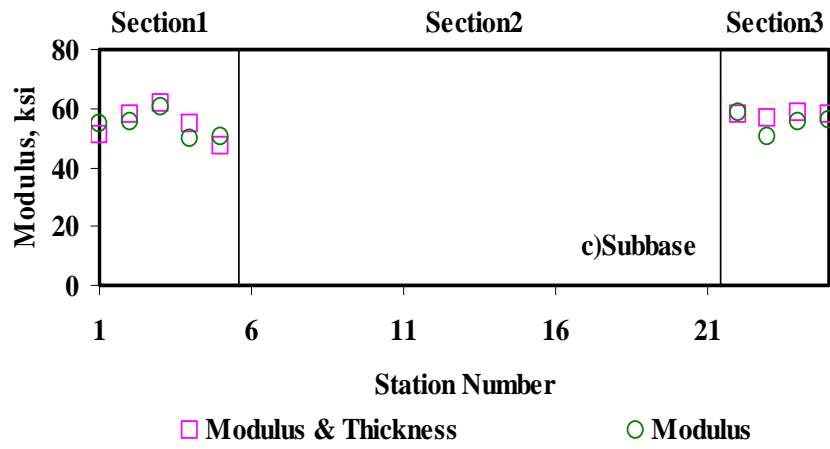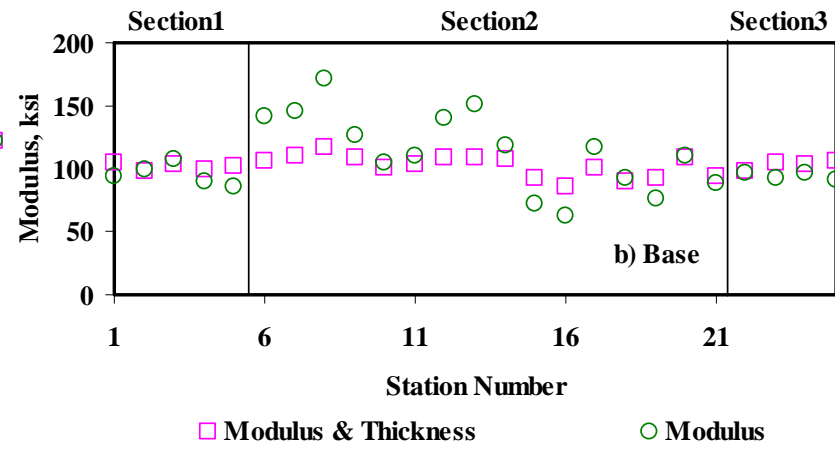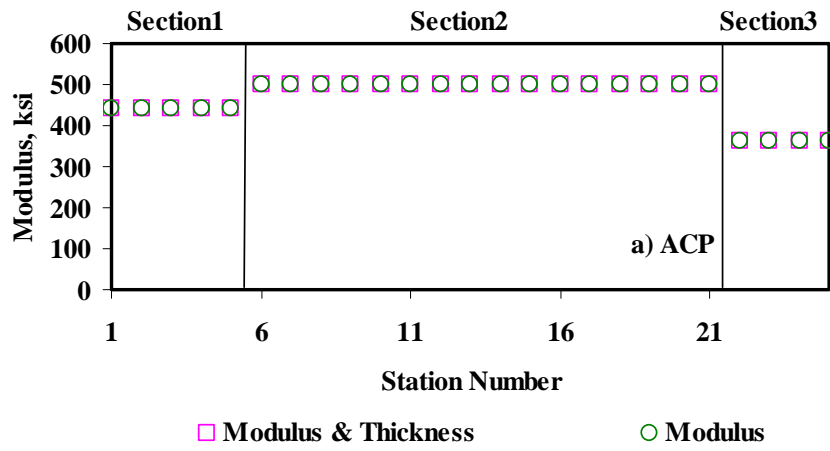| Section No.		Thickness, in.			Modulus, ksi							RMS Error, %
		ACP	Base	SB	ACP	Base		Subbase		Subgrade		
						Cons.	Avg.	Cons.	Avg.	Cons.	Avg.	
1	Average	2.4	6.5	8.4	441	74	101	32	55	12	13	2.5
	Std Dev	0.4	1.9	3.5	-	12.2	3.0	7.5	5.6	0.5	0.6	-
	COV	18%	29%	42%	-	16%	3%	24%	10%	4%	5%	-
2	Average	2.1	18.4	-	499	75	102	-	-	16	17	3.0
	Std Dev	0.4	1.8	-	-	13.2	8.8	-	-	1.7	1.9	-
	COV	17%	10%	-	-	18%	9%	-	-	11%	11%	-
3	Average	1.9	4.1	10.5	363	89	103	33	58	16	18	2.5
	Std Dev	0.1	0.8	5.4	-	9.3	3.5	4.5	0.9	2.3	2.5	-
	COV	6%	21%	51%	-	10%	3%	14%	2%	14%	14%	-

Figure C.3 - Comparison of Design Moduli from JIM Analysis with Constant and Backcalculated Thickness
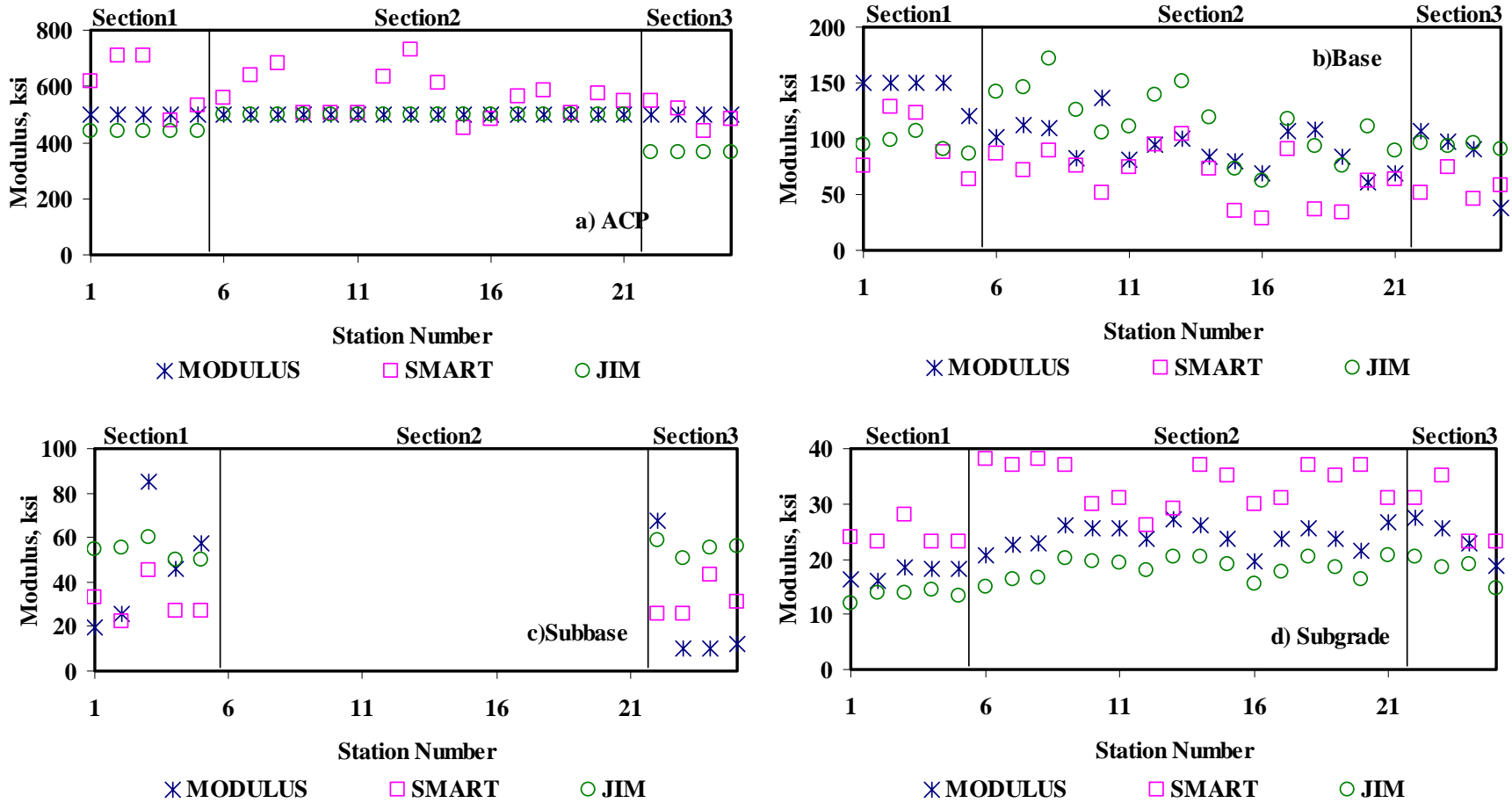
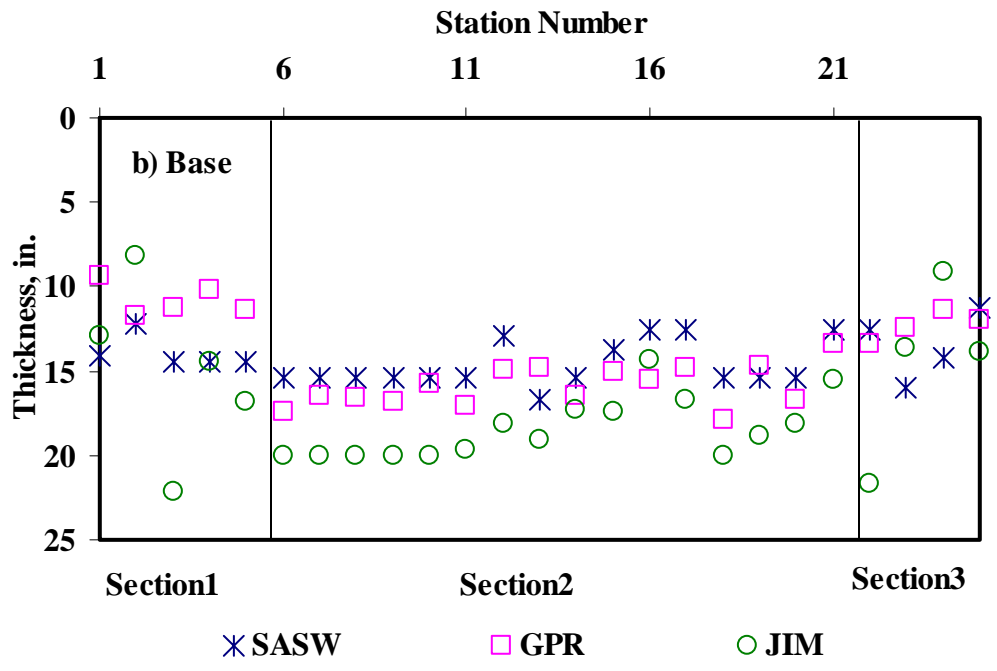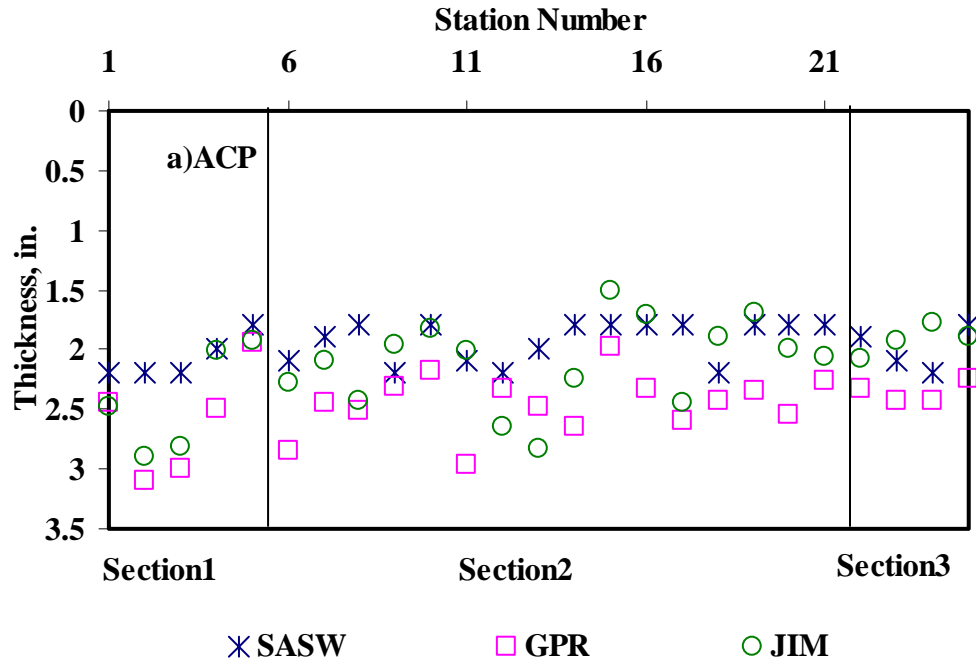**Figure C.4 - Comparison of Design Moduli from Different Analyses**

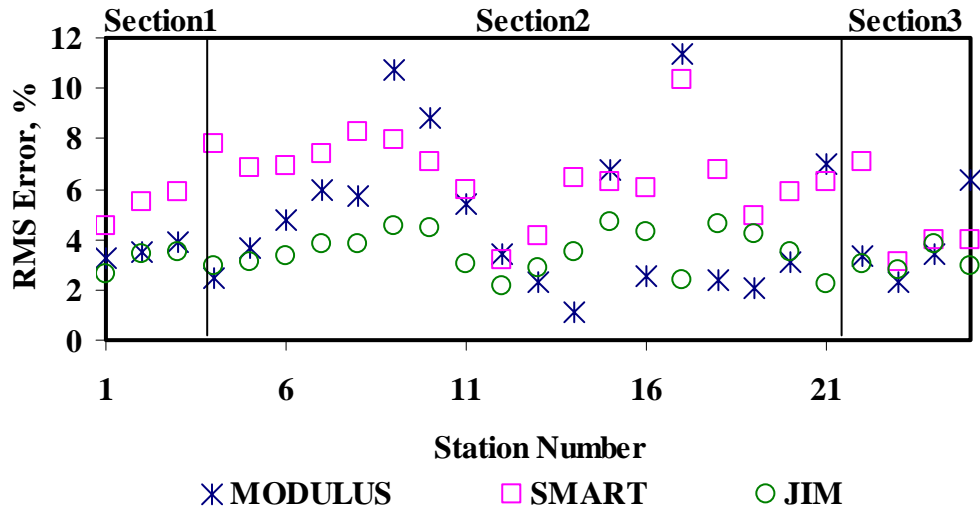**Figure C.5 - Comparison of Layer Thickness from Different Analyses**

Figure C.6 - Comparison of RMS Error from Different Analyses

Table C.8 - Summary of Design Modulus Values with Data Fusion Results

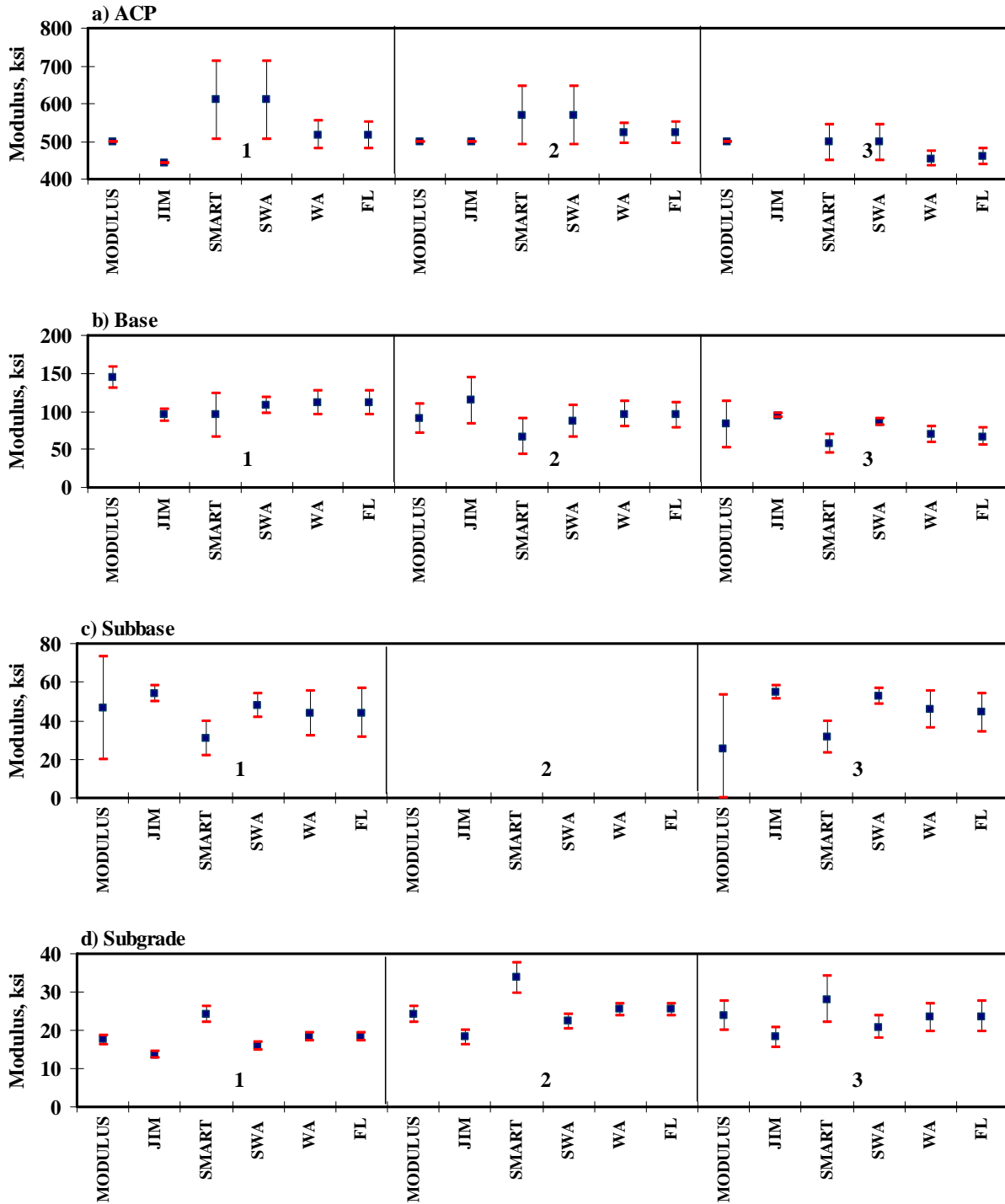| Section No.	Method	Modulus, ksi							
		ACP		Base		Subbase		Subgrade	
		Average	COV	Average	COV	Average	COV	Average	COV
1	MODULUS	500	-	144	9%	47	57%	18	7%
	JIM	441	-	95	9%	54	8%	14	7%
	SMART	609	17%	96	30%	31	29%	24	9%
	SWA	609	17%	108	10%	48	13%	16	6%
	WA	517	7%	112	14%	44	27%	18	6%
	FL	517	7%	112	14%	44	28%	18	6%
2	MODULUS	500	-	90	22%	-	-	24	9%
	JIM	499	-	114	27%	-	-	18	11%
	SMART	568	14%	67	36%	-	-	34	12%
	SWA	568	14%	87	25%	-	-	22	9%
	WA	522	5%	96	17%	-	-	25	6%
	FL	524	5%	95	17%	-	-	25	6%
3	MODULUS	500	-	83	37%	25	114%	24	16%
	JIM	363	-	94	3%	55	6%	18	14%
	SMART	498	10%	58	22%	32	25%	28	21%
	SWA	498	10%	86	5%	53	8%	21	14%
	WA	454	4%	70	16%	46	21%	23	16%
	FL	460	5%	67	17%	44	23%	24	17%

130

Figure C.7 - Statistical Comparison of Design Moduli of Different Analyses and Data Fusion Techniques

APPENDIX D - Results of Analyses for Eagle Pass Inspection Facility (Laredo)

Table D.1 - Results of SASW Analysis for Estimating Seismic Moduli

Section No.		Modulus, ksi			RMS Error, %
		ACP	Base	Subgrade	
Strip 2	Average	1377	283	45.7	6.1
	Std Dev	190	85	9.8	-
	COV	14%	30%	21%	-
Strip 4	Average	1244	209	44.5	6.3
	Std Dev	367	103	8.4	-
	COV	29%	49%	19%	-

Table D.2 - Results of SASW Analysis for Estimating Seismic Moduli and Thicknesses

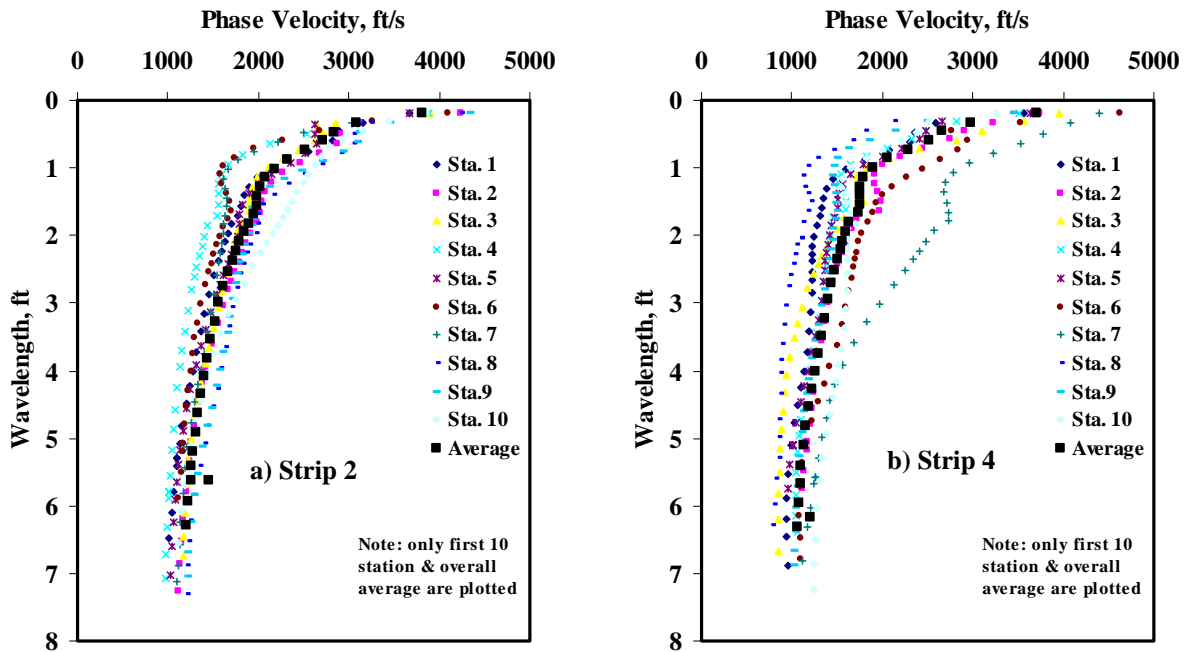| Section No.		Thickness, in.		Modulus, ksi			RMS Error, %
		ACP	Base	ACP	Base	Subgrade	
Strip 2	Average	2.0	11.7	1504	254	51.7	7.6
	Std Dev	0.2	1.2	217	33	7.2	-
	COV	10%	10%	14%	13%	14%	-
Strip 4	Average	1.9	11.2	1579	226	46.5	10.4
	Std Dev	0.1	1.1	212	45	5.0	-
	COV	8%	10%	13%	20%	11%	-

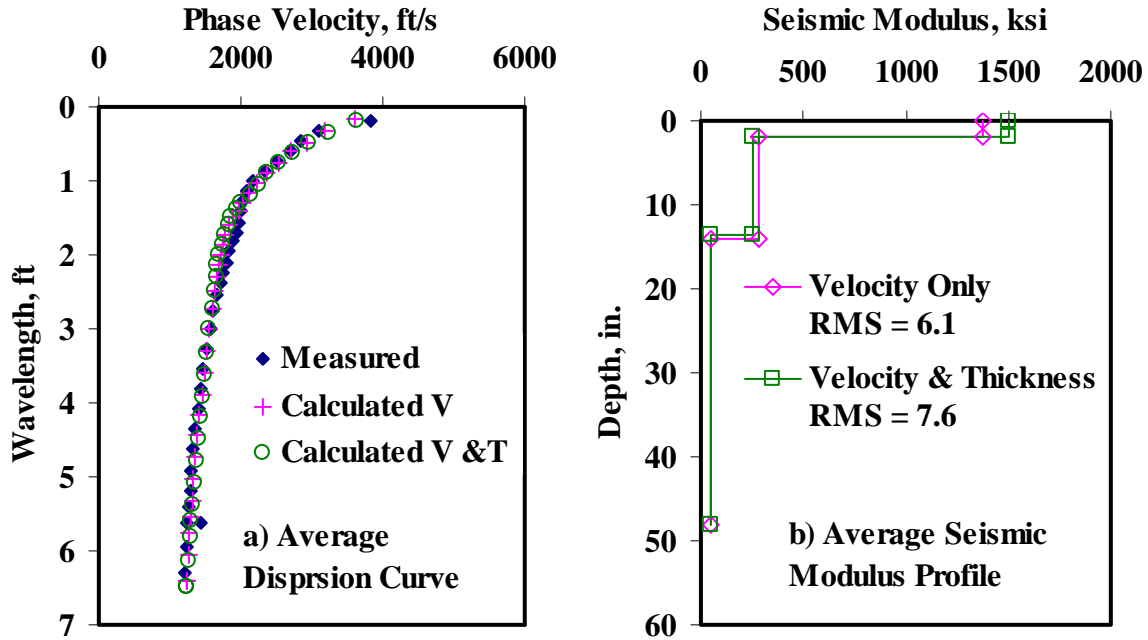**Figure D.1 - Results of Dispersion Curve from SASW Analysis**

135

Figure D.2 - Results of SASW Data Reduction Process (Strip 2)
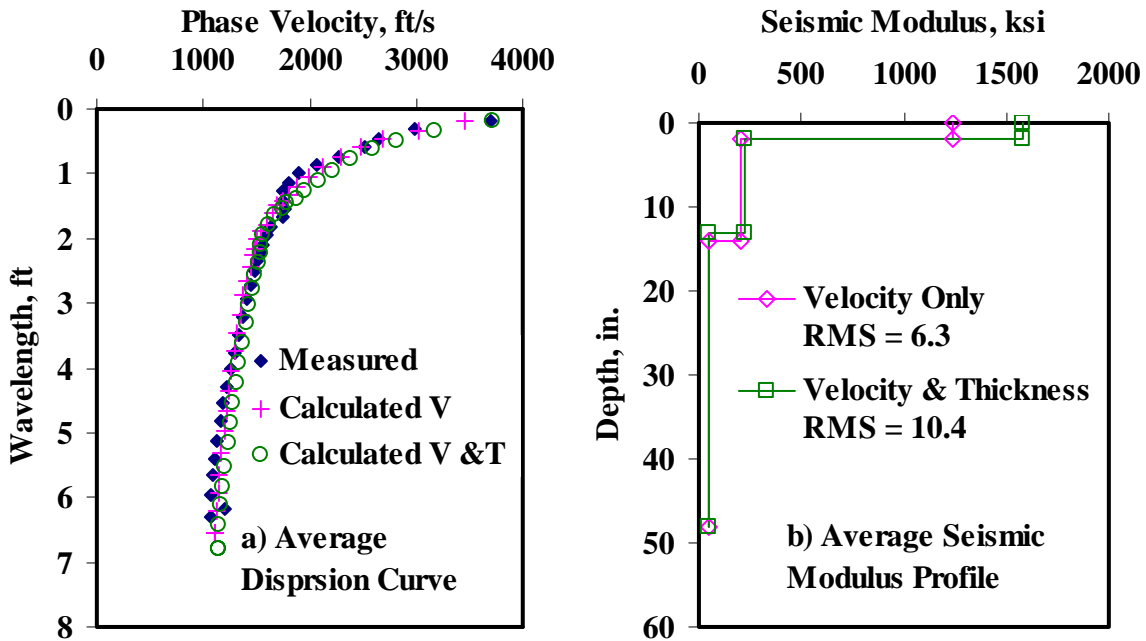

Figure D.3 - Results of SASW Data Reduction Process (Strip 4)

136

Table D.3 - Results of SMART Analysis for Estimating Design Moduli

Section No.		Modulus, ksi					RMS Error, %
		ACP	Base		Subgrade		
			Cons.	Avg.	Cons.	Avg.	
Strip 2	**Average**	**420**	**162**	**223**	**29**	**39**	**6.0**
	Std Dev	*64.6*	*49.5*	*63.5*	*7.0*	*9.6*	*-*
	COV	*15%*	*31%*	*28%*	*24%*	*25%*	*-*
Strip 4	**Average**	**389**	**120**	**167**	**27**	**38**	**6.4**
	Std Dev	*119.7*	*70.5*	*91.2*	*5.8*	*7.4*	*-*
	COV	*31%*	*59%*	*55%*	*21%*	*20%*	*-*

Table D.4 - Summary Statistics of Measured FWD Deflections

Section		Normalized Deflection, mils (12 in. Spacing)						
		d0	d1	d2	d3	d4	d5	d6
Strip 2	**Average**	**11.3**	**4.7**	**3.0**	**2.0**	**1.6**	**1.3**	**1.1**
	Std Dev	*5.7*	*1.7*	*0.9*	*0.5*	*0.4*	*0.3*	*0.2*
	COV	*50%*	*36%*	*31%*	*26%*	*25%*	*26%*	*22%*
Strip 4	**Average**	**13.3**	**5.8**	**3.2**	**2.2**	**1.6**	**1.3**	**1.0**
	Std Dev	*7.1*	*1.9*	*0.8*	*0.4*	*0.3*	*0.2*	*0.1*
	COV	*53%*	*33%*	*23%*	*20%*	*17%*	*15%*	*14%*

Table D.5 - Results MODULUS Analysis for Estimating Design Moduli

Section		Modulus, ksi			RMS Error, %
		ACP	Base	Subgrade	
Strip 2	**Average**	**500**	**105**	**41**	**12.0**
	Std Dev	*-*	*40.3*	*13.2*	*-*
	COV	*-*	*38%*	*32%*	*-*
Strip 4	**Average**	**500**	**93**	**36**	**11.1**
	Std Dev	*-*	*57.4*	*9.7*	*-*
	COV	*-*	*62%*	*27%*	*-*

Table D.6 - Results of JIM Analysis for Estimating Design Moduli

Section No.		Modulus, ksi					RMS Error, %
		ACP	Base		Subgrade		
			Cons.	Avg.	Cons.	Avg.	
Strip 2	Average	490	139	240	26	28	3.7
	Std Dev	87	25	37	7	8	-
	COV	18%	18%	15%	28%	28%	-
Strip 4	Average	440	114	203	24	26	3.8
	Std Dev	176	36	54	65	6	-
	COV	40%	31%	27%	23%	23%	-

Table D.7 - Results of JIM Analysis for Estimating Design Moduli and Thicknesses

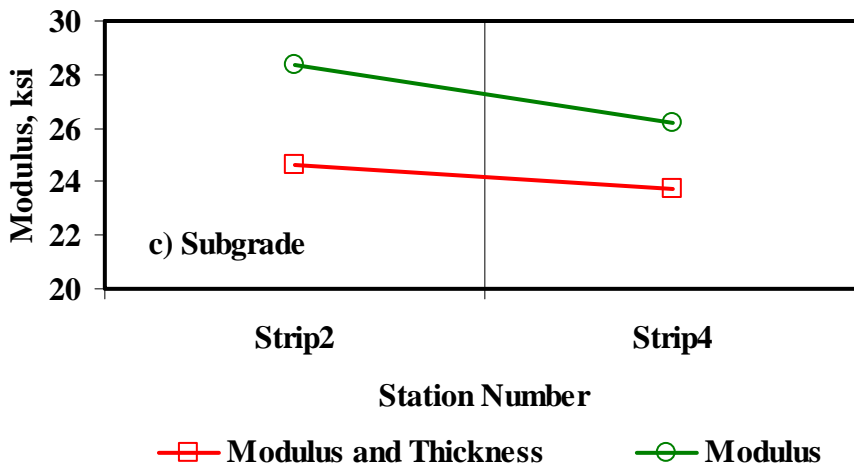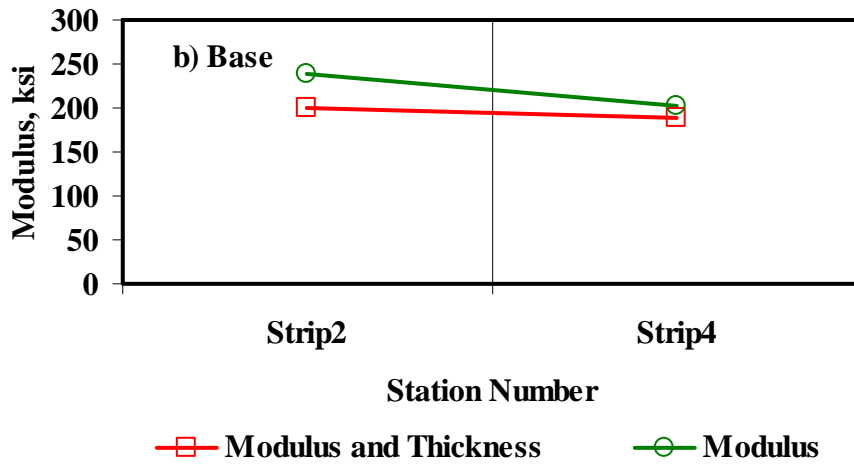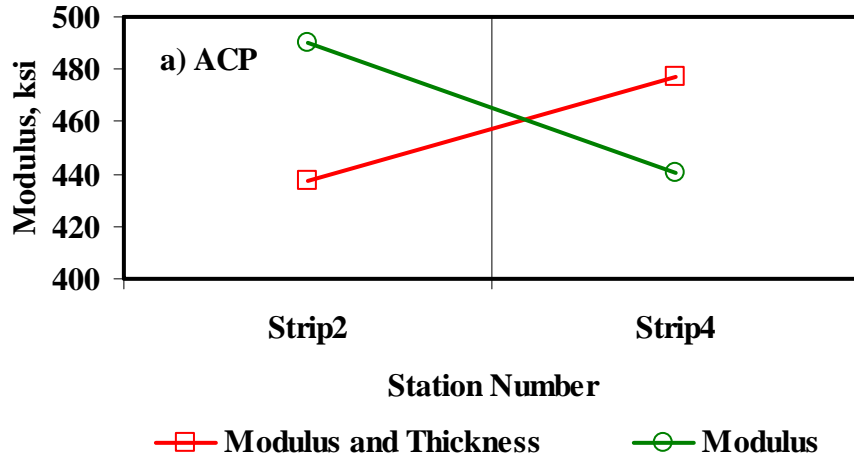| Section No.		Thickness, in.		Modulus, ksi					RMS Error, %
		ACP	Base	ACP	Base		Subgrade		
					Cons.	Avg.	Cons.	Avg.	
Strip 2	Average	2.7	18.0	437	187	200	23	25	3.2
	Std Dev	0.8	2.7	39.9	49.5	38.4	5.3	5.8	-
	COV	29%	15%	9%	27%	19%	23%	23%	-
Strip 4	Average	2.2	14.8	477	164.8	189.2	21.8	23.7	3.4
	Std Dev	0.8	4.5	36.3	63.1	48.5	3.8	4.1	-
	COV	38%	31%	8%	38%	26%	18%	17%	-

Figure D.4 - Comparison of Design Moduli from JIM Analysis with Constant and Backcalculated Thicknesses

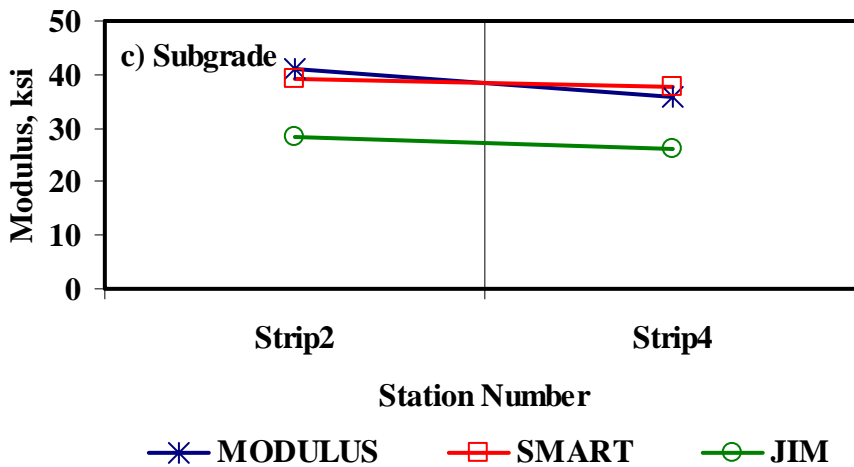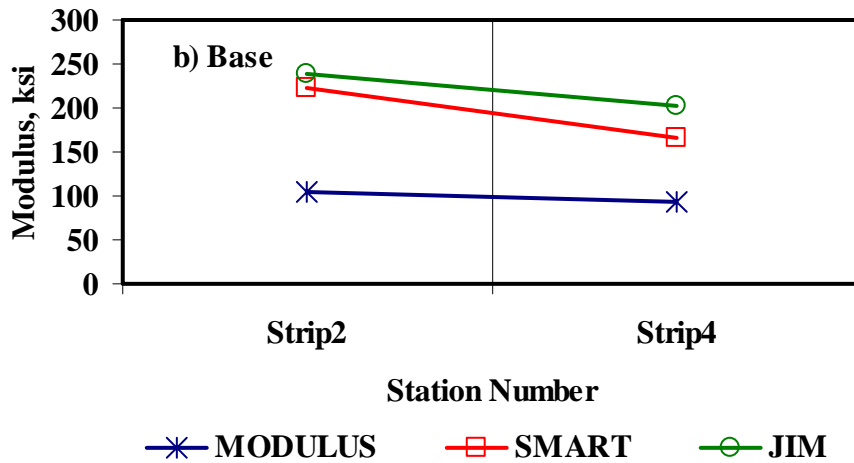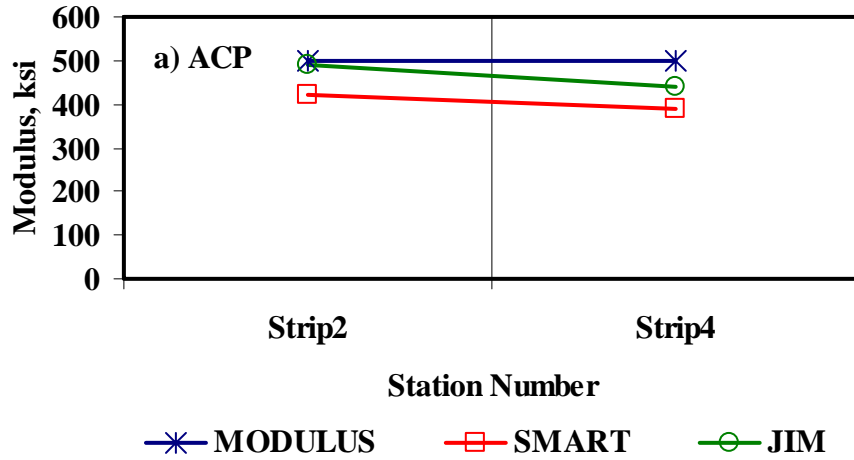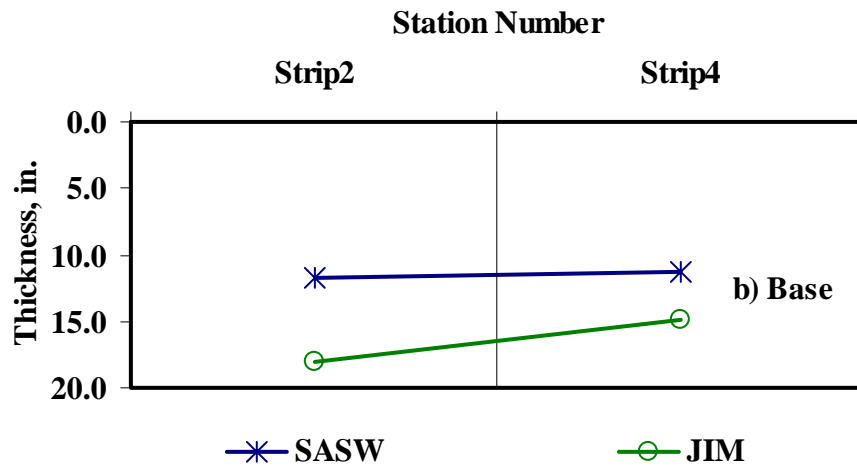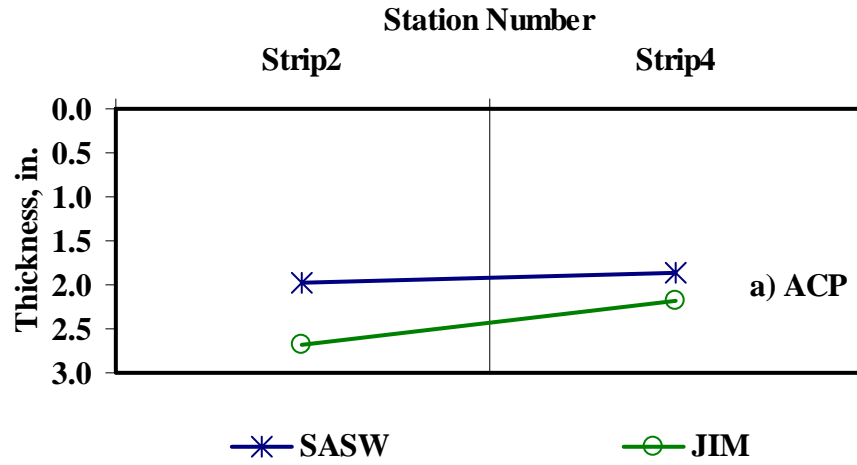**Figure D.5 - Comparison of Design Moduli from Different Analyses**

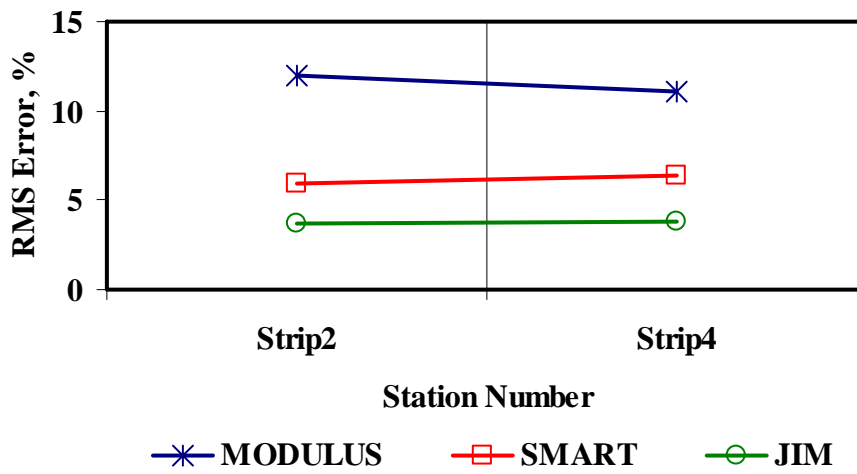Figure D.6 - Comparison of Layer Thickness from Different Analyses

Figure D.7 - Comparison of RMS Error from Different Analyses

Table D.8 - Summary of Design Modulus Values with Data Fusion Results

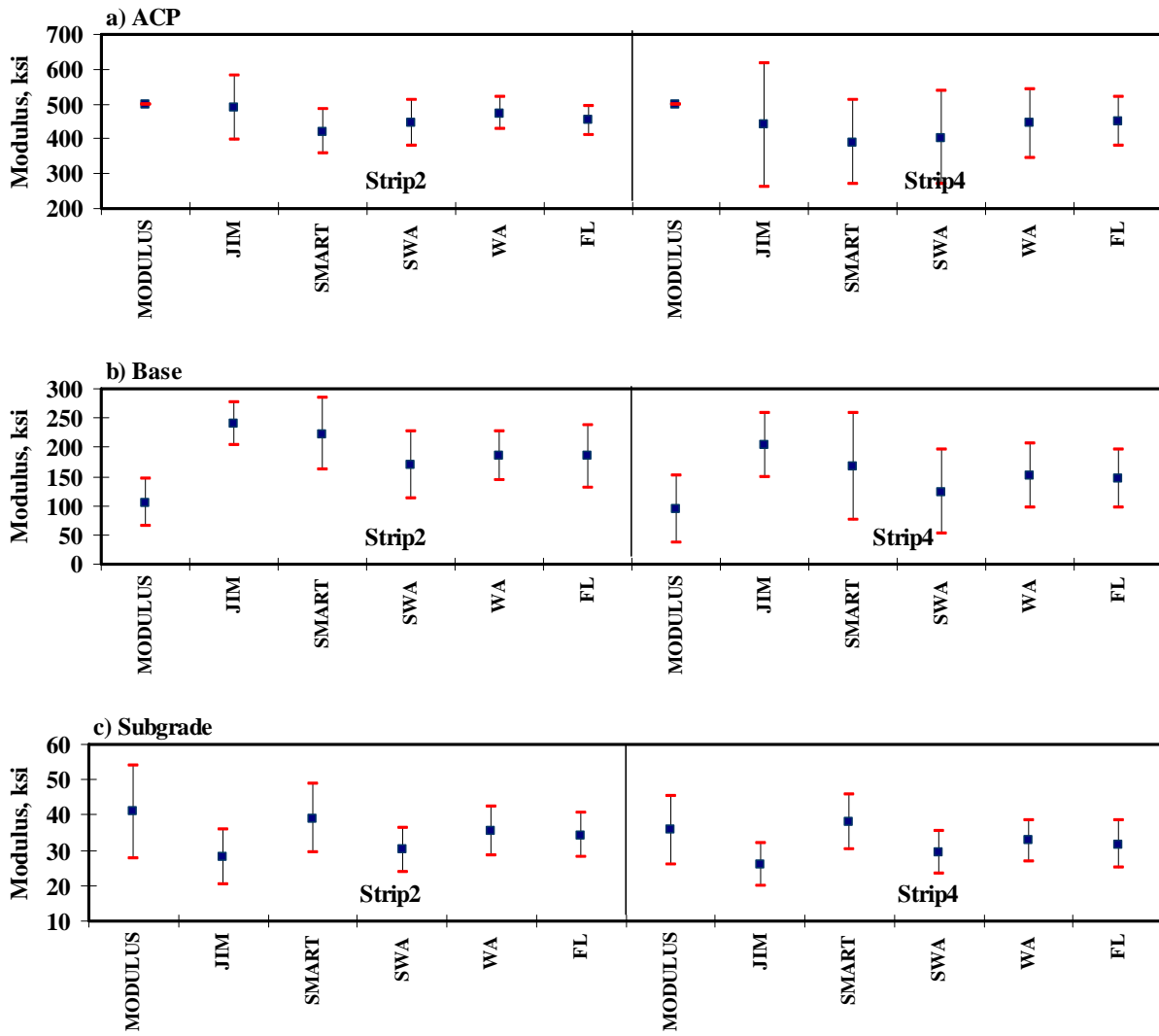| Section No. | Method | Modulus, ksi | | | | | |
| | | ACP | | Base | | Subgrade | |
		Average	COV	Average	COV	Average	COV
Strip2	MODULUS	500	-	105	38%	41	32%
	JIM	490	18%	240	15%	28	28%
	SMART	420	15%	223	28%	39	25%
	SWA	445	15%	170	34%	30	21%
	WA	474	10%	186	23%	36	20%
	FL	453	9%	184	29%	34	18%
Strip4	MODULUS	500	-	93	62%	36	27%
	JIM	440	40%	203	27%	26	23%
	SMART	389	31%	167	55%	38	20%
	SWA	403	33%	123	58%	29	20%
	WA	444	22%	152	36%	33	18%
	FL	450	15%	146	34%	32	21%

Figure D.8 - Statistical Comparison of Design Moduli of Different Analyses and Data Fusion Techniques

143

APPENDIX E - Results of Analyses for IH - I20 (Odessa, Ward)

Table E.1 - Results of SASW Analysis for Estimating Seismic Moduli

Section No.		Modulus, ksi			RMS Error, %
		ACP	Base	Subgrade	
1	Average	1591	133	144.2	6.3
	Std Dev	184	35	13.6	-
	COV	12%	26%	9%	-
2	Average	1770	141	151.4	5.3
	Std Dev	197	30	15.3	-
	COV	11%	21%	10%	-
3	Average	2373	202	140.7	5.2
	Std Dev	172	39	17.8	-
	COV	7%	19%	13%	-
4	Average	1846	137	147.9	4.6
	Std Dev	119	15	17.5	-
	COV	6%	11%	12%	-

Table E.2 - Results of SASW Analysis for Estimating Seismic Moduli and Thicknesses

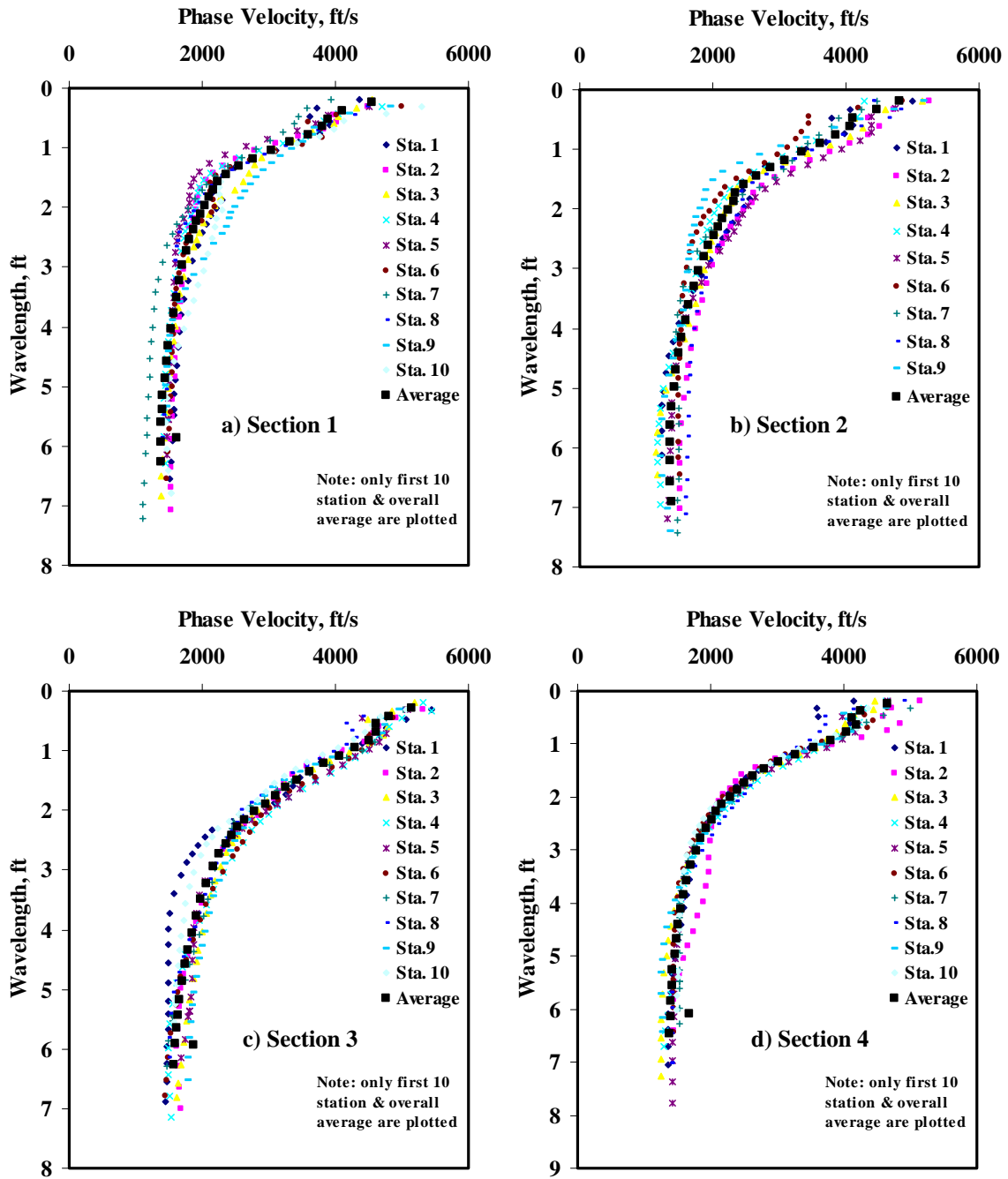| Section No.		Thickness, in.		Modulus, ksi			RMS Error, %
		ACP	Base	ACP	Base	Subgrade	
1	Average	4.5	17.3	1896	167	125.9	7.5
	Std Dev	0.2	1.7	299	44	17.2	-
	COV	6%	10%	16%	26%	14%	-
2	Average	4.7	16.9	1941	157	130.7	6.0
	Std Dev	0.3	2.3	212	20	27.2	-
	COV	7%	13%	11%	13%	21%	-
3	Average	5.5	16.1	2205	168	136.3	5.3
	Std Dev	0.5	1.8	184	33	21.6	-
	COV	8%	11%	8%	19%	16%	-
4	Average	5.0	18.7	1876	145	134.8	4.6
	Std Dev	0.4	1.6	191	20	20.0	-
	COV	8%	9%	10%	14%	15%	-

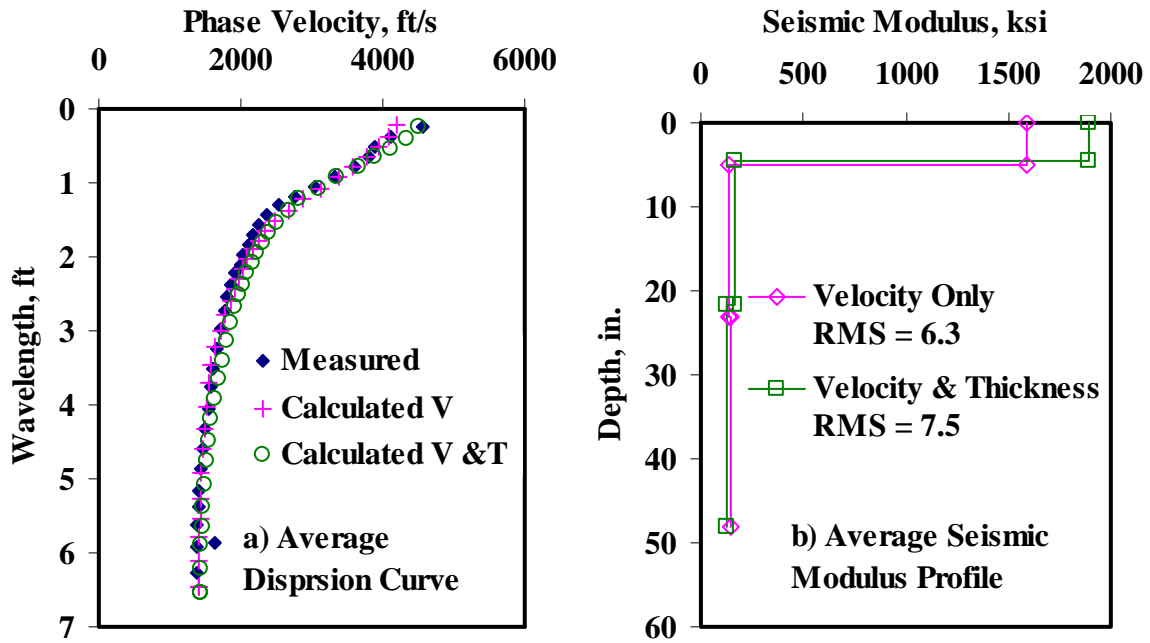**Figure E.1 - Results of Dispersion Curve from SASW Analysis**

148

Figure E.2 - Results of SASW Data Reduction Process (Section 1)
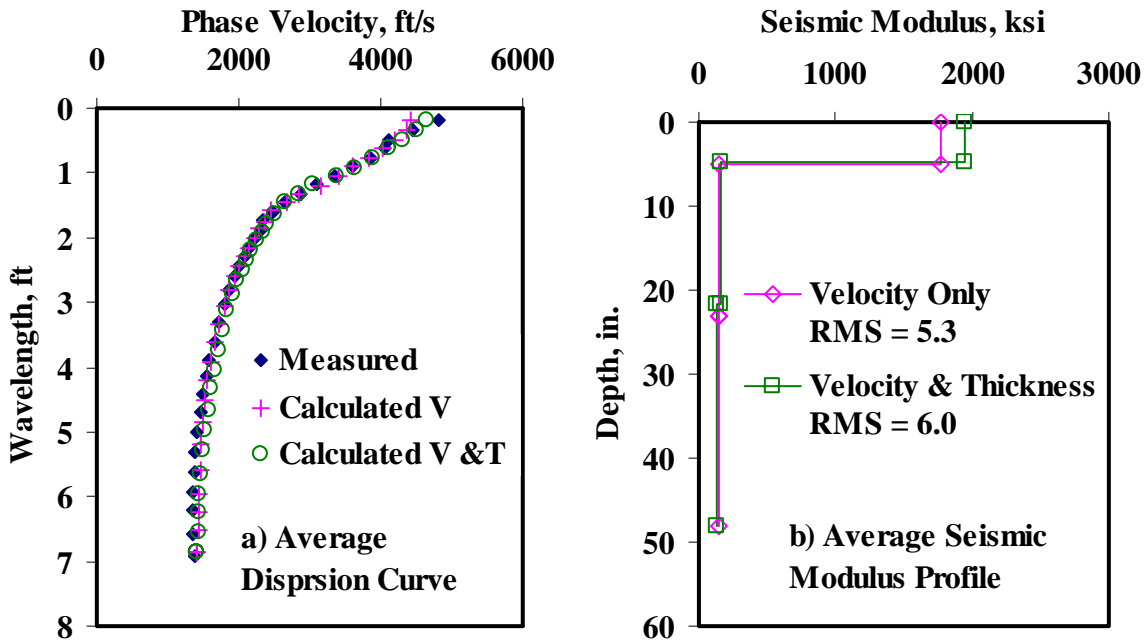

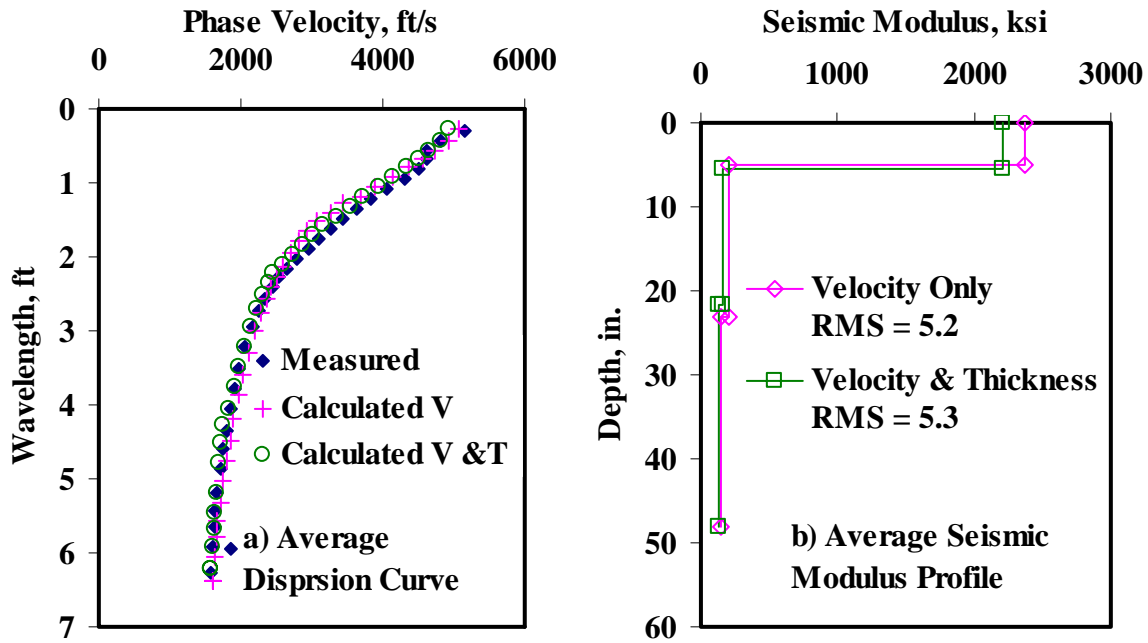**Figure E.3 - Results of SASW Data Reduction Process (Section 2)**

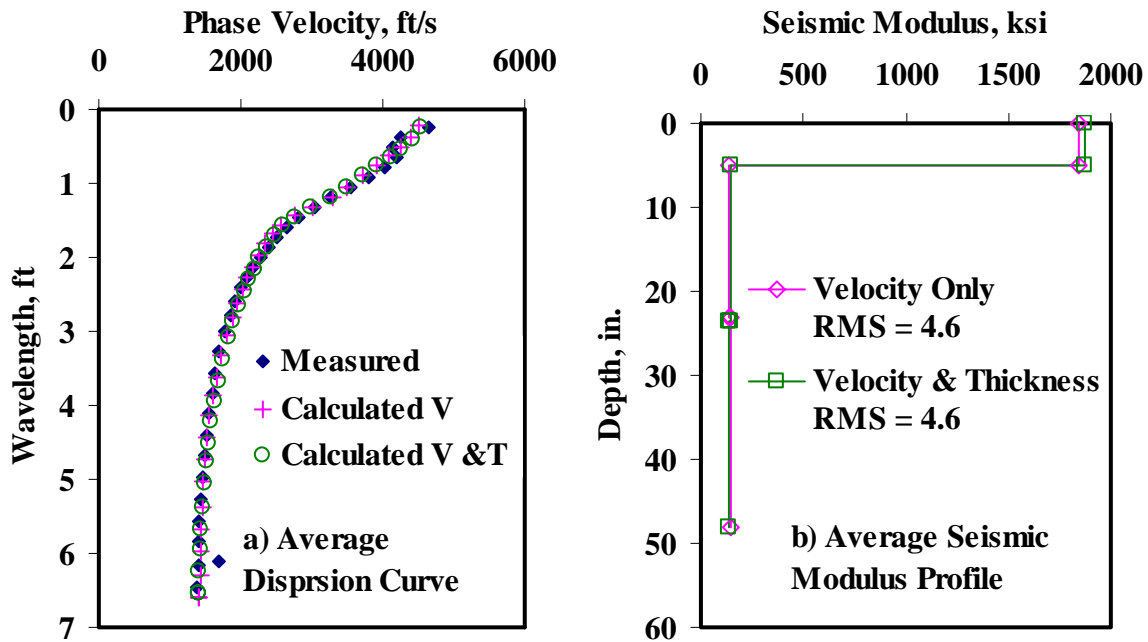**Figure E.4 - Results of SASW Data Reduction Process (Section 3)**

Figure E.5 - Results of SASW Data Reduction Process (Section 4)

150

Table E.3 - Results of SMART Analysis for Estimating Design Moduli

Section No.		ACP	Base		Subgrade		RMS Error, %
			Cons.	Avg.	Cons.	Avg.	
1	**Average**	**465**	**107**	**112**	**116**	**129**	**6.2**
	Std Dev	*53.9*	*30.5*	*34.4*	*12.5*	*12.0*	*-*
	COV	*12%*	*28%*	*31%*	*11%*	*9%*	*-*
2	**Average**	**516**	**118**	**122**	**125**	**137**	**5.3**
	Std Dev	*57.6*	*28.5*	*31.4*	*16.0*	*15.4*	*-*
	COV	*11%*	*24%*	*26%*	*13%*	*11%*	*-*
3	**Average**	**692**	**164**	**184**	**116**	**128**	**6.0**
	Std Dev	*50.5*	*28.9*	*38.8*	*17.7*	*17.3*	*-*
	COV	*7%*	*18%*	*21%*	*15%*	*14%*	*-*
4	**Average**	**545**	**114**	**119**	**118**	**131**	**5.4**
	Std Dev	*37.2*	*15.4*	*16.8*	*18.2*	*17.7*	*-*
	COV	*7%*	*13%*	*14%*	*15%*	*14%*	*-*

Modulus, ksi spans the ACP, Base, and Subgrade columns.

Table E.4 - Summary Statistics of Measured FWD Deflections

Section No.		Normalized Deflection, mils (12 in. Spacing)						
		d0	d1	d2	d3	d4	d5	d6
1	**Average**	**7.2**	**3.7**	**1.6**	**1.0**	**0.8**	**0.7**	**0.6**
	Std Dev	*1.2*	*0.7*	*0.4*	*0.3*	*0.3*	*0.2*	*0.2*
	COV	*16%*	*19%*	*25%*	*29%*	*31%*	*33%*	*37%*
2	**Average**	**7.6**	**4.2**	**1.9**	**1.1**	**0.8**	**0.6**	**0.5**
	Std Dev	*1.9*	*1.1*	*0.8*	*0.5*	*0.4*	*0.3*	*0.2*
	COV	*25%*	*27%*	*40%*	*48%*	*51%*	*52%*	*48%*
3	**Average**	**4.3**	**2.7**	**1.5**	**0.9**	**0.7**	**0.6**	**0.4**
	Std Dev	*0.7*	*0.6*	*0.5*	*0.3*	*0.3*	*0.2*	*0.2*
	COV	*17%*	*21%*	*30%*	*36%*	*36%*	*37%*	*35%*
4	**Average**	**6.9**	**3.9**	**1.8**	**1.0**	**0.8**	**0.7**	**0.5**
	Std Dev	*0.7*	*0.4*	*0.3*	*0.3*	*0.1*	*0.1*	*0.1*
	COV	*10%*	*11%*	*15%*	*27%*	*19%*	*22%*	*18%*

Table E.5 - Results MODULUS Analysis for Estimating Design Moduli

Section No.		Modulus, ksi			RMS Error, %
		ACP	Base	Subgrade	
1	Average	561	62	71	9.8
	Std Dev	163.4	15.4	19.8	-
	COV	29%	25%	28%	-
2	Average	803	49	76	6.0
	Std Dev	252.5	16.9	32.7	-
	COV	31%	34%	43%	-
3	Average	1682	96	80	5.4
	Std Dev	394.3	22.7	31.1	-
	COV	23%	24%	39%	-
4	Average	935	48	70	10.0
	Std Dev	318.6	12.1	11.4	-
	COV	34%	25%	16%	-

Table E.6 - Results of JIM Analysis for Estimating Design Moduli

Section No.		Modulus, ksi					RMS Error, %
		ACP	Base		Subgrade		
			Cons.	Avg.	Cons.	Avg.	
1	Average	586	101	145	49	52	3.3
	Std Dev	86	33	47	14	15	-
	COV	15%	33%	33%	28%	28%	-
2	Average	682	96	137	52	55	2.9
	Std Dev	95	20.2	29.6	22.5	24.4	-
	COV	14%	21%	22%	44%	44%	-
3	Average	914	162	224	54	57	3.0
	Std Dev	77	26.6	33.0	17.7	19.0	-
	COV	8%	16%	15%	33%	33%	-
4	Average	706	95	140	47	50	3.4
	Std Dev	63	21.3	31.6	7.9	8.6	-
	COV	9%	22%	23%	17%	17%	-

152

Table E.7 - Results of JIM Analysis for Estimating Design Moduli and Thicknesses

| Section No. | | Thickness, in. | | Modulus, ksi | | | | | RMS Error, % |
| | | | | ACP | Base | | Subgrade | | |
		ACP	Base		Cons.	Avg.	Cons.	Avg.	
1	Average	5.2	27.2	491	65	93	40	43	3.7
	Std Dev	0.8	5.8	43.7	14.3	17.6	14.2	15.4	-
	COV	15%	21%	9%	22%	19%	35%	36%	-
2	Average	5.5	18.8	535	74.6	104.6	50.2	54.0	2.6
	Std Dev	0.7	7.3	45.3	11.1	15.8	20.9	22.8	-
	COV	13%	39%	8%	15%	15%	42%	42%	-
3	Average	6.5	22.0	660	108	143	53	56	2.3
	Std Dev	0.8	7.7	46.4	22.0	23.5	16.2	17.6	-
	COV	12%	35%	7%	20%	16%	31%	31%	-
4	Average	5.8	21.9	544	65	93	44	47	3.2
	Std Dev	0.3	10.2	52.4	22.7	27.7	8.3	9.1	-
	COV	6%	46%	10%	35%	30%	19%	19%	-
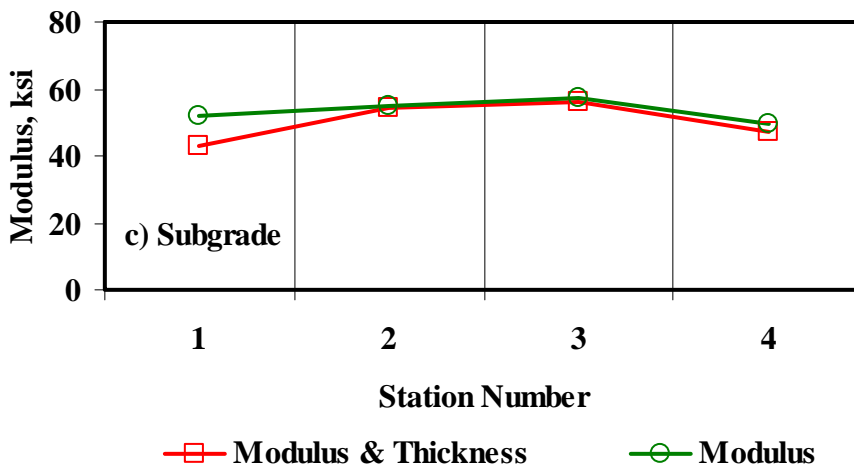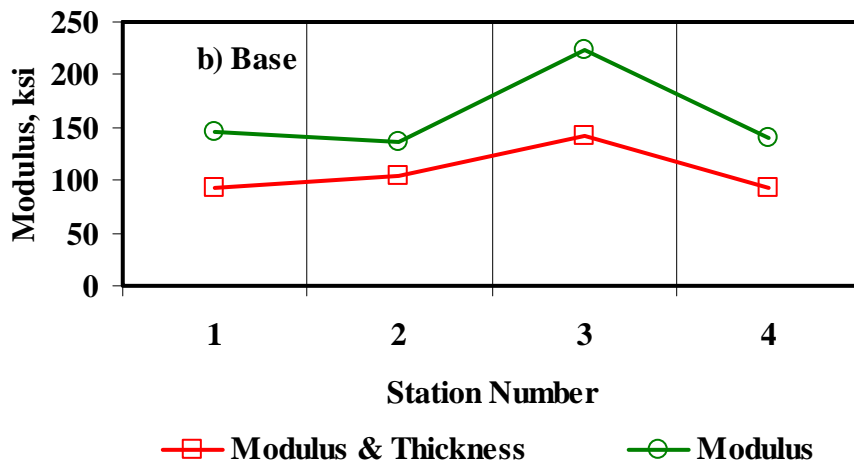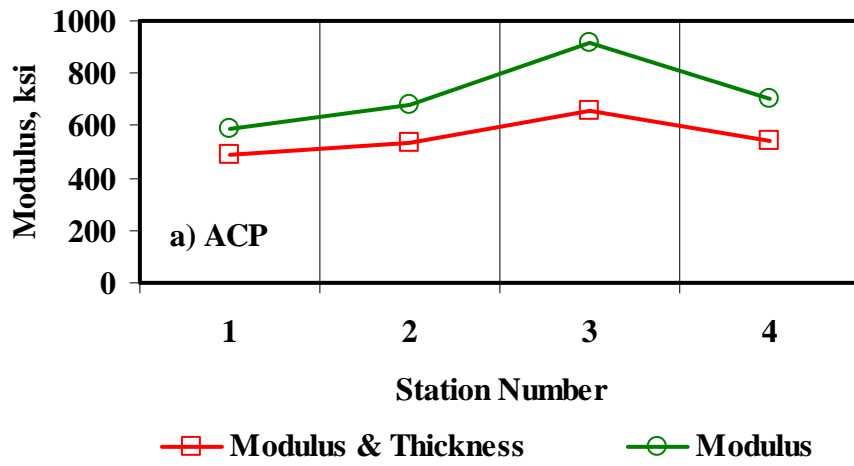
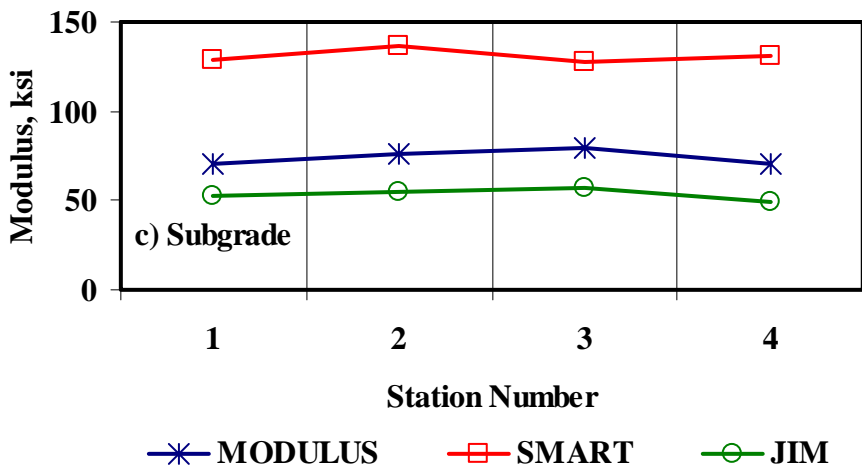**Figure E.6 - Comparison of Design Moduli from JIM Analysis with Constant and Backcalculated Thickness**

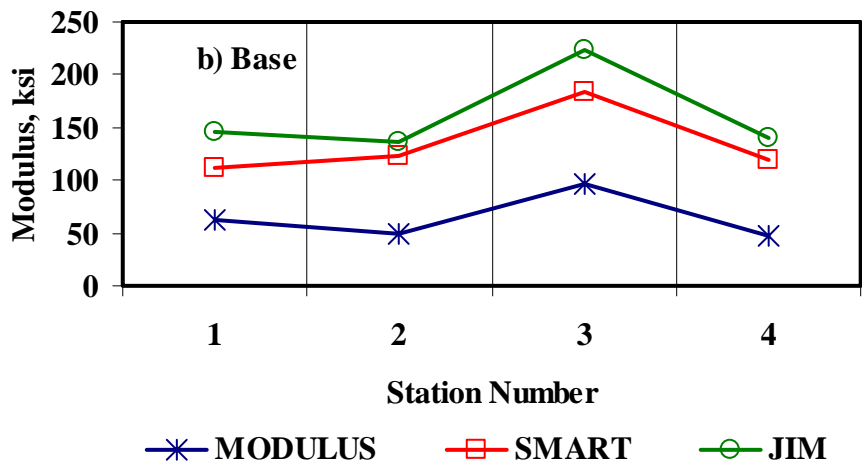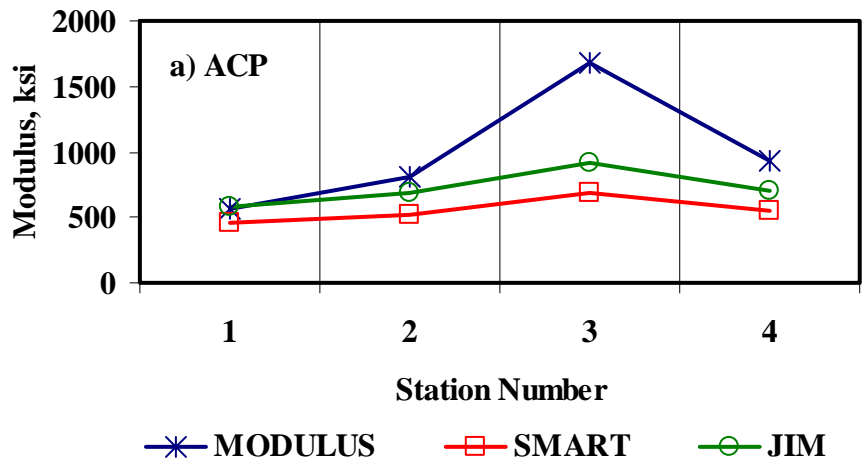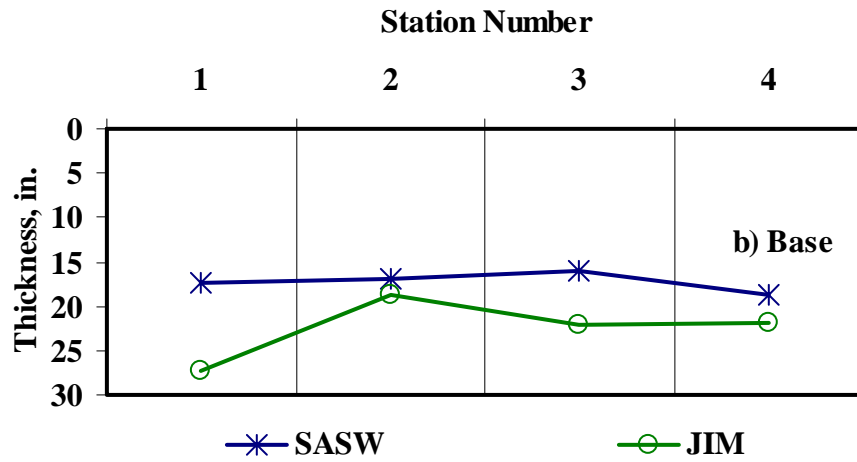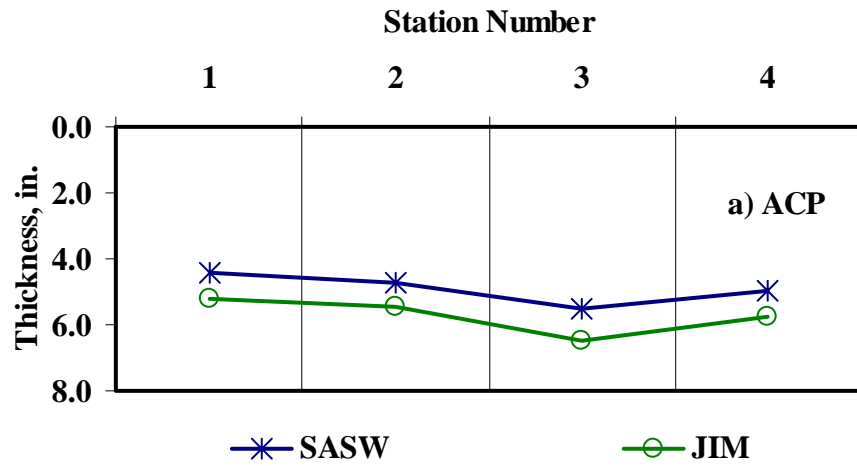**Figure E.7 - Comparison of Design Moduli from Different Analyses**

Figure E.8 - Comparison of Layer Thickness from Different Analyses
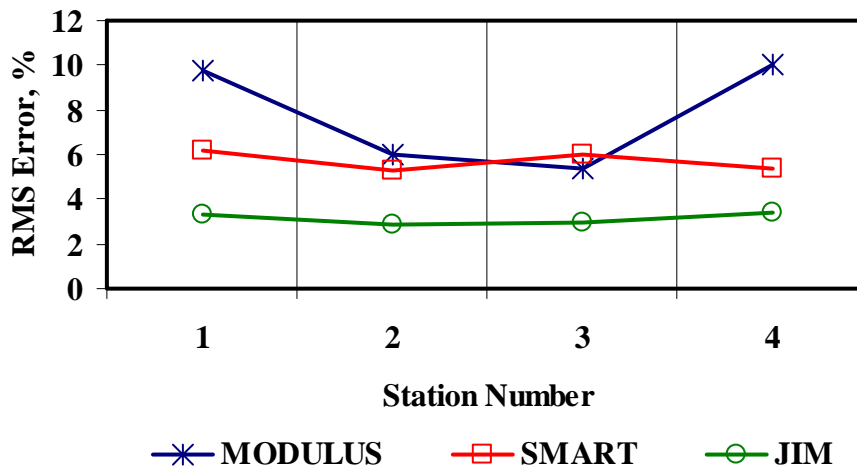

Figure E.9 - Comparison of RMS Error from Different Analyses

Table E.8 - Summary of Design Modulus Values with Data Fusion Results

| Section No.	Method	Modulus, ksi					
		ACP		Base		Subgrade	
		Average	COV	Average	COV	Average	COV
1	MODULUS	561	29%	62	25%	71	28%
	JIM	586	15%	145	33%	52	28%
	SMART	465	12%	112	31%	129	9%
	SWA	495	12%	80	22%	70	18%
	WA	525	15%	110	16%	82	10%
	FL	510	11%	101	19%	86	11%
2	MODULUS	803	31%	49	34%	76	43%
	JIM	682	14%	137	22%	55	44%
	SMART	516	11%	122	26%	137	11%
	SWA	564	12%	75	36%	97	31%
	WA	663	19%	101	21%	87	24%
	FL	628	15%	94	23%	95	16%
3	MODULUS	1682	23%	96	24%	80	39%
	JIM	914	8%	224	10%	57	30%
	SMART	692	7%	184	21%	128	14%
	SWA	769	7%	142	20%	86	25%
	WA	1096	14%	168	15%	88	18%
	FL	1015	18%	167	16%	90	21%
4	MODULUS	935	34%	48	25%	70	16%
	JIM	706	9%	140	23%	50	17%
	SMART	545	7%	119	14%	131	14%
	SWA	575	7%	77	22%	67	17%
	WA	727	15%	102	16%	85	14%
	FL	680	7%	95	12%	81	16%
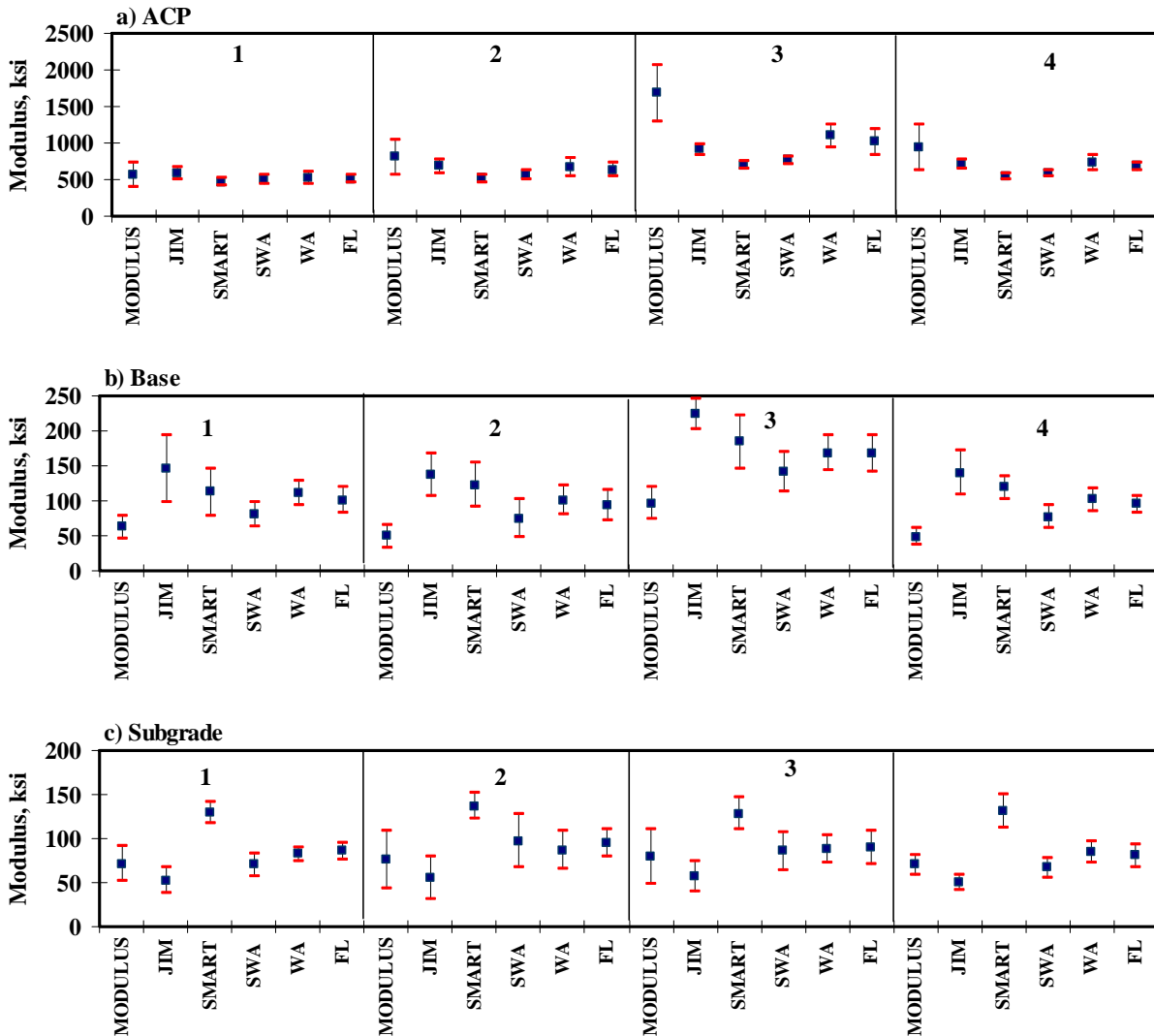
Figure E.10 - Statistical Comparison of Design Moduli of Different Analyses and Data Fusion Techniques

APPENDIX F - Results of Analyses for IH - I20 (Odessa, Ector)

160

Table F.1 - Results of SASW Analysis for Estimating Seismic Moduli

Section No.		Modulus, ksi			RMS Error, %
		ACP	Base	Subgrade	
1	Average	1074	90	95.6	4.6
	Std Dev	177	19	15.8	-
	COV	16%	21%	17%	-
2	Average	966	95	98.9	5.8
	Std Dev	89	23	14.9	-
	COV	9%	24%	15%	-
3	Average	980	111	115.0	5.1
	Std Dev	128	23	12.3	-
	COV	13%	21%	11%	-
4	Average	980	111	115.0	4.9
	Std Dev	128	23	12.3	-
	COV	13%	21%	11%	-

Table F.2 - Results of SASW Analysis for Estimating Seismic Moduli and Thicknesses

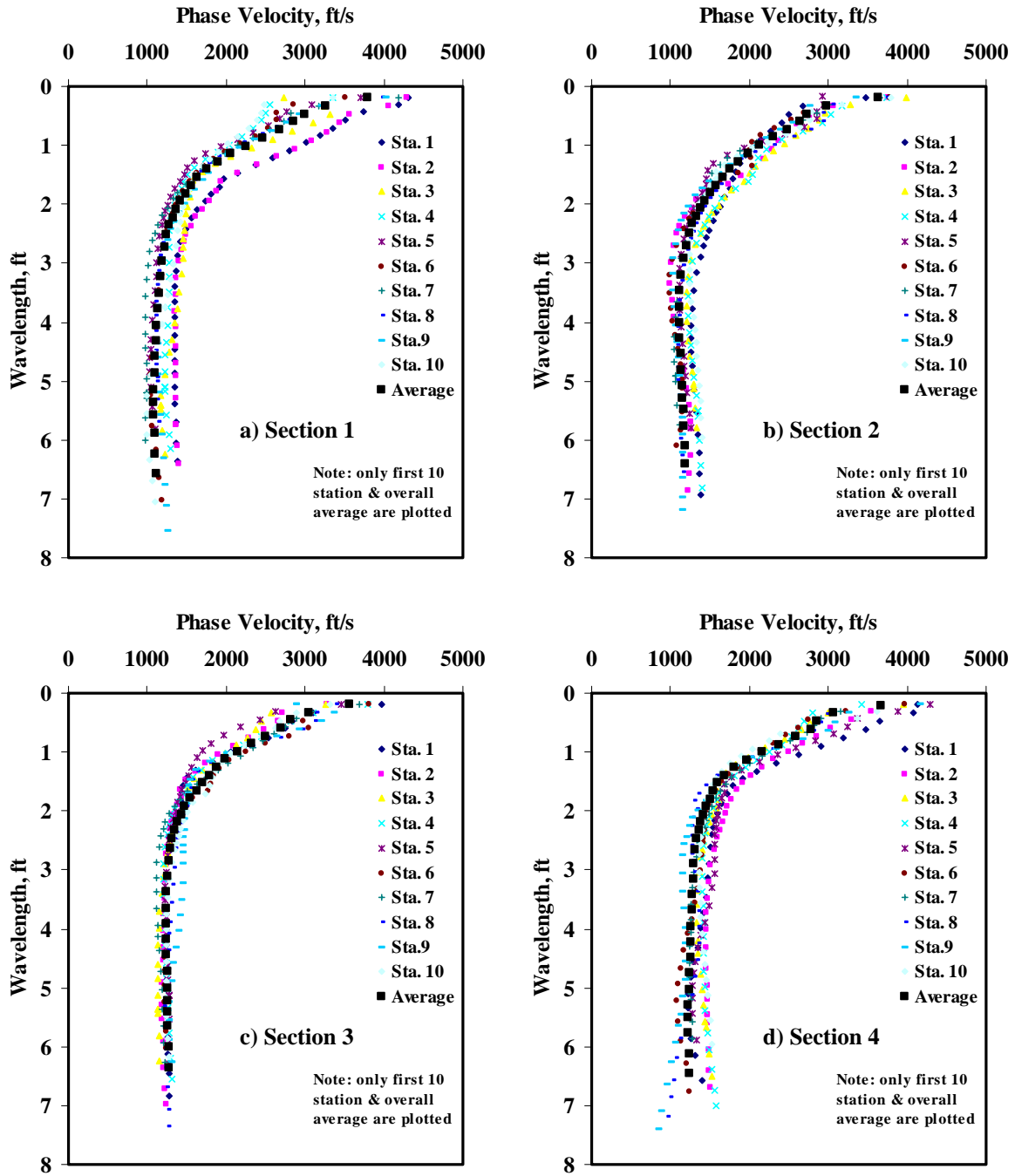| Section No.		Thickness, in.		Modulus, ksi			RMS Error, %
		ACP	Base	ACP	Base	Subgrade	
1	Average	3.2	23.5	1251	90	53.5	5.4
	Std Dev	0.2	2.2	213	18	5.7	-
	COV	8%	9%	17%	20%	11%	-
2	Average	3.2	24.3	1127	92	49.7	7.3
	Std Dev	0.2	1.4	167	19	7.5	-
	COV	7%	6%	15%	21%	15%	-
3	Average	3.3	24.3	1129	108	53.0	7.3
	Std Dev	0.2	1.0	167	17	6.3	-
	COV	5%	4%	15%	16%	12%	-
4	Average	3.3	24.3	1129	108	53.0	5.2
	Std Dev	0.2	1.0	167	17	6.3	-
	COV	5%	4%	15%	16%	12%	-

Figure F.1 - Results of Dispersion Curve from SASW Analysis
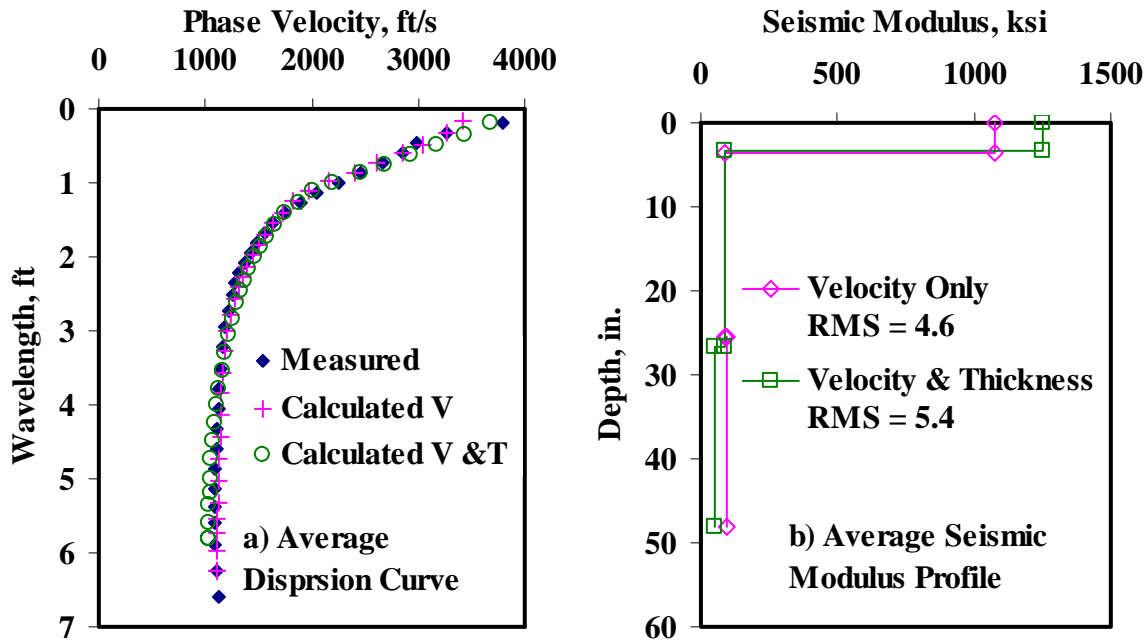
Figure F.2 - Results of SASW Data Reduction Process (Section 1)
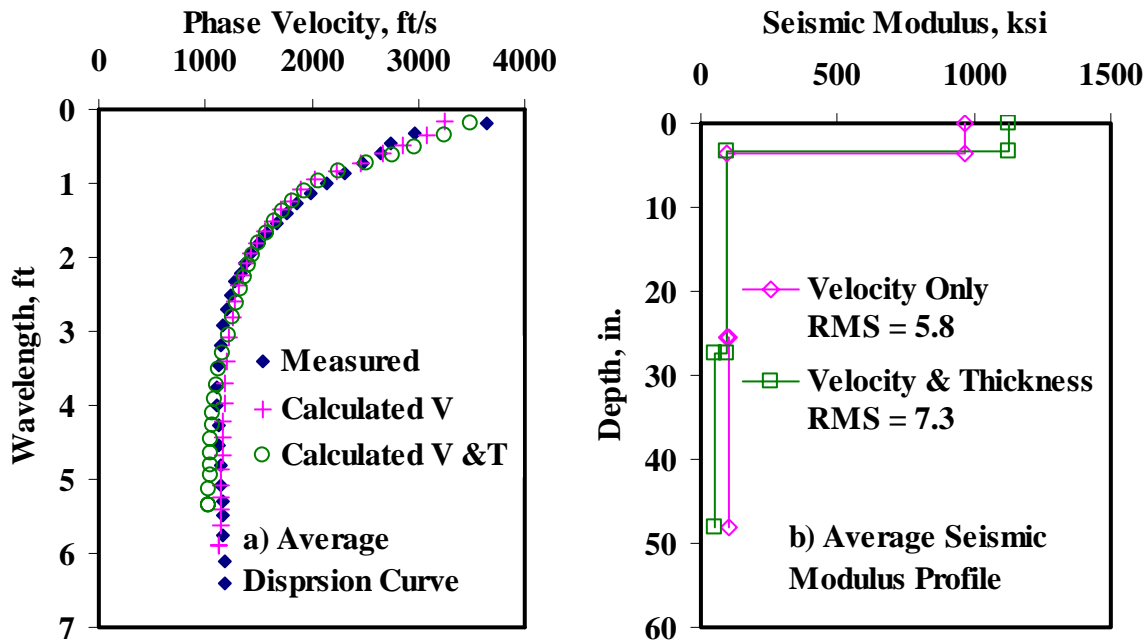

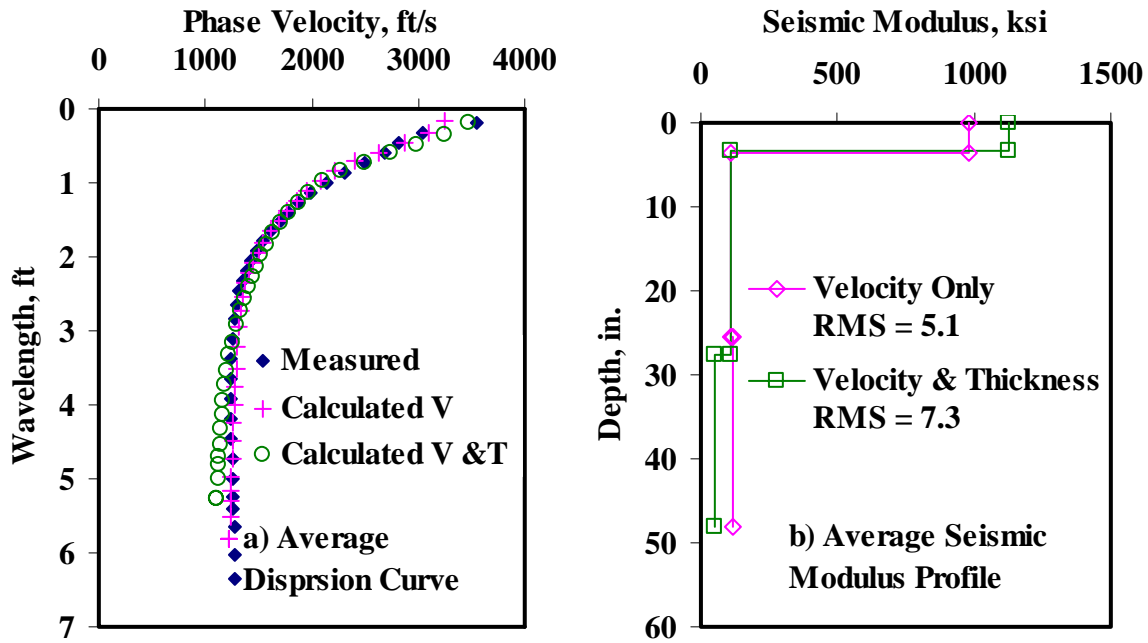**Figure F.3 - Results of SASW Data Reduction Process (Section 2)**

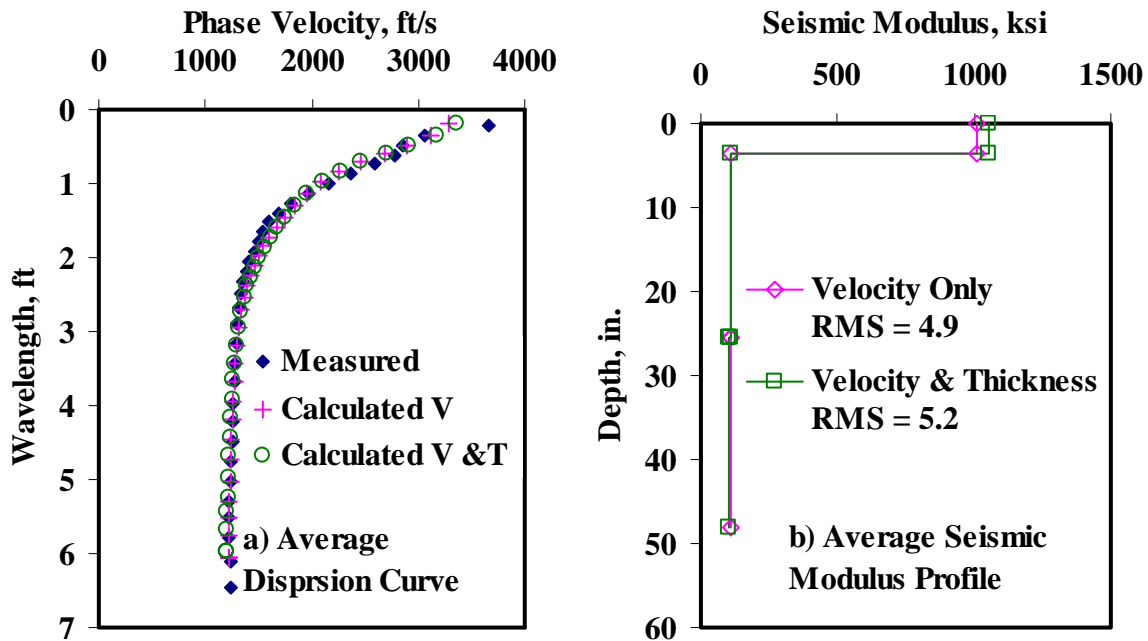**Figure F.4 - Results of SASW Data Reduction Process (Section 3)**

Figure F.5 - Results of SASW Data Reduction Process (Section 4)

164

Table F.3 - Results of SMART Analysis for Estimating Design Moduli

Section No.		Modulus, ksi					RMS Error, %
		ACP	Base		Subgrade		
			Cons.	Avg.	Cons.	Avg.	
1	Average	329	66	69	70	84	4.6
	Std Dev	51.6	15.4	16.4	12.9	13.3	-
	COV	16%	23%	24%	18%	16%	-
2	Average	313	69	72	73	87	5.6
	Std Dev	29.6	18.1	20.2	13.5	13.8	-
	COV	9%	26%	28%	19%	16%	-
3	Average	322	85	90	88	102	5.0
	Std Dev	42.6	22.0	24.1	12.5	12.0	-
	COV	13%	26%	27%	14%	12%	-
4	Average	316	86	91	86	101	4.9
	Std Dev	49.9	19.0	20.7	15.1	14.8	-
	COV	16%	22%	23%	18%	15%	-

Table F.4 - Summary Statistics of Measured FWD Deflections

Section No.		Normalized Deflection, mils (12 in. Spacing)						
		d0	d1	d2	d3	d4	d5	d6
1	Average	14.9	6.3	2.0	1.1	0.9	0.7	0.6
	Std Dev	3.3	1.4	0.6	0.5	0.3	0.3	0.2
	COV	22%	22%	31%	40%	40%	40%	41%
2	Average	13.7	5.2	1.5	0.9	0.7	0.5	0.4
	Std Dev	2.3	1.1	0.4	0.3	0.2	0.1	0.1
	COV	17%	20%	29%	30%	27%	27%	25%
3	Average	14.3	5.1	1.4	0.8	0.7	0.5	0.4
	Std Dev	3.4	1.3	0.4	0.3	0.3	0.3	0.2
	COV	24%	24%	32%	41%	44%	48%	49%
4	Average	13.6	5.6	1.6	0.9	0.7	0.6	0.5
	Std Dev	2.6	1.1	0.4	0.3	0.3	0.2	0.2
	COV	19%	19%	28%	35%	37%	44%	44%

165

Table F.5 - Results MODULUS Analysis for Estimating Design Moduli

Section No.		Modulus, ksi			RMS Error, %
		ACP	Base	Subgrade	
1	Average	512	31	65	9.0
	Std Dev	248.2	18.0	22.7	-
	COV	48%	58%	35%	-
2	Average	394	34	85	8.8
	Std Dev	119.1	7.5	30.2	-
	COV	30%	22%	35%	-
3	Average	318	37	107	12.7
	Std Dev	115.6	21.8	92.2	-
	COV	36%	59%	86%	-
4	Average	529	31	86	10.5
	Std Dev	219.8	7.1	37.2	-
	COV	42%	23%	43%	-

Table F.6 - Results of JIM Analysis for Estimating Design Moduli

Section No.		Modulus, ksi					RMS Error, %
		ACP	Base		Subgrade		
			Cons.	Avg.	Cons.	Avg.	
1	Average	373	49	70	45	48	3.6
	Std Dev	64.8	12	15	16	17	-
	COV	17%	25%	22%	36%	36%	-
2	Average	334	55	76	56	59	3.9
	Std Dev	36.2	11.7	14.6	13.1	14.3	-
	COV	11%	21%	19%	24%	24%	-
3	Average	346	70	96	58	63	4.9
	Std Dev	62.5	28.8	36.1	19.9	21.6	-
	COV	18%	41%	38%	34%	35%	-
4	Average	362	61	84	54	58	4.7
	Std Dev	64.2	13.1	16.6	17.3	18.8	-
	COV	18%	22%	20%	32%	32%	-

Table F.7 - Results of JIM Analysis for Estimating Design Moduli and Thicknesses

| Section No.		Thickness, in.		Modulus, ksi					RMS Error, %
				ACP	Base		Subgrade		
		AC	Base		Cons.	Avg.	Cons.	Avg.	
1	Average	2.6	21.0	466	75	104	43	46	3.9
	Std Dev	0.5	10.1	41.1	25.0	24.8	14.7	16.0	-
	COV	21%	48%	9%	33%	24%	34%	35%	-
2	Average	2.6	24.8	444	71.6	98.9	53.9	57.6	4.2
	Std Dev	0.5	9.7	24.6	24.5	24.5	12.8	13.9	-
	COV	18%	39%	6%	34%	25%	24%	24%	-
3	Average	3.0	30.9	424	76	106	55	59	5.0
	Std Dev	0.9	7.7	38.0	26.0	27.5	20.3	22.1	-
	COV	31%	25%	9%	34%	26%	37%	37%	-
4	Average	2.9	24.5	434	82	109	53	56	4.9
	Std Dev	0.9	10.2	47.1	32.8	30.4	17.4	19.0	-
	COV	32%	42%	11%	40%	28%	33%	34%	-
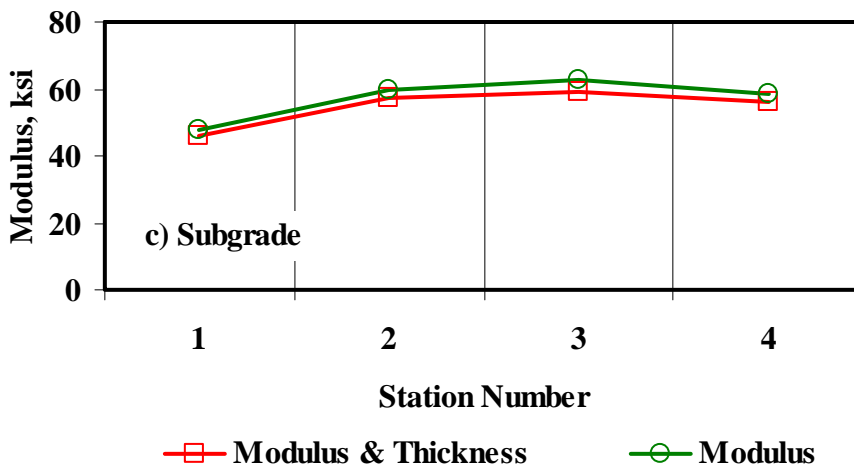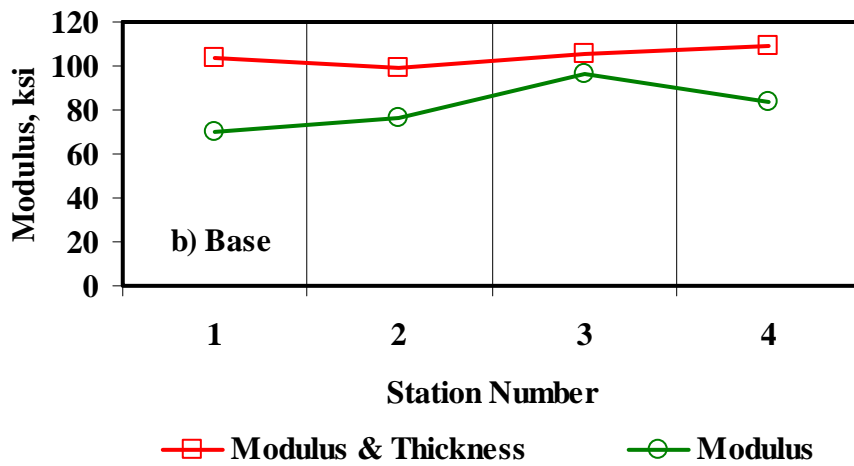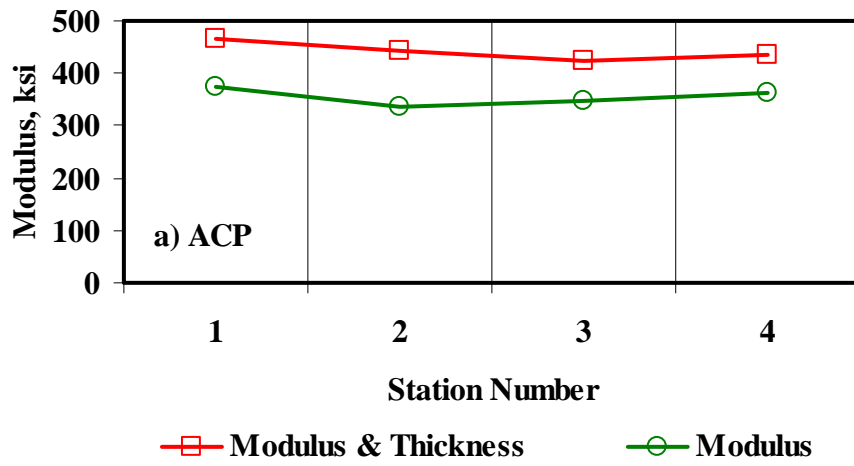
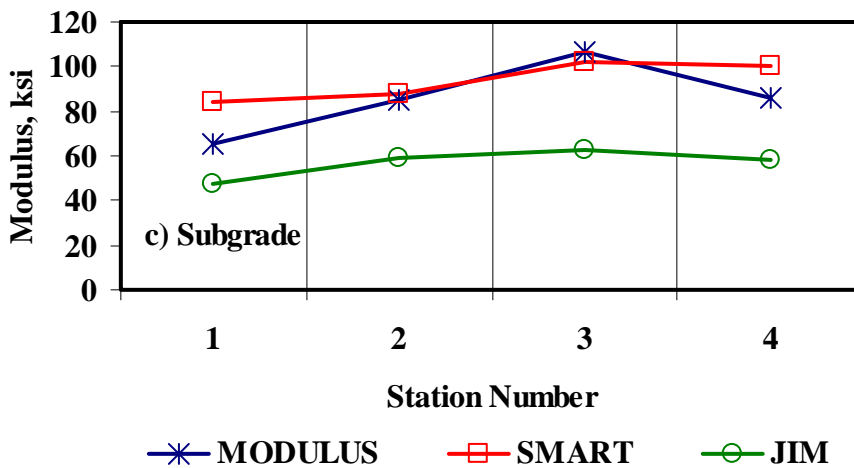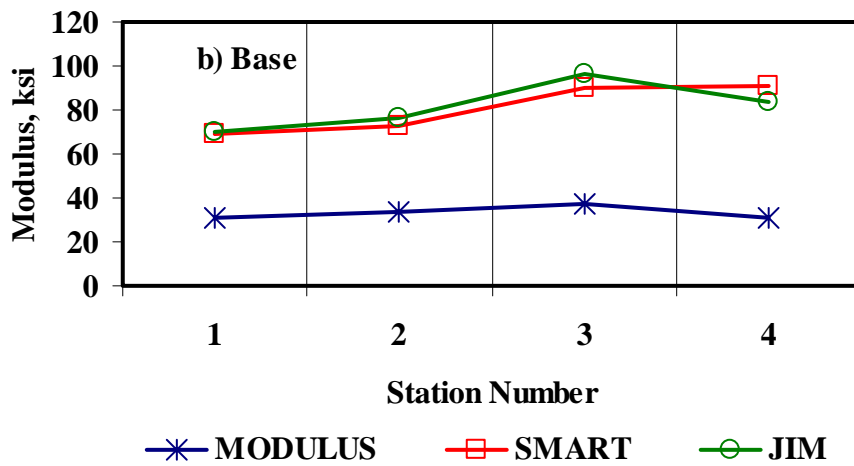**Figure F.6 - Comparison of Design Moduli from JIM Analysis with Constant and Backcalculated Thickness**
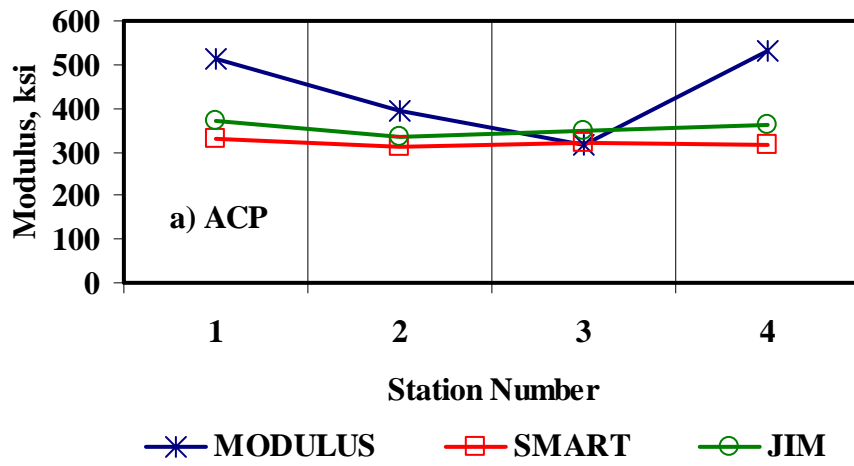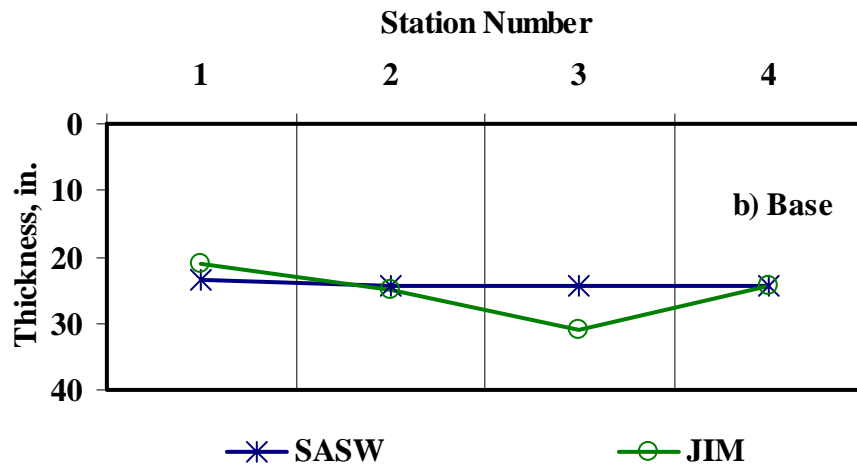
Figure F.7 - Comparison of Design Moduli from Different Analyses
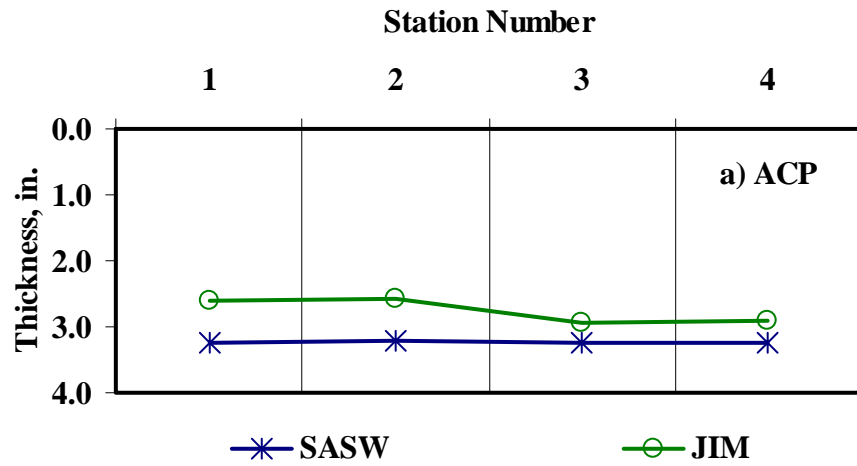
Figure F.8 - Comparison of Layer Thickness from Different Analyses
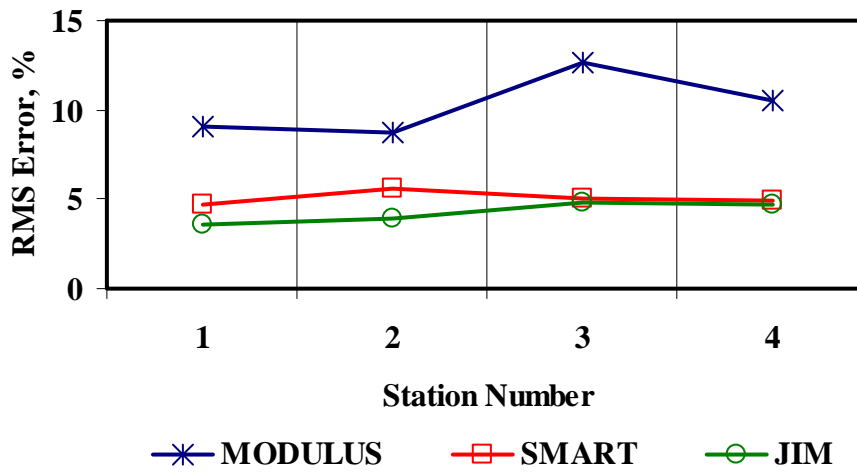
Figure F.9 - Comparison of RMS Error from Different Analyses

170

Table F.8 - Summary of Design Modulus Values with Data Fusion Results

Section No.	Method	Modulus, ksi					
		AC		Base		Subgrade	
		Average	COV	Average	COV	Average	COV
1	MODULUS	512	48%	31	58%	65	35%
	JIM	373	17%	70	22%	48	36%
	SMART	329	16%	69	24%	84	16%
	SWA	338	15%	41	23%	65	14%
	WA	405	19%	57	16%	66	17%
	FL	382	20%	54	20%	69	14%
2	MODULUS	394	30%	34	22%	85	35%
	JIM	334	11%	76	19%	59	24%
	SMART	313	9%	72	28%	87	16%
	SWA	323	8%	43	21%	77	19%
	WA	347	13%	61	18%	77	21%
	FL	337	9%	56	15%	82	16%
3	MODULUS	318	36%	37	59%	107	86%
	JIM	346	18%	96	40%	63	30%
	SMART	322	13%	90	27%	102	12%
	SWA	320	11%	72	15%	78	14%
	WA	329	15%	74	16%	91	37%
	FL	313	11%	72	14%	77	15%
4	MODULUS	529	42%	31	23%	86	43%
	JIM	362	18%	84	20%	58	32%
	SMART	316	16%	91	23%	101	15%
	SWA	348	14%	43	21%	82	16%
	WA	402	22%	69	15%	82	18%
	FL	409	23%	67	16%	88	16%

Figure F.10 - Statistical Comparison of Design Moduli of Different Analyses and Data Fusion Techniques

APPENDIX G - Results of Analyses for US380 (Lubbock)

Table G.1 - Results of SASW Analysis for Estimating Seismic Moduli

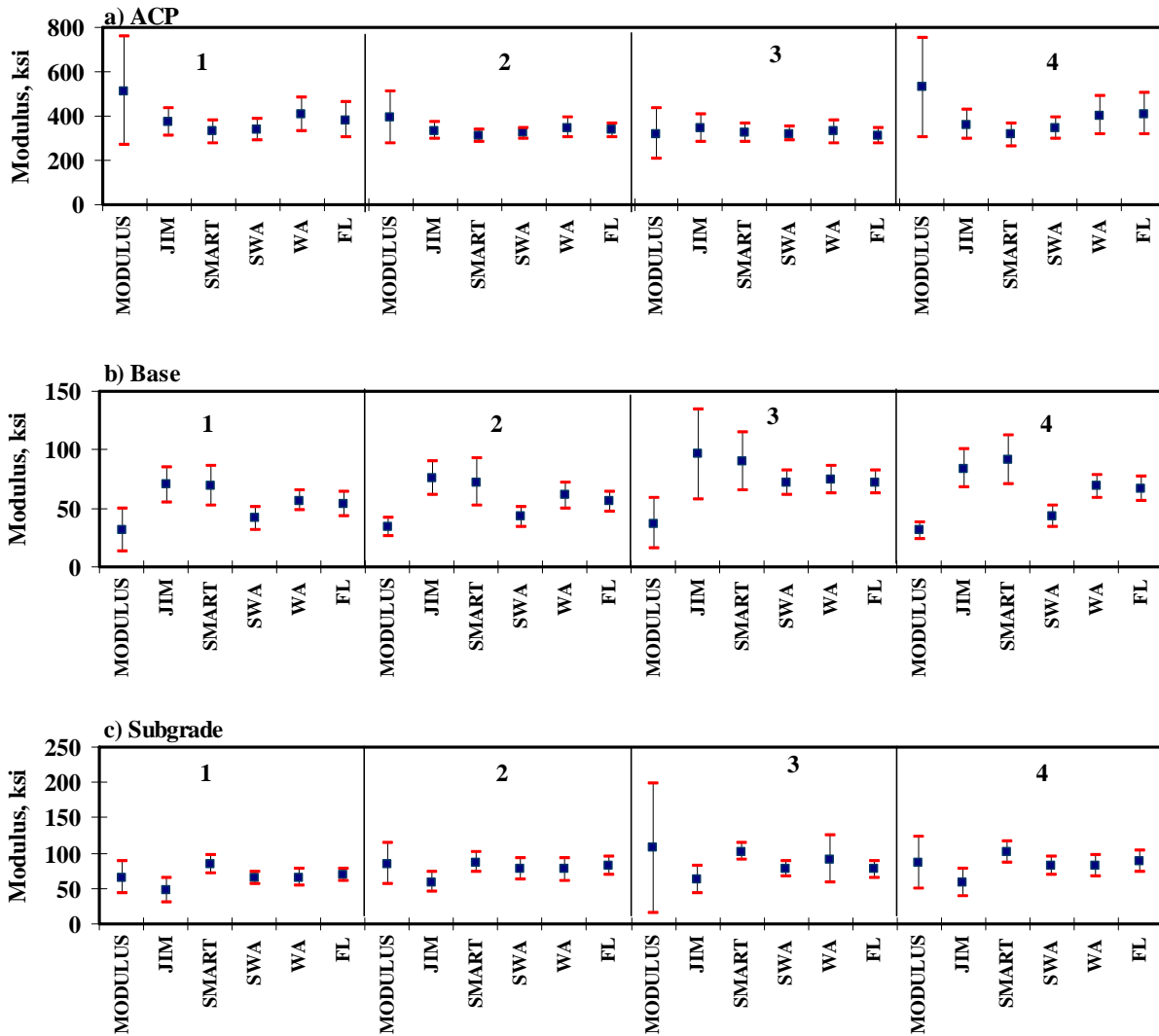| Section No.		Modulus, ksi			RMS Error, %
		ACP	Base	Subgrade	
EB1	Average	870	80	30.2	5.3
	Std Dev	276	42	4.5	-
	COV	32%	53%	15%	-
EB2	Average	988	91	29.7	5.9
	Std Dev	344	37	4.7	-
	COV	35%	41%	16%	-
WB1	Average	964	96	29.9	5.8
	Std Dev	403	42	6.4	-
	COV	42%	44%	22%	-
WB2	Average	768	83	23.9	8.8
	Std Dev	141	42	2.6	-
	COV	18%	50%	11%	-

Table G.2 - Results of SASW Analysis for Estimating Seismic Moduli and Thicknesses

Section No.		Thickness, in.		Modulus, ksi			RMS Error, %
		ACP	Base	ACP	Base	Subgrade	
EB1	Average	1.9	9.1	908	93	48.1	11.7
	Std Dev	0.2	0.6	306	27	4.4	-
	COV	9%	7%	34%	29%	9%	-
EB2	Average	2.0	9.2	1002	99	49.1	10.0
	Std Dev	0.2	0.6	274	27	6.1	-
	COV	10%	7%	27%	27%	12%	-
WB1	Average	2.0	9.1	1020	100	47.9	9.3
	Std Dev	0.2	0.5	404	29	5.6	-
	COV	10%	6%	40%	29%	12%	-
WB2	Average	2.0	9.2	663	88	14.8	9.5
	Std Dev	0.2	0.4	108	13	0.3	-
	COV	8%	4%	16%	14%	2%	-

174
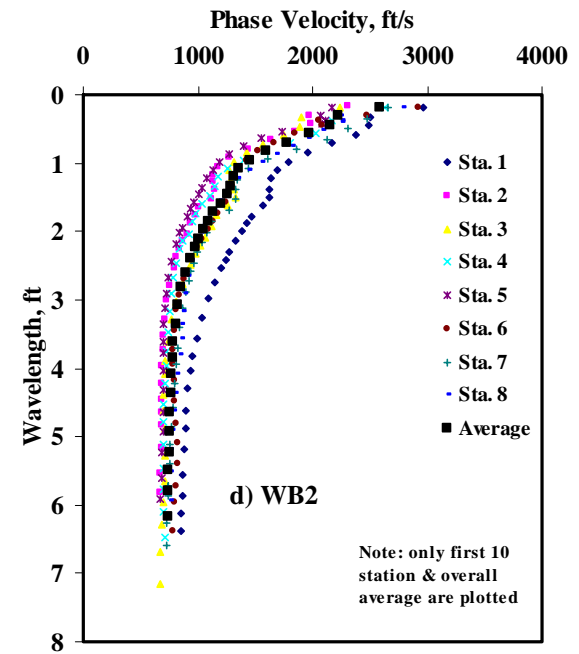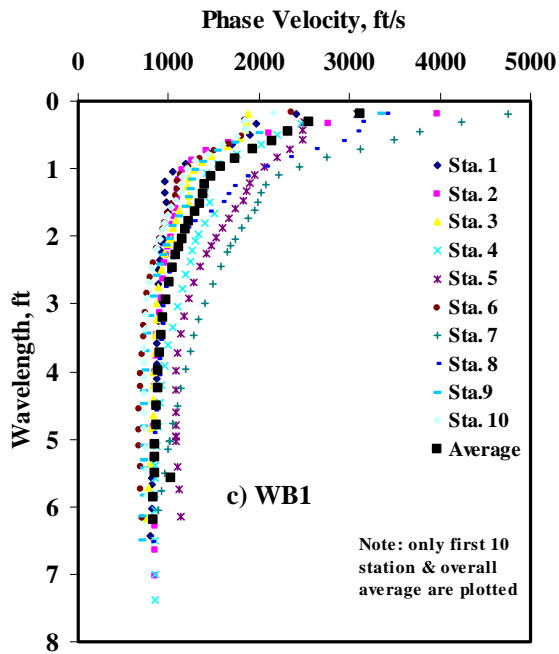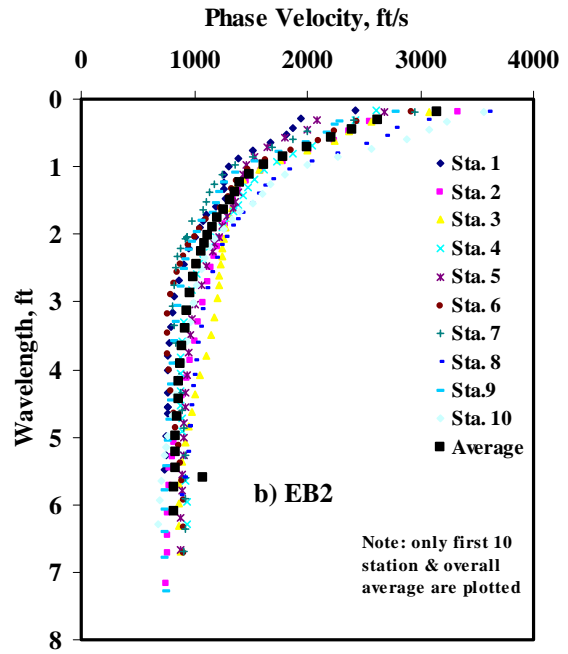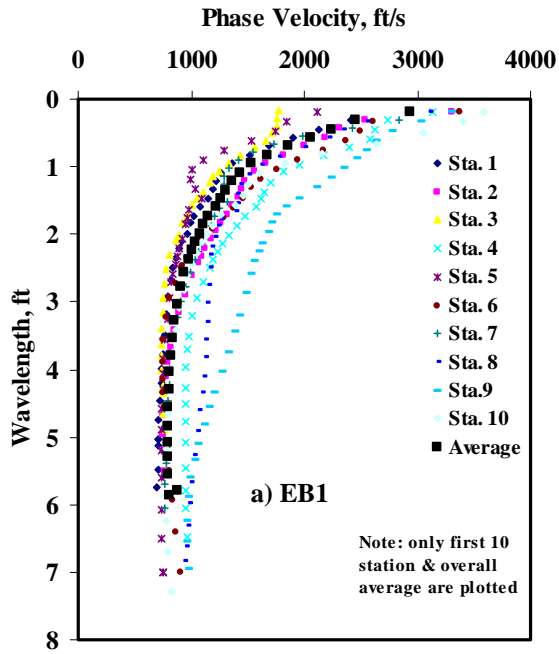
Figure G.1 - Results of Dispersion Curve from SASW Analysis

Figure G.2

Phase Velocity, ft/s — 0, 1000, 2000, 3000, 4000

Wavelength, ft — 0, 1, 2, 3, 4, 5, 6, 7

- ◆ Measured
- + Calculated V
- ○ Calculated V &T

a) Average
Disprsion Curve

Seismic Modulus, ksi — 0, 500, 1000

Depth, in. — 0, 10, 20, 30, 40, 50, 60

- ◇ Velocity Only
  RMS = 5.3
- □ Velocity & Thickness
  RMS = 11.7

b) Average Seismic
Modulus Profile

Figure G.2 - Results of SASW Data Reduction Process (EB1)

Figure G.3

Phase Velocity, ft/s — 0, 1000, 2000, 3000, 4000

Wavelength, ft — 0, 1, 2, 3, 4, 5, 6, 7, 8

- ◆ Measured
- + Calculated V
- ○ Calculated V &T

a) Average
Disprsion Curve

Seismic Modulus, ksi — 0, 500, 1000, 1500

Depth, in. — 0, 10, 20, 30, 40, 50, 60

- ◇ Velocity Only
  RMS = 5.9
- □ Velocity & Thickness
  RMS = 10.0

b) Average Seismic
Modulus Profile

Figure G.3 - Results of SASW Data Reduction Process (EB2)

Figure G.4 - Results of SASW Data Reduction Process (WB1)

Figure G.5 - Results of SASW Data Reduction Process (WB2)

Table G.3 - Results of SMART Analysis for Estimating Design Moduli

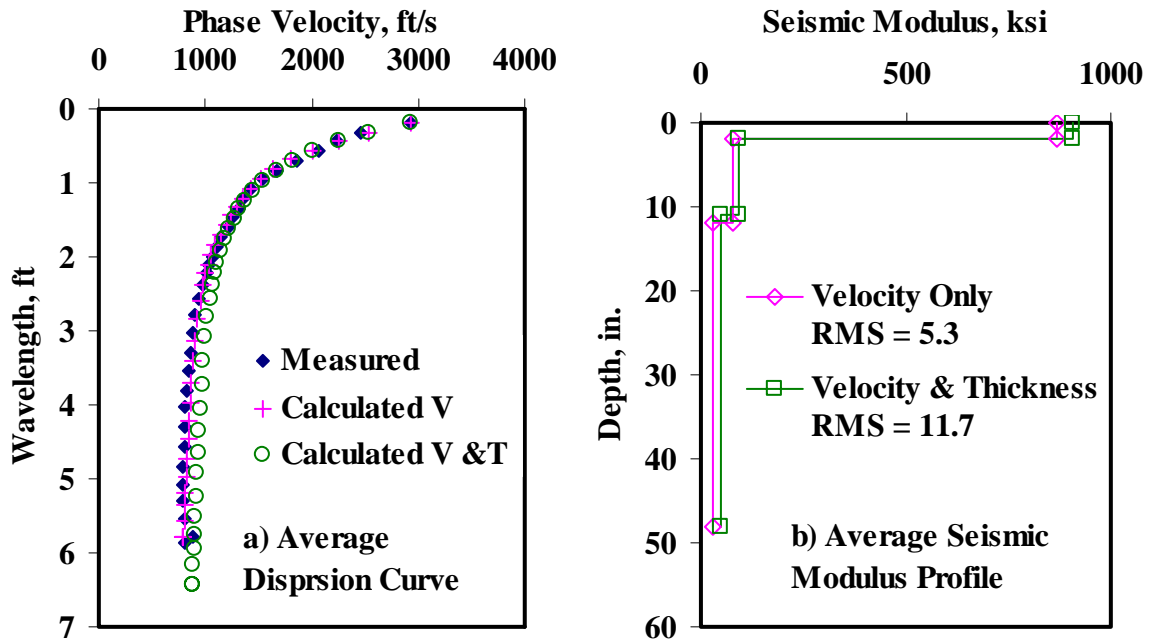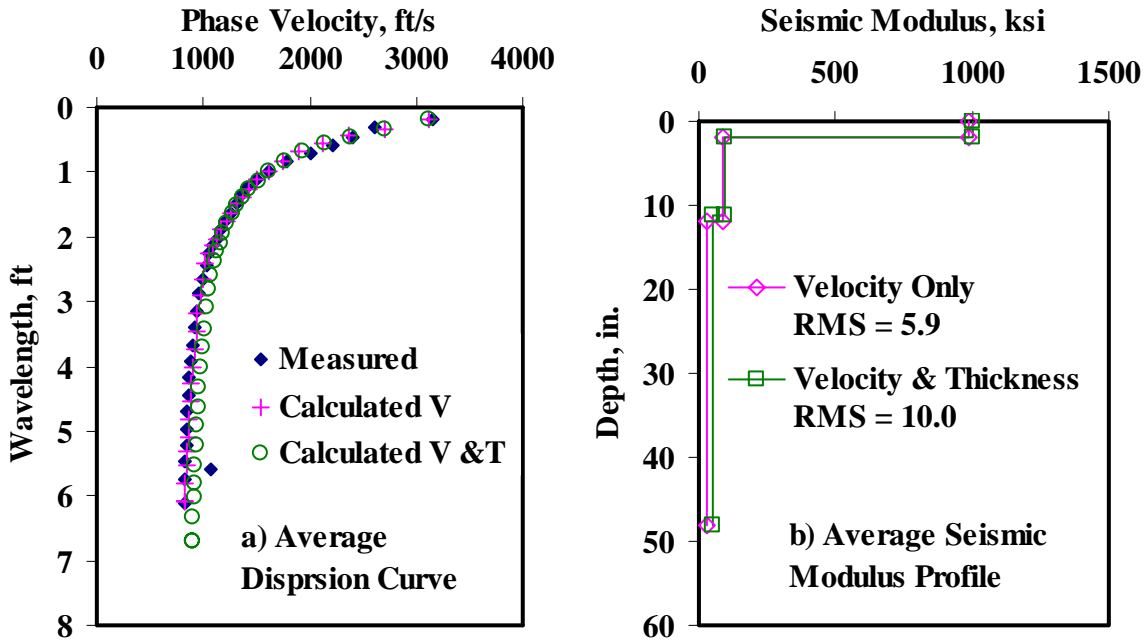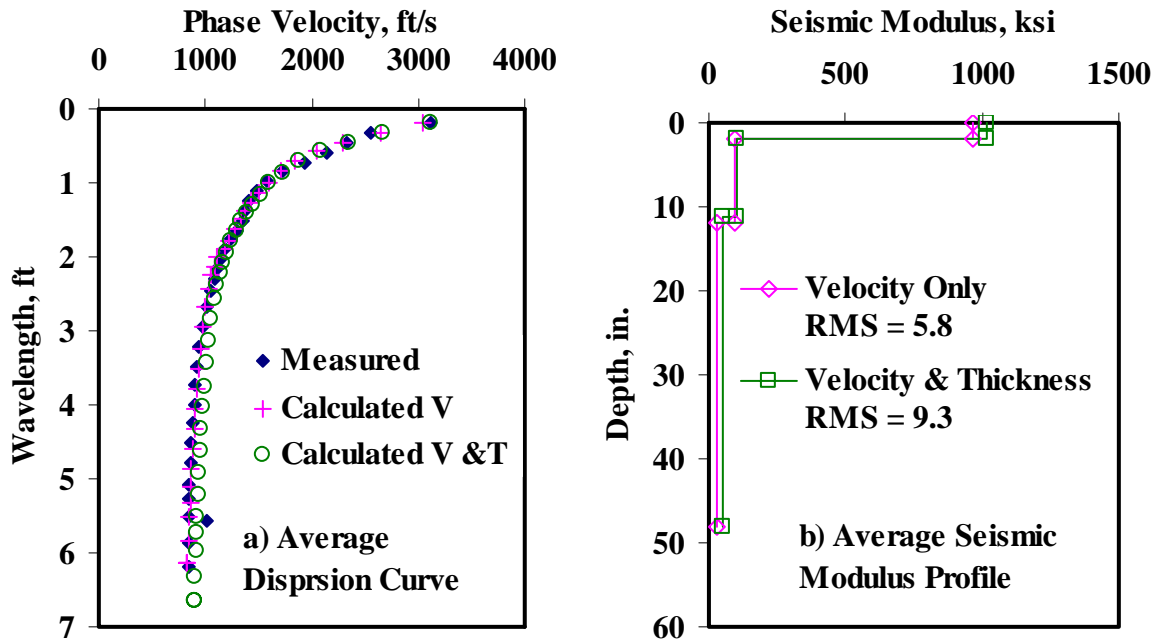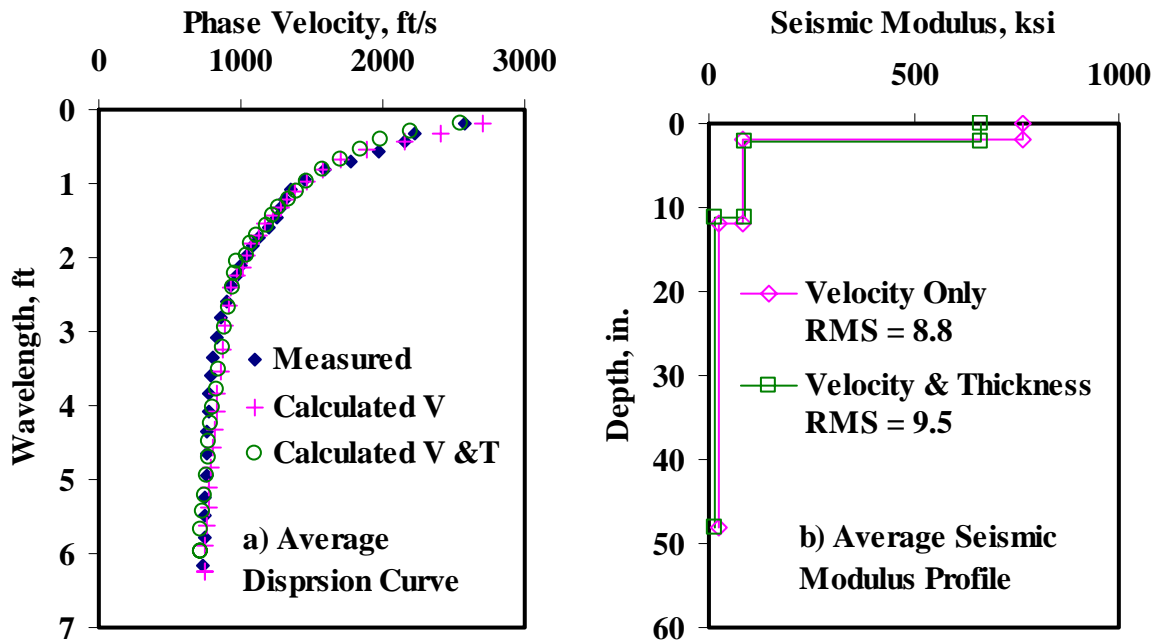| Section No.		ACP	Base		Subgrade		RMS Error, %
			Cons.	Avg.	Cons.	Avg.	
EB1	Average	241	34	48	16	25	5.3
	Std Dev	91.4	19.0	28.8	2.4	3.6	-
	COV	38%	57%	60%	15%	14%	-
EB2	Average	320	42	62	16	24	5.7
	Std Dev	86.4	17.4	25.4	2.1	3.3	-
	COV	27%	41%	41%	13%	14%	-
WB1	Average	293	42	62	17	26	5.7
	Std Dev	124.1	21.1	30.2	3.5	5.8	-
	COV	42%	50%	49%	20%	22%	-
WB2	Average	248	37	56	13	20	8.4
	Std Dev	54.1	20.1	29.7	1.3	1.9	-
	COV	22%	54%	53%	10%	10%	-

(Modulus, ksi column heading spans ACP, Base, and Subgrade columns)

Table G.4 - Summary Statistics of Measured FWD Deflections

Section No.		Normalized Deflection, mils (12 in. Spacing)						
		d0	d1	d2	d3	d4	d5	d6
EB1	Average	45.7	19.8	6.8	3.6	2.4	1.7	1.4
	Std Dev	18.3	8.0	2.5	1.3	0.9	0.7	0.5
	COV	40%	41%	37%	36%	38%	38%	38%
EB2	Average	42.8	21.5	8.9	5.0	3.4	2.5	1.9
	Std Dev	15.7	8.8	3.6	2.0	1.3	0.8	0.6
	COV	37%	41%	40%	40%	38%	32%	33%
WB1	Average	41.3	19.8	8.1	4.5	3.0	2.2	1.7
	Std Dev	17.6	10.4	4.2	2.1	1.3	0.8	0.7
	COV	43%	52%	52%	46%	44%	38%	40%
WB2	Average	49.2	22.4	8.0	4.3	2.8	1.9	1.5
	Std Dev	14.7	6.6	2.0	1.0	0.6	0.4	0.4
	COV	30%	29%	25%	24%	22%	22%	24%

178

Table G.5 - Results MODULUS Analysis for Estimating Design Moduli

Section No.		Modulus, ksi			RMS Error, %
		ACP	Base	Subgrade	
EB1	Average	500	20	19	34.9
	Std Dev	-	24.7	8.5	-
	COV	-	126%	46%	-
EB2	Average	500	20	14	23.2
	Std Dev	-	21.7	5.6	-
	COV	-	107%	39%	-
WB1	Average	500	20	17	23.0
	Std Dev	-	16.1	6.7	-
	COV	-	80%	40%	-
WB2	Average	500	14	14	39.1
	Std Dev	-	7.5	3.9	-
	COV	-	53%	27%	-

Table G.6 - Results of JIM Analysis for Estimating Design Moduli

Section No.		Modulus, ksi					RMS Error, %
		ACP	Base		Subgrade		
			Cons.	Avg.	Cons.	Avg.	
EB1	Average	299	41	83	16	17	4.1
	Std Dev	95	21	39	7	8	-
	COV	32%	52%	48%	44%	45%	-
EB2	Average	330	48	101	12	13	4.2
	Std Dev	118	17.1	31.1	3.9	4.4	-
	COV	36%	36%	31%	33%	34%	-
WB1	Average	320	52	109	13	15	4.0
	Std Dev	144	20.8	36.1	4.5	5.1	-
	COV	45%	40%	33%	33%	34%	-
WB2	Average	262	39	84	12	14	4.7
	Std Dev	56	17.5	32.5	3.0	3.4	-
	COV	21%	45%	39%	25%	25%	-

Table G.7 - Results of JIM Analysis for Estimating Design Moduli and Thicknesses

| Section No.		Thickness, in.		Modulus, ksi					RMS Error, %
				ACP	Base		Subgrade		
		ACP	Base		Cons.	Avg.	Cons.	Avg.	
EB1	Average	1.6	5.6	426	170	174	15	17	4.7
	Std Dev	0.4	1.7	72.0	44.4	40.1	6.6	7.4	-
	COV	24%	31%	17%	26%	23%	43%	44%	-
EB2	Average	1.6	7.2	468	84.8	142.5	12.7	12.8	4.4
	Std Dev	0.2	1.7	56.4	47.0	35.6	4.4	4.4	-
	COV	13%	24%	12%	55%	25%	34%	34%	-
WB1	Average	1.7	7.7	445	144	165	13	15	4.3
	Std Dev	0.3	3.1	94.9	68.4	55.1	4.5	5.0	-
	COV	18%	40%	21%	47%	33%	33%	34%	-
WB2	Average	1.6	4.9	385	192	193	12	13	5.0
	Std Dev	0.2	0.8	29.6	41.0	39.8	2.9	3.2	-
	COV	11%	16%	8%	21%	21%	24%	24%	-
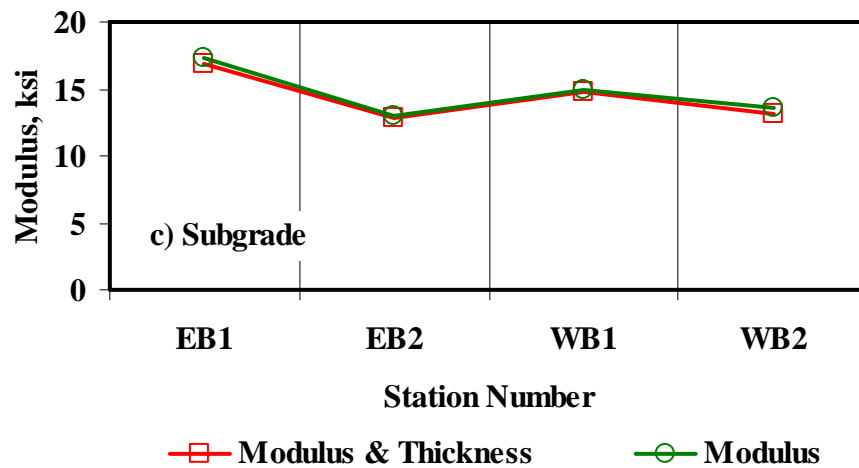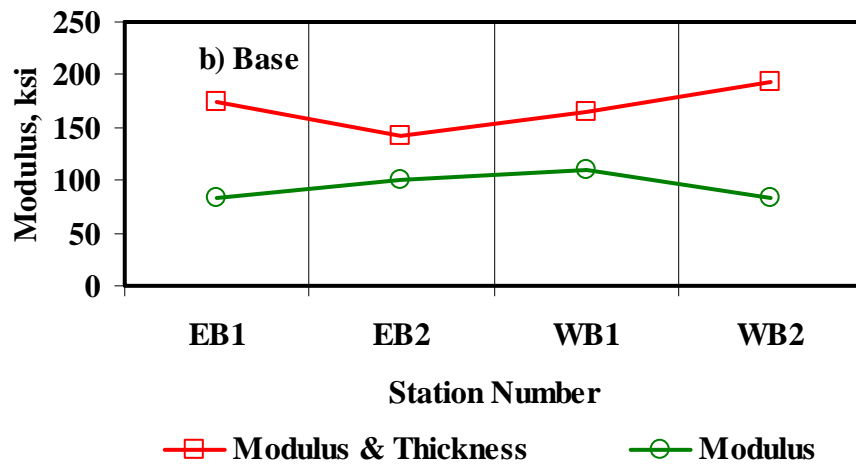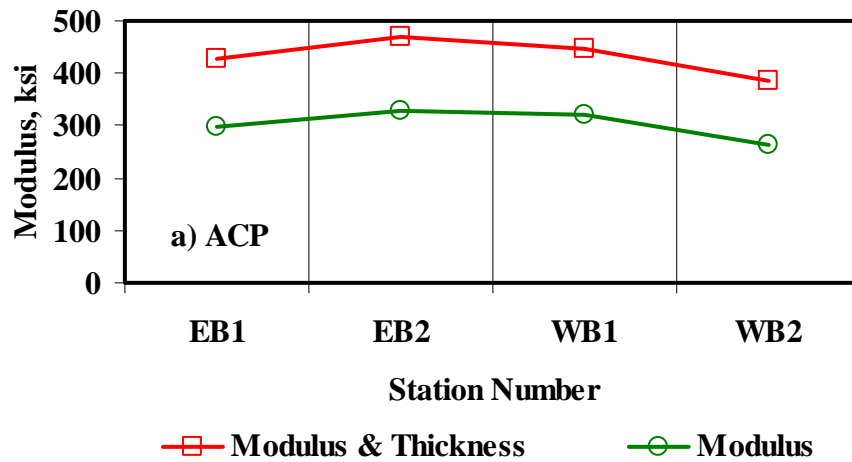
Figure G.6 - Comparison of Design Moduli from JIM Analysis with Constant and Backcalculated Thickness
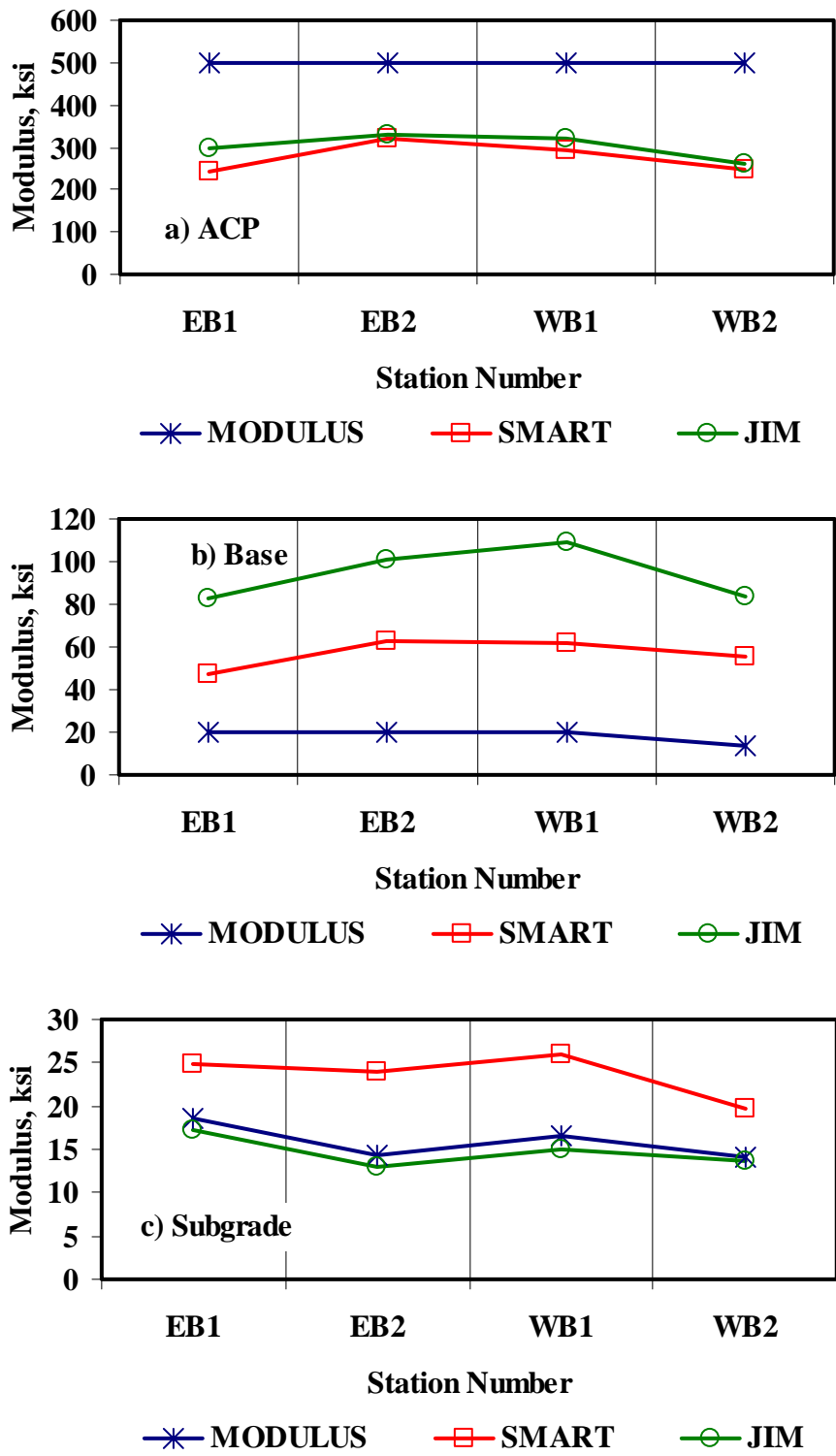
Figure G 7 - Comparison of Design Moduli from Different Analyses

182
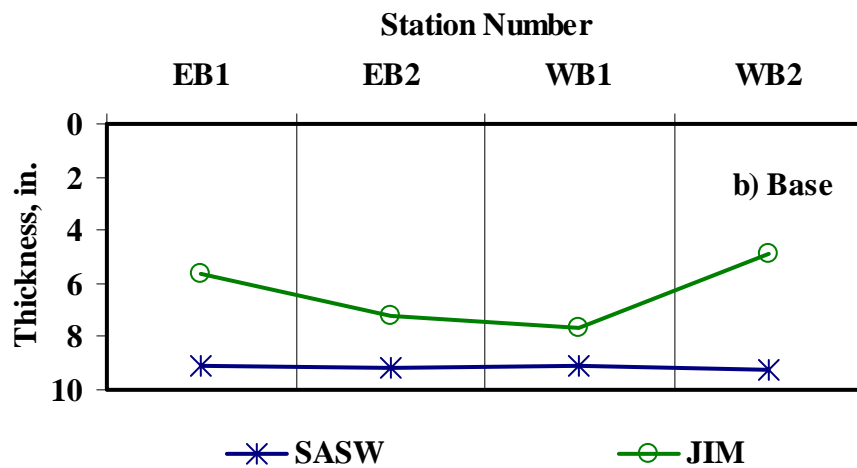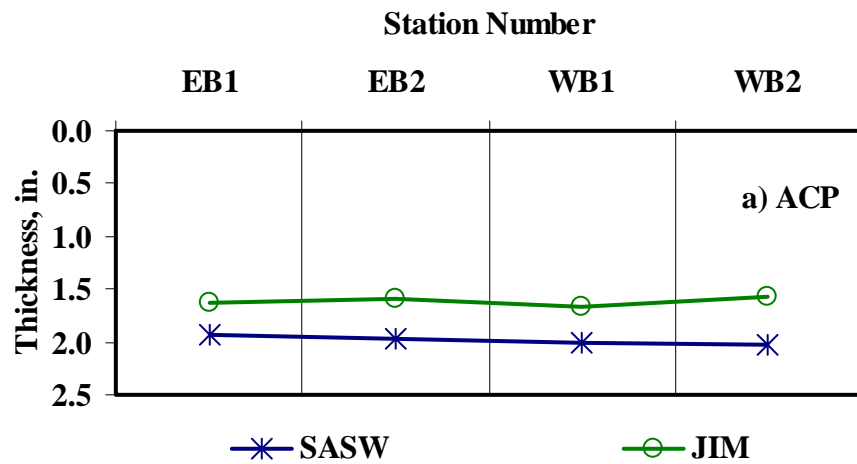
Figure G.8 - Comparison of Layer Thickness from Different Analyses
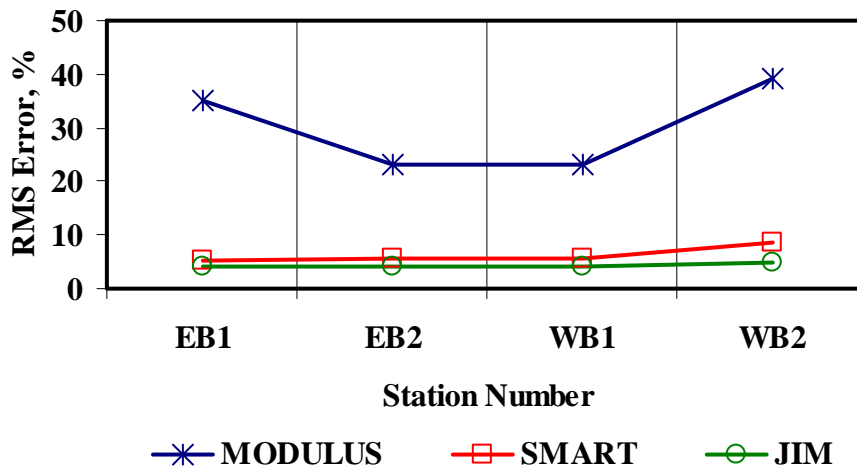
Figure G.9 - Comparison of RMS Error from Different Analyses

Table G.8 - Summary of Design Modulus Values with Data Fusion Results

Section No.	Method	Modulus, ksi					
		ACP		Base		Subgrade	
		Average	COV	Average	COV	Average	COV
EB1	FWD	500	-	20	126%	19	46%
	JIM	299	32%	83	48%	17	45%
	SMART	241	38%	48	60%	25	14%
	SWA	281	25%	60	94%	20	13%
	WA	347	13%	50	49%	20	22%
	FL	336	17%	55	55%	20	16%
EB2	FWD	500	-	20	107%	14	39%
	JIM	330	36%	101	31%	13	34%
	SMART	320	27%	62	41%	24	14%
	SWA	325	24%	40	60%	16	21%
	WA	383	12%	61	23%	17	15%
	FL	345	15%	58	26%	18	13%
WB1	FWD	500	-	20	80%	17	40%
	JIM	320	45%	109	30%	15	30%
	SMART	293	42%	62	49%	26	22%
	SWA	308	42%	48	65%	18	31%
	WA	371	24%	64	39%	19	25%
	FL	359	27%	58	44%	19	24%
WB2	FWD	500	-	14	53%	14	27%
	JIM	262	21%	84	39%	14	25%
	SMART	248	22%	56	53%	20	10%
	SWA	256	22%	48	55%	17	12%
	WA	337	11%	51	45%	16	16%
	FL	308	12%	47	42%	16	16%

184

Figure G.10 - Statistical Comparison of Design Moduli of Different Analyses and Data Fusion Techniques

APPENDIX H - Results of Analyses for APT Section (December 2003)

Table H.1 - Results of SASW Analysis for Estimating Seismic Moduli

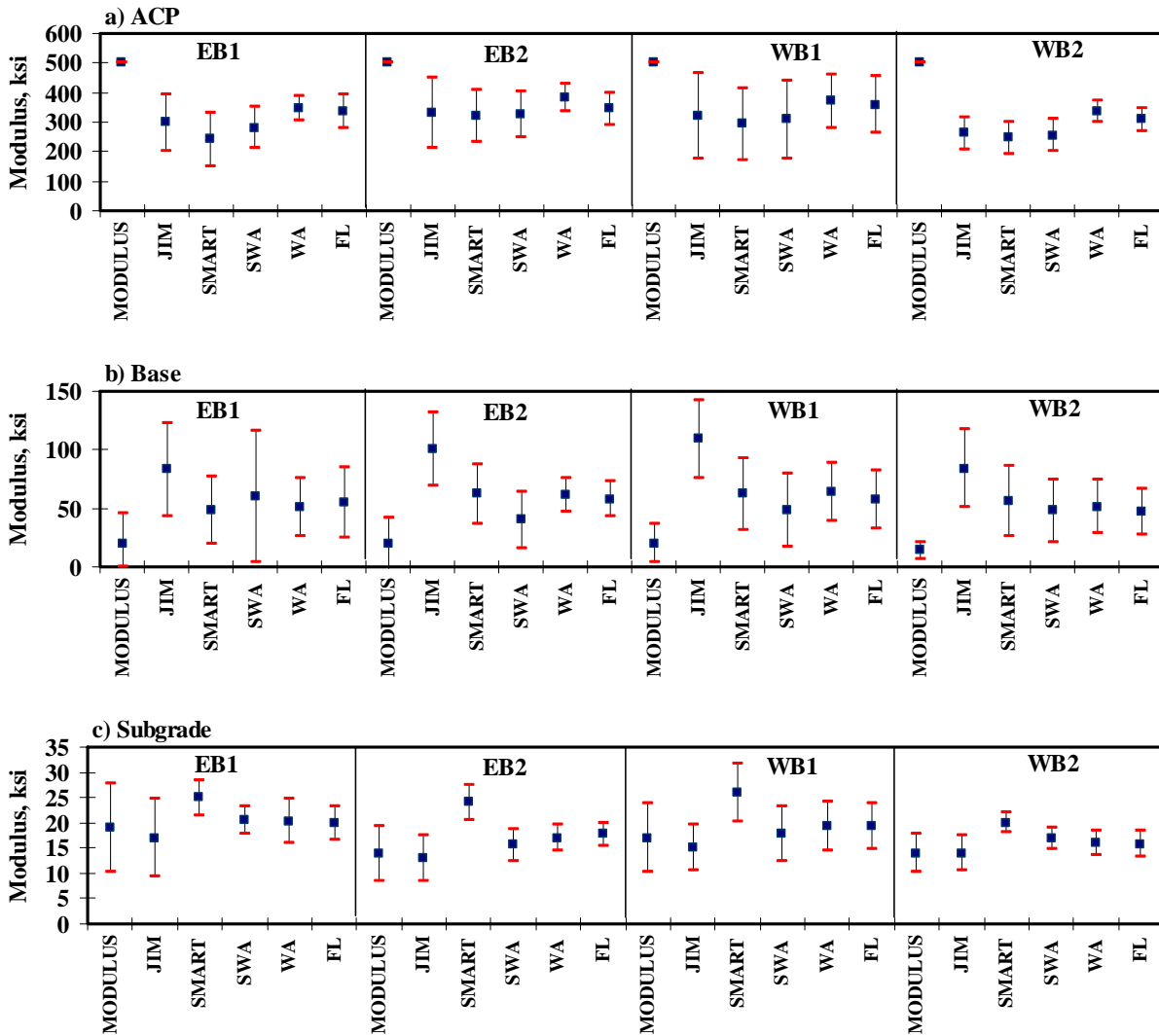| Section No.		Modulus, ksi			RMS Error, %
		ACP	Base	Subgrade	
L1	Average	1776	117	23.7	5.3
	Std Dev	140	16	2.5	-
	COV	8%	14%	10%	-
L2	Average	1609	113	25.0	8.4
	Std Dev	155	17	2.4	-
	COV	10%	15%	9%	-
L3	Average	1459	119	25.1	5.6
	Std Dev	177	19	3.8	-
	COV	12%	16%	15%	-
L4	Average	1723	111	24.5	5.8
	Std Dev	171	7	3.1	-
	COV	10%	6%	13%	-
Pad	Average	1735	116	23.3	6.5
	Std Dev	227	20	3.0	-
	COV	13%	17%	13%	-

Table H.2 - Results of SASW Analysis for Estimating Seismic Moduli and Thicknesses

| Section		Thickness, in.		Modulus, ksi			RMS Error, %
		ACP	Base	ACP	Base	subgrade	
L1	Average	1.9	7.8	1957	146	17.1	6.6
	Std Dev	0.2	0.8	220	48	1.4	-
	COV	9%	10%	11%	33%	8%	-
L2	Average	1.8	7.7	1975	122	16.7	8.2
	Std Dev	0.1	0.8	208	50	2.1	-
	COV	5%	11%	11%	41%	12%	-
L3	Average	1.9	8.2	1699	125	16.9	6.1
	Std Dev	0.1	0.8	347	35	2.0	-
	COV	7%	10%	20%	28%	12%	-
L4	Average	1.7	7.1	1801	107	15.5	5.7
	Std Dev	0.5	2.3	611	50	4.8	-
	COV	31%	32%	34%	47%	31%	-
Pad	Average	1.9	7.6	1799	126	17.1	6.7
	Std Dev	0.2	0.6	226	49	1.8	-
	COV	9%	9%	13%	39%	11%	-
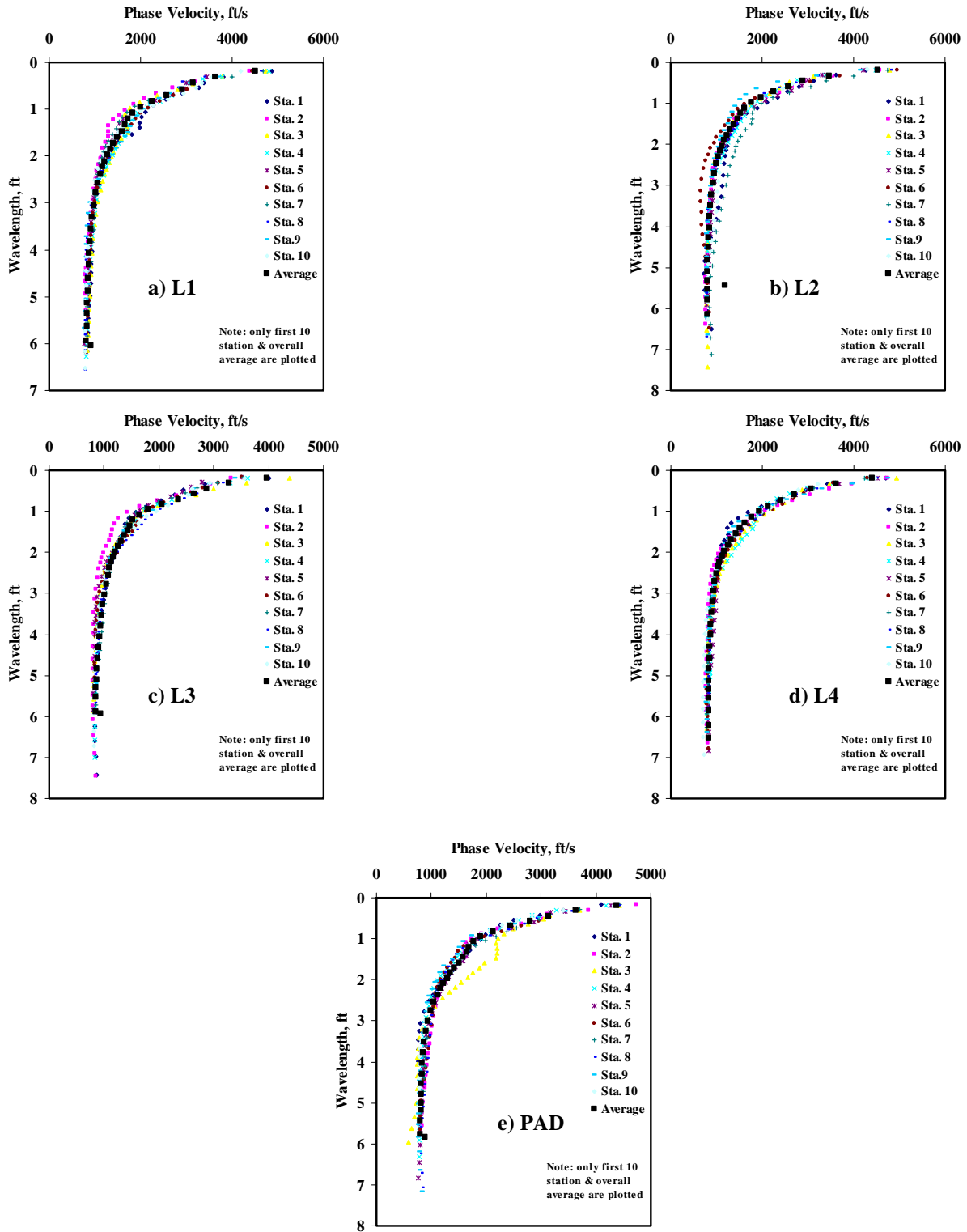
Figure H.1 - Results of Dispersion Curve from SASW Analysis

Figure H.2 - Results of SASW Data Reduction Process (Section L1)
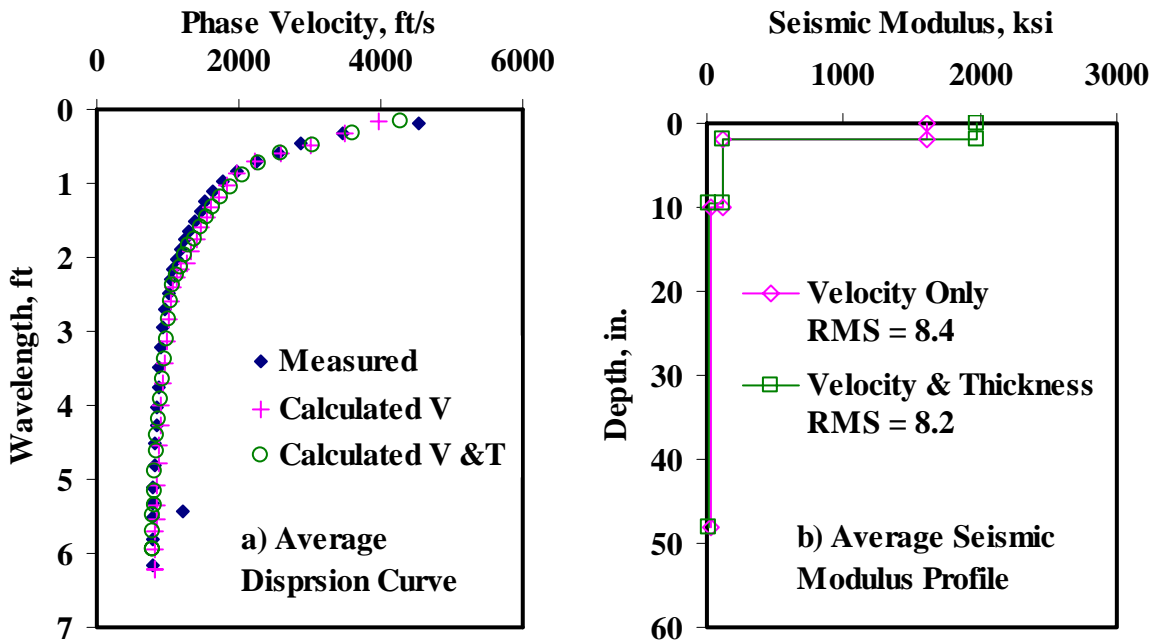
Figure H.3 - Results of SASW Data Reduction Process (Section L2)
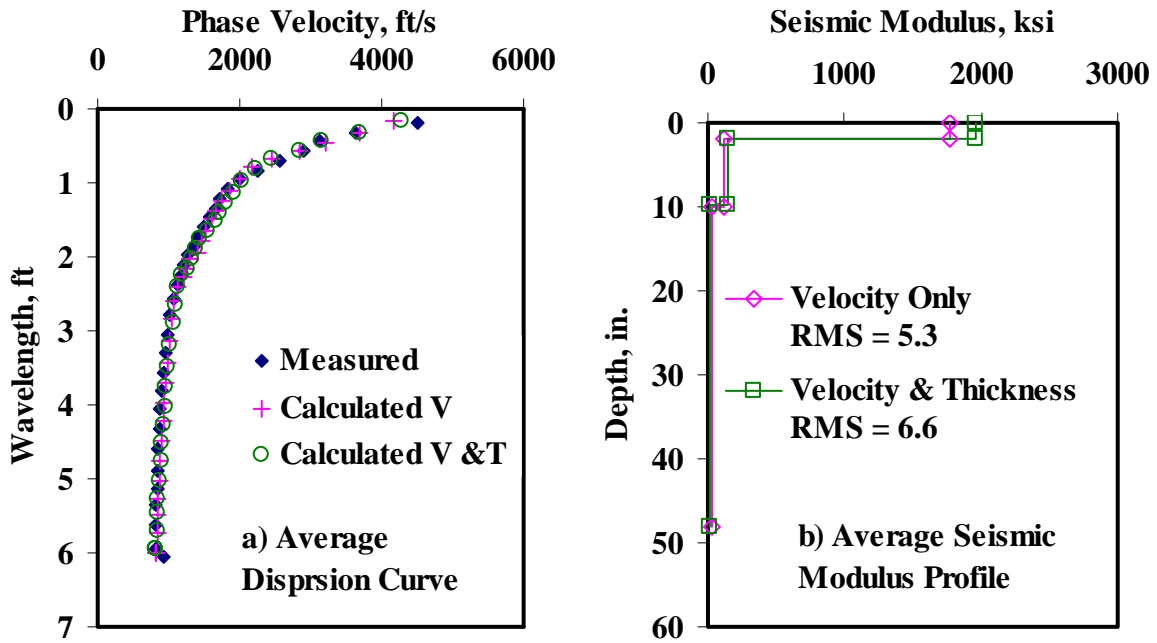
191
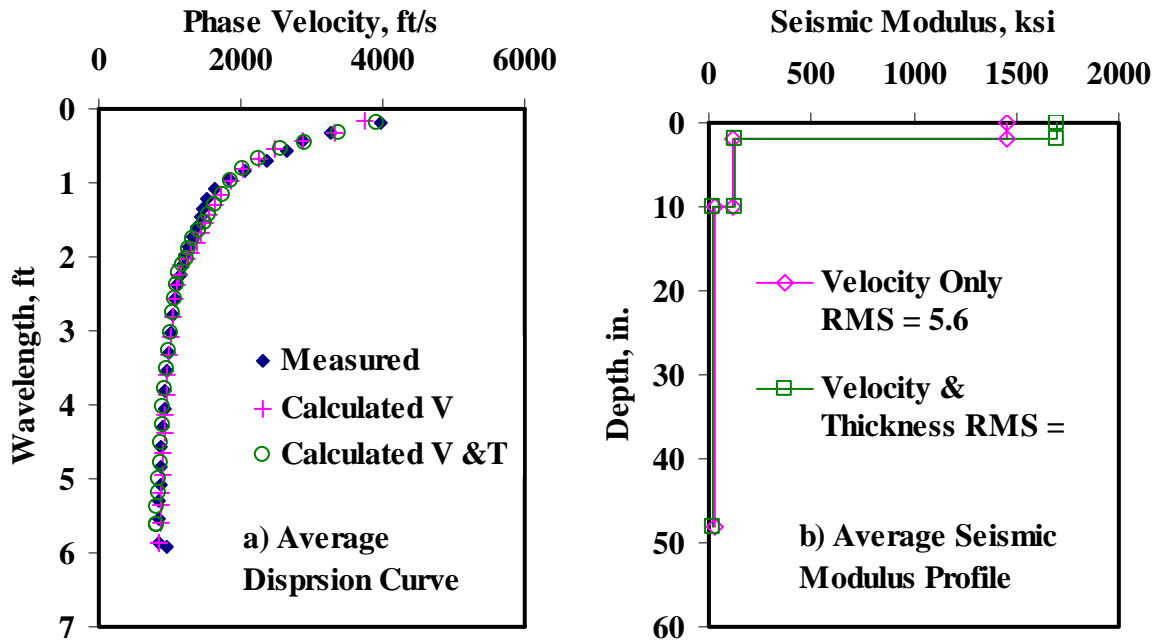
Figure H.4 - Results of SASW Data Reduction Process (Section L3)
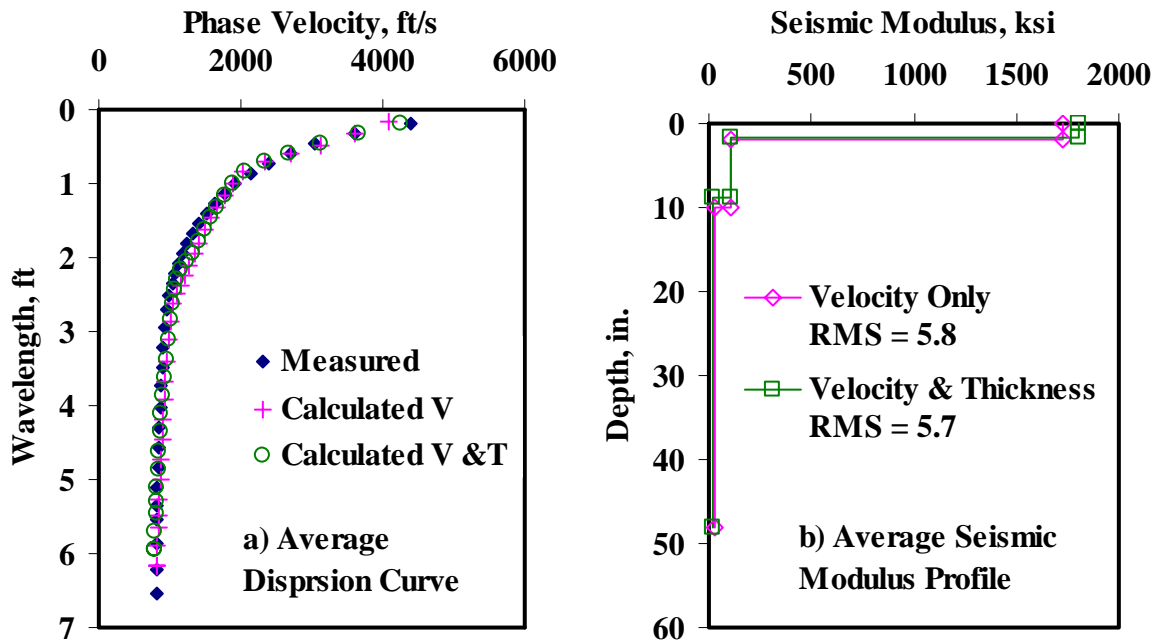
Figure H.5 - Results of SASW Data Reduction Process (Section L4)

192
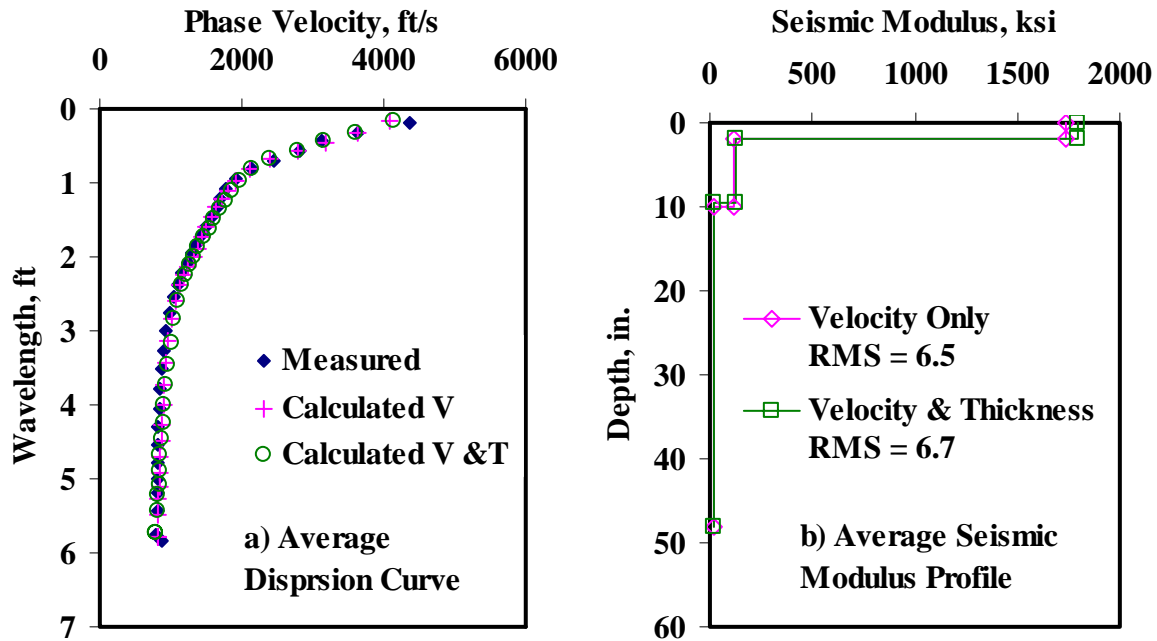
Figure H.6 - Results of SASW Data Reduction Process (Section PAD)

Table H.3 - Results of SMART Analysis for Estimating Design Moduli

Section No.		Modulus, ksi					RMS Error, %
		ACP	Base		Subgrade		
			Cons.	Avg.	Cons.	Avg.	
L1	**Average**	**526**	**80**	**99**	**13**	**20**	**5.3**
	Std Dev	*42.3*	*11.7*	*13.2*	*1.3*	*2.1*	*-*
	COV	*8%*	*15%*	*13%*	*10%*	*10%*	*-*
L2	**Average**	**471**	**77**	**96**	**14**	**21**	**8.0**
	Std Dev	*44.6*	*13.7*	*15.3*	*1.3*	*1.9*	*-*
	COV	*9%*	*18%*	*16%*	*10%*	*9%*	*-*
L3	**Average**	**432**	**81**	**101**	**14**	**21**	**5.6**
	Std Dev	*52.5*	*13.6*	*15.5*	*2.0*	*3.2*	*-*
	COV	*12%*	*17%*	*15%*	*14%*	*16%*	*-*
L4	**Average**	**510**	**75**	**94**	**13**	**20**	**5.8**
	Std Dev	*49.5*	*5.6*	*6.3*	*1.7*	*2.6*	*-*
	COV	*10%*	*7%*	*7%*	*13%*	*13%*	*-*
PAD	**Average**	**524**	**79**	**98**	**13**	**19**	**6.3**
	Std Dev	*57.7*	*15.2*	*17.3*	*1.5*	*2.5*	*-*
	COV	*11%*	*19%*	*18%*	*12%*	*13%*	*-*

Table H.4 - Summary Statistics of Measured FWD Deflections

Section No.		Normalized Deflection, mils (12 in. Spacing)						
		d0	d1	d2	d3	d4	d5	d6
L1	Average	17.7	8.7	3.9	2.2	1.4	1.0	0.7
	Std Dev	2.1	0.9	0.2	0.1	0.1	0.1	0.0
	COV	12%	10%	6%	5%	5%	6%	6%
L2	Average	17.5	8.6	3.9	2.2	1.4	1.0	0.7
	Std Dev	2.4	0.8	0.2	0.1	0.1	0.1	0.1
	COV	14%	9%	5%	4%	4%	6%	8%
L3	Average	19.0	8.6	3.6	2.1	1.3	0.9	0.7
	Std Dev	3.4	1.3	0.3	0.2	0.1	0.1	0.1
	COV	18%	15%	10%	7%	9%	12%	13%
L4	Average	19.6	8.6	3.6	2.1	1.4	0.9	0.7
	Std Dev	3.6	1.6	0.4	0.2	0.1	0.1	0.1
	COV	18%	18%	10%	9%	11%	12%	14%
PAD	Average	18.4	9.3	4.2	2.4	1.5	1.0	0.8
	Std Dev	2.5	1.3	0.3	0.1	0.1	0.0	0.0
	COV	14%	14%	7%	5%	4%	5%	5%

Table H.5 - Results MODULUS Analysis for Estimating Design Moduli

Section No.		Modulus, ksi			RMS Error, %
		AC	Base	Subgrade	
L1	Average	500	46	29	31.9
	Std Dev	-	9.9	1.7	-
	COV	-	21%	6%	-
L2	Average	500	49	29	31.0
	Std Dev	-	14.8	1.5	-
	COV	-	30%	5%	-
L3	Average	500	39	31	31.1
	Std Dev	-	12.1	3.2	-
	COV	-	31%	10%	-
L4	Average	500	37	31	30.6
	Std Dev	-	11.9	3.7	-
	COV	-	32%	12%	-
PAD	Average	500	46	28	32.4
	Std Dev	-	11.7	2.0	-
	COV	-	26%	7%	-

194

Table H.6 - Results of JIM Analysis for Estimating Design Moduli

Section No.		ACP	Base		Subgrade		RMS Error, %
			Cons.	Avg.	Cons.	Avg.	
L1	**Average**	**435**	**77**	**109**	**23**	**25**	**2.7**
	Std Dev	*-*	*13*	*16*	*1*	*1*	*-*
	COV	*-*	*16%*	*15%*	*5%*	*5%*	*-*
L2	**Average**	**509**	**61**	**86**	**22**	**25**	**3.0**
	Std Dev	*-*	*17.5*	*24.0*	*1.1*	*1.2*	*-*
	COV	*-*	*29%*	*28%*	*5%*	*5%*	*-*
L3	**Average**	**445**	**71**	**102**	**24**	**27**	**2.7**
	Std Dev	*-*	*10.4*	*13.4*	*2.6*	*2.9*	*-*
	COV	*-*	*15%*	*13%*	*11%*	*11%*	*-*
L4	**Average**	**448**	**66**	**94**	**24**	**27**	**2.6**
	Std Dev	*-*	*10.4*	*14.1*	*2.6*	*3.0*	*-*
	COV	*-*	*16%*	*15%*	*11%*	*11%*	*-*
PAD	**Average**	**445**	**70**	**103**	**21**	**24**	**2.6**
	Std Dev	*-*	*13.0*	*17.3*	*1.1*	*1.2*	*-*
	COV	*-*	*19%*	*17%*	*5%*	*5%*	*-*

Table H.7 - Results of JIM Analysis for Estimating Design Moduli and Thicknesses

| Section No.		Thickness, in.		ACP	Base		Subgrade		RMS Error, %
		AC	Base		Cons.	Avg.	Cons.	Avg.	
L1	**Average**	**2.5**	**4.6**	**435**	**102**	**105**	**23**	**26**	**2.1**
	Std Dev	*0.3*	*1.2*	*-*	*6.8*	*1.4*	*1.2*	*1.4*	*-*
	COV	*12%*	*26%*	*-*	*7%*	*1%*	*5%*	*5%*	*-*
L2	**Average**	**1.9**	**4.9**	**509**	**103.6**	**104.0**	**22.7**	**25.1**	**2.5**
	Std Dev	*0.4*	*1.1*	*-*	*2.8*	*2.6*	*1.1*	*1.2*	*-*
	COV	*19%*	*22%*	*-*	*3%*	*2%*	*5%*	*5%*	*-*
L3	**Average**	**2.1**	**5.5**	**445**	**98**	**106**	**25**	**27**	**2.4**
	Std Dev	*0.3*	*1.5*	*-*	*13.8*	*2.1*	*2.5*	*2.7*	*-*
	COV	*16%*	*27%*	*-*	*14%*	*2%*	*10%*	*10%*	*-*
L4	**Average**	**2.2**	**4.4**	**448**	**103**	**105**	**24**	**27**	**2.2**
	Std Dev	*0.2*	*1.1*	*-*	*7.1*	*2.0*	*2.5*	*2.8*	*-*
	COV	*11%*	*26%*	*-*	*7%*	*2%*	*10%*	*10%*	*-*
PAD	**Average**	**2.4**	**4.6**	**445**	**101**	**104**	**21**	**24**	**1.9**
	Std Dev	*0.3*	*1.2*	*-*	*9.6*	*2.0*	*1.2*	*1.3*	*-*
	COV	*14%*	*25%*	*-*	*9%*	*2%*	*6%*	*5%*	*-*
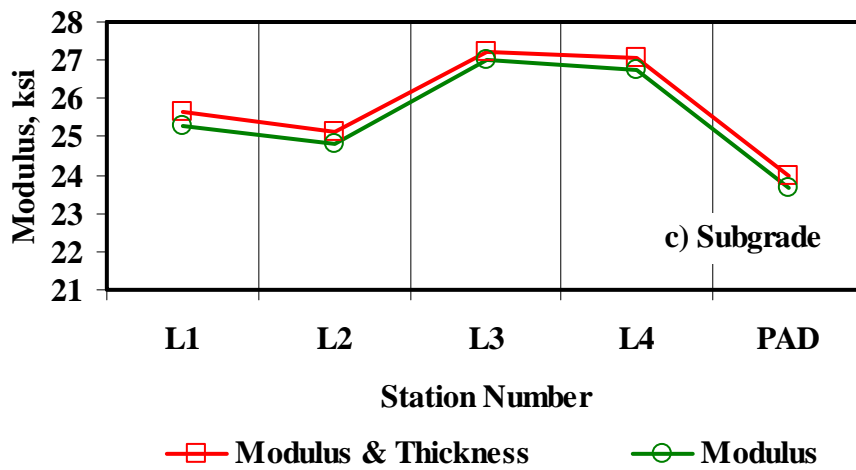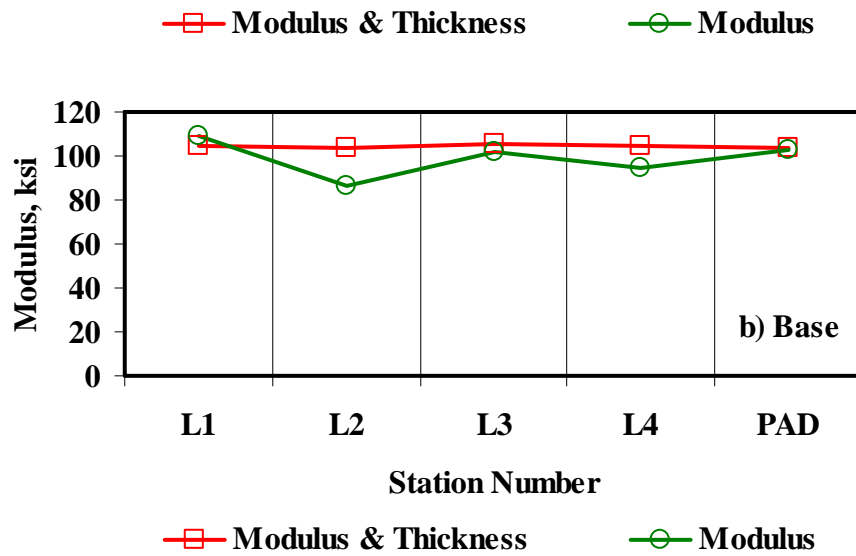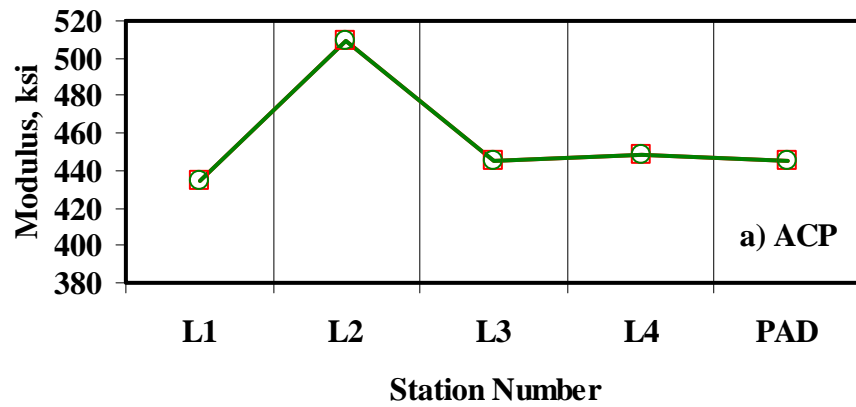
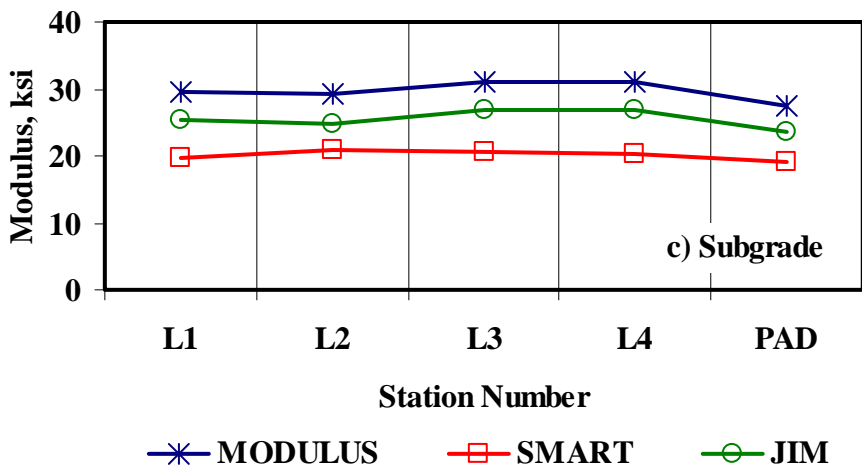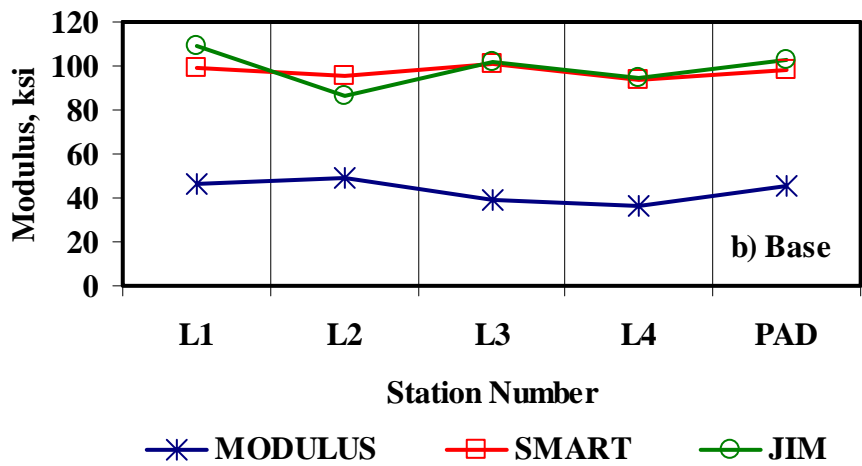**Figure H.7 - Comparison of Design Moduli from JIM Analysis with Constant and Backcalculated Thicknesses**
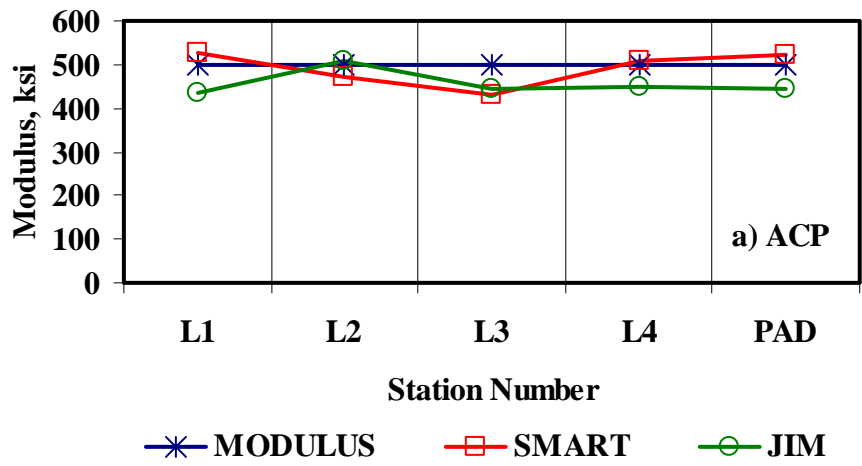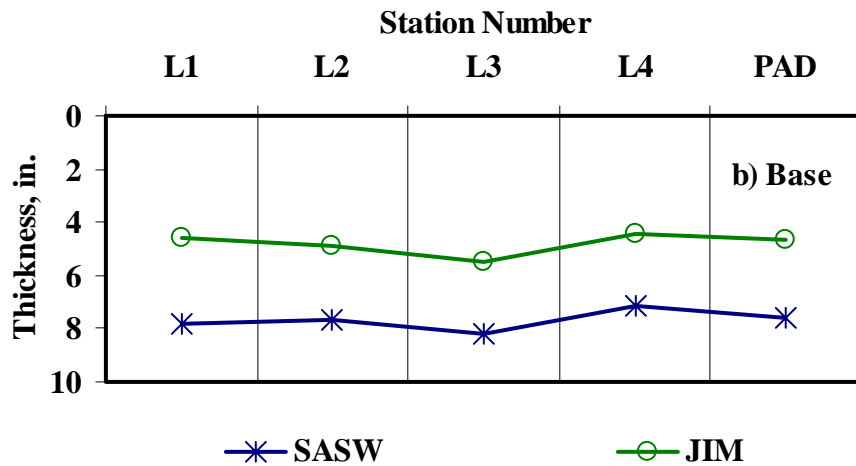
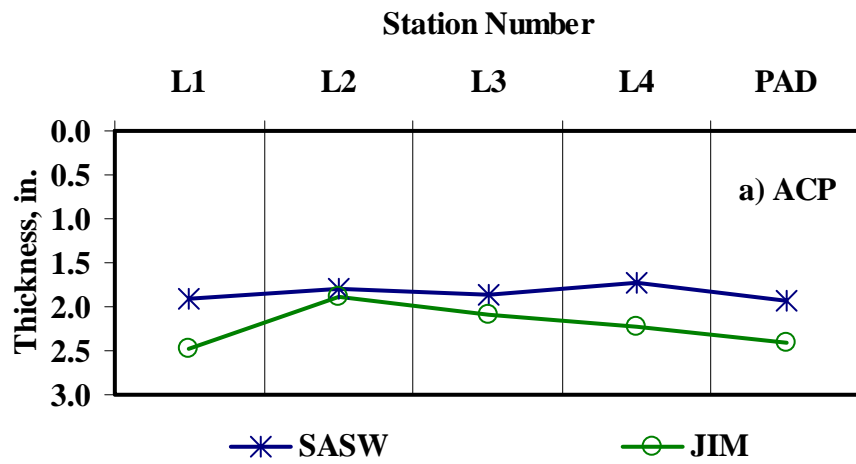196

Figure H.8 - Comparison of Design Moduli from Different Analyses

Figure H.9 - Comparison of Layer Thicknesses from Different Analyses
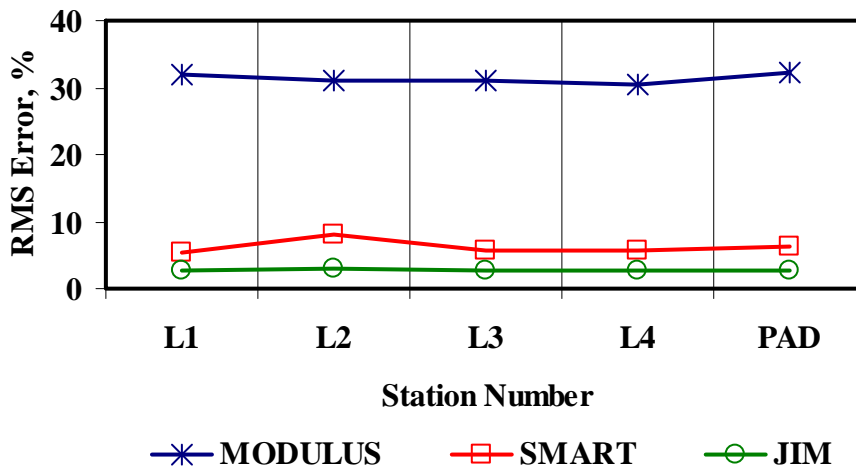

Figure H.10 - Comparison of RMS Error from Different Analyses

Table H.8 - Summary of Design Modulus Values with Data Fusion Results

| Section No.	Method	Modulus, ksi					
		ACP		Base		Subgrade	
		Average	COV	Average	COV	Average	COV
L1	MODULUS	500	-	46	21%	29	6%
	JIM	435	-	109	15%	25	5%
	SMART	526	8%	99	13%	20	10%
	SWA	526	8%	72	17%	25	3%
	WA	487	3%	85	10%	25	4%
	FL	491	3%	83	8%	25	4%
L2	MODULUS	500	-	49	30%	29	5%
	JIM	509	-	86	28%	25	5%
	SMART	471	9%	96	16%	21	9%
	SWA	471	9%	61	20%	25	4%
	WA	493	3%	77	10%	25	4%
	FL	490	4%	73	13%	24	6%
L3	MODULUS	500	-	39	31%	31	10%
	JIM	445	-	102	10%	27	10%
	SMART	432	12%	101	15%	21	16%
	SWA	432	12%	84	12%	25	5%
	WA	459	4%	78	11%	26	7%
	FL	458	4%	78	10%	26	7%
L4	MODULUS	500	-	37	32%	31	12%
	JIM	448	-	94	15%	27	11%
	SMART	510	10%	94	7%	20	13%
	SWA	510	10%	78	13%	24	4%
	WA	486	3%	73	10%	25	7%
	FL	495	3%	73	13%	25	8%
PAD	MODULUS	500	-	46	26%	28	7%
	JIM	445	-	103	17%	24	5%
	SMART	524	11%	98	18%	19	13%
	SWA	524	11%	79	17%	24	4%
	WA	490	4%	82	12%	24	5%
	FL	494	4%	82	11%	24	6%
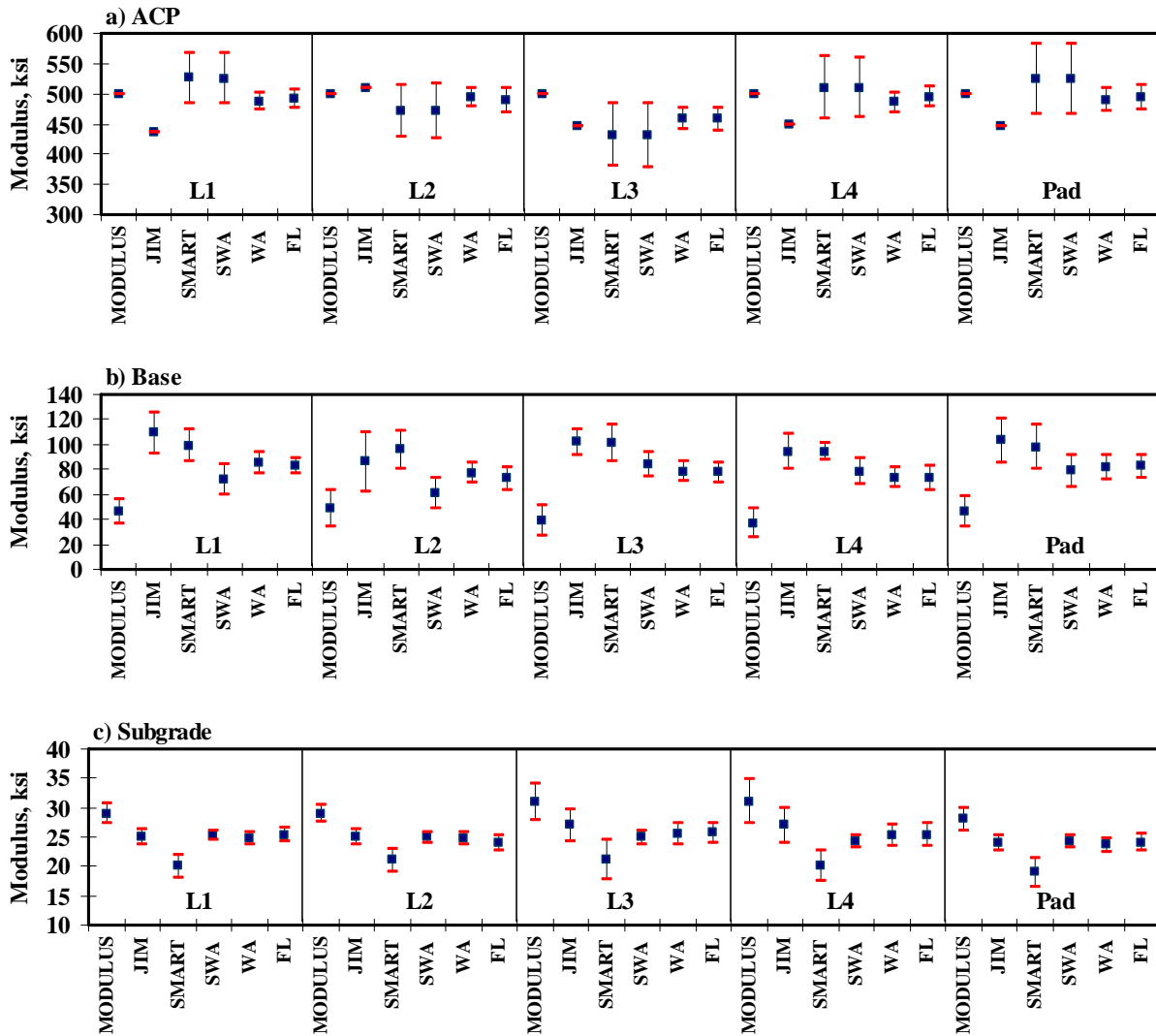
Figure H.11 - Statistical Comparison of Design Moduli of Different Analyses and Data Fusion Techniques

200

APPENDIX I - RESULTS OF ANALYSES FOR APT SECTION (SEPTEMBER 2004)

Table I.1 - Results of SASW Analysis for Estimating Seismic Moduli

Section No.		Modulus, ksi			RMS Error, %
		ACP	Base	Subgrade	
L1	**Average**	**1204**	**128**	**26.1**	**7.2**
	Std Dev	*145*	*24*	*1.7*	*-*
	COV	*12%*	*18%*	*7%*	*-*
L2	**Average**	**1068**	**116**	**26.1**	**7.3**
	Std Dev	*196*	*36*	*2.8*	*-*
	COV	*18%*	*31%*	*11%*	*-*
L4	**Average**	**1194**	**127**	**27.3**	**5.9**
	Std Dev	*183*	*35*	*3.7*	*-*
	COV	*15%*	*27%*	*14%*	*-*
LL	**Average**	**892**	**150**	**26.6**	**7.4**
	Std Dev	*225*	*32*	*2.6*	*-*
	COV	*25%*	*21%*	*10%*	*-*
RL	**Average**	**809**	**105**	**28.0**	**6.5**
	Std Dev	*196*	*49*	*2.8*	*-*
	COV	*24%*	*47%*	*10%*	*-*

Table I.2 - Results of SASW Analysis for Estimating Seismic Moduli and Thicknesses

Section No.		Thickness, in.		Modulus, ksi			RMS Error, %
		ACP	Base	ACP	Base	Subgrade	
L1	**Average**	**1.8**	**7.2**	**1102**	**259**	**20.5**	**12.4**
	Std Dev	*0.1*	*0.1*	*182*	*50*	*2.1*	*-*
	COV	*7%*	*2%*	*16%*	*19%*	*10%*	*-*
L2	**Average**	**1.8**	**7.2**	**1125**	**245**	**21.5**	**14.4**
	Std Dev	*0.1*	*0.2*	*206*	*58*	*2.1*	*-*
	COV	*3%*	*2%*	*18%*	*24%*	*10%*	*-*
L4	**Average**	**1.8**	**7.4**	**1296**	**233**	**19.9**	**10.0**
	Std Dev	*0.1*	*0.5*	*196*	*53*	*2.2*	*-*
	COV	*4%*	*7%*	*15%*	*23%*	*11%*	*-*
LL	**Average**	**1.9**	**7.3**	**967**	**232**	**19.8**	**8.4**
	Std Dev	*0.1*	*0.5*	*173*	*50*	*1.9*	*-*
	COV	*8%*	*7%*	*18%*	*21%*	*10%*	*-*
RL	**Average**	**1.8**	**7.5**	**1010**	**188**	**21.0**	**13.7**
	Std Dev	*0.0*	*0.5*	*264*	*47*	*2.2*	*-*
	COV	*2%*	*7%*	*26%*	*25%*	*10%*	*-*
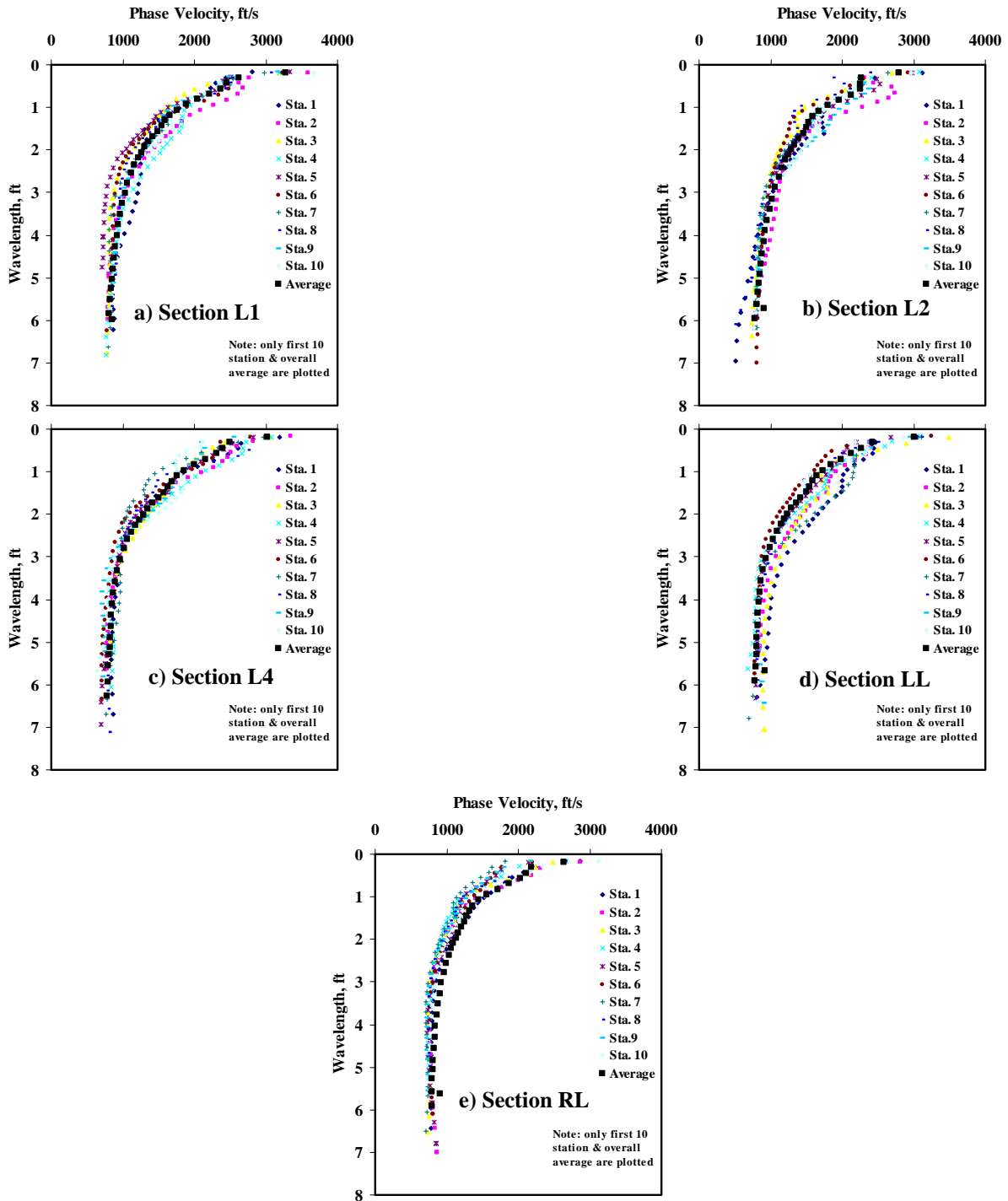
Figure I.1 - Results of Dispersion Curve from SASW Analysis

204

Phase Velocity, ft/s

Seismic Modulus, ksi

a) Average Disprsion Curve

- ◆ Measured
- + Calculated V
- ○ Calculated V &T

b) Average Seismic Modulus Profile

- ◇ Velocity Only RMS = 7.2
- ☐ Velocity & Thickness RMS = 12.4

Figure I.2 - Results of SASW Data Reduction Process (Section L1)

Phase Velocity, ft/s

Seismic Modulus, ksi

a) Average Disprsion Curve

- ◆ Measured
- + Calculated V
- ○ Calculated V &T

b) Average Seismic Modulus Profile

- ◇ Velocity Only RMS = 7.3
- ☐ Velocity & Thickness RMS = 14.4

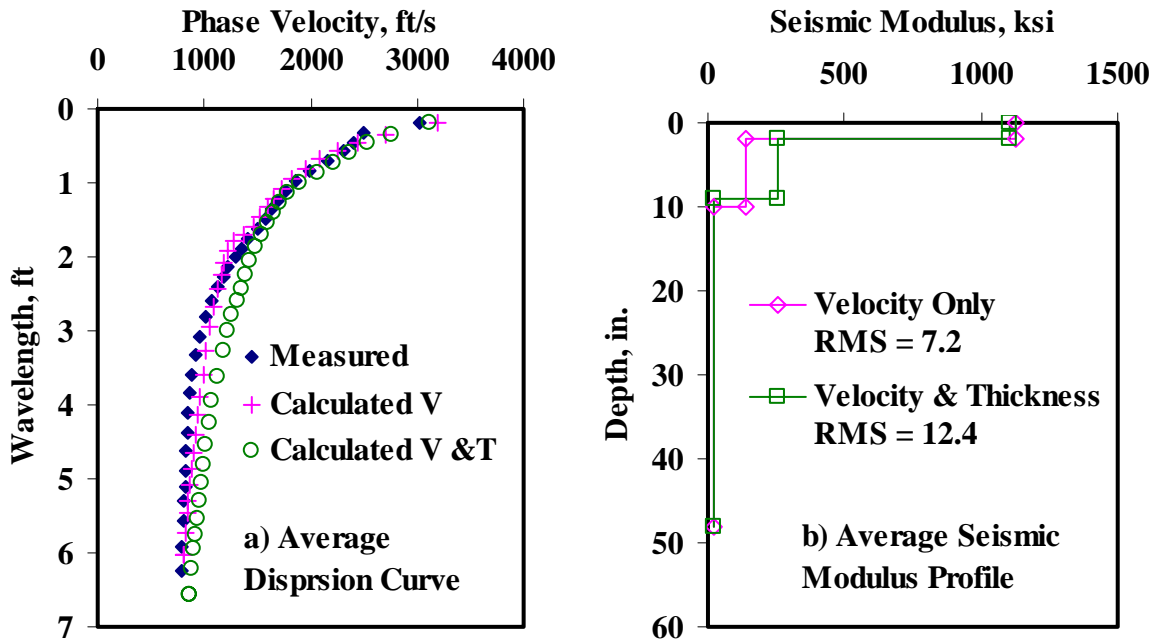**Figure I.3 - Results of SASW Data Reduction Process (Section L2)**

205

Figure I.4 - Results of SASW Data Reduction Process (Section L4)
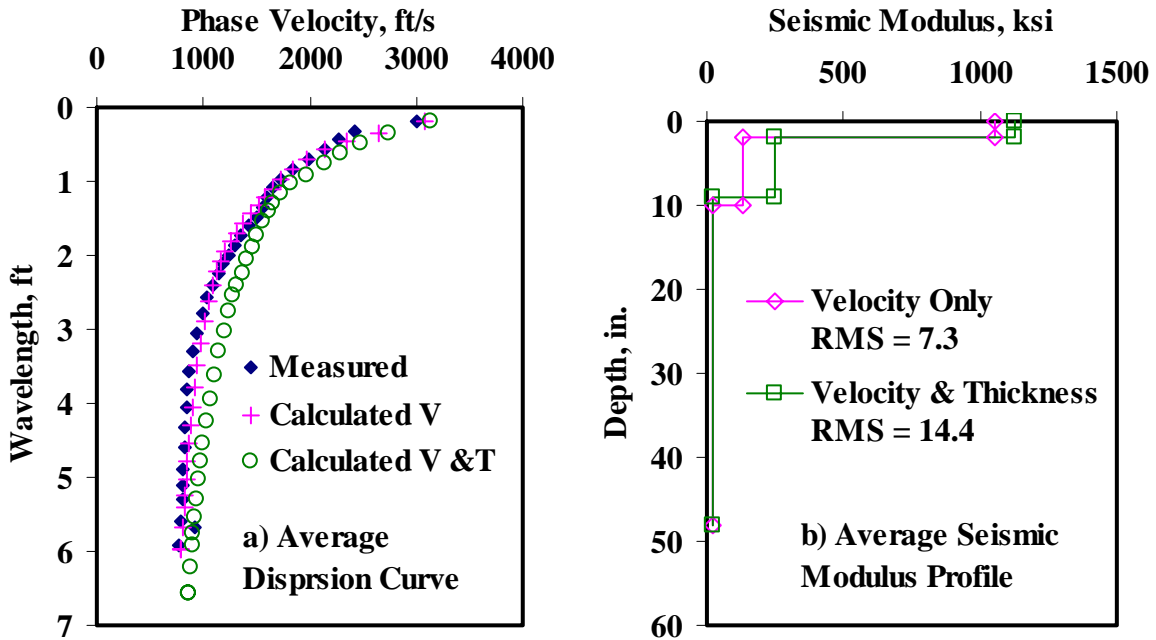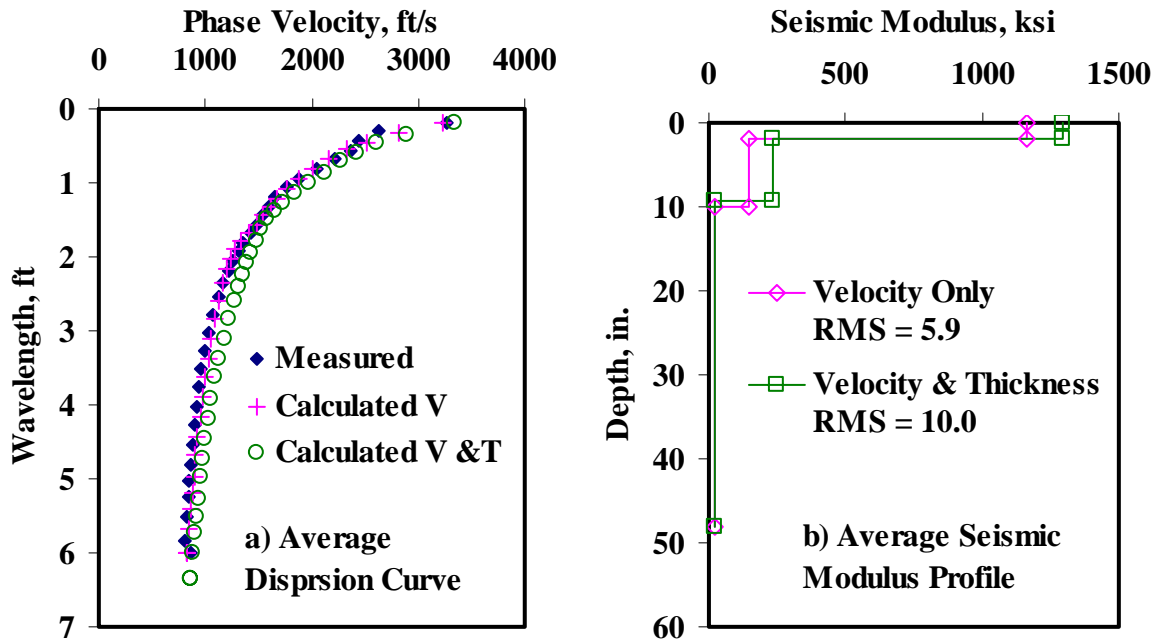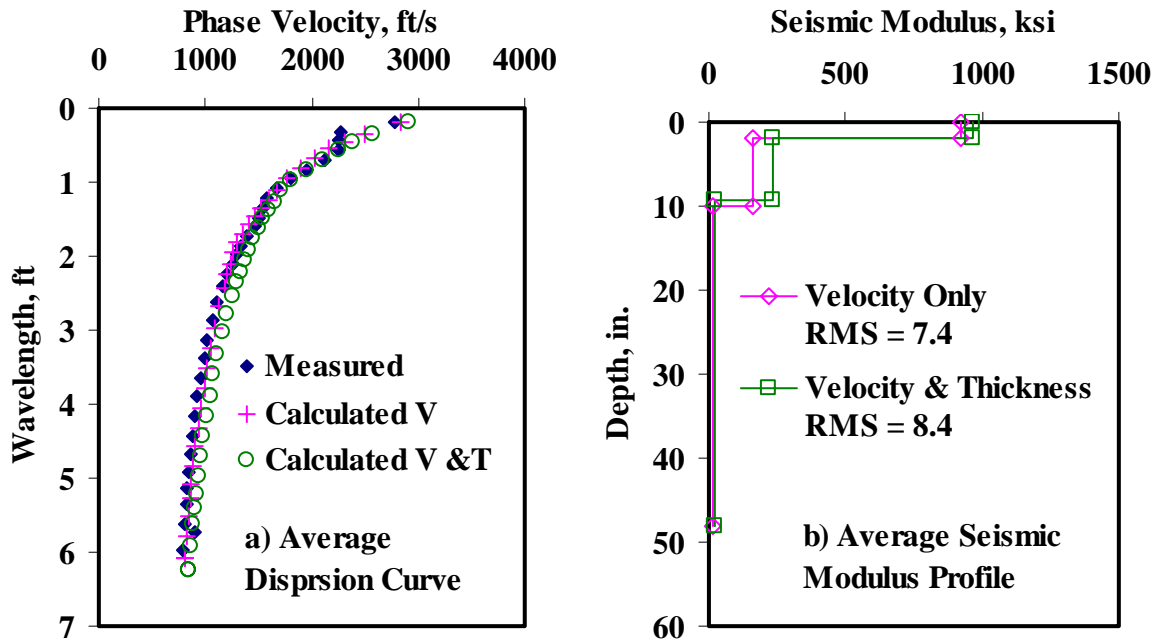
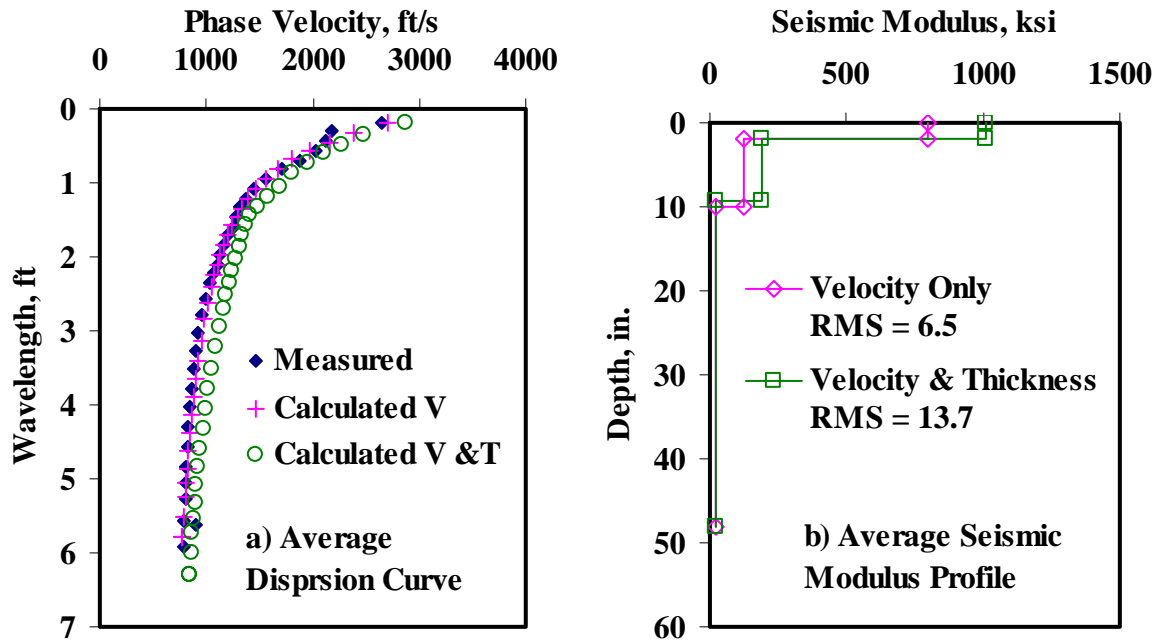**Figure I.5 - Results of SASW Data Reduction Process (Section LL)**

Figure I.6 - Results of SASW Data Reduction Process (Section RL)

Table I.3 - Results of SMART Analysis for Estimating Design Moduli

Section No.		Modulus, ksi					RMS Error, %
		ACP	Base		Subgrade		
			Cons.	Avg.	Cons.	Avg.	
L1	**Average**	**579**	**88**	**109**	**14**	**21**	**7.2**
	Std Dev	*69.5*	*17.6*	*20.5*	*0.9*	*1.4*	*-*
	COV	*12%*	*20%*	*19%*	*6%*	*6%*	*-*
L2	**Average**	**453**	**80**	**99**	**14**	**21**	**7.6**
	Std Dev	*77.4*	*26.4*	*30.7*	*1.3*	*2.1*	*-*
	COV	*17%*	*33%*	*31%*	*9%*	*10%*	*-*
L4	**Average**	**458**	**88**	**110**	**15**	**23**	**6.2**
	Std Dev	*77.4*	*26.3*	*30.3*	*1.8*	*2.9*	*-*
	COV	*17%*	*30%*	*28%*	*12%*	*13%*	*-*
LL	**Average**	**472**	**103**	**127**	**15**	**22**	**7.4**
	Std Dev	*116.6*	*24.3*	*28.6*	*1.3*	*2.1*	*-*
	COV	*25%*	*24%*	*23%*	*9%*	*10%*	*-*
RL	**Average**	**402**	**71**	**91**	**15**	**23**	**6.5**
	Std Dev	*101.0*	*36.3*	*41.8*	*1.5*	*2.3*	*-*
	COV	*25%*	*51%*	*46%*	*10%*	*10%*	*-*

Table I.4 - Summary Statistics of Measured FWD Deflections

Section No.		Normalized Deflection, mils (12 in. Spacing)						
		d0	d1	d2	d3	d4	d5	d6
L1	Average	18.6	9.3	4.2	2.4	1.5	0.9	0.7
	Std Dev	2.0	0.9	0.4	0.2	0.1	0.1	0.0
	COV	11%	10%	10%	9%	8%	7%	7%
L2	Average	18.6	8.8	3.9	2.2	1.4	0.9	0.6
	Std Dev	2.3	0.7	0.3	0.1	0.1	0.1	0.0
	COV	12%	8%	7%	6%	6%	7%	8%
L4	Average	17.4	8.3	3.8	2.2	1.4	0.9	0.6
	Std Dev	3.0	0.9	0.3	0.1	0.1	0.1	0.1
	COV	17%	11%	7%	6%	7%	9%	13%
LL	Average	16.9	8.4	4.0	2.3	1.4	0.9	0.6
	Std Dev	2.2	0.8	0.3	0.2	0.1	0.1	0.0
	COV	13%	10%	8%	7%	7%	6%	5%
RL	Average	26.2	10.6	4.4	2.7	1.7	1.1	0.8
	Std Dev	4.4	0.8	0.5	0.3	0.2	0.1	0.1
	COV	17%	7%	12%	11%	11%	12%	14%

Table I.5 - Results MODULUS Analysis for Estimating Design Moduli

Section		Modulus, ksi			RMS Error, %
		ACP	Base	Subgrade	
L1	Average	500	43	28	40.9
	Std Dev	-	7.6	2.4	-
	COV	-	18%	8%	-
L2	Average	500	41	30	39.6
	Std Dev	-	10.1	1.7	-
	COV	-	25%	6%	-
L4	Average	500	49	31	36.8
	Std Dev	-	16.0	2.3	-
	COV	-	33%	7%	-
LL	Average	500	52	30	38.9
	Std Dev	-	12.1	2.1	-
	COV	-	23%	7%	-
RL	Average	500	25	25	31.1
	Std Dev	-	11.3	2.2	-
	COV	-	46%	9%	-

Table I.6 - Results of JIM Analysis for Estimating Design Moduli

| Section No. | | ACP* | Modulus, ksi | | | | RMS Error, % |
| | | | Base | | Subgrade | | |
			Cons.	Avg.	Cons.	Avg.	
L1	Average	640	58	84	22	25	4.6
	Std Dev	76.2	9	13	2	2	-
	COV	12%	15%	16%	8%	8%	-
L2	Average	553	59	83	23	26	4.5
	Std Dev	68	13.9	22.7	1.3	1.5	-
	COV	12%	24%	27%	6%	6%	-
L4	Average	545	65	95	24	27	3.5
	Std Dev	63.8	11.4	16.4	2.0	2.3	-
	COV	12%	17%	17%	9%	9%	-
LL	Average	587	61	87	23	26	4.9
	Std Dev	42.1	11.3	18.4	1.4	1.6	-
	COV	8%	19%	21%	6%	6%	-
RL	Average	665	50	66	19	22	7.2
	Std Dev	102.4	22.7	36.2	1.9	2.1	-
	COV	15%	45%	55%	10%	10%	-

* - Based on PSPA results

Table I.7 - Results of JIM Analysis for Estimating Design Moduli and Thicknesses

| Section No. | | Thickness, in. | | Modulus, ksi | | | | | RMS Error, % |
| | | ACP | Base | ACP | Base | | Subgrade | | |
					Cons.	Avg.	Cons.	Avg.	
L1	Average	1.6	5.9	640	109	111	23	25	3.7
	Std Dev	0.1	1.0	-	8.7	3.8	1.7	1.9	-
	COV	9%	17%	-	8%	3%	7%	7%	-
L2	Average	1.6	5.6	553	105.2	109.2	23.6	26.6	3.6
	Std Dev	0.2	1.3	-	10.9	5.3	1.2	1.4	-
	COV	13%	23%	0%	10%	5%	5%	5%	-
L4	Average	1.7	6.6	545	101	110	24	27	3.0
	Std Dev	0.3	1.3	-	15.4	3.5	1.9	2.2	-
	COV	15%	19%	-	15%	3%	8%	8%	-
LL	Average	1.6	7.2	587	98	110	24	26	4.1
	Std Dev	0.1	1.3	-	16.2	5.0	1.3	1.5	-
	COV	6%	17%	-	17%	5%	6%	6%	-
RL	Average	1.5	5.9	665	97	107	20	22	5.5
	Std Dev	0.1	1.7	-	10.7	7.9	1.7	1.9	-
	COV	6%	29%	-	11%	7%	8%	9%	-
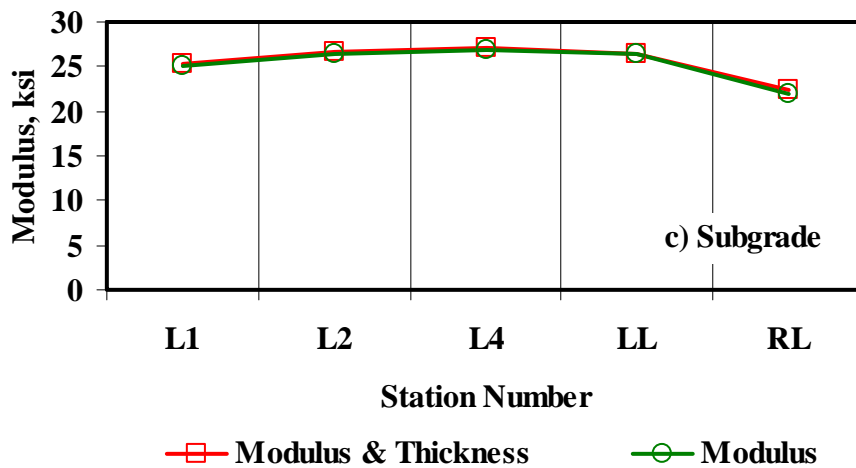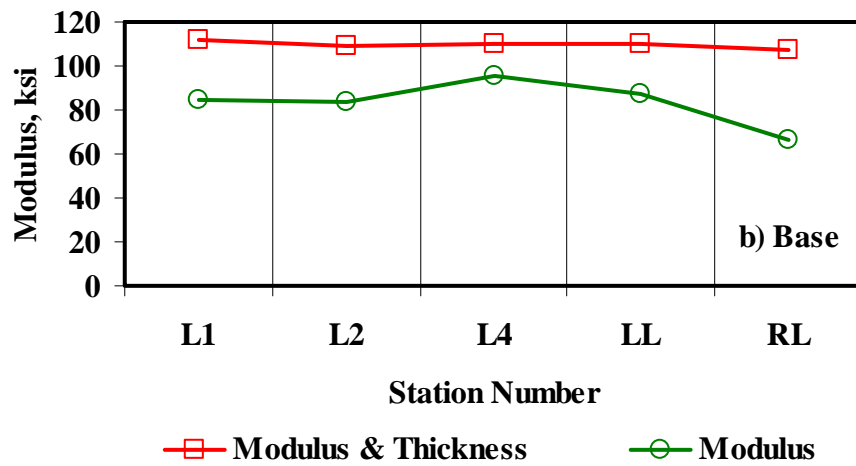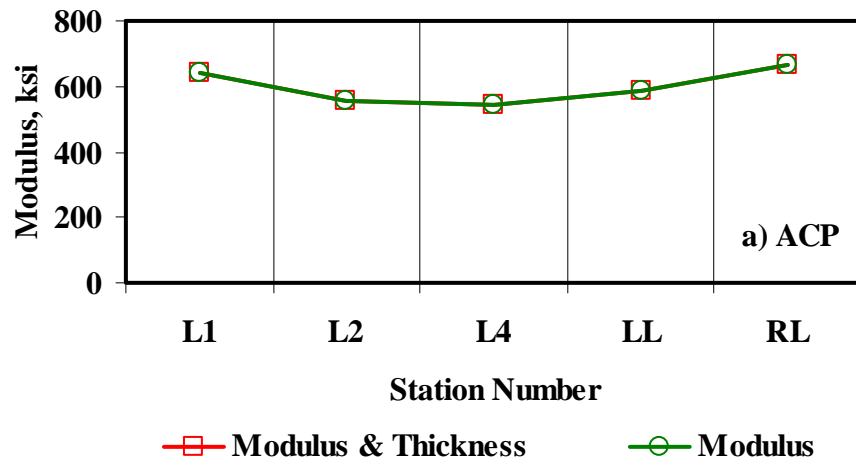
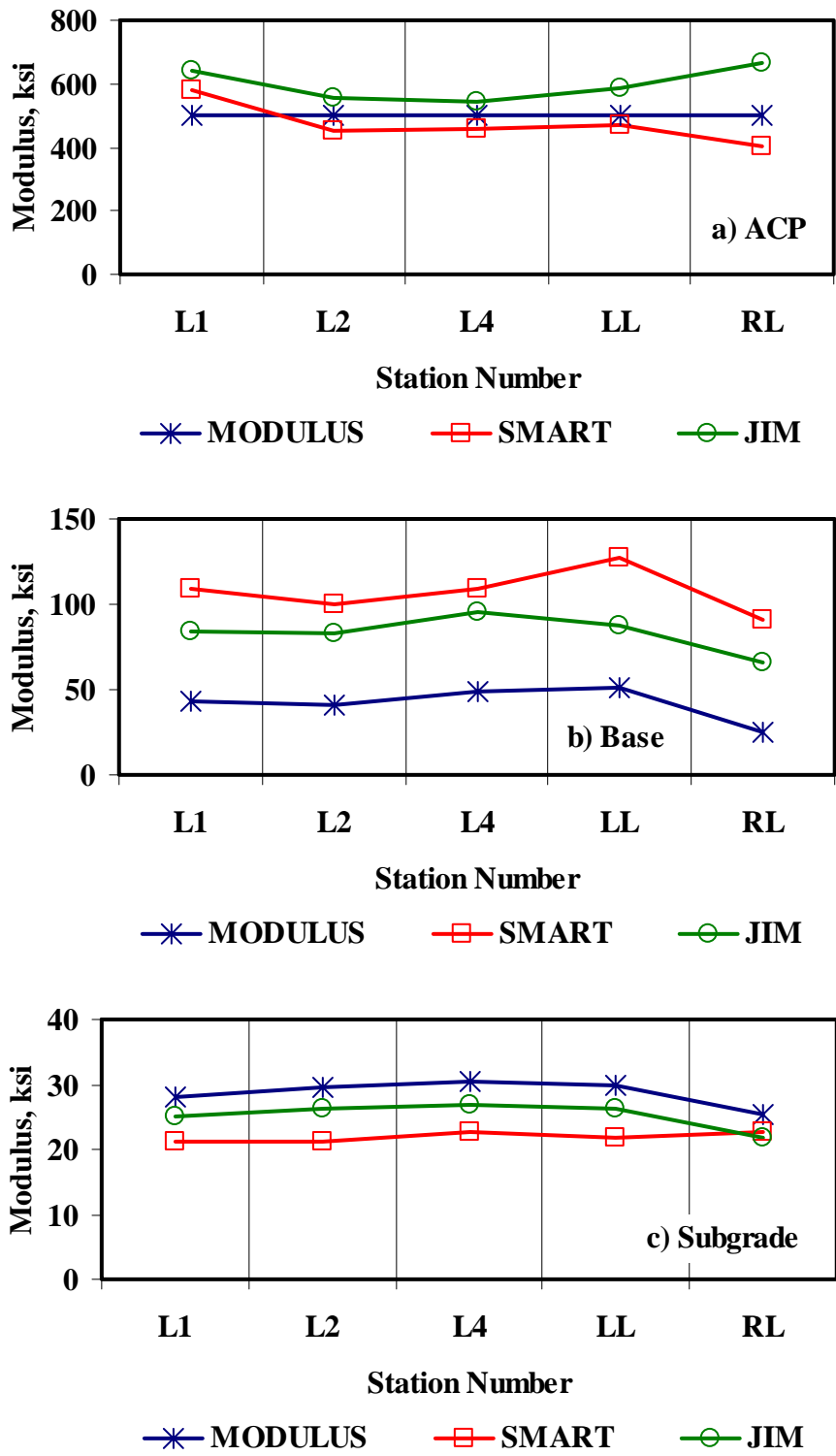**Figure I.7 - Comparison of Design Moduli from JIM Analysis with Constant and Backcalculated Thickness**

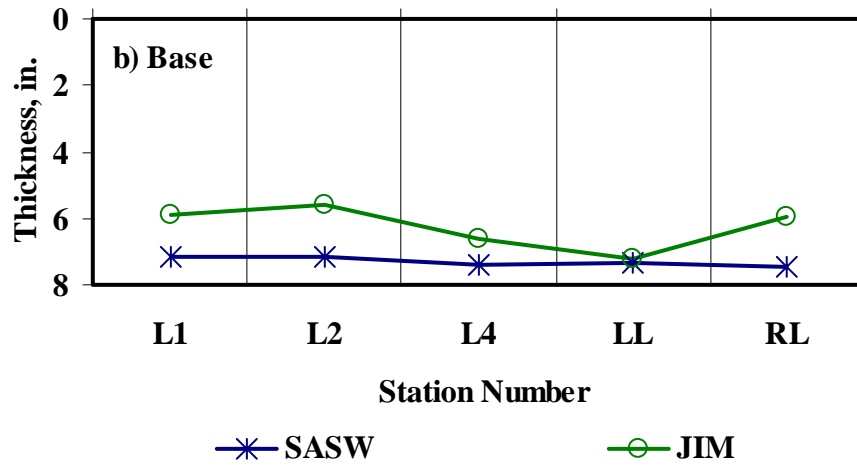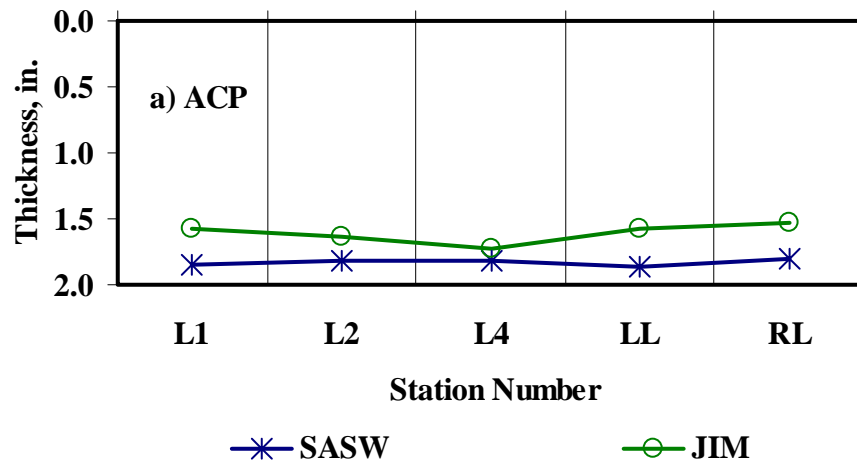**Figure I.8 - Comparison of Design Moduli from Different Analyses**

Figure I.9 - Comparison of Layer Thickness from Different Analyses
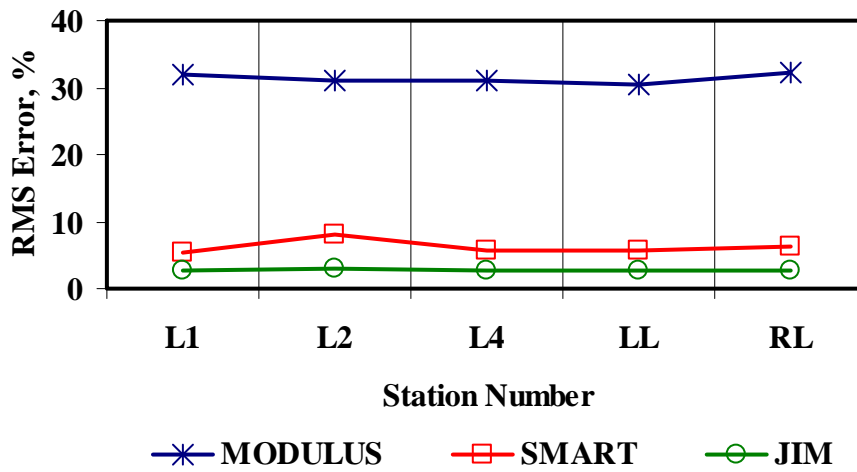

Figure I.10 - Comparison of RMS Error from Different Analyses

Table I.8 - Summary of Design Modulus Values with Data Fusion Results

| Section No.	Method	Modulus, ksi					
		ACP		Base		Subgrade	
		Average	COV	Average	COV	Average	COV
L1	MODULUS	500	-	43	18%	28	8%
	JIM	640	-	84	16%	25	8%
	SMART	579	12%	109	19%	21	6%
	SWA	579	12%	60	15%	24	5%
	WA	573	4%	77	12%	25	5%
	FL	565	4%	75	12%	25	5%
L2	MODULUS	500	-	41	25%	30	6%
	JIM	553	-	83	27%	26	6%
	SMART	453	17%	99	31%	21	10%
	SWA	458	18%	53	24%	26	4%
	WA	504	6%	79	20%	25	4%
	FL	490	8%	74	18%	26	6%
L3	MODULUS	500	-	49	33%	31	7%
	JIM	545	-	95	20%	27	10%
	SMART	457	17%	110	27%	22	12%
	SWA	463	15%	71	24%	25	2%
	WA	503	5%	83	18%	26	5%
	FL	498	5%	81	18%	27	5%
LL	MODULUS	500	-	52	23%	30	7%
	JIM	587	-	87	21%	26	6%
	SMART	474	25%	128	22%	22	10%
	SWA	474	25%	65	21%	26	2%
	WA	520	8%	87	14%	26	4%
	FL	507	10%	81	16%	26	8%
RL	MODULUS	500	-	25	46%	25	9%
	JIM	665	-	66	55%	22	10%
	SMART	402	25%	91	46%	23	10%
	SWA	402	25%	34	22%	23	6%
	WA	522	6%	52	33%	23	5%
	FL	498	7%	39	26%	24	5%
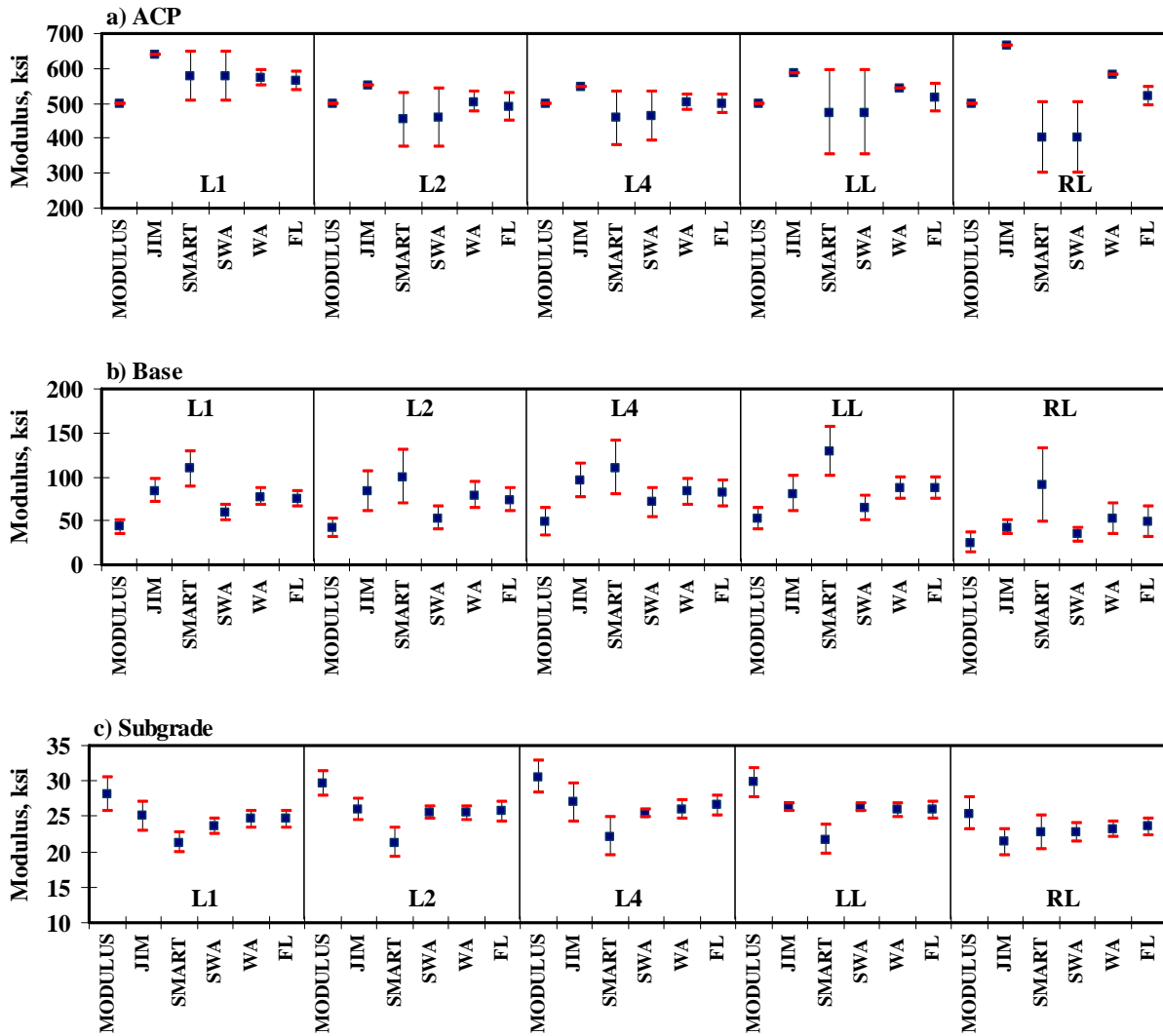
Figure I.11 - Statistical Comparison of Design Moduli of Different Analyses and Data Fusion Techniques